

# Cauchy-Navier Wavelet Solvers and Their Application in Deformation Analysis

M.K.Abeyratne

Geomathematics Group  
Department of Mathematics  
University of Kaiserslautern  
Germany

Vom Fachbereich Mathematik  
der Universität Kaiserslautern  
zur Erlangung des akademischen Grades  
Doktor der Naturwissenschaften  
(Doctor rerum naturalium, Dr. rer. nat.)  
genehmigte Dissertation

1. Gutachter: Prof. Dr. W. Freeden, Kaiserslautern
2. Gutachter: Prof. Dr. E. Groten, Darmstadt

Vollzug der Promotion: 28. August 2003

D 386

## Acknowledgements

First and foremost, I would like to express my deep gratitude to my advisor, Prof. Dr. Willi Freeden for his enthusiastic supervision of this work. He provided sound advice, good teaching, lots of valuable ideas, endless encouragement and good company. His willing support kept me going to the end. I am also obliged to Prof. Dr. E. Groten for reading and evaluation of my dissertation.

The members of the Geomathematics Group, University of Kaiserslautern have been a valuable source of knowledge in the field of my work. I have benefited from many valuable discussions with the group. Especially, HDoz. Dr. Volker Michel, Dr. Thorsten Maier, and Dip.-Math. Carsten Mayer always had time to consider my questions and gave me suggestions for improving various aspects. My sincere thanks go to all of them. I have great regard, and I wish to extend my warmest thanks to the secretary, Mrs. Claudia Korb and all the other members of the group for creating a friendly atmosphere.

The quality of this manuscript has improved substantially through the help of my colleagues; Dr. Helga Nutz, Dr. Thorsten Maier, and M.Sc. nat. Frank Bauer. I really admire their patience and staying power to carefully read the whole manuscript and would like to thank them for their helpful advice.

I am deeply indebted to Dr. Falk Triebisch, Department of Mathematics, University of Kaiserslautern, for his kindness and various assistance given to my family during our study period in Kaiserslautern.

The generous financial support provided by the German Academic Exchange Service (DAAD) and the University of Kaiserslautern is gratefully acknowledged. I would like to acknowledge with thanks and gratitude the University of Ruhuna, Sri Lanka for granting me study leave for the period of stay in Kaiserslautern. Special thank also goes to my colleagues of the Department of Mathematics, University of Ruhuna, for their friendly assistance.

I owe my loving thanks to my family; Gayanthi, Hans and Himani for their endless patience and encouragement when it was most required, during my work. Without their understanding it would have been impossible for me to finish this work. Finally, I express my sincere thanks to all my friends who helped me in numerous ways throughout my stay in Germany.

# Contents

<b>Introduction</b>	<b>1</b>
<b>1 Preliminaries</b>	<b>7</b>
1.1 Basic Notation and Definitions . . . . .	7
1.2 Spherical Function Spaces and Spherical Harmonics . . . . .	8
1.3 Spherical (Vectorial) Function Spaces and Vector Spherical Harmonics . . .	12
1.4 Regular Surfaces . . . . .	17
1.5 Mathematical Subjects of Elasticity . . . . .	18
1.5.1 Formulation of the Equations in Elasticity . . . . .	18
1.5.2 Boundary-value Problems of Classical Elasticity . . . . .	20
<b>2 Potential Methods for the Cauchy-Navier Equation</b>	<b>22</b>
2.1 Elastic Potentials on Regular Surfaces . . . . .	22
2.2 A Cauchy-Navier Vector Field Associated to Vector Harmonics . . . . .	23
2.3 Layer Potential Operators on Regular Surfaces . . . . .	24
2.3.1 Limit and Jump Relations . . . . .	25
2.4 Layer Potentials for the Dual Operators . . . . .	27
<b>3 Existence, Uniqueness and Regularity</b>	<b>31</b>
3.1 Inner Displacement Boundary-Value Problem . . . . .	31
3.2 $\ell^2(\Sigma)$ -closure of Cauchy-Navier Vector Fields . . . . .	33
3.3 A Generalized Fourier Series Approach to the Displacement Boundary-Value Problem . . . . .	35
<b>4 A Spatial Approach to Cauchy-Navier Wavelets</b>	<b>37</b>
4.1 Cauchy-Navier Wavelets Associated to Layer Potentials . . . . .	37
4.2 Scale Continuous Reconstruction Formula . . . . .	39
4.3 Scale Discrete Reconstruction Formula . . . . .	41

4.4	A Tree Algorithm . . . . .	45
4.5	Multiscale Solution of the Inner Displacement Boundary-Value Problem of Elastostatics . . . . .	48
4.6	Cauchy-Navier Wavelets Associated to Dual Layer Potentials . . . . .	51
<b>5</b>	<b>A Spectral Approach to Cauchy-Navier Wavelets</b>	<b>57</b>
5.1	Cauchy-Navier Vector Fields Corresponding to Vector Spherical Harmonics	59
5.2	Inner Displacement Boundary-Value Problem . . . . .	62
5.3	A Multiscale Approximation . . . . .	64
5.3.1	(Scale Discrete) Cauchy-Navier Scaling Functions . . . . .	65
5.3.2	(Scale Discrete) Cauchy-Navier Wavelets . . . . .	71
5.3.3	Computational Aspects . . . . .	75
5.3.4	Examples for Cauchy-Navier Wavelets . . . . .	78
5.4	Green's Function Associated to the Radial Boundary Displacements on the Unit Sphere . . . . .	84
<b>6</b>	<b>Numerical Results</b>	<b>88</b>
6.1	A Test Example - Use of Cauchy-Navier Wavelets Associated to Layer Potentials . . . . .	88
6.1.1	Spherical Approximation of Vector Fields by Layer Potentials . . . . .	88
6.2	Test Examples - Use of Cauchy-Navier Wavelets Associated to Vector Spherical Harmonics . . . . .	90
6.2.1	Multiscale Approximation - Scale and Detail Reconstructions (Global)	92
6.2.2	Multiscale Approximation - Scale and Detail Reconstructions (Local)	100
6.3	An Application to Deformation Analysis of the Earth . . . . .	102
6.3.1	Crustal Deformation . . . . .	103
6.3.2	Deformation Analysis for the Nevada Area Using GPS Measurements	103
<b>7</b>	<b>Concluding Remarks</b>	<b>109</b>
<b>A</b>	<b>Further Results on Cauchy-Navier Scaling Functions and Wavelets</b>	<b>111</b>
A.1	Shannon Scaling Functions and Wavelets . . . . .	111
A.2	Cubic Polynomial Scaling Functions and Wavelets . . . . .	115
<b>B</b>	<b>Auxiliary Results</b>	<b>120</b>
B.1	Partial Sums of Legendre Series via Clenshaw's Algorithm . . . . .	120



---

<b>C</b>	<b>Crustal Deformation Data</b>	<b>124</b>
C.1	GPS Measurements . . . . .	124

# Introduction

The theory of elasticity forms the central core of solid mechanics and deals with the systematic study of stress, strain, and displacement in an ideally elastic body under the influence of external forces (see, for example, [42],[46],[75]). It is a broad fundamental science having applications in a variety of areas such as materials science (modelling the mechanical properties of solids), geophysics (the Earth's deformation analysis, interpretation of seismic data using elastic wave analysis), engineering structural mechanics, etc. The underlying mathematical theory of elasticity provides a rich framework for the study of such applications and also offers many interesting and challenging mathematical concepts such as the governing partial differential equations and the qualitative and quantitative properties of their solutions. More precisely, in the theory of linear elastostatics, the displacement field can be modelled by a coupled linear system of elliptic partial differential equations called Cauchy-Navier equations. The corresponding mathematical concepts are known as Cauchy-Navier theory. Finding the solution of Cauchy-Navier equations in a bounded domain, where the solution satisfies given prescribed boundary conditions, represents the well-known inner displacement boundary-value problem of elastostatics ([46],[58]). The solution of this problem (i.e. the deformation analysis in a homogeneous isotropic elastic media) is a considerable issue of the theory of linear elasticity, and, in particular, is of practical significance in the field of geoscience.

When we look at the solution strategies available in handling such problems in elastostatics, several numerical approaches can be found in the literature. For example, the Finite Element Methods (FEM) ([8]), Methods of Fundamental Solutions (MFS) [55] and Boundary Element Methods (BEM) ([11],[48]), etc. Although, much progress has been made in the numerical analysis of these methods, some techniques have their own drawbacks and limitations in different applications. For example, it is generally recognized that mesh generations for 3D domains remain one of the major challenges for the FEM. Also MFS techniques are mostly applied to axisymmetric two-dimensional problems. Although, BEM is expected to be advantageous in large-scale problems due to the reduction of the dimensionality, nevertheless, it reveals serious shortcomings like the fact that the resulting system of linear algebraic equations is non-sparse and non-symmetric. Other inherent disadvantages are the sensitivity of the results to the choice of collocation points, the inaccuracy of the elastic (displacement) fields near boundaries and the smoothness constraints needed to treat the problems with hypersingular kernels.

From classical literature, it is evident that the framework of integral equations provides an appropriate tool to represent the boundary-value problems of elastostatics ([52]). In this framework, recalling the formulation of governing equations of linear elasticity in terms of displacements in  $\mathbb{R}^3$  (i.e. the Cauchy-Navier equations), the associated fundamental solutions can be established in a matrix form. The fundamental solutions then can be used to generate, by a layer theoretical method, boundary integral equations, which are used to replace the given original boundary-value problem. The existence of such equations can be found in literature, for example, in [58]. Uniqueness is assured under certain conditions on the material properties such as that the media are assumed to be homogeneous and isotropic (see, for example, [46]). The use of potential methods in elasticity and the associated theory of linear integral equations in elasticity has been investigated by several authors since the first issue of Fredholm (see, for example, [5],[29],[46],[52],[58]). In this respect, it should be mentioned that the differential equations for displacement vector fields in elastic equilibrium and, thereby, the corresponding integral forms for the inner displacement boundary-value problems can be prescribed in analogy to classical potential theory for harmonic functions. Thus, the displacement vector corresponds to the scalar harmonic function, whereas the integral formulae parallel the Gauss flux theorem and, moreover, the well known Betti's and Somigliana representations correspond to the Green formulae. Consequently, the fundamental existence and uniqueness theorems can be formulated in analogy to the corresponding theorems for harmonic functions. More detailed theoretical treatments on those topics are given, for example, in [58].

To solve such boundary integral equations using traditional numerical procedures, arbitrarily dense distributions of the boundary values are required. Moreover, boundary integral equations which consist of singular kernels like Green's representation on a boundary for elastostatic boundary-value problems, are hardly treatable (see, for example, [4],[75]). At this point, it is worth mentioning that, with the Runge framework of sphere oriented techniques, displacement boundary value-problems of linear elastostatics have been successfully treated by several techniques. For example, the global basis method ([37]), Navier spline interpolation ([28],[29],[81]), etc. The basic concept in behind all those topics is the use of comparatively simply structured tensorial kernel functions. Another traditional way of modelling the displacement vector field for a spherical boundary is the use of Fourier representations with vector spherical harmonics as basis functions (see, for example, [37],[43]). A major drawback of these methods, for example, in regional modelling, is that the spherical harmonics are globally supported and do not display any localization in the space domain. In consequence, local changes of a function may affect the whole set of Fourier coefficients, hence, changing the representation of the data function globally. Due to the well-known fact that ideal space and frequency localization are mutually exclusive (see, for example, [30],[33]), one has to consider kernel functions compromising the space and frequency localizations. In this respect, the use of special kernel functions like for example, scaling functions and associated wavelets become significant tools for handling the underlying problems. In such consideration, the scaling functions and wavelets are tensor type kernels representing bases in certain spaces and

characterized by their localization properties in both space and frequency domains.

Wavelet analysis is a relatively new mathematical discipline which has generated much interest in both pure and applied mathematics in the past fifteen years. It was originated as a powerful tool for signal and image analysis, and it has covered out the areas like time series analysis, matrix compression, data coding, analysis of signals and approximation theory, e.g. data compression in image processing (see, for example, [20],[63]). Wavelet methods are being used and applied in a large variety of fields of science, engineering and technology today, such as numerical solutions of partial differential equations, problems in geosciences, etc (see, for example, [51],[56]).

Wavelets are, in general, basis functions defined over  $\mathbb{R}^n$  or torus in certain function spaces, the elements of the function spaces can be represented using kernels at different positions and scales. Those are particularly well suited for representing complicated functions, for example, elastic displacement fields in our consideration, breaking up to simple pieces of functions. The reason is that wavelets are well localized in space domain as well as in frequency domain (see, for example, [12],[45],[53]). More precisely, the fundamental strength of wavelets lies in its ability to achieve a very high resolution locally using a certain number of localized functions. Today, wavelet analysis is well established in many scientific disciplines as an effective alternative tool in contrast to the extreme space-frequency tradeoff of the standard mathematics of Fourier theory.

Recently, wavelet methods became a new fast numerical tool, for example, for the solution of elliptic boundary-value problems, for solving boundary integral equations (see, for example, [3],[9],[15],[51],[73]). In geophysically relevant problems, there is a growing interest in wavelet applications based on sphere oriented techniques, i.e. based on spherical multiresolution analysis (see, for example, [30],[40],[41] for the scalar case, [6],[7],[10],[30] for the vectorial case, [30],[77] for the tensorial case). Moreover, geomathematical methods such as harmonic wavelets (see, for example, [26],[31],[39] and references therein) or wavelets for the numerical treatments of the pre-maxwell equations of geomagnetics have been investigated in a series of publications (see, for example, [62] and the literature therein). Those efforts have been devoted in the representations based on scalar, vector and tensor valued functions and a significant progress has been made in a variety of fields, like gravimetry ([33],[66]), gradiometry problems ([26],[32],[35],[77]) and magnetic field determination ([6],[7],[10],[62]). A detailed overview about the publications involving wavelet applications in geomathematical problems has been given in [69].

However, most of the previous work invested in the construction of those wavelet environments has focused on 'harmonic' type problems such as the outer harmonic multiscale modelling in potential theory ([26],[38]). Less effort, however, has been expended on handling wavelet applications in elliptic boundary-value problems in linear elasticity like Cauchy-Navier deformation analysis (cf. [1]). Even more, in the case of elasticity, it should be noted that the geophysically relevant multiscale approaches in a spherical

framework are still at a rudimentary level. It is the purpose of this work to establish a novel approach to the solution of the inner displacement boundary-value problem of elastostatics using tensor wavelet method which we introduce as Cauchy-Navier wavelet solvers. We focus on two essential topics: wavelets defined by layer potentials (a spatial approach to wavelets) and the wavelets associated to vector spherical harmonics (a spectral approach to wavelets).

The first method is based on the limit and jump relations defined on regular surfaces according to the potential theory in elasticity ([58]). In the standard potential theoretic framework, the inner displacement boundary-value problem defined on regular boundaries is transformed to a Fredholm integral equation of second kind such that the techniques of standard wavelet concept for solving integral equation become available (see, for example, [3],[14]). Kernels defined by limit and jump integral operators are considered as scaling functions to establish a new wavelet family on regular surfaces (cf. [1],[32]). The second technique is developed having the ultimate goal of constructing a suitable wavelet approximation associated to Green's integral representation for the displacement boundary-value problem of elastostatics. The starting point is the use of tensor product kernels defined on Cauchy-Navier vector fields as scaling functions (cf. [1],[34],[43],[81]). This technique is known to be a spectral approach to wavelets for the boundary-value problems of elastostatics associated to the geophysically relevant spherical boundaries.

When we turn to geophysically relevant applications, we see that geodetic measurements of crustal deformation provide direct tests of geophysical models which are used to describe the dynamics of the Earth. Two major tasks are to obtain geodetic measurements of surface displacements of the Earth crust, and to analyse the deformations of Earth interior using elastic properties. It is experienced that, by making precise measurements of deformation of the Earth's surface, one can model the static displacements of the interior of the Earth crust by the Cauchy-Navier theory. Hence, above mentioned solution strategies can be applied to solve such problems which is the goal of this work. Moreover, it should be remarked that the topics of Cauchy-Navier wavelet solvers have been studied in this work in order to apply these techniques to practical problems of deformation analysis. In this thesis we first discuss various test examples for three dimensional boundary value-problems for numerical realization. One real application is considered to show the applicability of the techniques so as to make the first step towards practical applications.

The outline of the thesis is as follows:

Chapter 1 presents the basic definitions and the principles of foundation within the scope necessary for this study. Hence, the main concepts of the scalar and vector spherical harmonics are reviewed. As the tensors take a prominent role throughout this investigation, the Legendre tensors and the tensor product kernel structures on vector spherical harmonics are briefly presented. Moreover, the theory of linear elasticity including the

derivation of the governing Cauchy-Navier equations and the associated boundary-value problems are recapitulated.

Chapter 2 is mainly devoted to discuss the potential methods in elasticity that parallel the classical potential theory. Starting from the definition of elastic potentials on regular surfaces a vector field satisfying the elasticity equation is derived in terms of vector harmonics. In analogy to classical potential theory we discuss the limit and jump relations within the framework of Hilbert spaces of square-integrable vector fields on regular surfaces. We examine how all those results can be extended to the (adjoint) dual layer potentials.

In Chapter 3, a general overview of the uniqueness, existence, and the regularity of the solution of the displacement problem is discussed. Moreover, in this chapter, a "generalized" Fourier series representation to the solution of the inner displacement boundary-value problem associated to a regular boundary is achieved. This is, of course, a global basis technique and this is done by taking a Fourier representation using a Cauchy-Navier vector field defined in terms of vector harmonics so that the vector field represents an orthonormal basis on the regular surface.

In Chapter 4, in the framework of layer potentials and their operator formulations discussed in Chapter 2, we introduce a wavelet technique (i.e. a spatial approach to Cauchy-Navier wavelets) in the nomenclature of the Hilbert space of square-integrable vector fields on a regular boundary. Introducing so-called Cauchy-Navier scaling functions and wavelets, the wavelet transforms and the reconstruction formulae both in continuous and discrete forms are explicitly established. Based on appropriate numerical integration rules a pyramid scheme is developed. This overall approach is then used to represent a multi-scale approximation of the solution of the inner displacement boundary-value problem of elastostatics. An extension of those techniques to dual layer potentials is briefly recapitulated.

Chapter 5 addresses a spectral approach to wavelets, introducing the so-called Cauchy-Navier wavelet solvers for the inner displacement boundary-value problem associated to the geophysically relevant case of a spherical boundary. Green's integral representation of the solution is taken into account. Essential tools are Cauchy-Navier vector fields possessing the vector spherical harmonics as boundary values. Using tensorial product kernels associated to the Cauchy-Navier vector field as scaling functions, a wavelet concept is introduced. More explicitly, a multiscale approximation of the solution of the displacement boundary value-problem is established via a wavelet approximation associated to Green's integral representation. Finally, as usual in a wavelet framework of elastic fields from prescribed displacement vectors, a tree algorithm is developed for the decomposition and reconstruction.

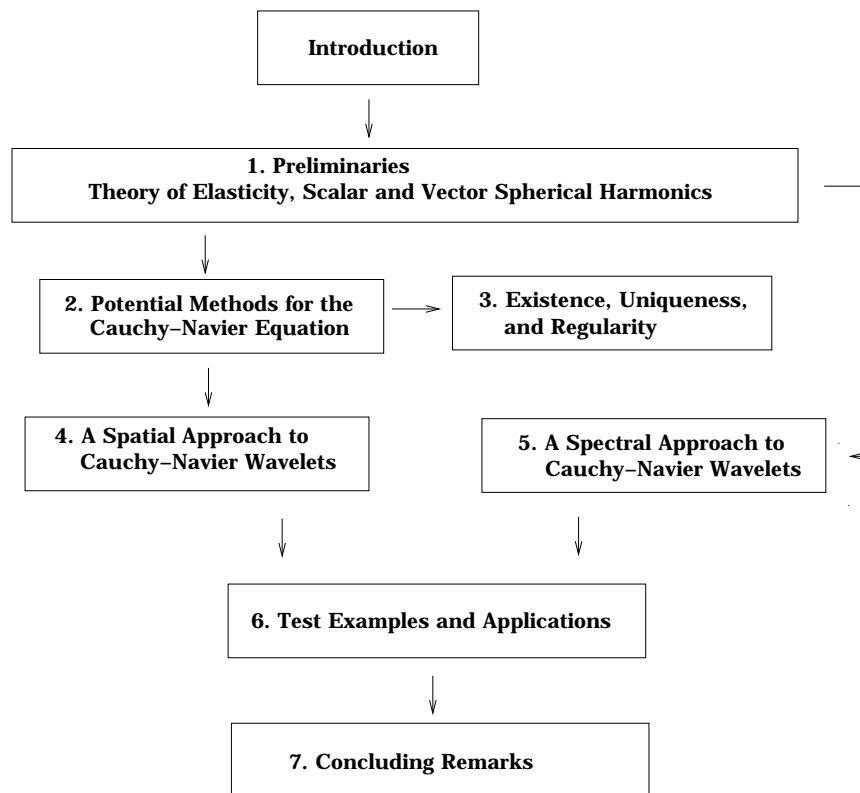
Chapter 6 deals with numerical results. Both methods are treated by test examples

in which geophysically relevant spherical boundaries such as spheres are used for the numerical realization. The potential theoretical approach is tested only for approximations of boundary functions, whereas the second wavelet approach associated to Green's representation is tested by solving an inner displacement boundary-value problem. Both global and local approximations produce accurate results by a lower scale approximation, when compared to exact solutions for the test problems under consideration. As a last example, the method is applied to the deformation analysis of a particular region of the Earth, viz. Nevada using a discrete set of surface displacements provided by satellite observations.

Chapter 7 contains a short summary of the work and some general conclusions. Moreover, in this Chapter new directions of research that opened up as outcomes of the work are briefly discussed.

Finally, the appendices are dedicated to technicalities, i.e. to present supplementary proofs, some computational tools, a table of real data and more detailed graphical illustrations of scaling functions and wavelets.

The interrelations between the chapters can be briefly illustrated as follows:



# Chapter 1

## Preliminaries

We start this chapter by introducing basic definitions and conventional notation we use throughout this study. Next we discuss the basic facts on scalar and vector spherical harmonics and some consequence results which are necessary in our work. It should be noticed that we only give the resulting facts on spherical harmonics. For more details the reader is referred to [30] and the literature therein. Finally, we give a detailed representation of the theory of linear elasticity including the derivation of the Cauchy-Navier equation which describes displacements in elastic media. Moreover, we give an overview of the boundary-value problems of linear elasticity and some remarks on the classical solution techniques.

### 1.1 Basic Notation and Definitions

Throughout this study we use the following conventional notation unless otherwise stated: the scalar functions are denoted by capital letters  $F, G, \dots$ , the vector fields are denoted by lower-case letters  $f, g, \dots$  and tensor fields of second rank are by boldface lower-case letters  $\mathbf{f}, \mathbf{g}, \dots$ .

We denote the set  $\mathbb{N} \cup \{0\}$  by  $\mathbb{N}_0$ , where  $\mathbb{N}$  represents the set of positive integers. The set of integers is represented by  $\mathbb{Z}$ .  $\mathbb{R}^3$  denotes the three-dimensional (real) Euclidean space. We consistently write  $x, y, \dots$  for the elements of  $\mathbb{R}^3$ . In components we have the representation

$$x = x_1\epsilon^1 + x_2\epsilon^2 + x_3\epsilon^3, \quad (1.1)$$

where the vectors  $\epsilon^1, \epsilon^2, \epsilon^3$  form the canonical orthonormal basis in  $\mathbb{R}^3$ ,

$$\epsilon^1 = \begin{pmatrix} 1 \\ 0 \\ 0 \end{pmatrix}, \quad \epsilon^2 = \begin{pmatrix} 0 \\ 1 \\ 0 \end{pmatrix}, \quad \epsilon^3 = \begin{pmatrix} 0 \\ 0 \\ 1 \end{pmatrix}.$$

The inner product, vector product, and the tensor product between  $x$  and  $y$ , respectively, are defined by



$$x \cdot y = x^T y = \sum_{i=1}^3 x_i y_i, \quad (1.2)$$

$$x \wedge y = (x_2 y_3 - x_3 y_2, x_3 y_1 - x_1 y_3, x_1 y_2 - x_2 y_1)^T, \quad (1.3)$$

$$x \otimes y = xy^T = \begin{pmatrix} x_1 y_1 & x_1 y_2 & x_1 y_3 \\ x_2 y_1 & x_2 y_2 & x_2 y_3 \\ x_3 y_1 & x_3 y_2 & x_3 y_3 \end{pmatrix} \quad (1.4)$$

An important relation between the scalar product and tensor product is given by

$$(x \otimes y)z = (y \cdot z)x, \quad (1.5)$$

for any  $x, y, z \in \mathbb{R}^3$ .

The Euclidean norm of  $x$  is denoted by  $|x|$  and defined as  $|x| = (x \cdot x)^{1/2}$ .

The so-called double dot product between two tensors  $\mathbf{t}_1, \mathbf{t}_2 \in \mathbb{R}^{3 \times 3}$ , is defined by

$$\mathbf{t}_1 : \mathbf{t}_2 = \sum_{i=1}^3 \sum_{j=1}^3 (\mathbf{t}_1)_{i,j} (\mathbf{t}_2)_{i,j}. \quad (1.6)$$

The sphere centered at the origin with radius  $R$  is denoted by

$$\Omega_R = \{x \in \mathbb{R}^3 \mid |x| = R\}, \quad (1.7)$$

while the unit sphere (i.e.  $R = 1$ ) is simply denoted by  $\Omega$ . Moreover, in order to represent the elements on  $\Omega$  we usually use Greek letters  $\xi, \eta, \dots$ .

## 1.2 Spherical Function Spaces and Spherical Harmonics

The set of scalar functions  $F : \Omega \rightarrow \mathbb{R}$  possessing  $k$  times continuous derivatives on the unit sphere is denoted by  $\mathcal{C}^{(k)}(\Omega)$ ,  $0 \leq k \leq \infty$ , in particular,  $\mathcal{C}^{(0)}(\Omega) = \mathcal{C}(\Omega)$ .  $\mathcal{L}^2(\Omega)$  denotes the set of all square-integrable scalar-valued functions  $F : \Omega \rightarrow \mathbb{R}$ . The space  $\mathcal{L}^2(\Omega)$  is the completion of  $\mathcal{C}(\Omega)$  with respect to the norm  $\|\cdot\|_{\mathcal{L}^2(\Omega)}$  equipped with the inner product  $\langle \cdot, \cdot \rangle_{\mathcal{L}^2(\Omega)}$  defined by

$$\langle F, G \rangle_{\mathcal{L}^2(\Omega)} = \int_{\Omega} F(\xi) G(\xi) d\omega(\xi), \quad F, G \in \mathcal{L}^2(\Omega), \quad (1.8)$$

i.e.

$$\mathcal{L}^2(\Omega) = \overline{\mathcal{C}(\Omega)}^{\|\cdot\|_{\mathcal{L}^2(\Omega)}}. \quad (1.9)$$

Moreover,

$$\|F\|_{C(\Omega)} = \sup_{\xi \in \Omega} |F(\xi)|, \quad F \in C(\Omega). \quad (1.10)$$

The norm  $\|\cdot\|_{\mathcal{L}^2(\Omega)}$  may be estimated by

$$\|F\|_{\mathcal{L}^2(\Omega)} \leq \sqrt{4\pi} \|F\|_{C(\Omega)}, \quad F \in C(\Omega). \quad (1.11)$$

For any  $x \in \mathbb{R}^3$ ,  $x \neq 0$ , we have the representation  $x = r\xi$ ,  $r = |x|$ , where  $\xi = (\xi_1, \xi_2, \xi_3)^T \in \Omega$  is the uniquely determined directional unit vector of  $x$ .

Any point  $\xi \in \Omega$  can be represented in spherical coordinates by

$$\xi = \sqrt{1-t^2}(\cos \varphi \epsilon^1 + \sin \varphi \epsilon^2) + t \epsilon^3, \quad (1.12)$$

where,

$$t = \cos \theta, \theta \in [0, \pi], \varphi \in [0, 2\pi).$$

( $\theta$  : latitude,  $\varphi$  : longitude,  $t$  : polar distance).

Moreover, we consider the directional unit vectors  $(\epsilon^r, \epsilon^\varphi, \epsilon^t)$  corresponding to spherical coordinates to be defined by (cf. [30])

$$\epsilon^r = \begin{pmatrix} \sqrt{1-t^2} \cos \varphi \\ \sqrt{1-t^2} \sin \varphi \\ t \end{pmatrix}, \quad \epsilon^\varphi = \begin{pmatrix} -\sin \varphi \\ \cos \varphi \\ 0 \end{pmatrix}, \quad \epsilon^t = \begin{pmatrix} -t \cos \varphi \\ -t \sin \varphi \\ \sqrt{1-t^2} \end{pmatrix}.$$

We list below a number of differential operators in coordinate free representation.

Symbol	Differential Operator
$\nabla$	Gradient
$\nabla^*$	Surface gradient
$\Delta = \nabla \cdot \nabla$	Laplace operator
$\Delta^* = \nabla^* \cdot \nabla^*$	Beltrami operator
$L^*$	Surface curl gradient

Table 1.1: Differential operators

For the convenience of the reader we also give the representation of those operators in local polar coordinates (1.20):

$$\nabla_x = \xi \frac{\partial}{\partial r} + \frac{1}{r} \nabla_\xi^*, \quad (1.13)$$

$$\nabla_\xi^* = \frac{1}{\sqrt{1-t^2}}(-\sin \varphi \epsilon^1 + \cos \varphi \epsilon^2) \frac{\partial}{\partial \varphi} \quad (1.14)$$

$$+ \sqrt{1-t^2}(-t \cos \varphi \epsilon^1 - t \sin \varphi \epsilon^2 + \sqrt{1-t^2} \epsilon^3) \frac{\partial}{\partial t}, \quad (1.15)$$

$$\Delta_x = \left(\frac{\partial}{\partial r}\right)^2 + \frac{2}{r}\left(\frac{\partial}{\partial r}\right) + \frac{1}{r^2}\Delta_\xi^*, \quad (1.16)$$

$$\Delta_\xi^* = \frac{\partial}{\partial t}(1-t^2)\frac{\partial}{\partial t} + \frac{1}{1-t^2}\left(\frac{\partial}{\partial \varphi}\right)^2, \quad (1.17)$$

$$L_\xi^* = \sqrt{1-t^2}(\sin \varphi \epsilon^1 - \cos \varphi \epsilon^2) \frac{\partial}{\partial t} \quad (1.18)$$

$$+ \frac{1}{\sqrt{1-t^2}}(-t \cos \varphi \epsilon^1 - t \sin \varphi \epsilon^2 + \sqrt{1-t^2} \epsilon^3) \frac{\partial}{\partial \varphi}. \quad (1.19)$$

The scalar spherical harmonics  $Y_n$  of degree  $n$  are defined as the everywhere on  $\Omega$  infinitely differentiable eigenfunctions corresponding to the eigenvalues  $\Delta^*(n) = -n(n+1)$ ,  $n = 0, 1, \dots$  of the Beltrami operator  $\Delta^*$ , i.e.  $(\Delta_\xi^* - n(n+1))Y_n(\xi) = 0$ ,  $\xi \in \Omega$ .

The space of all scalar spherical harmonics of degree  $n$  is a linear space of dimension  $2n+1$  and is denoted by  $Harm_n(\Omega)$ . Furthermore, the set of spherical harmonics given by  $\{Y_{n,j} : n = 0, 1, \dots, j = 1, \dots, 2n+1\}$  is always assumed to be an orthonormal system in the sense that

$$\int_{\Omega} Y_{n,j}(\xi) Y_{m,l}(\xi) d\omega(\xi) = \delta_{n,m} \delta_{j,l}, \quad (1.20)$$

where  $n$  and  $j$  are the degree and the order of the spherical harmonic  $Y_{n,j}$  respectively, and  $\delta$  is Kronecker's delta. The space  $Harm_{0\dots m}(\Omega)$  denotes the space of all spherical harmonics up to degree  $m$  and, hence,  $\dim(Harm_{0\dots m}(\Omega)) = \sum_{k=0}^m (2k+1) = (m+1)^2$ .

The functions  $H_n : \mathbb{R}^3 \rightarrow \mathbb{R}$  of the form  $H_n(x) = r^n Y_n(\xi)$ ,  $r = |x|$ ,  $\xi \in \Omega$  are homogeneous harmonic polynomials of degree  $n$ . Moreover, in connection with the eigenfunctions of the Beltrami operator, it can easily be checked that

$$\begin{aligned} \Delta(H_n(x)) &= \Delta(r^n Y_n(\xi)) \\ &= \left( \left(\frac{\partial}{\partial r}\right)^2 + \frac{2}{r} \frac{\partial}{\partial r} + \frac{1}{r^2} \Delta_\xi^* \right) r^n Y_n(\xi) \\ &= (n(n-1)r^{n-1} + 2nr^{n-2})Y_n(\xi) + r^{n-2}\Delta_\xi^* Y_n(\xi) \\ &= (n(n+1)r^{n-1})Y_n(\xi) - r^{n-2}n(n+1)Y_n(\xi) \\ &= 0. \end{aligned}$$

Many of the important properties of spherical harmonics can be found in literature, for example, [30],[68]. We review only some of them, which are necessary in our investigation. For more details the reader is referred to [30].

**Theorem 1.1** *The set of all spherical harmonics  $\{Y_{n,j} : n = 0, 1, \dots, j = 1, \dots, 2n+1\}$  is closed in  $\mathcal{L}^2(\Omega)$ , i.e. for every  $F \in \mathcal{L}^2(\Omega)$  and for any given  $\epsilon > 0$  there exist an integer*

$N = N(\epsilon)$  and coefficients  $a_{n,j} \in \mathbb{R}$  such that

$$\left\| \sum_{i=1}^N \sum_{j=1}^{2n+1} a_{n,j} Y_{n,j} - F \right\|_{\mathcal{L}^2(\Omega)} < \epsilon. \quad (1.21)$$

In the framework of Hilbert theory the closure is equivalent to the statement: For any  $F \in \mathcal{L}^2(\Omega)$  we have the Fourier expansion in the sense of  $\|\cdot\|_{\mathcal{L}^2(\Omega)}$

$$F = \sum_{n=0}^{\infty} \sum_{j=1}^{2n+1} F^{\wedge}(n, j) Y_{n,j}, \quad (1.22)$$

where the Fourier coefficients  $F^{\wedge}(n, j)$  are given by the formula

$$F^{\wedge}(n, j) = \int_{\Omega} F(\xi) Y_{n,j}(\xi) d\omega(\xi), \quad n \in \mathbb{N}_0, \quad j = 1, 2, \dots, 2n+1. \quad (1.23)$$

Equivalently, we have the Parseval identity for any  $F, G \in \mathcal{L}^2(\Omega)$

$$\langle F, G \rangle_{\mathcal{L}^2(\Omega)} = \sum_{n=0}^{\infty} \sum_{j=1}^{2n+1} F^{\wedge}(n, j) G^{\wedge}(n, j) \quad (1.24)$$

and, therefore, the norm can be reformulated as

$$\|F\|_{\mathcal{L}^2(\Omega)} = \left( \sum_{n=0}^{\infty} \sum_{j=1}^{2n+1} |F^{\wedge}(n, j)|^2 \right)^{1/2}, \quad F \in \mathcal{L}^2(\Omega). \quad (1.25)$$

The Legendre polynomials  $P_n$ ,  $n = 0, 1, 2, \dots$ , given by

$$P_n(t) = \sum_{k=1}^{[n/2]} (-1)^k \frac{(2n-2k)!}{2^n (n-2k)! (n-k)! k!} t^{n-2k}, \quad t \in [-1, 1], \quad (1.26)$$

are the infinitely differentiable eigenfunctions on the interval  $[-1, 1]$  corresponding to the Legendre operator

$$L_t = (1-t^2) \left( \frac{d}{dt} \right)^2 - 2t \left( \frac{d}{dt} \right)$$

which are bounded on  $[-1, +1]$  such that  $P_n(1) = 1$ .

Apart from a multiplicative factor the Legendre polynomial  $P_n(\epsilon^3 \cdot) : \xi \mapsto P_n(\epsilon^3 \cdot \xi)$ ,  $\xi \in \Omega$ , is the only spherical harmonic that is invariant under all orthonormal transformations keeping  $\epsilon^3$  fixed.

For any pair  $(\xi, \eta) \in \Omega \times \Omega$ , the sum

$$F_n(\xi, \eta) = \sum_{j=1}^{2n+1} Y_{n,j}(\xi) Y_{n,j}(\eta) \quad (1.27)$$

is invariant under the orthonormal transformation  $\mathbf{u}$  (cf. [30]), i.e.  $F_n(\mathbf{u}\xi, \mathbf{u}\eta) = F_n(\xi, \eta)$  for all  $\mathbf{u}$  satisfying  $\mathbf{u}^T \mathbf{u} = \mathbf{u} \mathbf{u}^T = \mathbf{i}_3$ , ( $\mathbf{i}_3$  is the unit matrix in  $\mathbb{R}^3$ ). This leads us to obtain the so called *addition theorem* for spherical harmonics:

$$\sum_{j=1}^{2n+1} Y_{n,j}(\xi) Y_{n,j}(\eta) = \frac{2n+1}{4\pi} P_n(\xi \cdot \eta), \quad (\xi, \eta) \in \Omega \times \Omega. \quad (1.28)$$

In particular, we have

$$\sum_{j=1}^{2n+1} |Y_{n,j}(\xi)|^2 = \frac{2n+1}{4\pi}, \quad \xi \in \Omega. \quad (1.29)$$

Furthermore, it is easy to see that

$$|Y_{n,j}(\xi)| \leq \sqrt{\frac{2n+1}{4\pi}}. \quad (1.30)$$

### 1.3 Spherical (Vectorial) Function Spaces and Vector Spherical Harmonics

Next we are concerned with vector-valued functions as known from [30] associated to scalar spherical harmonics. With the notation and definitions mentioned above, a vector valued function  $f : \Omega \longrightarrow \mathbb{R}^3$  can be represented in canonical form as

$$f(\xi) = \sum_{i=1}^3 F_i(\xi) \epsilon^i, \quad \xi \in \Omega, \quad F_i(\xi) = f(\xi) \cdot \epsilon^i, \quad i = 1, 2, 3. \quad (1.31)$$

As in the scalar case, the space of square-integrable vector valued functions defined on  $\Omega$  is denoted by  $\ell^2(\Omega)$ . Thus, the space  $\ell^2(\Omega)$  is a Hilbert space equipped with the inner product

$$\langle f, g \rangle_{\ell^2(\Omega)} = \int_{\Omega} f(\xi) \cdot g(\xi) d\omega(\xi) \quad f, g \in \ell^2(\Omega). \quad (1.32)$$

$c^{(k)}(\Omega)$ ,  $0 \leq k \leq \infty$ , consists of  $k$ -times continuously differentiable vector valued functions defined on  $\Omega$  and  $c(\Omega) = c^{(0)}(\Omega)$ .

Moreover,

$$\|f\|_{c(\Omega)} = \sup_{\xi \in \Omega} |f(\xi)|, \quad f \in c(\Omega). \quad (1.33)$$

It is known that

$$\ell^2(\Omega) = \overline{c^{(\infty)}(\Omega)}^{\|\cdot\|_{\ell^2(\Omega)}}. \quad (1.34)$$

The norm  $\|\cdot\|_{\ell^2(\Omega)}$  may be estimated by

$$\|f\|_{\ell^2(\Omega)} \leq \sqrt{4\pi} \|f\|_{c(\Omega)}, \quad f \in c(\Omega). \quad (1.35)$$

Any function  $f \in c^{(0)}(\Omega)$  can be decomposed into the normal and tangential components using the operators  $p_{nor}$  and  $p_{tan}$  defined by

$$p_{nor}(f(\xi)) = (f(\xi) \cdot \xi)\xi, \quad (1.36)$$

$$p_{tan}(f(\xi)) = f(\xi) - p_{nor}(f(\xi)), \quad (1.37)$$

respectively.

As an immediate consequence we are able to define

$$\ell_{nor}^2(\Omega) = \{p_{nor}(f) \mid f \in \ell^2(\Omega)\}, \quad (1.38)$$

$$\ell_{tan}^2(\Omega) = \{p_{tan}(f) \mid f \in \ell^2(\Omega)\}. \quad (1.39)$$

In consequence,

$$\ell^2(\Omega) = \ell_{nor}^2(\Omega) \oplus \ell_{tan}^2(\Omega). \quad (1.40)$$

**Definition 1.1** Let  $F$  be of class  $C^{(0_i)}(\Omega)$ ,  $i \in \{1, 2, 3\}$ , where

$$0_i = \begin{cases} 0 & \text{if } i = 1 \\ 1 & \text{if } i = 2, 3. \end{cases}$$

Then the operators  $o^{(i)} : C^{(0_i)}(\Omega) \longrightarrow c(\Omega)$ , respectively, are defined by

$$o_\xi^{(1)}F(\xi) = \xi F(\xi), \quad i = 1,$$

$$o_\xi^{(2)}F(\xi) = \nabla^*F(\xi), \quad i = 2,$$

$$o_\xi^{(3)}F(\xi) = \xi \wedge \nabla^*F(\xi) = L_\xi^*F(\xi), \quad i = 3,$$

$\xi \in \Omega$ .

It is clear that  $o_\xi^{(1)}F(\xi)$  is a radial vector field, while  $o_\xi^{(2)}F(\xi)$  and  $o_\xi^{(3)}F(\xi)$  are tangential.

As it is well-known (cf. [30]), any function  $f \in c^{(1)}(\Omega)$  can be represented in the form

$$f(\xi) = \xi F_1(\xi) + \nabla^*F_2(\xi) + L_\xi^*F_3(\xi), \quad x \in \Omega \quad (1.41)$$

with appropriately defined functions  $F_i : \Omega \longrightarrow \mathbb{R}$ .

The space of square-integrable vector valued functions defined on  $\Omega_{int}$  is denoted by  $\ell^2(\Omega_{int})$ . Thus, the space  $\ell^2(\Omega_{int})$  is a Hilbert space equipped with the inner product

$$\langle f, g \rangle_{\ell^2(\Omega_{int})} = \int_{\Omega_{int}} f(x) \cdot g(x) \, d\omega(x) \quad f, g \in \ell^2(\Omega_{int}). \quad (1.42)$$

Moreover, for all  $\mathcal{K} \subset \mathbb{R}^3$ ,  $c^{(k)}(\mathcal{K})$ ,  $0 \leq k \leq \infty$ , consists of all  $k$ -times continuously differentiable vector valued functions defined on  $\mathcal{K}$ . Conventionally,  $c(\mathcal{K}) = c^{(0)}(\mathcal{K})$ .

Accordingly,

$$\|f\|_{c(\mathcal{K})} = \sup_{x \in \mathcal{K}} |f(x)|, \quad f \in c(\mathcal{K}). \quad (1.43)$$

Now we recapitulate some concepts of vector spherical harmonics as given in the monograph [30].

**Definition 1.2** *Let  $Y_n$  be a scalar spherical harmonic of degree  $n$ , i.e.  $Y_n \in \text{Harm}_n(\Omega)$ . Let  $o^{(i)}$ ,  $i = 1, 2, 3$  be defined as above. Then the vector fields  $y_n^{(i)} : \Omega \rightarrow \mathbb{R}^3$  defined by  $y_n^{(i)}(\xi) = o_\xi^{(i)} Y_n(\xi)$ ,  $\xi \in \Omega$ ,  $i = 1, 2, 3$  are called vector spherical harmonics of degree  $n$  and kind  $i$ .*

Let the space of all vector spherical harmonics of degree  $n$  and kind  $i$  be denoted by  $\text{harm}_n^{(i)}(\Omega)$ .

Then we let

$$\text{harm}_{0_i, \dots, n}^{(i)}(\Omega) = \bigoplus_{k=0_i}^n \text{harm}_k^{(i)}(\Omega). \quad (1.44)$$

Consequently, we obtain

$$\ell_{(i)}^2(\Omega) = \overline{\bigoplus_{k=0_i}^{\infty} \text{harm}_k^{(i)}(\Omega)}^{\|\cdot\|_{\ell^2(\Omega)}} \quad (1.45)$$

and

$$\ell^2(\Omega) = \bigoplus_{i=1}^3 \ell_{(i)}^2(\Omega). \quad (1.46)$$

To obtain an orthonormal set of vector spherical harmonics (in  $\ell^2(\Omega)$ –sense) we choose the coefficients of normalization as

$$\mu_n^{(i)} = \begin{cases} 1 & \text{if } i = 1 \\ n(n+1) & \text{if } i = 2, 3. \end{cases} \quad (1.47)$$

Considering these coefficients we are able to construct the vector field  $y_{n,j}^{(i)}$  of the form

$$y_{n,j}^{(i)}(\xi) = (\mu_n^{(i)})^{-\frac{1}{2}} o_\xi^{(i)} Y_{n,j}(\xi), \quad i = 1, 2, 3, \quad n = 0_i, 0_i + 1, \dots, \quad j = 1, 2, \dots, 2n + 1,$$

which form an orthonormal set in the sense that

$$\int_{\Omega} y_{n,j}^{(i)}(\xi) \cdot y_{n',j'}^{(i')}(\xi) d\omega(\xi) = \delta_{n,n'} \delta_{j,j'} \delta_{i,i'}. \quad (1.48)$$

Now we come to another important result on vector spherical harmonics (proved in [30]).

**Theorem 1.2** *The system of vector spherical harmonics  $\{y_{n,j}^{(i)}, i = 1, 2, 3, n = 0_i, 0_i + 1, \dots, j = 1, 2, \dots, 2n + 1\}$  is closed in  $c(\Omega)$  and complete in  $\ell^2(\Omega)$  with respect to the corresponding norms.*

More precisely,

$$\ell^2(\Omega) = \overline{\text{span}\{y_{n,j}^{(i)}\}}^{\|\cdot\|_{\ell^2(\Omega)}}. \quad (1.49)$$

Furthermore, any  $f \in \ell^2(\Omega)$  can be represented in  $\|\cdot\|_{\ell^2(\Omega)}$ -sense by its Fourier series

$$f = \sum_{i=1}^3 \sum_{n=0_i}^{\infty} \sum_{j=1}^{2n+1} (f^{(i)})^{\wedge}(n, j) y_{n,j}^{(i)}, \quad (1.50)$$

where

$$(f^{(i)})^{\wedge}(n, j) = \int_{\Omega} f(\xi) \cdot y_{n,j}^{(i)}(\xi) d\omega(\xi). \quad (1.51)$$

For our purposes, it is worth to consider the addition theorem for vector spherical harmonics (see [30]).

Let  $f : \Omega \rightarrow \mathbb{R}^3$  be a smooth vector field of the form

$$f(\xi) = \sum_{k=1}^3 F_k(\xi) \epsilon^k. \quad (1.52)$$

By applying the operator  $o^{(i)}$  on each component of  $f$ ,  $o^{(i)}f$  can be defined as

$$o_{\xi}^{(i)} f = o_{\xi}^{(i)} \sum_{k=1}^3 F_k(\xi) \epsilon^k = \sum_{k=1}^3 (o_{\xi}^{(i)} F_k(\xi)) \otimes \epsilon^k, \quad i = 1, 2, 3. \quad (1.53)$$

This implies that for each  $i$ , the operator  $o^{(i)}$  represents a mapping from vectorial fields to tensorial fields. This property leads [30] to obtain the following explicit formula

$$\begin{aligned} \sum_{j=1}^{2n+1} y_{n,j}^{(i)}(\xi) \otimes y_{n,j}^{(k)}(\eta) &= \sum_{j=1}^{2n+1} \left( (\mu_n^{(i)})^{-\frac{1}{2}} o_{\xi}^{(i)} Y_{n,j}(\xi) \right) \otimes \left( (\mu_n^{(k)})^{-\frac{1}{2}} o_{\eta}^{(k)} Y_{n,j}(\eta) \right) \\ &= (\mu_n^{(i)})^{-\frac{1}{2}} (\mu_n^{(k)})^{-\frac{1}{2}} \sum_{j=1}^{2n+1} o_{\xi}^{(i)} Y_{n,j}(\xi) \otimes o_{\eta}^{(k)} Y_{n,j}(\eta) \\ &= (\mu_n^{(i)})^{-\frac{1}{2}} (\mu_n^{(k)})^{-\frac{1}{2}} o_{\xi}^{(i)} o_{\eta}^{(k)} \sum_{j=1}^{2n+1} Y_{n,j}(\xi) Y_{n,j}(\eta) \\ &= (\mu_n^{(i)})^{-\frac{1}{2}} (\mu_n^{(k)})^{-\frac{1}{2}} o_{\xi}^{(i)} o_{\eta}^{(k)} \frac{2n+1}{4\pi} P_n(\xi \cdot \eta) \\ &= (\mu_n^{(i)})^{-\frac{1}{2}} (\mu_n^{(k)})^{-\frac{1}{2}} \frac{2n+1}{4\pi} o_{\xi}^{(i)} o_{\eta}^{(k)} P_n(\xi \cdot \eta) \\ &= \frac{2n+1}{4\pi} \mathbf{p}_n^{(i,k)}(\xi, \eta). \end{aligned}$$

The last formula is known as the addition theorem for vector spherical harmonics ([30]). The tensorial functions  $\mathbf{p}_n^{(i,k)}(\xi, \eta)$  are called Legendre tensors of degree  $n$  of type  $(i, k)$ . It should be noted that these tensors can be shown to be given in the following form:



**Theorem 1.3**

$$\begin{aligned}
\mathbf{p}_n^{(1,1)}(\xi, \eta) &= P_n(\xi \cdot \eta) \xi \otimes \eta, \quad n \in \mathbb{N}_0, \\
\mathbf{p}_n^{(1,2)}(\xi, \eta) &= \frac{1}{[n(n+1)]^{\frac{1}{2}}} P'_n(\xi \cdot \eta) \xi \otimes [\xi - (\xi \cdot \eta) \eta], \quad n \in \mathbb{N}, \\
\mathbf{p}_n^{(2,1)}(\xi, \eta) &= \frac{1}{[n(n+1)]^{\frac{1}{2}}} P'_n(\xi \cdot \eta) [\eta - (\xi \cdot \eta) \xi] \otimes \eta, \quad n \in \mathbb{N}, \\
\mathbf{p}_n^{(2,2)}(\xi, \eta) &= \frac{1}{[n(n+1)]} \{ P''_n(\xi \cdot \eta) [\eta - (\xi \cdot \eta) \xi] \otimes [\xi - (\xi \cdot \eta) \eta] \\
&\quad + P'_n(\xi \cdot \eta) [\mathbf{i}_{tan}(\xi) - (\eta - (\xi \cdot \eta) \xi) \otimes \eta] \}, \quad n \in \mathbb{N}, \\
\mathbf{p}_n^{(2,3)}(\xi, \eta) &= \frac{1}{[n(n+1)]} \{ P''_n(\xi \cdot \eta) [\eta - (\xi \cdot \eta) \xi] \otimes [\eta \wedge \xi] \\
&\quad + P'_n(\xi \cdot \eta) [-\mathbf{j}_{tan}(\eta) - \xi \otimes \eta \wedge \xi] \}, \quad n \in \mathbb{N}, \\
\mathbf{p}_n^{(3,2)}(\xi, \eta) &= \frac{1}{[n(n+1)]} \{ P''_n(\xi \cdot \eta) [(\xi \wedge \eta) \otimes (\xi - (\xi \cdot \eta) \eta)] \\
&\quad + P'_n(\xi \cdot \eta) [\mathbf{j}_{tan}(\xi) - \xi \wedge \eta \otimes \eta] \}, \quad n \in \mathbb{N}, \\
\mathbf{p}_n^{(3,3)}(\xi, \eta) &= \frac{1}{[n(n+1)]} \{ P''_n(\xi \cdot \eta) [\xi \wedge \eta] \otimes [\eta \wedge \xi] \\
&\quad + P'_n(\xi \cdot \eta) [(\xi \cdot \eta)(\mathbf{i}_3 - \xi \otimes \xi) - (\eta - (\xi \cdot \eta) \xi) \otimes \xi] \}, \quad n \in \mathbb{N},
\end{aligned}$$

where we have used the abbreviations

$$\begin{aligned}
\mathbf{i}_3 &= \begin{pmatrix} 1 & 0 & 0 \\ 0 & 1 & 0 \\ 0 & 0 & 1 \end{pmatrix}, \\
\mathbf{i}_{tan}(\xi) &= \mathbf{i}_3 - \xi \otimes \xi, \\
\mathbf{j}_{tan}(\xi) &= \sum_{i=1}^3 (\xi \wedge \epsilon^i) \otimes \epsilon^i, \quad \xi, \eta \in \Omega.
\end{aligned}$$

As a consequence, the addition theorem (cf. [30]) may be used to represent any vector spherical function  $f \in \ell^2(\Omega)$  by means of Legendre tensors. To be more concrete, any function  $f \in \ell^2(\Omega)$  can be represented in  $\ell^2(\Omega)$ -sense as follows:

$$\begin{aligned}
f &= \sum_{i=1}^3 \sum_{n=0_i}^{\infty} \sum_{j=1}^{2n+1} (f^{(i)})^{\wedge}(n, j) y_{n,j}^{(i)} \\
&= \sum_{i=1}^3 \sum_{n=0_i}^{\infty} \sum_{j=1}^{2n+1} \int_{\Omega} f(\xi) \cdot y_{n,j}^{(i)}(\xi) d\omega(\xi) y_{n,j}^{(i)} \\
&= \sum_{i=1}^3 \sum_{n=0_i}^{\infty} \sum_{j=1}^{2n+1} \int_{\Omega} y_{n,j}^{(i)}(\cdot) \otimes y_{n,j}^{(i)}(\xi) f(\xi) d\omega(\xi)
\end{aligned}$$

$$\begin{aligned}
&= \sum_{i=1}^3 \sum_{n=0_i}^{\infty} \sum_{j=1}^{2n+1} \int_{\Omega} y_{n,j}^{(i)}(\cdot) \otimes y_{n,j}^{(i)}(\xi) f(\xi) d\omega(\xi) \\
&= \sum_{i=1}^3 \sum_{n=0_i}^{\infty} \int_{\Omega} \frac{2n+1}{4\pi} \mathbf{P}_n^{(i,i)}(\cdot, \xi) f(\xi) d\omega(\xi).
\end{aligned}$$

This representation provides us a certain approximate identity for  $\ell^2(\Omega)$ -functions. Roughly speaking, this tells us how a reproducing kernel structure can be used to establish wavelets via a spectral approach. In Chapter 5 we discuss those topics in detail.

## 1.4 Regular Surfaces

A surface  $\Sigma \subset \mathbb{R}^3$  is called *regular* (cf. [26]) if it satisfies the following properties:

- (i)  $\Sigma$  divides  $\mathbb{R}^3$  uniquely into the bounded region  $\Sigma_{int}$  (*inner space*) and the unbounded region  $\Sigma_{ext}$  (*outer space*) given by  $\Sigma_{ext} = \mathbb{R}^3 \setminus \overline{\Sigma_{int}}$ ,  $\overline{\Sigma_{int}} = \Sigma_{int} \cup \Sigma$ ,
- (ii)  $\Sigma$  is a closed and compact surface free of double points,
- (iii)  $\Sigma_{int}$  contains the origin,
- (iv)  $\Sigma$  is locally of class  $C^{(2)}$ .

Given a regular surface then there exist positive constants  $\alpha$  and  $\beta$  such that

$$\alpha < \sigma^{\inf} = \inf_{x \in \Sigma} |x| \leq \sup_{x \in \Sigma} |x| = \sigma^{\sup} < \beta. \quad (1.54)$$

$\Omega_{\alpha}$  and  $\Omega_{\beta}$  denote the spheres of radii  $\alpha$  and  $\beta$ , respectively. As usual,  $\Omega_{\beta}^{int}, \Omega_{\beta}^{ext}$  (and  $\Omega_{\alpha}^{int}, \Omega_{\alpha}^{ext}$ ) denote the inner and outer spaces of  $\Omega_{\beta}$  (and  $\Omega_{\alpha}$ ), respectively.

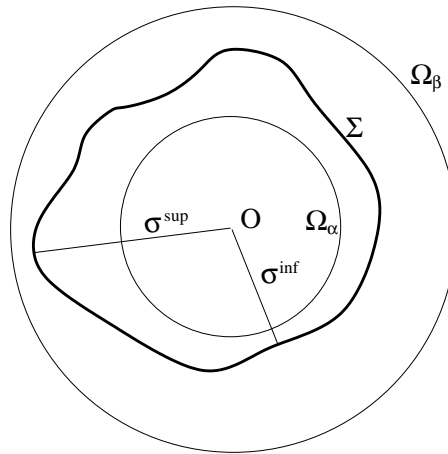


Figure 1.1: An illustration of a regular surface.

A vector field  $f$  defined on  $\Sigma$  possessing  $k$  continuous derivatives is said to be of class  $c^{(k)}(\Sigma)$ ,  $0 \leq k < \infty$ . As usual,  $c^{(0)}(\Sigma)$  ( $= c(\Sigma)$ ) is the class of continuous vector fields  $f$  defined on  $\Sigma$ . The space  $c(\Sigma)$  is a complete normed space endowed with the norm  $\|f\|_{c(\Sigma)} = \sup_{x \in \Sigma} |f(x)|$ . In  $c(\Sigma)$  we have the inner product  $\langle \cdot, \cdot \rangle_{\ell^2(\Sigma)}$  equipped with the norm

$$\|f\|_{\ell^2(\Sigma)} = \left( \int_{\Sigma} |f(x)|^2 d\omega(x) \right)^{\frac{1}{2}}, \quad (1.55)$$

where  $d\omega$  represents the surface element on  $\Sigma$ . Furthermore, for each  $f \in c(\Sigma)$ , we have the norm-estimate

$$\|f\|_{\ell^2(\Sigma)} \leq \sqrt{\|\Sigma\|} \|f\|_{c(\Sigma)}, \quad \|\Sigma\| = \int_{\Sigma} d\omega. \quad (1.56)$$

By  $\ell^2(\Sigma)$  we denote the space of (Lebesgue) square-integrable vector fields on  $\Sigma$ . It is known that  $\ell^2(\Sigma)$  is a Hilbert space with respect to the inner product  $\langle \cdot, \cdot \rangle_{\ell^2(\Sigma)}$  and a Banach space with respect to  $\|\cdot\|_{\ell^2(\Sigma)}$ .  $\ell^2(\Sigma)$  is the completion of  $c(\Sigma)$  with respect to the norm  $\|\cdot\|_{\ell^2(\Sigma)}$ , i.e.

$$\ell^2(\Sigma) = \overline{c(\Sigma)}^{\|\cdot\|_{\ell^2(\Sigma)}}. \quad (1.57)$$

## 1.5 Mathematical Subjects of Elasticity

In what follows we briefly motivate the Cauchy-Navier equation in linear elastostatics in terms of displacements, where the media are assumed to be homogeneous and isotropic.

### 1.5.1 Formulation of the Equations in Elasticity

First we recapitulate some results known from the theory of elasticity: we will always regard the inner space  $\Sigma_{int}$  of a closed surface  $\Sigma$  as a fixed reference configuration of a body. By a *deformation* of  $\overline{\Sigma_{int}}$  we mean a one-to-one  $c^1$ -function  $z : \overline{\Sigma_{int}} \rightarrow \mathbb{R}^3$  such that  $\det(\nabla \otimes z) > 0$ . The function  $u : \overline{\Sigma_{int}} \rightarrow \mathbb{R}^3$ , defined by  $u(x) = z(x) - x$ ,  $x \in \overline{\Sigma_{int}}$ , is called the *displacement* of  $\overline{\Sigma_{int}}$  relative to the deformation  $z$ . The tensor field  $(\nabla \otimes u)(x)$  is called the *displacement gradient*. The *(infinitesimal) strain tensor* is defined by  $\mathbf{e} = \frac{1}{2}((\nabla \otimes u) + (\nabla \otimes u)^T)$  as the symmetric part of the *displacement gradient*, while the antisymmetric part is used to define the *(infinitesimal) rotation tensor*  $\mathbf{d}$  as  $\mathbf{d} = \frac{1}{2}((\nabla \otimes u) - (\nabla \otimes u)^T)$ . While  $\mathbf{d}$  describes a 'rigid' displacement field,  $\mathbf{e}$  is responsible for the 'non-rigid' displacements. According to Kirchhoff's Theorem (see, for example, [64]) two displacement fields  $u$  and  $u'$  corresponding to the same strain field imply  $u = u' + w$  where  $w$  is a rigid displacement field. One calls  $\text{trace}(\mathbf{e}) = \nabla \cdot u$  the *(elastic) dilatation*. Thus the dilatation is determined by the diagonal elements of  $\mathbf{e}$ , the remaining elements of  $\mathbf{e}$  prescribe torsions. Every displacement field  $u$  can be decomposed into a pure torsion  $u_T$  (i.e.  $\nabla \cdot u_T = 0$ ) and a pure dilatation  $u_D$  (i.e.,  $\nabla \wedge u_D = 0$ ) so that  $u = u_T + u_D$ .

An elastic body in a strained configuration performs by definition a tendency of recovering its original form: this tendency is materialized by a field of forces on each part of the body by the other parts. This field of internal forces called (elastic) *stress*, is due to the interaction of the molecules of the body which have been removed from their relative position of equilibrium and to recover it, following the principle of action and interaction. If  $x$  is a point of a (regular) surface element in  $\Sigma_{int}$  with unit normal  $\nu$ , then the *stress vector*  $s_\nu(x) = T_\nu(u)(x)$  is the force per unit area at  $x$  exerted by the portion of  $\Sigma_{int}$  on the side of the surface element in  $\Sigma_{int}$  towards  $\nu(x)$  on the portion of  $\Sigma_{int}$  on the other side. For time-independent behaviour and in the absence of body stress fields there exists a symmetric tensor field  $\mathbf{s}$ , called *stress tensor field*, such that  $s_\nu = \mathbf{s}\nu$  for each vector  $\nu$  and  $\nabla(\mathbf{s}a) = 0$  for each fixed  $a \in \mathbb{R}^3$  (for more details see, for example, [46],[58],[80]).

Hooke's law relates the stress to strain, i.e. linear elasticity of the body implies that for each  $x \in \Sigma_{int}$  there exists a linear transformation  $\mathbf{c}$  from the space of all tensors into the space of all symmetric tensors such that  $\mathbf{s} = \mathbf{c}\mathbf{e}$ . Consequently, the linear theory of elasticity is based on the *strain-displacement* relation

$$\mathbf{e} = \frac{1}{2}((\nabla \otimes u) + (\nabla \otimes u)^T), \quad (1.58)$$

the *stress-strain* relation

$$\mathbf{s} = \mathbf{c}\mathbf{e} \quad (1.59)$$

and the *equation of equilibrium*

$$\nabla \cdot \mathbf{s} + b = 0, \quad (1.60)$$

where the divergence is applied on each column of the tensor  $\mathbf{s}$  and  $b$  is the body force field in  $\Sigma_{int}$ .

The above equations imply the *displacement equation of equilibrium* in  $\Sigma_{int}$

$$\nabla \cdot \mathbf{c}(\nabla \otimes u) + b = 0. \quad (1.61)$$

For given  $\mathbf{c}$  and  $b$ , this is a coupled linear system of partial differential equations for the fields  $u$ ,  $\mathbf{e}$  and  $\mathbf{s}$ . If the material is *isotropic*,  $\mathbf{c}$  is given by

$$\mathbf{c}\mathbf{e} = 2\mu\mathbf{e} + \lambda(\text{trace } \mathbf{e})\mathbf{i}_3, \quad (1.62)$$

where the scalars  $\lambda$  and  $\mu$  are called the Lamé moduli and  $\mathbf{i}_3$  is the identity matrix of order 3. Moreover, if the material is *homogeneous*,  $\lambda$  and  $\mu$  are constants (typical requirements imposed on  $\lambda$  and  $\mu$  are  $\mu > 0$ ,  $3\lambda + 2\mu > 0$  (see, for example, [57])). Therefore, in the homogeneous isotropic case, observing the identities (see, for example, [34])

$$\nabla \cdot (\mu(\nabla \otimes u)) = \mu\Delta u, \quad \nabla \cdot (\mu(\nabla \otimes u)^T) = 0, \quad \nabla \cdot (\lambda(\nabla \cdot u)\mathbf{i}) = \lambda\nabla(\nabla \cdot u), \quad (1.63)$$

we are led to the displacement equation of equilibrium in the form

$$\mu\Delta u + (\lambda + \mu)\nabla(\nabla \cdot u) + b = 0. \quad (1.64)$$

Finally, assuming that the body force field  $b$  vanishes, this equation can be reduced to the so-called *Cauchy-Navier equation* in  $\Sigma_{int}$

$$\mu \Delta u + (\lambda + \mu) \nabla \nabla u = 0. \quad (1.65)$$

This equation plays the same role in the theory of elasticity as the Laplace equation in the theory of harmonic functions and it formally reduces to it for  $\mu = 1$ ,  $\lambda = -1$ . The Cauchy-Navier equation allows an equivalent formulation in  $\Sigma_{int}$

$$\Delta u + \sigma \nabla \nabla \cdot u = 0, \quad (1.66)$$

where  $\sigma = (1 - 2\rho)^{-1}$ ,  $\rho = \lambda/2(\lambda + \mu)$ ,  $\mu \neq 0$ .  $\rho$  is the Poisson ratio. Equation (1.65) represents a coupled linear system of elliptic partial differential equations. For simplicity we let

$$\Diamond u = \mu \Delta u + (\lambda + \mu) \nabla \nabla u = 0, \quad (1.67)$$

in  $\Sigma_{int}$ . It is easy to show that the displacement field  $u$  is biharmonic and its divergence and curl are harmonic. This yields a deep relation between linear elasticity and potential theory (see, for example, [58]).

### 1.5.2 Boundary-value Problems of Classical Elasticity

The problems in elasticity consist of finding the stress and the displacement in an elastic body subject to surface forces, surface displacement and body forces. Particularly, the problem determining the displacements in  $\Sigma_{int} \subset \mathbb{R}^3$  subject to a given state of displacement on the boundary  $\Sigma$  is known as the inner displacement boundary-value problem. More precisely, we seek a vector valued function  $u : \Sigma_{int} \rightarrow \mathbb{R}^3$  such that the displacement field  $u$  satisfies the given boundary conditions  $f$  on  $\Sigma$ , i.e.  $u|_{\Sigma} = f$ . Subject to certain restrictions on the nature of the solution, the surface  $\Sigma$  and also the form of boundary conditions, the existence and the uniqueness of the problem is assured (cf. [58],[61]).

In solving boundary-value problems of elasticity, a variety of methods can be found in literature. Some of these methods depend primarily on intuition, while others are based on a systematic application of the techniques of applied mathematics. Roughly speaking, some of those methods are the inverse method, the method of potentials ([42],[58]), Betti's method, the integral transform methods ([79]), the complex variable methods ([23]), the variational methods, ([74],[76],[84]) and the Runge approximations ([5],[26],[27],[37]). Several investigations on those methods can be found in literature, for example, [58],[65],[75].

The solution of the interior boundary-value problem is of practical significance in several fields. For example, in geosciences, the analysis of elastic crustal deformation in a particular area can be modelled by the surface displacements. Moreover, this linear elastostatic Cauchy-Navier approach can be used to describe the deformation of an elastic plate of a particular thickness, such as tectonic plates (or Earth's crust itself) undergoing movements in response to the forces and loads (see, for example, [67],[71]). From

---

the mathematical point of view, once the boundary displacement vectors on an arbitrary but smooth bounded surface (the so-called regular surface of our consideration) has been given, the displacement problem is uniquely solvable (cf. [37]). However, in the most real problems the boundary functions cannot be expected to be available in closed forms. Instead, methods defined on a discrete pointset requiring computational numerical treatments are essential.

# Chapter 2

## Potential Methods for the Cauchy-Navier Equation

In what follows, the classical single- and double- layer potentials are considered in elastostatics. More accurately, we discuss three types of potential operators, namely, single layer, double layer and the derivative of single layer operators defined on a regular surface  $\Sigma$ . The well-known limit and jump relations are established (cf. [37],[58]). Moreover, in addition to the classical approach, we extend all the limit and jump relations to the dual case.

### 2.1 Elastic Potentials on Regular Surfaces

The set  $pot(\Sigma_{int})$  (more precisely,  $pot_{\lambda,\mu}(\Sigma_{int})$ ) denotes the space of (elastic) potentials  $u \in c^{(2)}(\Sigma_{int})$  satisfying the Cauchy-Navier equation  $\mu\Delta u + (\lambda + \mu)\nabla\nabla u = 0$  in  $\Sigma_{int}$  (with  $\lambda, \mu$  being fixed) ([37]). With  $pot(\overline{\Sigma_{int}})$  we denote the space of all vector fields  $u : \overline{\Sigma_{int}} \rightarrow \mathbb{R}^3$  satisfying the properties

- (i)  $u$  is of class  $c(\overline{\Sigma_{int}})$ ,
- (ii)  $u|_{\Sigma_{int}} \in pot(\Sigma_{int})$ .

Note that

$$\overline{pot(\overline{\Sigma_{int}})}|_{\Sigma}^{\|\cdot\|_{c^{(0)}(\Sigma)}} = c^{(0)}(\Sigma). \quad (2.1)$$

Moreover, the set  $pot(\Sigma_{ext})$  denotes the space of all vector fields  $u \in c^{(2)}(\Sigma_{ext})$  satisfying the Cauchy-Navier equation in  $\Sigma_{ext}$  and being regular at infinity, i.e.  $|u(x)| = o(1)$  (cf. [34]).

## 2.2 A Cauchy-Navier Vector Field Associated to Vector Harmonics

Let  $\Omega_R$  be the sphere of radius  $R$ . It is well known (see, for example, [37]) that any vector field  $h \in c(\Omega_R^{int})$  with  $\Delta h = 0$  in  $\Omega_R^{int}$  can be represented as series expansion in terms of the vector harmonics  $H_{n,j}\epsilon^k$ ,  $n = 0, 1, \dots, j = 1, 2, \dots, 2n+1$ ,  $k = 1, 2, 3$ , with  $H_{n,j}(x) = |x|^n Y_{n,j}(\xi)$ ,  $x = |x|\xi$ ,  $n = 0, 1, 2, \dots, j = 1, 2, \dots, 2n+1$  so that

$$h(x) = \sum_{n=0}^{\infty} \sum_{j=1}^{2n+1} \sum_{k=1}^3 b_{n,j}^{(k)} H_{n,j} \epsilon^k, \quad (2.2)$$

where

$$b_{n,j}^{(k)} |x|^n = \int_{\Omega} (h(|x|\xi) \cdot \epsilon^k) H_{n,j}(\xi) d\omega(\xi). \quad (2.3)$$

In other words, assuming that  $u \in c(\Omega_R^{int})$  with  $\diamond u(x) = 0$  in  $\Omega_R^{int}$ , i.e.  $u \in pot(\overline{\Omega_R^{int}})$ , we have

$$\diamond(u(x) + \frac{\lambda + \mu}{2\mu}(\nabla \cdot u(x))x) = 0 \quad \text{for all } x \in \Omega_R. \quad (2.4)$$

Moreover, for a given field  $u \in c^{(2)}(\Omega_R^{int})$  with  $\Delta h(x) = 0$  the equation

$$h(x) = u(x) + \frac{\lambda + \mu}{2\mu}(\nabla \cdot u(x))x = 0 \quad (2.5)$$

is uniquely solvable such that  $\diamond u = 0$  in  $\Omega_R^{int}$  (cf. [5],[37]). More explicitly,

$$u(x) = h(x) - \left( \frac{1}{|x|^\gamma} \int_{\rho=0}^{|x|} \rho^\gamma (\nabla \cdot h(x))|_{x=\rho\xi} d\rho \right) x, \quad (2.6)$$

where we used the abbreviations

$$\gamma = \frac{1 + 2\alpha}{\alpha}, \quad \alpha = \frac{\lambda + \mu}{2\mu}.$$

Hence, to any vector harmonic  $H_{n,j}\epsilon^k$ , there exists a uniquely defined vector field  $u_{n,j}^{(k)}$  such that  $\diamond u_{n,j}^{(k)} = 0$ , namely,

$$u_{n,j}^{(k)}(x) = H_{n,j}(x)\epsilon^k - \frac{\lambda + \mu}{(n+2)\lambda + (n+4)\mu}(\nabla H_{n,j}(x) \cdot \epsilon^k)x. \quad (2.7)$$

Consequently, any vector field  $u \in pot(\Omega_R^{int})$  can be represented by the series expansion

$$u(x) = \sum_{n=0}^{\infty} \sum_{j=1}^{2n+1} \sum_{k=1}^3 c_{n,j}^{(k)} u_{n,j}^{(k)}(x), \quad x \in \Omega_R^{int}, \quad (2.8)$$

where

$$c_{n,j}^{(k)} |x|^n = \int_{\Omega} \left( \left( u(x) + \frac{\lambda + \mu}{2\mu}(\nabla \cdot u(x))x \right) \Big|_{x=|x|\xi} \right) H_{n,j}(\xi) d\omega(\xi). \quad (2.9)$$

It is not difficult to see that the right hand side of (2.8) is convergent in  $\ell^2(\Omega_R)$  and absolutely and uniformly convergent in  $\ell^2(\Omega_R^{int})$  ([37]).



## 2.3 Layer Potential Operators on Regular Surfaces

At each point  $x$  of a regular surface  $\Sigma$  we can construct a normal  $\nu(x)$  pointing into the outer space  $\Sigma_{ext}$ . The set

$$\Sigma(\tau) = \{x_\tau \in \mathbb{R}^3 \mid x_\tau = x + \tau\nu(x), \quad x \in \Sigma\}, \quad (2.10)$$

generates a *parallel surface* which is exterior to surface  $\Sigma$  for  $\tau > 0$  and interior for  $\tau < 0$ . If  $|\tau|$  is sufficiently small the parallel surface is regular and the normal to one parallel surface is normal to the other parallel surface. More precisely, it is known from [68] that for a given regular surface  $\Sigma$  there exists a real number  $\bar{\tau} > 0$  such that each parallel surface  $\Sigma(\tau)$  represents a regular surface for each  $\tau$  with  $0 < \tau < \bar{\tau}$  in the sense as defined in Section 1.4. This is the reason why, in case of dual layer potentials, the parameter  $\tau$  is chosen such that  $\tau < \bar{\tau}$ . Moreover, it should be remarked that for larger values of  $\tau$ ,  $\Sigma(\tau)$  may not represent, in general, a regular surface.

The matrix  $\mathbf{\Gamma}(x)$ ,  $x \in \mathbb{R}^3$  with  $|x| \neq 0$ , given by

$$\mathbf{\Gamma}(x) = \frac{\lambda + 3\mu}{2\mu(\lambda + 2\mu)} \left( (\epsilon^i \cdot \epsilon^k + \frac{(\lambda + \mu)(x \cdot \epsilon^i)(x \cdot \epsilon^k)}{\lambda + 3\mu} \frac{1}{|x|^2}) \frac{1}{|x|} \right)_{i,k=1,2,3} \quad (2.11)$$

is constituted by the so-called fundamental solutions  $\Gamma_k(x) = \mathbf{\Gamma}(x)\epsilon^k$ ,  $k = 1, 2, 3$ , associated to the operator  $\diamond$  (cf. [58]).

Equivalently, the right hand side of (2.11) can be represented as

$$\mathbf{\Gamma}(x) = \frac{\lambda + 3\mu}{2\mu(\lambda + 2\mu)} \left( \frac{\mathbf{i}_3}{|x|} + \frac{(\lambda + \mu)(x \otimes x)}{\lambda + 3\mu} \frac{1}{|x|^3} \right). \quad (2.12)$$

The differential operator

$$n = \frac{1}{\lambda + 3\mu} \left( 2\mu(\lambda + 2\mu) \frac{\partial}{\partial \nu} + (\lambda + \mu)(\lambda + 2\mu)\nu \nabla + \mu(\lambda + \mu)\nu \times \nabla \times \right) \quad (2.13)$$

is called the *(pseudo-)stress operator*. Furthermore,  $n_x \Gamma_k(x)$ ,  $x \in \mathbb{R}^3$  with  $|x| \neq 0$ , is given by

$$n_x \Gamma_k(x) = \left( \frac{\partial}{\partial \nu(x)} \frac{1}{|x|} \right) \Lambda_k(x), \quad (2.14)$$

where

$$\Lambda_k(x) = \frac{2\mu}{\lambda + 3\mu} \left( \epsilon^k + \frac{3(\lambda + \mu)}{2\mu} \frac{(\epsilon^k \cdot x)x}{|x|^2} \right), \quad k = 1, 2, 3. \quad (2.15)$$

We let

$$\mathbf{\Lambda}(x) = (\Lambda_i(x) \cdot \epsilon^k)_{i,k}, \quad i, k = 1, 2, 3. \quad (2.16)$$

It should be recapitulated that the boldface capital (Greek) letters are used to denote the tensor-valued kernels  $\mathbf{\Gamma}$  and  $\mathbf{\Lambda}$ .

We introduce  $\mathbf{p}(\tau)$ ,  $\mathbf{p}_n(\tau)$  and  $\mathbf{n}_p(\tau)$  as the operators of the single, double and the  $n$ -derivative of the single layer potential, respectively.

$$\mathbf{p}(\tau)g(x) = \int_{\Sigma} \Gamma(x_{\tau} - y)g(y) d\omega(y) \quad (2.17)$$

$\mathbf{p}(\tau)$  : operator of the *single layer potential* on  $\Sigma$  for values on  $\Sigma(\tau)$ ,

$$\mathbf{p}_n(\tau)g(x) = \int_{\Sigma} \left( \frac{\partial}{\partial \nu(y)} \frac{1}{|x_{\tau} - y|} \right) \Lambda(x_{\tau} - y)g(y) d\omega(y) \quad (2.18)$$

$\mathbf{p}_n(\tau)$  : operator of the *double layer potential* on  $\Sigma$  for values on  $\Sigma(\tau)$ ,

$$\begin{aligned} \mathbf{n}_p(\tau)g(x) &= \int_{\Sigma} \left( \frac{\partial}{\partial \nu(x)} \frac{1}{|x_{\tau} - y|} \right) \Lambda(x_{\tau} - y)g(y) d\omega(y) \\ &= n_x \int_{\Sigma} \Gamma(x_{\tau} - y)g(y) d\omega(y) \end{aligned} \quad (2.19)$$

$\mathbf{n}_p(\tau)$  :  $n$ -derivative of the *single layer potential* on  $\Sigma$  for values on  $\Sigma(\tau)$ .

The operators  $\mathbf{p}(\tau)$ ,  $\mathbf{p}_n(\tau)$ ,  $\mathbf{n}_p(\tau)$  form mappings from  $\ell^2(\Sigma)$  into  $c(\Sigma)$  provided that  $|\tau|$  is sufficiently small. Furthermore, the integrals formally defined by

$$\mathbf{p}(0)g(x) = \int_{\Sigma} \Gamma(x - y)g(y) d\omega(y), \quad (2.20)$$

$$\mathbf{p}_n(0)g(x) = \int_{\Sigma} \left( \frac{\partial}{\partial \nu(y)} \frac{1}{|x - y|} \right) \Lambda(x - y)g(y) d\omega(y), \quad (2.21)$$

$$\mathbf{n}_p(0)g(x) = \int_{\Sigma} \left( \frac{\partial}{\partial \nu(x)} \frac{1}{|x - y|} \right) \Lambda(x - y)g(y) d\omega(y) \quad (2.22)$$

exist and define linear bounded operators  $\mathbf{p}(0)$ ,  $\mathbf{p}_n(0)$ ,  $\mathbf{n}_p(0)$  mapping  $\ell^2(\Sigma)$  into  $c(\Sigma)$ .

Note that a more detailed description of those properties can be found, for example, in [5],[37].

### 2.3.1 Limit and Jump Relations

As mentioned before, the potential operators in elastostatics behave near the boundary much like the ordinary harmonic potential operators (cf. [5],[37],[58]). In particular, *limit formulae* and *jump relations* can be formulated in analogy to the potential theoretical case. To be more explicit, let  $\mathbf{i}$  be the identity operator in  $\ell^2(\Sigma)$ . For all  $\tau > 0$  sufficiently

small the limit operators  $\mathbf{l}_i^\pm(\tau)$ ,  $i = 1, 2, 3$ , and the jump operators  $\mathbf{j}_j(\tau)$ ,  $j = 1, 2, 3, 4, 5$ , are defined by

$$\mathbf{l}_1^\pm(\tau) = \mathbf{p}(\pm\tau) - \mathbf{p}(0), \quad (2.23)$$

$$\mathbf{l}_2^\pm(\tau) = \mathbf{p}_n(\pm\tau) - \mathbf{p}_n(0) \mp 2\pi\mathbf{i}, \quad (2.24)$$

$$\mathbf{l}_3^\pm(\tau) = \mathbf{n}_p(\pm\tau) - \mathbf{n}_p(0) \pm 2\pi\mathbf{i}, \quad (2.25)$$

$$\mathbf{j}_1(\tau) = \mathbf{p}(\tau) - \mathbf{p}(-\tau), \quad (2.26)$$

$$\mathbf{j}_2(\tau) = \mathbf{p}_n(\tau) - \mathbf{p}_n(-\tau) - 4\pi\mathbf{i}, \quad (2.27)$$

$$\mathbf{j}_3(\tau) = \mathbf{n}_p(\tau) - \mathbf{n}_p(-\tau) + 4\pi\mathbf{i}, \quad (2.28)$$

$$\mathbf{j}_4(\tau) = \mathbf{p}_n(\tau) + \mathbf{p}_n(-\tau) - 2\mathbf{p}_n(0), \quad (2.29)$$

$$\mathbf{j}_5(\tau) = \mathbf{n}_p(\tau) + \mathbf{n}_p(-\tau) - 2\mathbf{n}_p(0), \quad (2.30)$$

respectively.

Furthermore, it should be remarked that the first three representations (2.23)-(2.25) are often called limit relations, while the latter five (2.26)-(2.30) are being considered as jump relations.

Then, the classical results of Cauchy-Navier theory (cf. [58]) tell us that, for all  $g \in c(\Sigma)$ ,

$$\lim_{\substack{\tau \rightarrow 0 \\ \tau > 0}} \|\mathbf{l}_i^\pm(\tau)g\|_{c(\Sigma)} = 0, \quad i = 1, 2, 3, \quad (2.31)$$

$$\lim_{\substack{\tau \rightarrow 0 \\ \tau > 0}} \|\mathbf{j}_j(\tau)g\|_{c(\Sigma)} = 0, \quad j = 1, 2, 3, 4, 5. \quad (2.32)$$

In [5],[37] these limit relations are formulated within the  $\ell^2(\Sigma)$ -nomenclature.

**Theorem 2.1** *For all  $g \in \ell^2(\Sigma)$*

$$\lim_{\substack{\tau \rightarrow 0 \\ \tau > 0}} \|\mathbf{l}_i^\pm(\tau)g\|_{\ell^2(\Sigma)} = 0, \quad i = 1, 2, 3, \quad (2.33)$$

and

$$\lim_{\substack{\tau \rightarrow 0 \\ \tau > 0}} \|\mathbf{j}_j(\tau)g\|_{\ell^2(\Sigma)} = 0, \quad j = 1, 2, 3, 4, 5. \quad (2.34)$$

**Proof.** We use a modification of a technique due to Lax [59]. Denote by  $\mathbf{t}(\tau)$  one of the operators  $\mathbf{l}_i^\pm(\tau)$ ,  $i = 1, 2, 3$ ,  $\mathbf{j}_j(\tau)$ ,  $j = 1, 2, 3, 4, 5$ . Let  $\mathbf{t}^*(\tau)$  be the adjoint operator with respect to the inner product  $\langle \cdot, \cdot \rangle_{\ell^2(\Sigma)}$ . According to the Cauchy-Schwarz inequality we find

$$\|\mathbf{t}(\tau)g\|_{\ell^2(\Sigma)}^2 \leq \|g\|_{\ell^2(\Sigma)} \|\mathbf{t}^*(\tau)\mathbf{t}(\tau)\|_{\ell^2(\Sigma)}. \quad (2.35)$$

Therefore, it follows that

$$\begin{aligned} \|\mathbf{t}(\tau)g\|_{\ell^2(\Sigma)}^2 &\leq \|g\|_{\ell^2(\Sigma)}^2 \|\mathbf{t}^*(\tau)\mathbf{t}(\tau)\|_{\ell^2(\Sigma)}^2 \\ &\leq \|g\|_{\ell^2(\Sigma)}^2 \|g\|_{\ell^2(\Sigma)} \|(\mathbf{t}^*(\tau)\mathbf{t}(\tau))^2 g\|_{\ell^2(\Sigma)}. \end{aligned} \quad (2.36)$$

Induction yields that for all  $n \geq 2$ ,

$$\|\mathbf{t}(\tau)g\|_{\ell^2(\Sigma)}^{2^n} \leq \|g\|_{\ell^2(\Sigma)}^{2^n-1} \|(\mathbf{t}^*(\tau)\mathbf{t}(\tau))^{2^{n-1}}g\|_{\ell^2(\Sigma)}. \quad (2.37)$$

Because of the boundedness of the operators  $\mathbf{t}^*(\tau)$  and  $\mathbf{t}(\tau)$  with respect to  $\|\cdot\|_{c(\Sigma)}$  there exists a positive constant  $D$  such that

$$\|\mathbf{t}(\tau)g\|_{\ell^2(\Sigma)}^{2^n} \leq \|\Sigma\| D^{2^n} \|g\|_{\ell^2(\Sigma)}^{2^n-1} \|g\|_{c(\Sigma)}, \quad \|\Sigma\| = \left(\int_{\Sigma} d\omega\right)^{1/2}. \quad (2.38)$$

Thus, for all  $n \geq 2$  and  $g \in c(\Sigma)$  with  $g \neq 0$ , we obtain

$$\frac{\|\mathbf{t}(\tau)g\|_{\ell^2(\Sigma)}}{\|g\|_{\ell^2(\Sigma)}} \leq D \left( \frac{\|\Sigma\| \|g\|_{c(\Sigma)}}{\|g\|_{\ell^2(\Sigma)}} \right)^{2^{-n}}. \quad (2.39)$$

Letting  $n$  tend to infinity we obtain for all  $g \neq 0$

$$\lim_{n \rightarrow \infty} \left( \frac{\|g\|_{c(\Sigma)}}{\|g\|_{\ell^2(\Sigma)}} \right)^{2^{-n}} = 1. \quad (2.40)$$

This shows that  $\|\mathbf{t}(\tau)\|_{\ell^2(\Sigma)} \leq D$  for all  $g \in c(\Sigma)$ . Since  $c(\Sigma)$  is a dense linear subspace of  $\ell^2(\Sigma)$ , we are able to extend the operator  $\mathbf{t}(\tau)$  from  $c(\Sigma)$  to  $\ell^2(\Sigma)$  without enlarging its norm (cf. [2],[37],[60]). Therefore,  $\mathbf{t}(\tau)$  is bounded with respect to  $\|\cdot\|_{\ell^2(\Sigma)}$  and we have

$$\|\mathbf{t}(\tau)\|_{\ell^2(\Sigma)} \leq \sqrt{\|\mathbf{t}(\tau)\|_{c(\Sigma)} \|\mathbf{t}^*(\tau)\|_{c(\Sigma)}}. \quad (2.41)$$

Hence, it follows that  $\|\mathbf{t}(\tau)\|_{\ell^2(\Sigma)} \rightarrow 0$  as  $\tau \rightarrow 0$ ,  $\tau > 0$ .  $\square$

## 2.4 Layer Potentials for the Dual Operators

Using the limit and jump operators for the potentials, i.e.  $\mathbf{p}(\pm\tau)$ ,  $\mathbf{p}_n(\pm\tau)$  and  $\mathbf{n}_p(\pm\tau)$  listed in Section 2.3, we now define the limit and jump relations corresponding to dual operators. Note that a similar consideration for limit and jump relations on dual operators associated to the Laplace has been discussed in [24].

As usual, the dual (adjoint) operators  $\mathbf{p}^*(\tau)$ ,  $\mathbf{p}_n^*(\tau)$  and  $\mathbf{n}_p^*(\tau)$  of the potential operators  $\mathbf{p}(\tau)$ ,  $\mathbf{p}_n(\tau)$  and  $\mathbf{n}_p(\tau)$  are given, respectively, by

$$\langle f, \mathbf{p}(\tau)g \rangle_{\ell^2(\Sigma)} = \langle \mathbf{p}^*(\tau)f, g \rangle_{\ell^2(\Sigma)}, \quad (2.42)$$

$$\langle f, \mathbf{p}_n(\tau)g \rangle_{\ell^2(\Sigma)} = \langle \mathbf{p}_n^*(\tau)f, g \rangle_{\ell^2(\Sigma)}, \quad (2.43)$$

$$\langle f, \mathbf{n}_p(\tau)g \rangle_{\ell^2(\Sigma)} = \langle \mathbf{n}_p^*(\tau)f, g \rangle_{\ell^2(\Sigma)}, \quad (2.44)$$

for  $f, g \in \ell^2(\Sigma)$ .

To obtain the explicit representations for the dual (potential) operators we observe that

$$\begin{aligned}
\langle f, \mathbf{p}(\tau)g \rangle_{\ell^2(\Sigma)} &= \int_{\Sigma} f(x) \cdot \mathbf{p}(\tau)g(x) \, d\omega(x) \\
&= \int_{\Sigma} f(x) \cdot \int_{\Sigma} \mathbf{\Gamma}(x_{\tau} - y)g(y) \, d\omega(y) d\omega(x) \\
&= \int_{\Sigma} \int_{\Sigma} \mathbf{\Gamma}(x_{\tau} - y)g(y) \, d\omega(y) \cdot f(x) \, d\omega(x) \\
&= \int_{\Sigma} \int_{\Sigma} \mathbf{\Gamma}(x_{\tau} - y)f(x) \, d\omega(x) \cdot g(y) \, d\omega(y) \\
&= \langle \int_{\Sigma} \mathbf{\Gamma}(x_{\tau} - \cdot)f(x) \, d\omega(x), g \rangle_{\ell^2(\Sigma)} \\
&= \langle \mathbf{p}^*(\tau)f, g \rangle_{\ell^2(\Sigma)}.
\end{aligned} \tag{2.45}$$

Hence, by virtue of the property  $\mathbf{\Gamma}(x) = \mathbf{\Gamma}(-x)$ , we are able to write

$$\mathbf{p}^*(\tau)g(x) = \int_{\Sigma} \mathbf{\Gamma}(x - y_{\tau})g(y) \, d\omega(y). \tag{2.46}$$

This provides the dual (or adjoint) single layer potential operator  $\mathbf{p}^*(\tau)$  defined on the parallel surface  $\Sigma(\tau)$  for the values on  $\Sigma$ .

Note that Equation (2.46) can also be formulated for the inner parallel surface  $\Sigma(-\tau)$  (by formally replacing  $\tau$  by  $-\tau$ ).

Since the matrix  $\mathbf{\Lambda}$  is symmetric, we use similar arguments as above to derive the explicit forms of  $\mathbf{p}_n^*(\tau)$  and  $\mathbf{n}_p^*(\tau)$ . In detail, we have

$$\begin{aligned}
\langle f, \mathbf{p}_n(\tau)g \rangle_{\ell^2(\Sigma)} &= \int_{\Sigma} f(x) \cdot \mathbf{p}_n(\tau)g(x) \, d\omega(x) \\
&= \int_{\Sigma} f(x) \cdot \int_{\Sigma} \left( \frac{\partial}{\partial \nu(y)} \frac{1}{|x_{\tau} - y|} \right) \mathbf{\Lambda}(x_{\tau} - y)g(y) \, d\omega(y) d\omega(x) \\
&= \int_{\Sigma} \int_{\Sigma} \left( \frac{\partial}{\partial \nu(y)} \frac{1}{|x_{\tau} - y|} \right) \mathbf{\Lambda}(x_{\tau} - y)f(x) \, d\omega(x) \cdot g(y) \, d\omega(y) \\
&= \langle \int_{\Sigma} \left( \frac{\partial}{\partial \nu(\cdot)} \frac{1}{|x_{\tau} - \cdot|} \right) \mathbf{\Lambda}(x_{\tau} - \cdot)f(x) \, d\omega(x), g \rangle_{\ell^2(\Sigma)} \\
&= \langle \mathbf{p}_n^*(\tau)f, g \rangle_{\ell^2(\Sigma)}.
\end{aligned} \tag{2.47}$$

Finally, we obtain

$$\mathbf{p}_n^*(\tau)g(x) = \int_{\Sigma} \left( \frac{\partial}{\partial \nu(x)} \frac{1}{|x - y_{\tau}|} \right) \mathbf{\Lambda}(x - y_{\tau})g(y) \, d\omega(y). \tag{2.48}$$

This provides the dual (or adjoint)  $n$ -derivative of the single layer potential operator  $\mathbf{p}_n^*(\tau)$  defined on the parallel surface  $\Sigma(\tau)$  for the values on  $\Sigma$ .

Finally, we see that

$$\begin{aligned}
\langle f, \mathbf{n}_p(\tau)g \rangle_{\ell^2(\Sigma)} &= \int_{\Sigma} f(x) \cdot \mathbf{n}_p(\tau)g(x) \, d\omega(x) \\
&= \int_{\Sigma} f(x) \cdot \int_{\Sigma} \left( \frac{\partial}{\partial \nu(x)} \frac{1}{|x_{\tau} - y|} \right) \mathbf{\Lambda}(x_{\tau} - y)g(y) \, d\omega(y) d\omega(x) \\
&= \int_{\Sigma} \int_{\Sigma} \left( \frac{\partial}{\partial \nu(x)} \frac{1}{|x_{\tau} - y|} \right) \mathbf{\Lambda}(x_{\tau} - y) f(x) \, d\omega(x) \cdot g(y) \, d\omega(y) \\
&= \langle \int_{\Sigma} \left( \frac{\partial}{\partial \nu(x)} \frac{1}{|x_{\tau} - \cdot|} \right) \mathbf{\Lambda}(x_{\tau} - \cdot) f(x) \, d\omega(x), g \rangle_{\ell^2(\Sigma)} \\
&= \langle \mathbf{p}_n^*(\tau)f, g \rangle_{\ell^2(\Sigma)}. \tag{2.49}
\end{aligned}$$

Hence, we have

$$\mathbf{n}_p^*(\tau)g(x) = \int_{\Sigma} \left( \frac{\partial}{\partial \nu(y)} \frac{1}{|x - y_{\tau}|} \right) \mathbf{\Lambda}(x - y_{\tau})g(y) \, d\omega(y). \tag{2.50}$$

This provides the dual (or adjoint) double layer potential operator  $\mathbf{n}_p^*(\tau)$  defined on the parallel surface  $\Sigma(\tau)$  for the values on  $\Sigma$ .

Finally, we arrive at the following theorem.

**Theorem 2.2** *Suppose that for all  $\tau$  with  $0 < \tau \leq \bar{\tau}$ , the limit operators  $\mathbf{l}_i^{*\pm}(\tau)$ ,  $i = 1, 2, 3$ , and the jump operators  $\mathbf{j}_j^*(\tau)$ ,  $j = 1, 2, 3, 4, 5$ , are defined by*

$$\mathbf{l}_1^{*\pm}(\tau) = \mathbf{p}^*(\pm\tau) - \mathbf{p}^*(0), \tag{2.51}$$

$$\mathbf{l}_2^{*\pm}(\tau) = \mathbf{p}_n^*(\pm\tau) - \mathbf{p}_n^*(0) \mp 2\pi\mathbf{i}, \tag{2.52}$$

$$\mathbf{l}_3^{*\pm}(\tau) = \mathbf{n}_p^*(\pm\tau) - \mathbf{n}_p^*(0) \pm 2\pi\mathbf{i}, \tag{2.53}$$

$$\mathbf{j}_1^*(\tau) = \mathbf{p}^*(\tau) - \mathbf{p}^*(-\tau), \tag{2.54}$$

$$\mathbf{j}_2^*(\tau) = \mathbf{p}_n^*(\tau) - \mathbf{p}_n^*(-\tau) - 4\pi\mathbf{i}, \tag{2.55}$$

$$\mathbf{j}_3^*(\tau) = \mathbf{n}_p^*(\tau) - \mathbf{n}_p^*(-\tau) + 4\pi\mathbf{i}, \tag{2.56}$$

$$\mathbf{j}_4^*(\tau) = \mathbf{p}_n^*(\tau) + \mathbf{p}_n^*(-\tau) - 2\mathbf{p}_n^*(0), \tag{2.57}$$

$$\mathbf{j}_5^*(\tau) = \mathbf{n}_p^*(\tau) + \mathbf{n}_p^*(-\tau) - 2\mathbf{n}_p^*(0). \tag{2.58}$$

Then for all  $g \in c(\Sigma)$ ,

$$\lim_{\substack{\tau \rightarrow 0 \\ \tau > 0}} \|\mathbf{l}_i^{*\pm}(\tau)g\|_{c(\Sigma)} = 0, \quad i = 1, 2, 3, \tag{2.59}$$

$$\lim_{\substack{\tau \rightarrow 0 \\ \tau > 0}} \|\mathbf{j}_j^*(\tau)g\|_{c(\Sigma)} = 0, \quad j = 1, 2, 3, 4, 5, \tag{2.60}$$

and for all  $g \in \ell^2(\Sigma)$ ,

$$\lim_{\substack{\tau \rightarrow 0 \\ \tau > 0}} \|\mathbf{l}_i^{*\pm}(\tau)g\|_{\ell^2(\Sigma)} = 0, \quad i = 1, 2, 3, \quad (2.61)$$

$$\lim_{\substack{\tau \rightarrow 0 \\ \tau > 0}} \|\mathbf{j}_j^*(\tau)g\|_{\ell^2(\Sigma)} = 0, \quad j = 1, 2, 3, 4, 5. \quad (2.62)$$

**Proof.** The cornerstones for the validity of Theorem 2.2 are the boundedness of the dual operators (see, for example, [5]).  $\square$

# Chapter 3

## Existence, Uniqueness and Regularity

### 3.1 Inner Displacement Boundary Value Problem

In the notations given above the homogeneous isotropic elastic displacement boundary-value problem can be formulated as follows (cf. [29]): Given  $f \in c(\Sigma)$ , find a vector field  $u \in \text{pot}(\overline{\Sigma_{int}})$  satisfying the boundary condition  $u|_{\Sigma} = f$ .

As it is well-known, the boundary-value problem has a unique solution (see, for example [57]). In order to prove the existence (cf. [37]) we use the double layer potential

$$\begin{aligned} u(x) &= \mathbf{p}_n(0)g(x) \\ &= \int_{\Sigma} \left( \frac{\partial}{\partial \nu(y)} \frac{1}{|x - y|} \right) \mathbf{\Lambda}(x - y)g(y) d\omega(y), \quad g \in c(\Sigma). \end{aligned} \quad (3.1)$$

Observing the discontinuity of the double layer potential we obtain from (2.24)

$$f(x) = -2\pi g(x) + \int_{\Sigma} \left( \frac{\partial}{\partial \nu(y)} \frac{1}{|x - y|} \right) \mathbf{\Lambda}(x - y)g(y) d\omega(y), \quad (3.2)$$

for all  $x \in \Sigma$ . The resulting integral equation  $-f = (2\pi \mathbf{i} - \mathbf{p}_n(0))g$ ,  $g \in c(\Sigma)$  fulfills all standard Fredholm theorems (see, for example, [52]).

The homogeneous integral equation  $(2\pi \mathbf{i} - \mathbf{p}_n(0))g = 0$  has no solution different from  $g = 0$ . Thus, the solution of the boundary-value problem exists and is representable by a double layer potential as indicated in (3.1). For details the reader is referred to [58]. The operator  $\mathbf{t} = 2\pi \mathbf{i} - \mathbf{p}_n(0)$  and its adjoint operator  $\mathbf{t}^*$  (with respect to the scalar product  $\langle \cdot, \cdot \rangle_{\ell^2(\Sigma)}$ ) form mappings from  $c(\Sigma)$  into  $c(\Sigma)$  which are linear and bounded with respect to the norm  $\| \cdot \|_{c(\Sigma)}$ . The operators  $\mathbf{t}, \mathbf{t}^*$  in  $c(\Sigma)$  are injective and, by the Fredholm alternative, bijective in the Banach space  $c(\Sigma)$ . Consequently, by the open mapping theorem (see, for example, [85]) the operators  $\mathbf{t}^{-1}$ ,  $\mathbf{t}^{*-1}$  are linear and bounded



with respect to  $\|\cdot\|_{c(\Sigma)}$ . Moreover,  $(\mathbf{t}^*)^{-1} = (\mathbf{t}^{-1})^*$ . But this implies that both  $\mathbf{t}^{-1}$  and  $(\mathbf{t}^*)^{-1}$  are bounded with respect to the norm  $\|\cdot\|_{\ell^2(\Sigma)}$  in  $c(\Sigma)$ . As we have shown, for a given  $f \in c(\Sigma)$ , there exists a vector field  $g \in c(\Sigma)$  determined by (3.2) such that  $u$  is representable in the form (3.1). Suppose that  $\mathcal{K}$  is a subset of  $\Sigma_{int}$  with  $\text{dist}(\overline{\mathcal{K}}, \Sigma) > 0$ . Then the Cauchy-Schwarz inequality applied to (3.1) gives for each  $x \in \overline{\mathcal{K}}$

$$|u(x)| \leq \left( \int_{\Sigma} \sum_{k=1}^3 \left| \left( \frac{\partial}{\partial \nu(y)} \frac{1}{|x-y|} \right) \Lambda_k(x-y) \right|^2 d\omega(y) \right)^{\frac{1}{2}} \left( \int_{\Sigma} |g(y)|^2 d\omega(y) \right)^{\frac{1}{2}}. \quad (3.3)$$

But this means that

$$\|u\|_{c(\overline{\mathcal{K}})} = \sup_{x \in \overline{\mathcal{K}}} |u(x)| \leq E \|g\|_{\ell^2(\Sigma)}, \quad (3.4)$$

where

$$E = \sup_{x \in \overline{\mathcal{K}}} \left( \int_{\Sigma} \sum_{k=1}^3 \left| \left( \frac{\partial}{\partial \nu(y)} \frac{1}{|x-y|} \right) \Lambda_k(x-y) \right|^2 d\omega(y) \right)^{\frac{1}{2}}. \quad (3.5)$$

In connection with (3.2) this implies the existence of a positive constant  $B$  (depending on  $\Sigma$  and  $\mathcal{K}$ ) such that

$$\|u\|_{c(\overline{\mathcal{K}})} \leq E \|\mathbf{t}^{-1} f\|_{\ell^2(\Sigma)} \leq B \|f\|_{\ell^2(\Sigma)}. \quad (3.6)$$

Summarizing our result we obtain the following regularity condition.

**Theorem 3.1** *Let  $u$  be a vector field of class  $\text{pot}(\overline{\Sigma_{int}})$  and  $\mathcal{K}$  a subset of  $\Sigma_{int}$  with  $\text{dist}(\overline{\mathcal{K}}, \Sigma) > 0$ . Then*

$$\|u\|_{c(\overline{\mathcal{K}})} \leq B \left( \int_{\Sigma} |u(x)|^2 d\omega(x) \right)^{1/2} = B \|u\|_{\ell^2(\Sigma)}. \quad (3.7)$$

Finally, as in the case of harmonic functions, we are able to formulate an  $\ell^2(\Sigma)$ –regularity theorem associated to the aforementioned boundary-value problem as follows:

**Theorem 3.2** *Let  $u$  be any vector field of class  $\text{pot}(\overline{\Sigma_{int}})$  and  $\mathcal{K}$  a subset of  $\Sigma_{int}$  with  $\text{dist}(\overline{\mathcal{K}}, \Sigma) \geq \rho > 0$ , where  $\rho$  is a sufficiently small real number. Then, there exists a constant  $C = C(\rho, \mathcal{K})$ , such that*

$$\|u\|_{c(\overline{\mathcal{K}})} \leq C \|f\|_{\ell^2(\Sigma)},$$

where  $f = u|_{\Sigma}$ .

The proofs are omitted here, for the details the reader is referred to [37].

### 3.2 $\ell^2(\Sigma)$ –closure of Cauchy-Navier Vector Fields

Our starting point is the construction of an  $\ell^2(\Sigma)$ –basis (cf. [37]).

**Definition 3.1** *A countable system  $\{u_n\} \subset \text{pot}(\overline{\Sigma_{int}})$  is said to be an  $\ell^2(\Sigma)$ –basis system on  $\Sigma$ , if the closure of  $\text{span}\{u_n|_{\Sigma}\}$  is equal to  $\ell^2(\Sigma)$  (understood in the sense of  $\|\cdot\|_{\ell^2(\Sigma)}$ ):*

$$\overline{\text{span}\{u_n|_{\Sigma}\}}^{\|\cdot\|_{\ell^2(\Sigma)}} = \ell^2(\Sigma). \quad (3.8)$$

Assuming that  $\{u_n\}$  possesses the  $\ell^2(\Sigma)$ –basis property we are able to formulate the next theorem.

**Theorem 3.3** *Let  $f$  be a given field of class  $c(\Sigma)$ . Let  $u$  be the unique solution of the inner displacement boundary-value problem  $u \in \text{pot}(\overline{\Sigma_{int}})$ ,  $u|_{\Sigma} = f$ . Suppose that  $\{u_n\}$  is a countable system in  $\text{pot}(\overline{\Sigma_{int}})$  such that*

$$\overline{\text{span}\{u_n|_{\Sigma}\}}^{\|\cdot\|_{\ell^2(\Sigma)}} = \ell^2(\Sigma).$$

*Then, for any given  $\varepsilon$  and any given subset  $\mathcal{K} \subset \Sigma_{int}$  with  $\text{dist}(\overline{\mathcal{K}}, \Sigma) > 0$ , there exists an integer  $N_0 = N_0(\varepsilon)$  and coefficients  $a_1, a_2, \dots, a_{N_0}$  such that*

$$\left( \int_{\Sigma} \left| f(x) - \sum_{n=1}^{N_0} a_n u_n(x) \right|^2 d\omega(x) \right)^{1/2} \leq \varepsilon \quad (3.9)$$

and

$$\sup_{x \in \overline{\mathcal{K}}} \left| u(x) - \sum_{n=1}^{N_0} a_n u_n(x) \right| \leq B\varepsilon \quad (3.10)$$

In other words, the  $\ell^2(\Sigma)$ –approximation using a system  $\{u_n\}$  on  $\Sigma$  implies uniform approximation (in the ordinary sense) on each  $\mathcal{K} \subset \Sigma_{int}$  with  $\text{dist}(\overline{\mathcal{K}}, \Sigma) > 0$ , i.e. locally uniform approximation in  $\Sigma_{int}$ .

Our interest now is to list some systems  $\{u_n\} \subset \text{pot}(\overline{\Sigma_{int}})$  possessing the  $\ell^2(\Sigma)$ –basis property on  $\Sigma$  and, in particular, being suitable for numerical purposes (for more details, see, for example, [37],[34]).

**Lemma 3.1** *Let  $(x_n)$  be a fundamental system in  $\mathbb{R}^3 \setminus \overline{\Sigma_{int}}$  with the following properties:*

1.  $\text{dist}((x_n), \Sigma) \geq \rho > 0$ ,
2. for each  $u \in c(\mathbb{R}^3 \setminus \overline{\Sigma_{int}})$  satisfying  $\diamond u = 0$  in  $\mathbb{R}^3 \setminus \overline{\Sigma_{int}}$ , regular at infinity, the equations  $u(x_n) = 0$  for  $n = 1, 2, \dots$  imply  $u = 0$  in  $\mathbb{R}^3 \setminus \overline{\Sigma_{int}}$ .

*Then the system  $\Gamma_k(x - x_n)$ ,  $n = 1, 2, \dots$ ;  $k = 1, 2, 3$ , is linearly independent such that*

$$\overline{\text{span}\{\Gamma_k(x - x_k)|_{x \in \Sigma}\}}^{\|\cdot\|_{\ell^2(\Sigma)}} = \ell^2(\Sigma). \quad (3.11)$$

**Proof.** The linear independence follows from the fact that  $x_n \neq x_m$  for  $n \neq m$ . Therefore, it remains to show that

$$\Gamma_k(x - x_n), \quad n = 1, 2, \dots; \quad k = 1, 2, 3, \quad (3.12)$$

forms a basis in  $\ell^2(\Sigma)$ , i.e. for given  $g \in \ell^2(\Sigma)$ , the assumptions

$$\int_{\Sigma} \Gamma_k(y - x_n) \cdot g(y) \, d\omega(y) = 0, \quad n = 1, 2, \dots, \quad k = 1, 2, 3 \quad (3.13)$$

imply  $g = 0$ . For that purpose we observe that the single layer potential

$$u(x) = \sum_{k=1}^3 \int_{\Sigma} \Gamma_k(y - x_n) \cdot g(y) \, d\omega(y) \epsilon^k \quad (3.14)$$

vanishes at all points  $x_n$ ,  $n = 1, 2, \dots$ ; consequently,  $u(x) = 0$  for all  $x \in \mathbb{R}^3 \setminus \overline{\Sigma_{int}}$ . Thus the assertion of Lemma 3.1 is proved by Theorem 3.3.  $\square$

**Lemma 3.2** *The sequence  $\{u_{n,j}^{(k)}\}$ ,  $n = 0, 1, \dots$ ,  $j = 1, 2, \dots, 2n+1$ ,  $k = 1, 2, 3$  as defined in (2.7), is linearly independent such that*

$$\overline{\text{span}\{u_{n,j}^{(k)}|_{\Sigma}\}}^{\|\cdot\|_{\ell^2(\Sigma)}} = \ell^2(\Sigma). \quad (3.15)$$

**Proof.** Let  $g$  be of class  $\ell^2(\Sigma)$  satisfying

$$\int_{\Sigma} g(y) \cdot u_{n,j}^{(k)}(y) \, d\omega(y) = 0, \quad n = 0, 1, \dots, \quad j = 1, 2, \dots, 2n+1, \quad k = 1, 2, 3. \quad (3.16)$$

We have to show that  $g = 0$ . To this end we observe that the series expansion of  $\Gamma_k(x - y)$  (considered as a function of  $x$ )

$$\Gamma_k(x - y) = \sum_{n=1}^{\infty} \sum_{j=1}^{2n+1} a_{n,j}(x) u_{n,j}^{(k)}(y) \quad (3.17)$$

with

$$a_{n,j}(x) = \frac{\lambda + 3\mu}{2\mu(\lambda + 2\mu)} \frac{4\pi}{2n+1} \frac{1}{|x|^{2n+1}} H_{n,j}(x) \quad (3.18)$$

is analytic for all  $x \in \mathbb{R}^3 \setminus \overline{\Omega_R^{int}}$ . For all  $x \in \mathbb{R}^3 \setminus \overline{\Omega_R^{int}}$  we thus find

$$\begin{aligned} u(x) &= \sum_{k=1}^3 \int_{\Sigma} \Gamma_k(x - y) \cdot g(y) \, d\omega(y) \epsilon^k \\ &= \sum_{n=1}^{\infty} \sum_{j=1}^{2n+1} \sum_{k=1}^3 a_{n,j}(x) \int_{\Sigma} u_{n,j}^{(k)}(y) \cdot g(y) \, d\omega(y) \epsilon^k \\ &= 0. \end{aligned} \quad (3.19)$$

However, this implies by analytic continuation that  $u = 0$  in  $\mathbb{R}^3 \setminus \overline{\Sigma_{int}}$ . Hence, again by virtue of Theorem 3.3, we have the desired result.  $\square$

### 3.3 A Generalized Fourier Series Approach to the Displacement Boundary-Value Problem

We now arrive at formulating the following approximation scheme for computing the solution  $u$  of the inner displacement boundary-value problem: given  $f \in c(\Sigma)$ , find  $u \in \text{pot}(\overline{\Sigma_{int}})$  with  $u|_{\Sigma} = f$ .

- (i) Choose a system  $\{u_n\} \subset \text{pot}(\overline{\Sigma_{int}})$  satisfying

$$\ell^2(\Sigma) = \overline{\text{span}\{u_n|_{\Sigma}\}}^{\|\cdot\|_{\ell^2(\Sigma)}}.$$

- (ii) Compute the vector fields

$$f^{(m)} = \sum_{n=1}^m a_n u_n|_{\Sigma}, \quad u^{(m)} = \sum_{n=1}^m a_n u_n, \quad (3.20)$$

by solving the linear equations

$$\sum_{n=1}^m \int_{\Sigma} u_l(x) \cdot u_n(x) \, d\omega(x) a_n = \int_{\Sigma} f(x) \cdot u_l(x) \, d\omega(x), \quad l = 1, 2, \dots, m. \quad (3.21)$$

Then the field  $u^{(m)}$  determined as above serves as approximation to  $u$ . The linear combination  $f^{(m)}$  is best in the sense that

$$\left( \int_{\Sigma} \left| f(x) - \sum_{n=1}^m a_n u_n(x) \right|^2 d\omega(x) \right)^{1/2} \leq \left( \int_{\Sigma} \left| f(x) - \sum_{n=1}^m b_n u_n(x) \right|^2 d\omega(x) \right)^{1/2} \quad (3.22)$$

for any selection of constants  $b_1, b_2, \dots, b_m$ . According to the Gram-Schmidt orthonormalization process, there exists a system  $\{u_n^*\}$  given by

$$u_n^* = \sum_{l=1}^n d_{n,l} u_l, \quad (3.23)$$

where  $d_{n,l}$  are the corresponding (constant) coefficients, such that  $\{u_n^*|_{\Sigma}\}$  is orthonormal in the sense that

$$\int_{\Sigma} u_l^*(x) \cdot u_n^*(x) \, d\omega(x) = \delta_{l,n}. \quad (3.24)$$

In terms of the orthonormal system  $\{u_n^*\}$  the best approximation  $f^{(m)}$  now reads

$$f^{(m)} = \sum_{n=1}^m f^{\wedge}(n) u_n^*, \quad (3.25)$$

where the Fourier coefficients of  $f$  with respect to the system  $\{u_n^*|_\Sigma\}$  are given by

$$f^\wedge(n) = \int_\Sigma f(x) \cdot u_n^*(x) \, d\omega(x). \quad (3.26)$$

According to Theorem 3.3, the  $\ell^2$ -convergence of  $f^{(m)}$  to  $f$

$$\lim_{m \rightarrow \infty} \left( \int_\Sigma \left| f(x) - \sum_{l=1}^m f^\wedge(l) u_l^*(x) \right|^2 d\omega(x) \right)^{1/2} = 0 \quad (3.27)$$

implies ordinary pointwise convergence of the  $u^{(m)}$  to  $u$  for each  $x \in \Sigma_{int}$ :

$$u(x) = \lim_{m \rightarrow \infty} u^{(m)}(x), \quad u^{(m)}(x) = \sum_{l=1}^m f^\wedge(l) u_l(x). \quad (3.28)$$

The series (3.25) is uniformly convergent on every subset  $\mathcal{K} \subset \Sigma_{int}$  with  $\text{dist}(\overline{\mathcal{K}}, \Sigma) > 0$ . Moreover, because of the estimate (3.22), we have for each  $m \in \mathbb{N}$

$$\begin{aligned} \sup_{x \in \overline{\mathcal{K}}} \left| u(x) - \sum_{l=1}^m f^\wedge(l) u_l^*(x) \right| &\leq B \left( \left| u(x) - \sum_{l=1}^m f^\wedge(l) u_l^*(x) \right| d\omega(x) \right)^{1/2} \\ &\leq B \left( \int_\Sigma |f(x)|^2 d\omega(x) - \sum_{l=1}^m |f^\wedge(l)|^2 \right)^{1/2}. \end{aligned} \quad (3.29)$$

In conclusion, once a complete orthonormal basis  $\{u_n^*\}$  on  $\Sigma$  is specified, the uniform approximation for the solution on every compact subset of  $\Sigma_{int}$  can be established. Hence, this generalized Fourier series approach can be used as a 'global technique' for numerical purposes in solving discrete boundary-value problems of elastostatics (see, for example, [37]).

# Chapter 4

## A Spatial Approach to Cauchy-Navier Wavelets

In what follows, we establish a general setup for multiscale approximation of elastic fields based on the limit and jump relations of the potential operators defined in the framework of the Hilbert space of square-integrable functions  $\ell^2(\Sigma)$ . Moreover, we develop a tree algorithm for the decomposition and reconstruction of elastic fields as a significant part of our wavelet analysis. It should be mentioned that the wavelet theory as presented here admits two essential origins: On the one hand side, the conventional wavelet approach is based on the classical limit and jump relations in the usual  $\ell^2(\Sigma)$ -framework, on the other hand a different wavelet approach can be deduced from the dual limit and jump relations in the  $\ell^2(\Sigma)$ -framework.

### 4.1 Cauchy-Navier Wavelets Associated to Layer Potentials

Our point of departure is the tensor kernel functions occurring in the potential integral operators (2.23)-(2.30) which act as scaling functions within our wavelet approach.

**Definition 4.1** *Let the tensor-valued kernels,  $\Phi_\tau^{(i)} : \Sigma \times \Sigma \longrightarrow \mathbb{R}^{3 \times 3}$ ,  $i = 1, \dots, 8$ , be defined by*

$$\begin{aligned}\Phi_\tau^{(1)}(x, y) &= \Gamma(x_\tau - y), \\ \Phi_\tau^{(2)}(x, y) &= \frac{1}{2\pi} \left( \left( \frac{\partial}{\partial \nu(y)} \frac{1}{|x_\tau - y|} \right) \Lambda(x_\tau - y) - \left( \frac{\partial}{\partial \nu(y)} \frac{1}{|x - y|} \right) \Lambda(x - y) \right), \\ \Phi_\tau^{(3)}(x, y) &= -\frac{1}{2\pi} \left( \left( \frac{\partial}{\partial \nu(x)} \frac{1}{|x_\tau - y|} \right) \Lambda(x_\tau - y) - \left( \frac{\partial}{\partial \nu(x)} \frac{1}{|x - y|} \right) \Lambda(x - y) \right), \\ \Phi_\tau^{(4)}(x, y) &= \Gamma(x_\tau - y) - \Gamma(x_{-\tau} - y), \\ \Phi_\tau^{(5)}(x, y) &= \frac{1}{4\pi} \left( \left( \frac{\partial}{\partial \nu(y)} \frac{1}{|x_\tau - y|} \right) \Lambda(x_\tau - y) - \left( \frac{\partial}{\partial \nu(y)} \frac{1}{|x_{-\tau} - y|} \right) \Lambda(x_{-\tau} - y) \right),\end{aligned}$$

$$\begin{aligned}
\Phi_\tau^{(6)}(x, y) &= -\frac{1}{4\pi} \left( \left( \frac{\partial}{\partial \nu(x)} \frac{1}{|x_\tau - y|} \right) \Lambda(x_\tau - y) - \left( \frac{\partial}{\partial \nu(x)} \frac{1}{|x_{-\tau} - y|} \right) \Lambda(x_{-\tau} - y) \right), \\
\Phi_\tau^{(7)}(x, y) &= \frac{1}{2} \left( \left( \frac{\partial}{\partial \nu(y)} \frac{1}{|x_\tau - y|} \right) \Lambda(x_\tau - y) + \left( \frac{\partial}{\partial \nu(y)} \frac{1}{|x_{-\tau} - y|} \right) \Lambda(x_{-\tau} - y) \right), \\
\Phi_\tau^{(8)}(x, y) &= \frac{1}{2} \left( \left( \frac{\partial}{\partial \nu(x)} \frac{1}{|x_\tau - y|} \right) \Lambda(x_\tau - y) + \left( \frac{\partial}{\partial \nu(x)} \frac{1}{|x_{-\tau} - y|} \right) \Lambda(x_{-\tau} - y) \right),
\end{aligned}$$

where  $\tau$  is a positive real number and  $(x, y) \in \Sigma \times \Sigma$ . Then, for  $i = 1, \dots, 8$ , the family  $\{\Phi_\tau^{(i)}\}$  of kernels  $\Phi_\tau^{(i)} : \Sigma \times \Sigma \longrightarrow \mathbb{R}^{3 \times 3}$  is called a (Cauchy-Navier)  $\Sigma$ -scaling function of type  $i$ . Moreover,  $\Phi_1^{(i)} : \Sigma \times \Sigma \longrightarrow \mathbb{R}^{3 \times 3}$  (i.e.  $\tau = 1$ ) is called the mother kernel of the (Cauchy-Navier)  $\Sigma$ -scaling function of type  $i$ .

More detailed calculation gives us the following result.

**Lemma 4.1** For  $x, y \in \Sigma$ ,

$$\begin{aligned}
\Phi_\tau^{(5)}(x, y) &= \frac{1}{4\pi} \left\{ \left( \frac{2\mu}{\lambda + 3\mu} \right) \left[ ((x - y) \cdot \nu(y)) \left( \frac{1}{|x_\tau - y|^3} - \frac{1}{|x_{-\tau} - y|^3} \right) \mathbf{i}_3 \right. \right. \\
&+ (\nu(x) \cdot \nu(y)) \left( \frac{\tau}{|x_\tau - y|^3} + \frac{\tau}{|x_{-\tau} - y|^3} \right) \mathbf{i}_3 \Big] \\
&+ \left( \frac{3(\lambda + \mu)}{\lambda + 3\mu} \right) \left[ ((x - y) \cdot \nu(y)(x - y) \otimes (x - y)) \left( \frac{1}{|x_\tau - y|^5} - \frac{1}{|x_{-\tau} - y|^5} \right) \right. \\
&+ ((x - y) \cdot \nu(y)(\nu(x) \otimes \nu(y)) \left( \frac{\tau^2}{|x_\tau - y|^5} - \frac{\tau^2}{|x_{-\tau} - y|^5} \right) \\
&+ (\nu(x) \cdot \nu(y)((x - y) \otimes \nu(x) + \nu(x) \otimes (x - y)) \left( \frac{\tau^2}{|x_\tau - y|^5} - \frac{\tau^2}{|x_{-\tau} - y|^5} \right) \\
&+ ((x - y) \cdot \nu(y)((x - y) \otimes \nu(x) + \nu(x) \otimes (x - y)) \left( \frac{\tau}{|x_\tau - y|^5} + \frac{\tau}{|x_{-\tau} - y|^5} \right) \\
&+ (\nu(x) \cdot \nu(y)(x - y) \otimes (x - y)) \left( \frac{\tau}{|x_\tau - y|^5} + \frac{\tau}{|x_{-\tau} - y|^5} \right) \\
&\left. \left. + (\nu(x) \cdot \nu(y)\nu(x) \otimes \nu(y)) \left( \frac{\tau^3}{|x_\tau - y|^5} + \frac{\tau^3}{|x_{-\tau} - y|^5} \right) \right] \right\}. \tag{4.1}
\end{aligned}$$

As an immediate consequence of Theorem 2.1 we are led to the following result, which may be understood in  $\ell^2(\Sigma)$ -sense.

**Theorem 4.1** For  $f \in \ell^2(\Sigma)$ ,  $x \in \Sigma$ , we have

$$\lim_{\substack{\tau \rightarrow 0 \\ \tau > 0}} \int_{\Sigma} \Phi_\tau^{(i)}(x, y) f(y) \, d\omega(y) = \begin{cases} \int_{\Sigma} \Gamma(x - y) f(y) \, d\omega(y), & i = 1 \\ 0, & i = 4 \\ f(x), & i = 2, 3, 5, 6 \\ \int_{\Sigma} \left( \frac{\partial}{\partial \nu(y)} \frac{1}{|x - y|} \right) \Lambda(x - y) f(y) \, d\omega(y), & i = 7 \\ \int_{\Sigma} \left( \frac{\partial}{\partial \nu(x)} \frac{1}{|x - y|} \right) \Lambda(x - y) f(y) \, d\omega(y), & i = 8. \end{cases} \tag{4.2}$$

Theorem 4.1 enables us to introduce wavelet functions via an appropriate scaling equation.

**Definition 4.2** *Let  $\{\Phi_\tau^{(i)}\}$  be a family of  $\Sigma$ -scaling functions of type  $i$  defined as above. Then the family  $\{\Psi_\tau^{(i)}\}$  of kernels  $\Psi_\tau^{(i)} : \Sigma \times \Sigma \longrightarrow \mathbb{R}^{3 \times 3}$  defined by*

$$\Psi_\tau^{(i)}(x, y) = -(\alpha(\tau))^{-1} \frac{d}{d\tau} \Phi_\tau^{(i)}(x, y), \quad x, y \in \Sigma, \quad (4.3)$$

*is called a (Cauchy-Navier)  $\Sigma$ -wavelet function of type  $i$ , where  $\alpha$  is a given positive real-valued function depending upon  $\tau$ . Moreover,  $\Psi_1^{(i)} : \Sigma \times \Sigma \longrightarrow \mathbb{R}^{3 \times 3}$  defines the so-called mother kernel of the (Cauchy-Navier)  $\Sigma$ -wavelet of type  $i$ .*

It should be noted that, in wavelet terminology, (4.3) is called the (scale continuous)  $\Sigma$ -scaling equation. The factor  $\alpha(\tau)^{-1}$  can be chosen in an appropriate way. For simplicity, throughout the remainder of this work, we use  $\alpha(\tau) = \tau^{-1}$ ,  $\tau > 0$ .

**Definition 4.3** *Let  $\{\Phi_\tau^{(i)}\}$  be a  $\Sigma$ -scaling function of type  $i$ . Then the associated  $\Sigma$ -wavelet transform of type  $i$ ,  $(\mathbf{WT})_\tau^{(i)} : \ell^2(\Sigma) \longrightarrow \ell^2(\Sigma)$  of a function  $f \in \ell^2(\Sigma)$  is defined by*

$$(\mathbf{WT})_\tau^{(i)}(f)(x) = \int_\Sigma \Psi_\tau^{(i)}(x, y) f(y) d\omega(y), \quad x \in \Sigma. \quad (4.4)$$

According to our definitions we obtain explicit formulae for the  $\Sigma$ -scaling and  $\Sigma$ -wavelet functions by means of the ordinary differential equations

$$\Psi_\tau^{(i)}(x, y) = -\tau \frac{d}{d\tau} \Phi_\tau^{(i)}(x, y), \quad i = 1, \dots, 8. \quad (4.5)$$

## 4.2 Scale Continuous Reconstruction Formula

It is not difficult to show that the  $\Sigma$ -wavelet functions  $\{\Psi_\tau^{(i)}\}$ ,  $i = 1, \dots, 8$ , behave (componentwise) like  $\mathcal{O}(\tau^{-1})$ , hence, the convergence of the integrals occurring in the next theorem is guaranteed (cf. [1],[32],[37]).

**Theorem 4.2** *Let  $\{\Phi_\tau^{(i)}\}$  be a  $\Sigma$ -scaling function of type  $i$ . Suppose that  $f$  is of class  $\ell^2(\Sigma)$ . Then the reconstruction formula*

$$\int_0^\infty (\mathbf{WT})_\tau^{(i)}(f)(x) \frac{d\tau}{\tau} = \begin{cases} \int_\Sigma \Gamma(x - y) f(y) d\omega(y), & i = 1 \\ 0, & i = 4 \\ f(x), & i = 2, 3, 5, 6 \\ \int_\Sigma \left( \frac{\partial}{\partial \nu(y)} \frac{1}{|x - y|} \right) \Lambda(x - y) f(y) d\omega(y), & i = 7 \\ \int_\Sigma \left( \frac{\partial}{\partial \nu(x)} \frac{1}{|x - y|} \right) \Lambda(x - y) f(y) d\omega(y), & i = 8 \end{cases} \quad (4.6)$$

*holds in the sense of  $\|\cdot\|_{\ell^2(\Sigma)}$ .*



**Proof.** Let  $R > 0$  be arbitrary. Taking the identity

$$\Phi_R^{(i)}(x, y) = \int_R^\infty \Psi_\tau^{(i)}(x, y) \frac{d\tau}{\tau}, \quad x, y \in \Sigma, \quad (4.7)$$

we obtain

$$\begin{aligned} \int_R^\infty (\mathbf{WT})_\tau^{(i)}(f)(x) \frac{d\tau}{\tau} &= \int_R^\infty \int_\Sigma \Psi_\tau^{(i)}(x, y) f(y) d\omega(y) \frac{d\tau}{\tau} \\ &= \int_\Sigma \left( \int_R^\infty \Psi_\tau^{(i)}(x, y) \frac{d\tau}{\tau} \right) f(y) d\omega(y) \\ &= \int_\Sigma \Phi_R^{(i)}(x, y) f(y) d\omega(y). \end{aligned}$$

Letting  $R$  tend to 0 we get the desired result.  $\square$

Next we are interested in formulating the wavelet transform and the reconstruction formula by formally using the so-called 'shift' and 'dilation' operators. Those enable us to form a family of wavelets using the mother wavelet  $\Psi_1$ . To be more specific, we define the  $x$ -shift and  $\tau$ -dilation operators of a mother kernel, respectively, by

$$T_x : \Psi_1^{(i)} \longmapsto T_x \Psi_1^{(i)} = \Psi_1^{(i)}(x, \cdot), \quad (4.8)$$

$$D_\tau : \Psi_1^{(i)} \longmapsto D_\tau \Psi_1^{(i)} = \Psi_\tau^{(i)}. \quad (4.9)$$

Consequently, this yields by composition

$$T_x D_\tau \Psi_1^{(i)} = T_x \Psi_\tau^{(i)} = \Psi_\tau^{(i)}(x, \cdot), \quad i = 1, \dots, 8. \quad (4.10)$$

Summarizing our results we therefore obtain

**Theorem 4.3** For  $x \in \Sigma$  and  $f \in \ell^2(\Sigma)$

$$\lim_{\substack{\tau \rightarrow 0 \\ \tau > 0}} \int_\Sigma T_x D_\tau \Phi_1^{(i)}(x, y) f(y) d\omega(y) = \begin{cases} \int_\Sigma \Gamma(x - y) f(y) d\omega(y), & i = 1 \\ 0, & i = 4 \\ f(x), & i = 2, 3, 5, 6 \\ \int_\Sigma \left( \frac{\partial}{\partial \nu(y)} \frac{1}{|x - y|} \right) \Lambda(x - y) f(y) d\omega(y), & i = 7 \\ \int_\Sigma \left( \frac{\partial}{\partial \nu(x)} \frac{1}{|x - y|} \right) \Lambda(x - y) f(y) d\omega(y), & i = 8 \end{cases} \quad (4.11)$$

and

$$\int_0^\infty \int_\Sigma T_x D_\tau \Psi_1^{(i)}(x, y) f(y) d\omega(y) \frac{d\tau}{\tau} = \begin{cases} \int_\Sigma \Gamma(x - y) f(y) d\omega(y), & i = 1 \\ 0, & i = 4 \\ f(x), & i = 2, 3, 5, 6 \\ \int_\Sigma \left( \frac{\partial}{\partial \nu(y)} \frac{1}{|x - y|} \right) \Lambda(x - y) f(y) d\omega(y), & i = 7 \\ \int_\Sigma \left( \frac{\partial}{\partial \nu(x)} \frac{1}{|x - y|} \right) \Lambda(x - y) f(y) d\omega(y), & i = 8 \end{cases} \quad (4.12)$$

hold in the sense of  $\|\cdot\|_{\ell^2(\Sigma)}$ .

**Proof.** The proof follows immediately from the results stated in Theorem 4.2.  $\square$

### 4.3 Scale Discrete Reconstruction Formula

Let  $(\tau_j)_{j \in \mathbb{Z}}$  denote a monotonically decreasing sequence of real numbers satisfying the properties

$$\lim_{j \rightarrow \infty} \tau_j = 0, \quad \lim_{j \rightarrow -\infty} \tau_j = \infty, \quad (4.13)$$

(for example,  $\tau_j = 2^{-j}$ ).

Given a  $\Sigma$ -scaling function  $\{\Phi_\tau^{(i)}\}$  of type  $i$ , we define the (scale) discretized  $\Sigma$ -scaling function and wavelets of type  $i$  by  $\{\Phi_j^{D;(i)}\}, \{\Psi_j^{D;(i)}\}$  with

$$\Phi_j^{D;(i)} = \Phi_{\tau_j}^{(i)}, \quad j \in \mathbb{Z}.$$

Then we are led to the following result.

**Theorem 4.4** *For  $f \in \ell^2(\Sigma)$ , the limit*

$$\lim_{j \rightarrow \infty} \int_{\Sigma} \Phi_j^{D;(i)}(x, y) f(y) d\omega(y) = \begin{cases} \int_{\Sigma} \Gamma(x - y) f(y) d\omega(y), & i = 1 \\ 0, & i = 4 \\ f(x), & i = 2, 3, 5, 6 \\ \int_{\Sigma} \left( \frac{\partial}{\partial \nu(y)} \frac{1}{|x - y|} \right) \Lambda(x - y) f(y) d\omega(y), & i = 7 \\ \int_{\Sigma} \left( \frac{\partial}{\partial \nu(x)} \frac{1}{|x - y|} \right) \Lambda(x - y) f(y) d\omega(y), & i = 8 \end{cases} \quad (4.14)$$

holds in the  $\|\cdot\|_{\ell^2(\Sigma)}$ -sense.

**Proof.** Obviously, Theorem 4.4 is just a discretization of Theorem 4.1.  $\square$

**Definition 4.4** *Let  $\{\Phi_j^{D;(i)}\}_{j \in \mathbb{Z}}$  be a scale discretized  $\Sigma$ -scaling function of type  $i$ . Then the (scale) discretized  $\Sigma$ -wavelet function  $\Psi_j^{D;(i)}$  of type  $i$  is defined by*

$$\Psi_j^{D;(i)}(x, y) = \Psi_{\tau_j}^{(i)}(x, y) = \int_{\tau_{j+1}}^{\tau_j} \Psi_{\tau}^{(i)}(x, y) \frac{d\tau}{\tau}, \quad j \in \mathbb{Z}, \quad x, y \in \Sigma, \quad i = 1, \dots, 8. \quad (4.15)$$

With the definition of  $\Psi_{\tau}^{(i)}$  we immediately obtain

$$\Psi_j^{D;(i)}(x, y) = - \int_{\tau_{j+1}}^{\tau_j} \tau \frac{d}{d\tau} \Phi_{\tau}^{(i)}(x, y) \frac{d\tau}{\tau} = \Phi_{j+1}^{D;(i)}(x, y) - \Phi_j^{D;(i)}(x, y), \quad x, y \in \Sigma. \quad (4.16)$$

In the wavelet terminology, the equation (4.16) is called the (scale) discretized  $\Sigma$ -scaling equation of type  $i$ . It should be remarked that, with a suitably chosen  $\tau_j$ , formula (4.16) can easily be used to formulate the scale discrete  $\Sigma$ -wavelets. As examples, the following figures show the localization property of both scaling functions and wavelets.

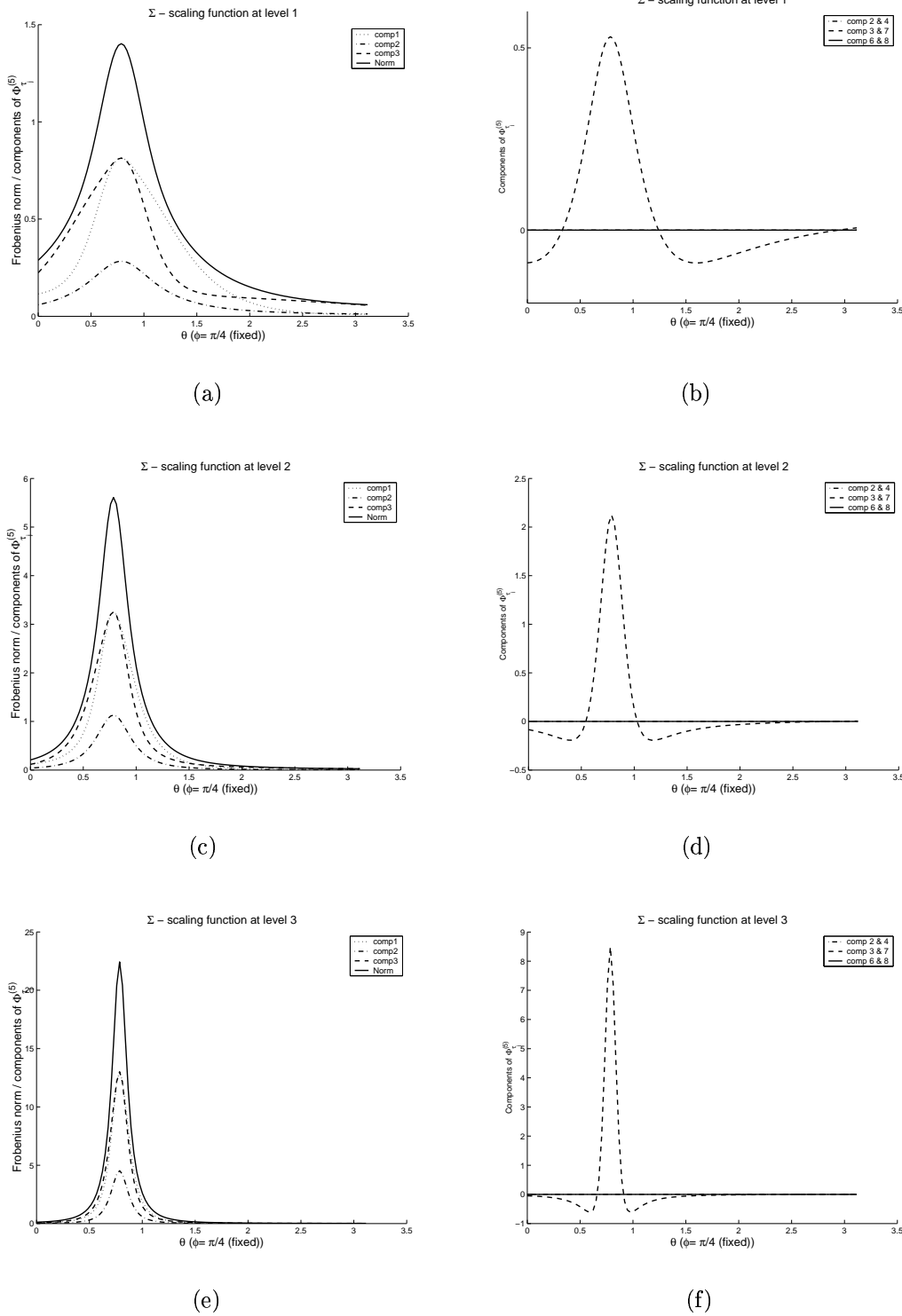


Figure 4.1: Sectional illustration of scale discrete  $\Sigma$ –scaling function  $\Phi_j^{D;(5)}(x, \cdot)$  at levels 1, 2 and 3 with  $\theta$  variable and  $\varphi = \pi/4$  and  $x$  fixed.  $\Phi_j^{D;(5)}(x, \cdot) = \Phi_{\tau_j}^{(5)}(x, \cdot)$  for  $\tau = 2^{-j}$ ,  $j = 1, 2, 3$ . Frobenius norm, diagonal components (left) and non-diagonal components (right).

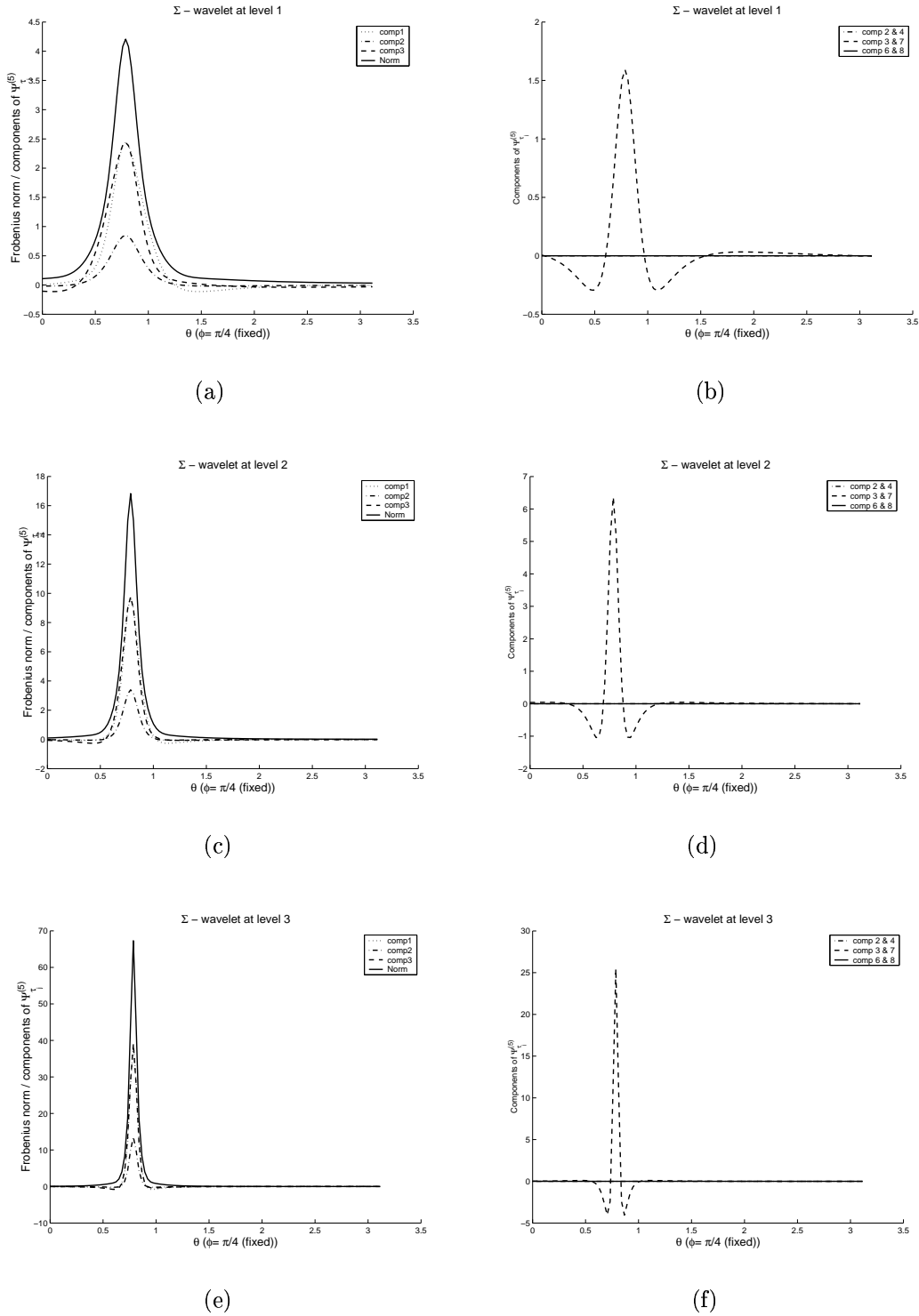


Figure 4.2: Sectional illustration of scale discrete  $\Sigma$ -wavelet  $\Psi_j^{D;(5)}(x, \cdot)$  at levels 1, 2 and 3 with  $\theta$  variable and  $\varphi = \pi/4$  and  $x$  fixed.  $\Psi_j^{D;(5)}(x, \cdot) = \Psi_{\tau_j}^{(5)}(x, \cdot)$  for  $\tau = 2^{-j}$ ,  $j = 1, 2, 3$ . Frobenius norm, diagonal components (left) and non-diagonal components (right).

Assume that  $f$  is a vector field of class  $\ell^2(\Sigma)$  and consider the discretized  $\Sigma$ -scaling equation of type  $i$  (see, Equation 4.16). Then, for  $J \in \mathbb{Z}$  sufficiently large and  $N \in \mathbb{N}$ , we have

$$\begin{aligned} \int_{\Sigma} \Phi_{J+N}^{D;(i)}(x, y) f(y) d\omega(y) &= \int_{\Sigma} \Phi_J^{D;(i)}(x, y) f(y) d\omega(y) \\ &\quad + \sum_{j=J}^{J+N-1} \int_{\Sigma} \Psi_j^{D;(i)}(x, y) f(y) d\omega(y), \quad x \in \Sigma. \end{aligned} \quad (4.17)$$

By taking into account the property (4.15) we find in connection with Theorem 4.3 the following result.

**Theorem 4.5** *Let  $\{\Phi_j^{D;(i)}\}$  be a (scale) discretized  $\Sigma$ -scaling function of type  $i$ . Then the multiscale representation of a function  $f \in \ell^2(\Sigma)$*

$$\begin{aligned} \int_{\Sigma} \Phi_J^{D;(i)}(x, y) f(y) d\omega(y) + \sum_{j=J}^{\infty} \int_{\Sigma} \Psi_j^{D;(i)}(x, y) f(y) d\omega(y) \\ = \begin{cases} \int_{\Sigma} \Gamma(x - y) f(y) d\omega(y), & i = 1 \\ 0, & i = 4 \\ f(x), & i = 2, 3, 5, 6 \\ \int_{\Sigma} \left( \frac{\partial}{\partial \nu(y)} \frac{1}{|x-y|} \right) \Lambda(x - y) f(y) d\omega(y), & i = 7 \\ \int_{\Sigma} \left( \frac{\partial}{\partial \nu(x)} \frac{1}{|x-y|} \right) \Lambda(x - y) f(y) d\omega(y), & i = 8 \end{cases} \end{aligned} \quad (4.18)$$

holds for all  $J \in \mathbb{Z}$  (in the sense of  $\|\cdot\|_{\ell^2(\Sigma)}$ ).

Our considerations lead us in canonical way to the definition of the (scale) discretized  $\Sigma$ -wavelet transform of type  $i$  by

$$(\mathbf{WT})_j^{D;(i)}(f)(x) = \int_{\Sigma} \Psi_j^{D;(i)}(x, y) f(y) d\omega(y), \quad x \in \Sigma. \quad (4.19)$$

We are able to derive the following corollary.

**Corollary 4.1** *Let  $\{\Phi_j^{D;(i)}\}$  be a (scale) discretized  $\Sigma$ -scaling function of type  $i$ . Then, for all  $f \in \ell^2(\Sigma)$ ,*

$$\sum_{j=-\infty}^{\infty} (\mathbf{WT})_j^{D;(i)}(f)(x) = \begin{cases} \int_{\Sigma} \Gamma(x - y) f(y) d\omega(y), & i = 1 \\ 0, & i = 4 \\ f(x), & i = 2, 3, 5, 6 \\ \int_{\Sigma} \left( \frac{\partial}{\partial \nu(y)} \frac{1}{|x-y|} \right) \Lambda(x - y) f(y) d\omega(y), & i = 7 \\ \int_{\Sigma} \left( \frac{\partial}{\partial \nu(x)} \frac{1}{|x-y|} \right) \Lambda(x - y) f(y) d\omega(y), & i = 8 \end{cases} \quad (4.20)$$

holds in the  $\|\cdot\|_{\ell^2(\Sigma)}$ -sense.

In conclusion, any function  $f \in \ell^2(\Sigma)$  can be represented as a multiscale sum of the wavelet transforms corresponding to  $\Psi_j^{D;(i)}$ ,  $i \in \{2, 3, 5, 6\}$ .

As always in the theory of wavelets (cf. [26],[30],[41]), the operators  $\mathbf{p}_j^{D;(i)}$ ,  $\mathbf{r}_j^{D;(i)}$  defined by

$$\mathbf{p}_j^{D;(i)} f = \int_{\Sigma} \Phi_j^{D;(i)}(\cdot, y) f(y) d\omega(y), \quad f \in \ell^2(\Sigma), \quad (4.21)$$

$$\mathbf{r}_j^{D;(i)} f = \int_{\Sigma} \Psi_j^{D;(i)}(\cdot, y) f(y) d\omega(y), \quad f \in \ell^2(\Sigma) \quad (4.22)$$

may be understood as filters for scale and detail information, respectively.

The scale spaces  $v_j^{D;(i)}$  and details spaces  $w_j^{D;(i)}$  of type  $i$  are defined by

$$v_j^{D;(i)} = \{\mathbf{p}_j^{D;(i)}(f) \mid f \in \ell^2(\Sigma)\}, \quad (4.23)$$

$$w_j^{D;(i)} = \{\mathbf{r}_j^{D;(i)}(f) \mid f \in \ell^2(\Sigma)\}, \quad (4.24)$$

respectively.

It is clear that

$$\mathbf{p}_{J+1}^{D;(i)}(f) = \mathbf{p}_J^{D;(i)}(f) + \mathbf{r}_J^{D;(i)}(f), \quad J \in \mathbb{Z}. \quad (4.25)$$

Consequently,

$$v_{J+1}^{D;(i)} = v_J^{D;(i)} + w_J^{D;(i)}, \quad (4.26)$$

$$v_{J+1}^{D;(i)} = v_{J_0}^{D;(i)} + \sum_{j=J_0}^J w_j^{D;(i)}. \quad (4.27)$$

However, it should be remarked that the sum (4.25), in general, is neither direct nor orthogonal (cf. [32]).

## 4.4 A Tree Algorithm

In what follows, we present a particular scheme which simplifies the computational process of the reconstruction and decomposition of the wavelet approximation. This is known as a *tree algorithm* that provides a recursive process to compute the integrals  $\mathbf{p}_j^{D;(i)}(f)$  and  $\mathbf{r}_j^{D;(i)}(f)$  on different levels starting from an initial approximation of a given  $f \in \ell^2(\Sigma)$  without falling upon the original vector field  $f$  in each step.

For this purpose, we use appropriately chosen approximate integration rules such that

$$\mathbf{p}_j^{D;(i)}(f)(x) \approx \sum_{k=1}^{N_j} W_k^{N_j} \Phi_j^{D;(i)}(x, y_k^{N_j}) f(y_k^{N_j}), \quad (4.28)$$

$$\mathbf{r}_{j-1}^{D;(i)}(f)(x) \approx \sum_{k=1}^{N_{j-1}} W_k^{N_{j-1}} \Psi_{j-1}^{D;(i)}(x, y_k^{N_{j-1}}) f(y_k^{N_{j-1}}), \quad (4.29)$$

where  $\{(y_k^{N_j}, W_k^{N_j}) \in \Sigma \times \mathbb{R}\}$  are the prescribed integration points and weights and the symbol ' $\approx$ ' means that the error is negligible.

From (4.28), we conclude that for sufficiently large  $J \in \mathbb{N}$  there exist coefficient vectors  $a_k^{N_J} \in \mathbb{R}^3$ ,  $k = 1, \dots, N_J$ , such that

$$\mathbf{p}_J^{D;(i)}(f)(x) \approx \sum_{k=1}^{N_J} \Phi_J^{D;(i)}(x, y_k^{N_J}) a_k^{N_J}, \quad i = 1, \dots, 8, \quad x \in \Sigma, \quad (4.30)$$

where,

$$a_k^{N_J} = W_k^{N_J} f(y_k^{N_J}), \quad k = 1, \dots, N_J.$$

Now we want to introduce an algorithm to obtain the coefficients

$$\mathbf{a}^{N_j} = (a_1^{N_j}, \dots, a_{N_j}^{N_j}) \in \mathbb{R}^{3 \times N_j}, \quad j = J_0, \dots, J,$$

such that

(a) the vector  $\mathbf{a}^{N_j}$  is obtainable from  $\mathbf{a}^{N_{j+1}}$ ,  $j = J_0, \dots, J-1$ ,

(b) the expressions  $\mathbf{p}_j^{D;(i)}(f)(x)$ ,  $\mathbf{r}_{j-1}^{D;(i)}(f)(x)$  can be written as

$$\mathbf{p}_j^{D;(i)}(f)(x) = \sum_{k=1}^{N_j} \Phi_j^{D;(i)}(x, y_k^{N_j}) a_k^{N_j}, \quad j = J_0, \dots, J, \quad (4.31)$$

$$\mathbf{r}_{j-1}^{D;(i)}(f)(x) = \sum_{k=1}^{N_{j-1}} \Psi_{j-1}^{D;(i)}(x, y_k^{N_{j-1}}) a_k^{N_{j-1}}, \quad j = J_0 + 1, \dots, J. \quad (4.32)$$

The tree algorithm can be divided into two parts, namely the initial step and the pyramid step.

For the *initial step* we consider  $J \in \mathbb{N}$  to be sufficiently large and thus we see that

$$a_k^{N_J} = W_k^{N_J} f(y_k^{N_J}), \quad k = 1, \dots, N_J. \quad (4.33)$$

The aim of the pyramid step is to construct  $\mathbf{a}^{N_j}$  from  $\mathbf{a}^{N_{j+1}}$  by recursion. At this point, it is essential to assume that there exist (tensor) kernel functions  $\Xi_j^{(i)} : \Sigma \times \Sigma \longrightarrow \mathbb{R}^{3 \times 3}$  such that

$$\Phi_j^{D(i)}(x, y) \approx \int_{\Sigma} \Phi_j^{D(i)}(x, z) \Xi_j^{(i)}(z, y) d\omega(z), \quad (4.34)$$

$$\Xi_j^{(i)}(x, y) \approx \int_{\Sigma} \Xi_j^{(i)}(x, z) \Xi_{j+1}^{(i)}(z, y) d\omega(z) \quad (4.35)$$

for  $j = J_0, \dots, J$ . A reasonable choice for  $\Xi_j^{(i)}$  is

$$\Xi_j^{(i)} = \Phi_{J+L}^{D(i)}, \quad j = J_0, \dots, J; \quad i \in \{2, 3, 5, 6\}$$

with  $L \in \mathbb{N}$  suitably large. By the approximate integration rules we obtain

$$\begin{aligned} \int_{\Sigma} \Phi_j^{D(i)}(x, y) f(y) d\omega(y) &\approx \int_{\Sigma} \left[ \int_{\Sigma} \Phi_j^{D(i)}(x, z) \Xi_j^{(i)}(z, y) d\omega(z) \right] f(y) d\omega(y) \\ &= \int_{\Sigma} \Phi_j^{D(i)}(x, z) \left[ \int_{\Sigma} \Xi_j^{(i)}(z, y) f(y) d\omega(y) \right] d\omega(z) \\ &\approx \sum_{k=1}^{N_j} \Phi_j^{D(i)}(x, y_k^{N_j}) a_k^{N_j}, \end{aligned} \quad (4.36)$$

where

$$a_k^{N_j} = W_k^{N_j} \int_{\Sigma} \Xi_j^{(i)}(y_k^{N_j}, y) f(y) d\omega(y), \quad j = J_0, \dots, J. \quad (4.37)$$

Hence, in connection with (4.35) we find

$$\begin{aligned} a_k^{N_j} &= W_k^{N_j} \int_{\Sigma} \Xi_j^{(i)}(y_k^{N_j}, y) f(y) d\omega(y) \\ &\approx W_k^{N_j} \int_{\Sigma} \left[ \int_{\Sigma} \Xi_j^{(i)}(y_k^{N_j}, x) \Xi_{j+1}^{(i)}(x, y) d\omega(y) \right] f(y) d\omega(x) \\ &\approx W_k^{N_j} \int_{\Sigma} \sum_{l=1}^{N_{j+1}} \Xi_j^{(i)}(y_k^{N_j}, y_l^{N_{j+1}}) \Xi_{j+1}^{(i)}(y_l^{N_{j+1}}, y) f(y) d\omega(y) \\ &= W_k^{N_j} \sum_{l=1}^{N_{j+1}} \Xi_j^{(i)}(y_k^{N_j}, y_l^{N_{j+1}}) a_l^{N_{j+1}} \end{aligned} \quad (4.38)$$

for  $j = J - 1, \dots, J_0$  and  $k = 1, \dots, N_j$ .

The last formula is known as the pyramid step.

We see that once the coefficients  $\mathbf{a}^{N_j}$  are calculated, the coefficients  $\mathbf{a}^{N_{j-1}}$  are obtained



by (4.38).

Altogether, starting from an initial value  $\mathbf{a}^{N_J}$  all the coefficient vectors can be calculated recursively. Note that the coefficients  $\mathbf{a}^{N_J}$  in the initial step do not depend on the choice of  $\Xi_J^{(i)} = \Phi_{J+L}^{D;(i)}$ . Furthermore, the functions  $\Xi_j^{(i)}$ ,  $j = J_0, \dots, J$ , can be chosen independently of the  $\Sigma$ -scaling function used in the integrals  $\mathbf{p}_j^{D;(i)}(f)$  and  $\mathbf{r}_j^{D;(i)}(f)$ .

Finally, following the proposed pyramid scheme described by (4.33) and (4.38), the decomposition and reconstruction process of the wavelet approximation can be illustrated briefly as follows:

$$\begin{array}{ccccccc}
 f & \rightarrow & \mathbf{a}^{N_J} & \rightarrow & \mathbf{a}^{N_{J-1}} & \rightarrow \dots \rightarrow & \mathbf{a}^{N_{J_0+1}} & \rightarrow & \mathbf{a}^{N_{J_0}} \\
 & & \downarrow & & \downarrow & & \downarrow & \swarrow \searrow & \\
 & & \mathbf{r}_J^{D;(i)}(f) & & \mathbf{r}_{J-1}^{D;(i)}(f) & & \mathbf{r}_{J_0+1}^{D;(i)}(f) & \mathbf{r}_{J_0}^{D;(i)}(f) & \mathbf{p}_{J_0}^{D;(i)}(f)
 \end{array}$$

(decomposition scheme)

$$\begin{array}{ccccccc}
 \mathbf{a}^{N_{J_0}} & & \mathbf{a}^{N_{J_0+1}} & & \mathbf{a}^{N_{J-1}} & & \\
 \downarrow & & \downarrow & & \downarrow & & \\
 \mathbf{r}_{J_0}^{D;(i)}(f) & & \mathbf{r}_{J_0+1}^{D;(i)}(f) & & \mathbf{r}_{J-1}^{D;(i)}(f) & & \\
 \swarrow & & \swarrow & & \swarrow & & \\
 \mathbf{p}_{J_0}^{D;(i)}(f) & \rightarrow + \rightarrow & \mathbf{p}_{J_0+1}^{D;(i)}(f) & \rightarrow + \dots + \rightarrow & \mathbf{p}_{J-1}^{D;(i)}(f) & \rightarrow + \rightarrow & \mathbf{p}_J^{D;(i)}(f)
 \end{array}$$

(reconstruction scheme).

## 4.5 Multiscale Solution of the Inner Displacement Boundary-Value Problem of Elastostatics

In the sequel, we discuss the solution of the inner displacement boundary-value problem by means of wavelet approximation techniques derived in the preceding chapters. Existence, uniqueness and regularity of the solution of the problem are known from Chapter 3.

For given  $f \in c(\Sigma)$  the solution  $u \in \text{pot}(\overline{\Sigma_{int}})$  with  $u|_{\Sigma} = f$  of the (inner) displacement problem can be expressed uniquely by a double layer potential

$$u(x) = \int_{\Sigma} \left( \frac{\partial}{\partial \nu(y)} \frac{1}{|x-y|} \right) \mathbf{\Lambda}(x-y) g(y) d\omega(y), \quad g \in \ell^2(\Sigma). \quad (4.39)$$

As it is known, the corresponding integral equation reads as follows

$$(2\pi I - \mathbf{p}_n(0))g = -f, \quad g \in \ell^2(\Sigma). \quad (4.40)$$

More explicitly,

$$2\pi g(x) - \int_{\Sigma} \left( \frac{\partial}{\partial \nu(y)} \frac{1}{|x - y|} \right) \Lambda(x - y) g(y) d\omega(y) = -f(x), \quad g \in \ell^2(\Sigma), \quad x \in \Sigma. \quad (4.41)$$

To approximate  $u$  given by the double layer potential in (4.39), we use the concept stated in Theorem 4.1. In accordance with this approach we are able to rewrite (4.41) approximately in the form

$$2\pi g(x) - \int_{\Sigma} \Phi_L^{D;(7)}(x, y) g(y) d\omega(y) = -f(x), \quad x \in \Sigma, \quad (4.42)$$

provided that  $L \in \mathbb{N}$  is sufficiently large. Once the boundary integral equation (4.40) has been solved, the density function  $g$  is inserted into (4.39) and thereby the (approximate) solution  $u$  is obtained in  $\Sigma_{int}$ . Like in many cases of boundary integral equations there is, in general, no straightforward way of constructing the unknown function  $g$ . It is, therefore, necessary to apply a suitable approximation method. In this respect we again go back to Theorem 4.1 that enables us to formulate

$$g(y) = \lim_{j \rightarrow \infty} \int_{\Sigma} \Phi_j^{D;(5)}(y, z) g(z) d\omega(z). \quad (4.43)$$

Using an appropriate numerical integration technique, an approximation of  $g$  of level  $J$ , denoted by  $g_J$ , can be expressed by

$$\begin{aligned} g_J(y) &= \sum_{l=1}^{N_J} W_l^{N_J} \Phi_J^{D;(5)}(y, y_l^{N_J}) g(y_l^{N_J}) \\ &= \sum_{l=1}^{N_J} \Phi_J^{D;(5)}(y, y_l^{N_J}) b_l^{N_J}, \end{aligned} \quad (4.44)$$

where  $W_l^{N_J}$ ,  $l = 1, \dots, N_J$  are the integration weights corresponding to the nodal points  $y_l^{N_J} \in \Sigma$ ,  $l = 1, \dots, N_J$  and  $b_l^{N_J} \in \mathbb{R}^3$ ,  $l = 1, \dots, N_J$ .

The unknowns  $b_l^{N_J} \in \mathbb{R}^3$ ,  $l = 1, \dots, N_J$ , are deducible from (4.40) by solving a system of linear equations obtained by a suitable approximation method such as collocation, Galerkin procedure, least square approximation etc. (see for example, [25]). In consequence, we are led to the following system of equations for the unknowns  $b_l^{N_J}$ ,  $l = 1, \dots, N_J$ ,

$$\sum_{l=1}^{N_J} \left( 2\pi \Phi_J^{D;(5)}(y_m^{N_J}, y_l^{N_J}) - \sum_{k=1}^{N_J} W_k^{N_J} \Phi_J^{D;(5)}(y_m^{N_J}, y_k^{N_J}) \Phi_L^{D;(7)}(y_k^{N_J}, y_l^{N_J}) \right) b_l^{N_J} = -f(y_m^{N_J}), \quad (4.45)$$

$m = 1, \dots, N_J$ .

It should be mentioned that such a consideration leads to a system of linear equations with a 'full' matrix which seems to require much computational work for the definition of the matrix as well as for the solution. In this context, taking into consideration the localization behavior of the kernel functions, suitable accelerating techniques such as panel clustering, domain decomposition etc can efficiently be used (see, for example, [44],[47],[49]), which is, however, beyond the scope of this work. Moreover, further modifications of such techniques relevant to this particular consideration will be needed.

In this respect, a variant of our tree algorithm comes into play: once the starting values  $\mathbf{b}^{N_J} = (b_1^{N_J}, \dots, b_{N_J}^{N_J})^T \in \mathbb{R}^{3 \times N_J}$  are given, the coefficients  $\mathbf{b}^{N_j} = (b_1^{N_j}, \dots, b_{N_j}^{N_j})^T \in \mathbb{R}^{3 \times N_j}$ ,  $j = J_0, \dots, J-1$ , are obtained by the recursion formula

$$b_k^{N_j} = W_k^{N_j} \sum_{l=1}^{N_{j+1}} \Xi_j^{(i)}(y_k^{N_j}, y_l^{N_{j+1}}) b_l^{N_{j+1}}, \quad k = 1, \dots, N_j. \quad (4.46)$$

The corresponding approximate integrals are obtained by

$$\mathbf{p}_j^{D;(i)}(g)(x) \approx \sum_{k=1}^{N_j} \Phi_j^{D;(5)}(x, y_k^{N_j}) b_k^{N_j}, \quad x \in \Sigma, \quad j = J_0, \dots, J, \quad (4.47)$$

and

$$\mathbf{r}_{j-1}^{D;(i)}(g)(x) \approx \sum_{k=1}^{N_j} \Psi_{j-1}^{D;(5)}(x, y_k^{N_j}) b_k^{N_j}, \quad x \in \Sigma, \quad j = J_0 + 1, \dots, J, \quad (4.48)$$

where

$$\mathbf{r}_{j-1}^{D;(i)}(g)(x) = \mathbf{p}_j^{D;(i)}(g)(x) - \mathbf{p}_{j-1}^{D;(i)}(g)(x). \quad (4.49)$$

Hence, we finally arrive at the following theorem for the inner displacement boundary-value problems of the Cauchy-Navier theory.

**Theorem 4.6** *Let  $\Sigma$  be a regular surface. For given  $f \in c(\Sigma)$ , let  $u$  be the potential of class  $\text{pot}(\overline{\Sigma_{int}})$  with  $u|_{\Sigma} = f$ . Then the function  $f_J \in c(\Sigma)$  given by*

$$\begin{aligned} f_J(x) = & -2\pi \sum_{l=1}^{N_{J_0}} \Phi_{J_0}^{D;(i)}(x, y_l^{N_{J_0}}) b_l^{N_{J_0}} - 2\pi \sum_{j=J_0}^{J-1} \sum_{l=1}^{N_j} \Psi_j^{D;(i)}(x, y_l^{N_j}) b_l^{N_j} \\ & + \sum_{l=1}^{N_{J_0}} \left( \int_{\Sigma} \Phi_L^{D;(7)}(x, y) \Phi_{J_0}^{D;(i)}(y, y_l^{N_{J_0}}) d\omega(y) \right) b_l^{N_{J_0}} \\ & + \sum_{j=J_0}^{J-1} \sum_{l=1}^{N_j} \left( \int_{\Sigma} \Phi_L^{D;(7)}(x, y) \Psi_j^{D;(i)}(y, y_l^{N_j}) d\omega(y) \right) b_l^{N_j}, \end{aligned} \quad (4.50)$$

$x \in \Sigma$ , represents a  $J$ -scale approximation of  $f \in c(\Sigma)$ , in the sense of  $\|\cdot\|_{\ell^2(\Sigma)}$ , where  $i = 2, 3, 5, 6$  and  $L \in \mathbb{N}$  is sufficiently large. Furthermore,

$$u_J = \sum_{l=1}^{N_{J_0}} \int_{\Sigma} \Phi_L^{D;(7)}(\cdot, y) \Phi_{J_0}^{D;(i)}(y, y_l^{N_{J_0}}) d\omega(y) b_l^{N_{J_0}} \\ + \sum_{j=J_0}^{J-1} \sum_{l=1}^{N_J} \int_{\Sigma} \Phi_L^{D;(7)}(\cdot, y) \Psi_J^{D;(i)}(y, y_l^{N_J}) d\omega(y) b_l^{N_J} \quad (4.51)$$

represents a  $J$ -scale approximation of  $u$  in the sense of  $\|\cdot\|_{c(\overline{\mathcal{K}})}$  for every subset  $\mathcal{K} \subset \Sigma_{int}$  with  $\text{dist}(\overline{\mathcal{K}}, \Sigma) > 0$ .

In other words, locally uniform approximation on  $\Sigma_{int}$  is established from quadratic approximation on  $\Sigma$  by means of Cauchy-Navier wavelets.

## 4.6 Cauchy-Navier Wavelets associated to Dual Layer Potentials

In preceding sections, our wavelet construction was based on layer potentials in Cauchy-Navier theory of elasticity and the associated limit and jump relations. The corresponding wavelets canonically involve integration over  $\Sigma$  to approximate the (boundary) function at a particular point  $x \in \Sigma$ , in which the different resolutions are taken letting  $x_\tau$  tend to  $x$  (or equivalently  $\tau$  tend to 0). In contrast to the above wavelet approach based on integration procedures over the regular surface  $\Sigma$ , one can introduce an alternative wavelet procedure by means of dual layer potentials.

In what follows, we develop the Cauchy-Navier wavelet method by means of jump relations (2.51)-(2.58) associated to dual layer potential operators. In this context, we only investigate the resulting facts which are different from the classical case. The remaining results can easily be established in analogy to the theory developed in previous sections. Moreover, we are concerned with scale discrete wavelet reconstructions, which provide an alternative technique to treat the inner displacement boundary-value problems in a multistep setting.

We start from the following definition.

**Definition 4.5** Suppose that  $\tau$  is a positive real number such that  $0 < \tau \leq \bar{\tau}$  (where  $\bar{\tau}$  is defined in Section 2.3). Then the family  $\{\Phi_\tau^{*(i)}\}$  of kernels  $\Phi_\tau^{*(i)} : \Sigma \times \Sigma \longrightarrow \mathbb{R}^{3 \times 3}$ ,  $i = 1, \dots, 8$ , defined by

$$\begin{aligned}
\Phi_\tau^{*(1)}(x, y) &= \Gamma(x - y_\tau), \\
\Phi_\tau^{*(2)}(x, y) &= \frac{1}{2\pi} \left( \left( \frac{\partial}{\partial \nu(x)} \frac{1}{|x - y_\tau|} \right) \Lambda(x - y_\tau) - \left( \frac{\partial}{\partial \nu(x)} \frac{1}{|x - y|} \right) \Lambda(x - y) \right), \\
\Phi_\tau^{*(3)}(x, y) &= -\frac{1}{2\pi} \left( \left( \frac{\partial}{\partial \nu(y)} \frac{1}{|x - y_\tau|} \right) \Lambda(x - y_\tau) - \left( \frac{\partial}{\partial \nu(y)} \frac{1}{|x - y|} \right) \Lambda(x - y) \right), \\
\Phi_\tau^{*(4)}(x, y) &= \Gamma(x - y_\tau) - \Gamma(x - y_{-\tau}), \\
\Phi_\tau^{*(5)}(x, y) &= \frac{1}{4\pi} \left( \left( \frac{\partial}{\partial \nu(x)} \frac{1}{|x - y_\tau|} \right) \Lambda(x - y_\tau) - \left( \frac{\partial}{\partial \nu(x)} \frac{1}{|x - y_{-\tau}|} \right) \Lambda(x - y_{-\tau}) \right), \\
\Phi_\tau^{*(6)}(x, y) &= -\frac{1}{4\pi} \left( \left( \frac{\partial}{\partial \nu(y)} \frac{1}{|x - y_\tau|} \right) \Lambda(x - y_\tau) - \left( \frac{\partial}{\partial \nu(y)} \frac{1}{|x - y_{-\tau}|} \right) \Lambda(x - y_{-\tau}) \right), \\
\Phi_\tau^{*(7)}(x, y) &= \frac{1}{2} \left( \left( \frac{\partial}{\partial \nu(x)} \frac{1}{|x - y_\tau|} \right) \Lambda(x - y_\tau) + \left( \frac{\partial}{\partial \nu(x)} \frac{1}{|x - y_{-\tau}|} \right) \Lambda(x - y_{-\tau}) \right), \\
\Phi_\tau^{*(8)}(x, y) &= \frac{1}{2} \left( \left( \frac{\partial}{\partial \nu(y)} \frac{1}{|x - y_\tau|} \right) \Lambda(x - y_\tau) + \left( \frac{\partial}{\partial \nu(y)} \frac{1}{|x - y_{-\tau}|} \right) \Lambda(x - y_{-\tau}) \right),
\end{aligned}$$

is called dual (Cauchy-Navier)  $\Sigma$ -scaling function of type  $i$ . Correspondingly, the family  $\{\Psi_\tau^{*(i)}\}$  of kernels  $\Psi_\tau^{*(i)} : \Sigma \times \Sigma \longrightarrow \mathbb{R}^{3 \times 3}$ ,  $i = 1, \dots, 8$ , given by

$$\Psi_\tau^{*(i)}(x, y) = -(\alpha(\tau))^{-1} \frac{d}{d\tau} \Phi_\tau^{*(i)}(x, y),$$

is called a dual (Cauchy-Navier)  $\Sigma$ -wavelet of type  $i$ .

Note that we have chosen  $\alpha(\tau) = \tau^{-1}$ .

As a consequence of Theorem 2.1 we are led to the following result in analogy to Theorem 4.1, which is to be understood in the  $\ell^2(\Sigma)$ -sense.

**Theorem 4.7** For  $f \in \ell^2(\Sigma)$ ,  $x \in \Sigma$ , we have

$$\lim_{\substack{\tau \rightarrow 0 \\ \tau > 0}} \int_{\Sigma} \Phi_\tau^{*(i)}(x, y) f(y) d\omega(y) = \begin{cases} \int_{\Sigma} \Gamma(x - y) f(y) d\omega(y), & i = 1 \\ 0, & i = 4 \\ f(x), & i = 2, 3, 5, 6 \\ \int_{\Sigma} \left( \frac{\partial}{\partial \nu(x)} \frac{1}{|x - y|} \right) \Lambda(x - y) f(y) d\omega(y), & i = 7 \\ \int_{\Sigma} \left( \frac{\partial}{\partial \nu(y)} \frac{1}{|x - y|} \right) \Lambda(x - y) f(y) d\omega(y), & i = 8. \end{cases} \quad (4.52)$$

In connection with Definition 4.3 we easily define the wavelet transform for the dual case.

**Definition 4.6** Suppose that  $\tau$  is a positive real number such that  $\tau \leq \bar{\tau}$ . Let  $\{\Phi_\tau^{*(i)}\}$  be a dual  $\Sigma$ -scaling function of type  $i$ . Then the associated  $\Sigma$ -wavelet transform of type  $i$ ,  $(\mathbf{WT})_\tau^{*(i)} : \ell^2(\Sigma) \longrightarrow \ell^2(\Sigma)$  of a function  $f \in \ell^2(\Sigma)$  is defined by

$$(\mathbf{WT})_\tau^{*(i)}(f)(x) = \int_{\Sigma} \Psi_\tau^{*(i)}(x, y) f(y) d\omega(y). \quad (4.53)$$

Parallel to the classical approach, we now arrive at a scale continuous reconstruction formula with respect to the dual wavelets, however, in general, we have to restrict the scale parameter  $\tau$  to the finite interval  $(0, \bar{\tau}]$ .

We restrict ourselves to the investigation of scale discrete scaling functions and wavelets.

Let the set  $\mathbb{Z}_{\bar{\tau}}$  be defined by

$$\mathbb{Z}_{\bar{\tau}} = \{j \in \mathbb{Z} \mid \tau_j < \bar{\tau}\} \quad (4.54)$$

for appropriately chosen parameter  $\tau_j$ , where  $\{\tau_j\}_{j \in \mathbb{Z}}$  denotes a monotonically decreasing sequence of positive real numbers satisfying the property

$$\lim_{j \rightarrow \infty} \tau_j = 0. \quad (4.55)$$

Moreover, we let

$$J_0 = \min_j \{j \in \mathbb{Z} \mid \tau_j < \bar{\tau}\}.$$

Given a dual  $\Sigma$ -scaling function  $\{\Phi_{\tau}^{*(i)}\}$ ,  $0 < \tau \leq \bar{\tau}$  of type  $i$ , we are able to define the (scale) discretized dual  $\Sigma$ -scaling function  $\{\Phi_j^{D*;(i)}\}$ , and wavelets  $\{\Psi_j^{D*;(i)}\}$ ,  $J_0 \leq j < \infty$  of type  $i$ .

Hence, we let

$$\Phi_j^{D*;(i)} = \Phi_{\tau_j}^{D*;(i)}. \quad (4.56)$$

In connection with Theorem 4.4 we are now led to the following result.

**Theorem 4.8** *For  $f \in \ell^2(\Sigma)$ , the limit*

$$\lim_{j \rightarrow \infty} \int_{\Sigma} \Phi_j^{D*;(i)}(x, y) f(y) d\omega(y) = \begin{cases} \int_{\Sigma} \Gamma(x - y) f(y) d\omega(y), & i = 1 \\ 0, & i = 4 \\ f(x), & i = 2, 3, 5, 6 \\ \int_{\Sigma} \left( \frac{\partial}{\partial \nu(x)} \frac{1}{|x - y|} \right) \Lambda(x - y) f(y) d\omega(y), & i = 7 \\ \int_{\Sigma} \left( \frac{\partial}{\partial \nu(y)} \frac{1}{|x - y|} \right) \Lambda(x - y) f(y) d\omega(y), & i = 8 \end{cases} \quad (4.57)$$

holds in the  $\|\cdot\|_{\ell^2(\Sigma)}$ -sense, where  $(x, y) \in \Sigma \times \Sigma$ .

**Proof.** This result follows from the proof of Theorem 4.4.  $\square$

**Definition 4.7** *Let  $\{\Phi_j^{D*;(i)}\}$ ,  $J_0 \leq j < \infty$ , be a scale discretized dual  $\Sigma$ -scaling function of type  $i$ . Then the corresponding (scale) discretized dual  $\Sigma$ -wavelet function  $\Psi_j^{D*;(i)}$  of type  $i$  is defined by*

$$\Psi_j^{D*;(i)}(x, y) = \Psi_{\tau_j}^{*(i)}(x, y) = \int_{\tau_{j+1}}^{\tau_j} \Psi_{\tau}^{*(i)}(x, y) \frac{d\tau}{\tau}, \quad J_0 \leq j < \infty, \quad x, y \in \Sigma, \quad i = 1, \dots, 8. \quad (4.58)$$

With the definition of  $\Psi_\tau^{*(i)}$  we immediately obtain

$$\Psi_j^{D*;(i)}(x, y) = - \int_{\tau_{j+1}}^{\tau_j} \tau \frac{d}{d\tau} \Psi_\tau^{*(i)}(x, y) \frac{d\tau}{\tau} = \Phi_{j+1}^{D*;(i)}(x, y) - \Phi_j^{D*;(i)}(x, y), \quad x, y \in \Sigma. \quad (4.59)$$

**Theorem 4.9** For  $f \in \ell^2(\Sigma)$ , the limit

$$\lim_{\substack{j \rightarrow \infty \\ j \geq J_0}} \int_{\Sigma} \Phi_j^{D*;(i)}(x, y) f(y) d\omega(y) = \begin{cases} \int_{\Sigma} \Gamma(x - y) f(y) d\omega(y), & i = 1 \\ 0, & i = 4 \\ f(x), & i = 2, 3, 5, 6 \\ \int_{\Sigma} \left( \frac{\partial}{\partial \nu(x)} \frac{1}{|x - y|} \right) \Lambda(x - y) f(y) d\omega(y), & i = 7 \\ \int_{\Sigma} \left( \frac{\partial}{\partial \nu(y)} \frac{1}{|x - y|} \right) \Lambda(x - y) f(y) d\omega(y), & i = 8 \end{cases} \quad (4.60)$$

holds for all  $x \in \Sigma$ .

**Definition 4.8** Let  $\{\Phi_j^{D*;(i)}\}$  be a dual  $\Sigma$ -scaling function of type  $i$ . Then the associated dual  $\Sigma$ -wavelet transform of type  $i$   $(\mathbf{WT})_j^{D*;(i)} : \ell^2(\Sigma) \longrightarrow \ell^2(\Sigma)$  of a function  $f \in \ell^2(\Sigma)$  is defined by

$$(\mathbf{WT})_j^{D*;(i)}(f)(x) = \int_{\Sigma} \Psi_j^{D*;(i)}(x, y) f(y) d\omega(y), \quad x \in \Sigma. \quad (4.61)$$

Finally, we arrive at the following important theorem.

**Theorem 4.10** Let  $\{\Phi_j^{D*;(i)}\}$ ,  $J_0 \leq j < \infty$ , be a (scale) discretized  $\Sigma$ -scaling function of type  $i$ . Then the multiscale representation of a function  $f \in \ell^2(\Sigma)$

$$\begin{aligned} & \int_{\Sigma} \Phi_{\tau_J}^{*(i)}(x, y) f(y) d\omega(y) + \sum_{j=J}^{\infty} \int_{\Sigma} \Psi_j^{D*;(i)}(x, y) f(y) d\omega(y) \\ &= \begin{cases} \int_{\Sigma} \Gamma(x - y) f(y) d\omega(y), & i = 1 \\ 0, & i = 4 \\ f(x), & i = 2, 3, 5, 6 \\ \int_{\Sigma} \left( \frac{\partial}{\partial \nu(x)} \frac{1}{|x - y|} \right) \Lambda(x - y) f(y) d\omega(y), & i = 7 \\ \int_{\Sigma} \left( \frac{\partial}{\partial \nu(y)} \frac{1}{|x - y|} \right) \Lambda(x - y) f(y) d\omega(y), & i = 8 \end{cases} \end{aligned} \quad (4.62)$$

holds for all  $J \in \mathbb{Z}$  with  $J \geq J_0$ .

Moreover, the operators defined by

$$\mathbf{p}_j^{D*;(i)}(f) = \int_{\Sigma} \Phi_j^{D*;(i)}(\cdot, y) f(y) d\omega(y), \quad f \in \ell^2(\Sigma), \quad (4.63)$$

$$\mathbf{r}_j^{D*;(i)}(f) = \int_{\Sigma} \Psi_j^{D*;(i)}(\cdot, y) f(y) d\omega(y), \quad f \in \ell^2(\Sigma) \quad (4.64)$$

represent scale and detail information, respectively. Moreover, it should be remarked that the above definition of wavelet transform can be regarded as a filter detail information as well.

In the computations of those filters we have a certain restriction for the choice of  $j$ , i.e.  $j \geq J_0$ . Therefore, for the reconstruction formula of a given function  $f \in \ell^2(\Sigma)$ , we need a starting filtered version  $\mathbf{p}_{\tau_J}^{*(i)}(f)$  with suitably chosen  $J$ .

More explicitly, for  $f \in \ell^2(\Sigma)$ , we have an approximate identity

$$\lim_{\substack{j \rightarrow \infty \\ j \geq J_0}} \|f - \mathbf{p}_j^{D*(i)}(f)\|_{\ell^2(\Sigma)} = 0, \quad (4.65)$$

and the multiscale representation of  $f$  can be represented by

$$\mathbf{p}_J^{D*(i)}(f) + \sum_{j=J}^{\infty} \mathbf{r}_j^{D*(i)}(f) = f \quad (4.66)$$

for all  $J \geq J_0$ , where  $i = 2, 3, 5, 6$ .

In consequence, it is not difficult to show that the filters  $\mathbf{p}_j^{*(i)}$  and  $\mathbf{p}_j^{(i)}$  and also the filters  $\mathbf{r}_j^{*(i)}$  and  $\mathbf{r}_j^{(i)}$  represent dual relations with respect to  $\ell^2(\Sigma)$ -topology. To be more explicit, we state the following theorem.

**Theorem 4.11**

- (i) Let  $\mathbf{p}_j^{D;(i)}$  and  $\mathbf{p}_j^{D*,(i)}$ ,  $J_0 \leq j < \infty$ , be the filters of type  $i$  corresponding to the scale discrete  $\Sigma$  scaling functions  $\Phi_j^{D;(i)}$  and  $\Phi_j^{D*,(i)}$ , respectively. Then

$$\langle \mathbf{p}_j^{D*,(i)}(f), g \rangle_{\ell^2(\Sigma)} = \langle f, \mathbf{p}_j^{D;(i)}(g) \rangle_{\ell^2(\Sigma)} \quad (4.67)$$

holds for all  $f, g \in \ell^2(\Sigma)$ .

- (ii) Let  $\mathbf{r}_j^{D;(i)}$  and  $\mathbf{r}_j^{D*,(i)}$ ,  $J_0 \leq j < \infty$ , be the filters of type  $i$  corresponding to the scale discrete  $\Sigma$  wavelets  $\Psi_j^{D;(i)}$  and  $\Psi_j^{D*,(i)}$ , respectively. Then

$$\langle \mathbf{r}_j^{D*,(i)}(f), g \rangle_{\ell^2(\Sigma)} = \langle f, \mathbf{r}_j^{D;(i)}(g) \rangle_{\ell^2(\Sigma)} \quad (4.68)$$

holds for all  $f, g \in \ell^2(\Sigma)$ .

**Proof.**

- (i) Let  $f, g \in \ell^2(\Sigma)$ . For simplicity, we consider the case  $i = 1$ . Thus, the connection with



the symmetry of kernel functions, the straightforward calculations yield

$$\begin{aligned}
\langle \mathbf{p}_j^{D*; (1)}(f), g \rangle_{\ell^2(\Sigma)} &= \int_{\Sigma} \left( \int_{\Sigma} \Gamma(x - y_{\tau_j}) f(y) \, d\omega(y) \right) \cdot g(x) \, d\omega(x) \\
&= \int_{\Sigma} \int_{\Sigma} \Gamma(y_{\tau_j} - x) g(x) \, d\omega(x) \cdot f(y) \, d\omega(y) \\
&= \int_{\Sigma} \int_{\Sigma} \Gamma(x_{\tau_j} - y) g(y) \, d\omega(y) \cdot f(x) \, d\omega(x) \\
&= \int_{\Sigma} f(x) \cdot \left( \int_{\Sigma} \Gamma(x_{\tau_j} - y) g(y) \, d\omega(y) \right) \, d\omega(x) \\
&= \langle f, \mathbf{p}_j^{D; (1)}(g) \rangle_{\ell^2(\Sigma)} .
\end{aligned}$$

(ii) In connection with Part (i) the scale discretized scaling equation (4.59) leads to

$$\begin{aligned}
\langle \mathbf{r}_j^{D*; (i)}(f), g \rangle_{\ell^2(\Sigma)} &= \langle \mathbf{p}_{j+1}^{D*; (i)}(f) - \mathbf{p}_j^{D*; (i)}(f), g \rangle_{\ell^2(\Sigma)} \\
&= \langle \mathbf{p}_{j+1}^{D*; (i)}(f), g \rangle_{\ell^2(\Sigma)} - \langle \mathbf{p}_j^{D*; (i)}(f), g \rangle_{\ell^2(\Sigma)} \\
&= \langle f, \mathbf{p}_{j+1}^{D; (i)}(g) \rangle_{\ell^2(\Sigma)} - \langle f, \mathbf{p}_j^{D; (i)}(g) \rangle_{\ell^2(\Sigma)} \\
&= \langle f, \mathbf{r}_j^{D; (i)}(g) \rangle_{\ell^2(\Sigma)} .
\end{aligned}$$

□

Finally, it should be noted that the above dual multiscale representation also enables us to guarantee fast computation using a suitable tree algorithm. An appropriate pyramid scheme can be obtained in analogy to the classical case, taking into account the integrations over parallel surfaces  $\Sigma(\tau)$  as well as suitable restrictions for the choice of  $\tau$  (cf. Section 4.3, [1],[32]).

# Chapter 5

## A Spectral Approach to Cauchy-Navier Wavelets

The wavelets defined in the last chapter are introduced on particular properties of kernel functions involving the fundamental solutions  $\Gamma_1, \Gamma_2, \Gamma_3$ . In doing so a wavelet concept associated to the Cauchy-Navier equation is established by limit relations in the space domain. In what follows, we restrict ourselves to the geophysically interesting interior Dirichlet problem of linear elasticity corresponding to a spherical boundary. To be more concrete, we use the properties of closure and completeness of the particular system of vector spherical harmonics in the space of  $\ell^2(\Omega)$  of square-integrable vector fields on the unit sphere to deduce a wavelet concept based on limit relations in the spectral domain. The approach is closely related to the vector wavelet theory developed in [30].

We first give a brief overview of this approach as an introductory remark: Once the Cauchy-Navier vector field  $v_{n,l}^{(i)}$  corresponding to the vector spherical harmonics  $y_{n,l}^{(i)}$  has been specified within the spherical framework of the inner space  $\overline{\Omega_{int}}$  of the unit sphere  $\Omega$ , the Green tensor of the inner displacement boundary-value problem can be represented as follows:

$$\mathbf{g}(x, \eta) = \sum_{i=1}^3 \sum_{n=0_i}^{\infty} \sum_{l=1}^{2n+1} v_{n,l}^{(i)}(x) \otimes y_{n,l}^{(i)}(\eta), \quad x \in \overline{\Omega_{int}}, \quad \eta \in \Omega. \quad (5.1)$$

The solution of the associated displacement boundary-value problem then reads as follows: Given a continuous vector field  $f : \Omega \rightarrow \mathbb{R}^3$ , find  $u \in \text{pot}(\overline{\Omega_{int}})$  such that  $u|_{\Omega} = f$ . The displacement boundary-value problem is uniquely solvable in integral form by

$$u(x) = \int_{\Omega} \mathbf{g}(x, \eta) f(\eta) \, d\omega(\eta), \quad x \in \Omega_{int}. \quad (5.2)$$

In consequence, as the Green tensor is explicitly available in spherical nomenclature,  $u$  can be determined by numerical integration avoiding any solution of linear equations. For appropriate integration rules see, for example, [22].

A multiscale approach to the inner displacement boundary-value problem, i.e. a space-dependent frequency analysis in deformation analysis can be obtained by introducing a scaling tensor  $\{\Phi_j^D\}$ ,  $j \in \mathbb{Z}$ . Roughly speaking, a (discrete) Cauchy-Navier scaling function  $\Phi_j^D$  with  $\varphi_j(n)$ , can be represented by a tensor kernel

$$\Phi_j^D(x, \eta) = \sum_{i=1}^3 \sum_{n=0_i}^{\infty} \sum_{l=1}^{2n+1} \varphi_j(n) v_{n,l}^{(i)}(x) \otimes y_{n,l}^{(i)}(\eta), \quad x \in \overline{\Omega_{int}}, \quad (5.3)$$

which converges to the 'Green kernel'  $\mathbf{g}$  as  $j$  tends to infinity. As a matter of fact,  $\{\varphi_j(n)\}$  essentially is understood to be a real monotonically increasing sequence satisfying

$$\lim_{j \rightarrow \infty} \varphi_j(n) = 1 \quad (5.4)$$

for each  $n = 0, 1, \dots$

According to this multiscale principle,  $\Phi_j^D$  constitutes an approximate convolution identity, i.e. the convolution integral

$$\int_{\Omega} \Phi_j^D(x, \eta) f(\eta) d\omega(\eta) \quad (5.5)$$

formally converges to the solution of the inner displacement boundary-value problem

$$\int_{\Omega} \mathbf{g}(x, \eta) f(\eta) d\omega(\eta) = u(x) \quad (5.6)$$

for all  $x \in \overline{\Omega_{int}}$  as  $j$  tends to infinity.

In more detail, if  $u$  is the displacement field corresponding to vector field  $f$  on the unit sphere  $\Omega$ , then

$$\lim_{j \rightarrow \infty} \|u - \Phi_j^D * f\|_{\ell^2(\Omega)} = 0. \quad (5.7)$$

Moreover, in connection with the regularity condition (see Theorem 3.2), for all subsets  $\mathcal{K} \subset \Omega_{int}$  with  $\text{dist}(\overline{\mathcal{K}}, \Omega) > 0$ , we have the approximate identity

$$\lim_{j \rightarrow \infty} \sup_{x \in \overline{\mathcal{K}}} |u(x) - (\Phi_j^D * f)(x)| = 0, \quad (5.8)$$

i.e.,

$$\lim_{j \rightarrow \infty} \|u - \Phi_j^D * f\|_{\ell^c(\overline{\mathcal{K}})} = 0. \quad (5.9)$$

It should be noted that the wavelet transform acts as a space and frequency localization process in the following way: if  $\{\Phi_j^D\}$  is a Cauchy-Navier scaling function and  $j$  is a sufficiently large positive value, then  $\Phi_j^D(x, \cdot)$ ,  $x \in \Omega$ , is highly concentrated around the point  $x$ . Moreover, as  $j$  becomes smaller,  $\Phi_j^D(x, \cdot)$  becomes more and more localized in

frequency. Correspondingly, the space localization is more and more decreasing. In conclusion, the products  $x \mapsto \Phi_j^D(x, \eta)f(\eta)$ ,  $x \in \overline{\Omega_{int}}$ ,  $\eta \in \Omega$ , for each fixed value  $j$ , display information  $u$  at various levels of spatial resolution or frequency bands. Consequently, as  $j$  decreases, the convolution integrals  $\Phi_j^D * f$  display coarser, lower-frequency features. As  $j$  approaches infinity, the integrals give sharper and sharper spatial resolutions. This is quite comparable to the (discrete) wavelet approach in Chapter 4 based on the limit relations of elastic potentials in space domain.

Each scale-space approximation  $\Phi_j^D * f$  must be made directly by computing the relevant convolution integrals. In doing so, however, it is inefficient to use no information from the approximation  $\Phi_j^D * f$  within the computational process of  $\Phi_{j'}^D * f$  provided that  $j < j'$ . In fact, the efficient construction of wavelets begins by a recursive method which is ideal for computation.

$$\lim_{J \rightarrow \infty} \|u - (\Phi_0^D * f) + \sum_{j=0}^J \Psi_j^D * f\|_{\ell^2(\Omega)} = 0 \quad (5.10)$$

provided that

$$\Psi_j^D(x, \eta) = \sum_{i=1}^3 \sum_{n=0_i}^{\infty} \sum_{l=1}^{2n+1} \psi_j(n) v_{n,l}^{(i)}(x) \otimes y_{n,l}^{(i)}(\eta), \quad x \in \overline{\Omega_{int}}, \quad (5.11)$$

is given such that

$$\psi_j(n) = \varphi_{j+1}(n) - \varphi_j(n) \quad (5.12)$$

for  $n = 0, 1, \dots$ . Conventionally, the family  $\{\Psi_j^D\}$  is called a wavelet. The wavelet transform is defined by

$$(\Psi_j^D * f)(x) = \int_{\Omega} \Psi_j^D(x, \eta) f(\eta) d\omega(\eta). \quad (5.13)$$

## 5.1 Cauchy-Navier Vector Fields Corresponding to Vector Spherical Harmonics

First we briefly recapitulate some well-known results on Cauchy-Navier vector fields. For details the reader is referred to [27],[34],[43],[81]. In particular we are interested in finding the vector fields  $v_{n,l}^{(i)} \in \text{pot}(\overline{\Omega_{int}})$  such that  $v_{n,l}^{(i)}|_{\Omega} = y_{n,l}^{(i)}$ ,  $i = 1, 2, 3$ ,  $n = 0_i, 0_i + 1, \dots$ ,  $l = 1, \dots, 2n + 1$ .

We start our investigations by considering some properties of homogeneous harmonic polynomials defined in  $\mathbb{R}^3$ .

**Lemma 5.1** *Let  $H_n : \mathbb{R}^3 \rightarrow \mathbb{R}$ ,  $n \in \mathbb{N}_0$ , be a homogeneous harmonic polynomial of degree  $n$ . Then, for all  $x \in \mathbb{R}^3$ , we have*

- (i)  $\diamond(\nabla_x H_n(x)) = 0$ ,
- (ii)  $\diamond(x \wedge \nabla_x H_n(x)) = 0$ ,
- (iii)  $\diamond(x H_n(x) + \alpha_n |x|^2 \nabla_x H_n(x)) = 0$ ,

where

$$\alpha_n = -\frac{n\sigma + 2 + 3\sigma}{2(n(\sigma + 2) + 1)}. \quad (5.14)$$

**Proof.** These results can be obtained by straightforward calculations.  $\square$

Let  $\{H_{n,l} \mid l = 1, 2, \dots, 2n+1\}$  be a maximal linearly independent system of homogeneous harmonic polynomials of degree  $n$ . We seek a vector field  $v_{n,l}^{(i)} : \overline{\Omega_{int}} \rightarrow \mathbb{R}^3$  in  $\text{pot}(\overline{\Omega_{int}})$  such that  $v_{n,l}^{(i)}|_{\Omega} = y_{n,l}^{(i)}$  (cf. [34]).

**Lemma 5.2** *Let  $v_{n,l}^{(i)} : \Omega_{int} \rightarrow \mathbb{R}^3$ ,  $i = 1, 2, 3$ , be defined by*

$$\begin{aligned} v_{n,l}^{(1)}(x) &= x H_{n,l}(x) + \alpha_n(|x|^2 - 1) \nabla_x H_{n,l}(x), \quad n = 0, 1, \dots, j = 1, \dots, 2n+1, \\ v_{n,l}^{(2)}(x) &= (n(n+1))^{-\frac{1}{2}} (\nabla_x H_{n,l}(x)) - n v_{n,l}^{(1)}(x), \quad n = 1, \dots, j = 1, \dots, 2n+1, \\ v_{n,l}^{(3)}(x) &= (n(n+1))^{-\frac{1}{2}} (x \wedge \nabla_x H_{n,l}(x)), \quad n = 1, \dots, l = 1, \dots, 2n+1, \end{aligned} \quad (5.15)$$

where  $\alpha_n$  is as defined in Lemma 5.1, and  $H_{n,l}$  is given by  $H_{n,l} = |x|^n Y_{n,l}$ ,  $x = |x|\xi$ ,  $\xi \in \Omega$ . Then  $v_{n,l}^{(i)}$  is the only vector field of class  $\text{pot}(\overline{\Omega_{int}})$  such that  $v_{n,l}^{(i)}|_{\Omega} = y_{n,l}^{(i)}$ .

**Proof.** The results of Lemma 5.2 follow from straightforward calculations.  $\square$

In terms of vector spherical harmonics the system (5.15) can be written as

$$\begin{aligned} v_{n,l}^{(1)}(x) &= \sigma_n^{(1)}(r) y_{n,l}^{(1)}(\xi) + \tau_n^{(1)}(r) y_{n,l}^{(2)}(\xi), \\ v_{n,l}^{(2)}(x) &= \sigma_n^{(2)}(r) y_{n,l}^{(1)}(\xi) + \tau_n^{(2)}(r) y_{n,l}^{(2)}(\xi), \\ v_{n,l}^{(3)}(x) &= \sigma_n^{(3)}(r) y_{n,l}^{(3)}(\xi), \end{aligned} \quad (5.16)$$

where  $r = |x|$ ,  $x = r\xi$ ,  $\xi \in \Omega$  and

$$\begin{aligned} \sigma_n^{(1)}(r) &= r^{n-1}(r^2 + n\alpha_n(r^2 - 1)), \\ \sigma_n^{(2)}(r) &= [n(n+1)]^{-\frac{1}{2}} n(1 + n\alpha_n) r^{n-1}(1 - r^2), \\ \sigma_n^{(3)}(r) &= r^n, \\ \tau_n^{(1)}(r) &= \alpha_n [n(n+1)]^{\frac{1}{2}} r^{n-1}(r^2 - 1), \\ \tau_n^{(2)}(r) &= r^{n-1}(1 - n\alpha_n(r^2 - 1)). \end{aligned} \quad (5.17)$$

The (Cauchy-Navier) system  $\{v_{n,l}^{(i)} \mid i = 1, 2, 3, n = 0_i, 0_i + 1, \dots, l = 1, \dots, 2n + 1\}$  is, indeed, orthonormal in the sense that

$$\int_{\Omega} v_{n,l}^{(i)}(\xi) \cdot v_{n',l'}^{(i')}(\xi) d\omega(\xi) = \delta_{i,i'} \delta_{n,n'} \delta_{l,l'}. \quad (5.18)$$

**Remark.** By obvious modifications, this system can be reformulated with respect to a sphere  $\Omega_{\beta}$  of radius  $\beta$ . More precisely, we are easily able to obtain vector fields  $v_{n,l}^{(i)}(\beta, \cdot)$  in  $\text{pot}(\overline{\Omega_{\beta}^{int}})$  satisfying  $v_{n,j}^{(i)}(\beta, \cdot)|_{\Omega_{\beta}} = \frac{1}{\beta} y_{n,j}^{(i)}$  and an orthonormal condition in the sense of  $\ell^2(\Omega_{\beta})$ . The details will be omitted.

**Remark.** Under the assumptions  $3\lambda + 2\mu > 0$ ,  $\mu > 0$  it is not difficult to deduce the following estimates (cf. [34]).

$$\sigma = \frac{\lambda + \mu}{\mu} = \frac{1}{3} + \frac{3\lambda + 2\mu}{3\mu} > \frac{1}{3}.$$

Hence, for all  $n \geq 3$ ,

$$\begin{aligned} |\alpha_n| &= \frac{1}{2} \frac{n\sigma + 2 + 3\sigma}{n\sigma + 2n + 1} \\ &= \frac{1}{2} \frac{1 + \frac{2}{n\sigma} + \frac{3}{n}}{1 + \frac{2}{n} + \frac{1}{n\sigma}} \\ &\leq \frac{1}{2} \frac{2 + \frac{2}{n\sigma}}{1 + \frac{1}{n\sigma}} = 1. \end{aligned}$$

Moreover, for all  $n \geq 1$ , we have

$$|\alpha_n| \leq \frac{1}{2} + \frac{\frac{3}{2n}}{1 + \frac{2}{n\sigma}} \leq 2.$$

Finally, we state the following lemma.

**Lemma 5.3** *Let  $\mathcal{K} \subset \Omega_{int}$  such that  $\text{dist}(\bar{\mathcal{K}}, \Omega) \geq \gamma > 0$ . Then, for all  $x \in \mathcal{K}$ ,*

$$\begin{aligned} |\sigma_n^{(1)}(r)| &\leq (1 - \gamma)^{n-1} (1 + n), \\ |\sigma_n^{(2)}(r)| &\leq (n(n + 1))^{1/2} (1 - \gamma)^{n-1} \\ |\sigma_n^{(3)}(r)| &\leq (1 - \gamma)^n, \\ |\tau_n^{(1)}(r)| &\leq (n(n + 1))^{1/2} (1 - \gamma)^{n-1}, \\ |\tau_n^{(2)}(r)| &\leq (1 - \gamma)^{n-1} (1 + n), \end{aligned}$$

*provided that  $n \geq 3$ , where  $r = |x|$ .*

Finally, it should be mentioned that

$$\|v_{n,l}^{(i)}\|_{c(\overline{\Omega_{int}})} = \sup_{x \in \overline{\Omega_{int}}} |v_{n,l}^{(i)}(x)| \leq 2(1 + n)(1 - \gamma)^{n-1} \sqrt{\frac{2n + 1}{4\pi}}; \quad i \in \{1, 2, 3\}. \quad (5.19)$$

## 5.2 Inner Displacement Boundary-Value Problem

As pointed out above, we deal with the following displacement problem. Given a continuous vector field  $f : \Omega \longrightarrow \mathbb{R}^3$ , find  $u \in \text{pot}(\overline{\Omega_{int}})$  such that  $u|_{\Omega} = f$ .

It is well-known (see, for example, [43]) that the unique solution of this displacement boundary-value problem can be written as

$$u(x) = \int_{\Omega} \mathbf{g}(x, \eta) f(\eta) \, d\omega(\eta), \quad x \in \Omega_{int}, \quad (5.20)$$

where  $\mathbf{g}$  is the Green function of the displacement problem.

In particular, we obtain the following result.

**Lemma 5.4** For  $x \in \overline{\Omega_{int}}$ ,  $i \in \{1, 2, 3\}$ ,

$$v_{n,l}^{(i)}(x) = \int_{\Omega} \mathbf{g}(x, \eta) y_{n,l}^{(i)}(\eta) \, d\omega(\eta). \quad (5.21)$$

**Proof.** The field  $v_{n,l}^{(i)}$  corresponds to the solution of Cauchy-Navier equation associated to the boundary values  $y_{n,l}^{(i)}$  on  $\Omega$ . Hence, in connection with the uniqueness theorem the representation (5.20) implies the required result.  $\square$

Observing this property we are able to formulate (see, for example [43])

**Theorem 5.1** Let  $u$  be the unique solution of the inner displacement boundary-value problem: for a given continuous vector field  $f : \Omega \longrightarrow \mathbb{R}^3$ , find  $u \in \text{pot}(\overline{\Omega_{int}})$  so that  $u|_{\Omega} = f$ . Then  $u$  can be represented in integral form

$$u(x) = \int_{\Omega} \mathbf{g}(x, \eta) f(\eta) \, d\omega(\eta), \quad x \in \Omega_{int}. \quad (5.22)$$

Moreover,  $u$  admits a series representation of the form

$$u(x) = \sum_{i=1}^3 \sum_{n=0_i}^{\infty} \sum_{l=1}^{2n+1} \langle f, y_{n,l}^{(i)} \rangle_{\ell^2(\Omega)} v_{n,l}^{(i)}(x), \quad (5.23)$$

in the sense that

$$\lim_{N \rightarrow \infty} \left( \int_{\Omega} \left| f(\xi) - \sum_{i=1}^3 \sum_{n=0_i}^N \sum_{l=1}^{2n+1} \langle f, y_{n,l}^{(i)} \rangle_{\ell^2(\Omega)} y_{n,l}^{(i)}(\xi) \right|^2 d\omega(\xi) \right)^{1/2} = 0 \quad (5.24)$$

implies that the uniform convergence of the series to  $u$  on every subset  $\mathcal{K} \subset \Omega_{int}$  with  $\text{dist}(\overline{\mathcal{K}}, \Omega) > 0$ , i.e.

$$\lim_{N \rightarrow \infty} \sup_{x \in \overline{\mathcal{K}}} \left| u(x) - \sum_{i=1}^3 \sum_{n=0_i}^N \sum_{l=1}^{2n+1} \langle f, y_{n,l}^{(i)} \rangle_{\ell^2(\Omega)} v_{n,l}^{(i)}(x) \right| = 0. \quad (5.25)$$

Once again, it should be remarked that the convergence in  $\ell^2(\Omega)$ —topology on  $\Omega$  implies that the convergence in the sense of  $\|\cdot\|_{\ell^2(\overline{\mathcal{K}})}$  for all subsets  $\mathcal{K} \subset \overline{\Omega_{int}}$  with  $\text{dist}(\overline{\mathcal{K}}, \Omega) > 0$  (cf. [34]).

**Proof.** (cf. [43]). By the completeness of the system  $\{y_{n,l}^{(i)}\}$  in  $\ell^2(\Omega)$  we have,

$$\left\| f - \sum_{i=1}^3 \sum_{n=0_i}^N \sum_{l=1}^{2n+1} (f^{(i)})^\wedge(n, l) y_{n,l}^{(i)} \right\|_{\ell^2(\Omega)} \longrightarrow 0, \quad \text{as } N \longrightarrow \infty, \quad (5.26)$$

for all  $f \in \ell^2(\Omega)$ .

Moreover,

$$u(x) = \int_{\Omega} \mathbf{g}(x, \eta) f(\eta) d\omega(\eta) \quad (5.27)$$

and

$$v_{n,l}^{(i)}(x) = \int_{\Omega} \mathbf{g}(x, \eta) y_{n,l}^{(i)} d\omega(\eta). \quad (5.28)$$

It follows that

$$\begin{aligned} & \left| u(x) - \sum_{i=1}^3 \sum_{n=0_i}^N \sum_{l=1}^{2n+1} (f^{(i)})^\wedge(n, l) v_{n,l}^{(i)}(x) \right| \\ &= \left| \int_{\Omega} \mathbf{g}(x, \eta) f(\eta) d\omega(\eta) - \sum_{i=1}^3 \sum_{n=0_i}^N \sum_{l=1}^{2n+1} (f^{(i)})^\wedge(n, l) \int_{\Omega} \mathbf{g}(x, \eta) y_{n,l}^{(i)}(\eta) d\omega(\eta) \right| \\ &= \left| \int_{\Omega} \mathbf{g}(x, \eta) \left( f(\eta) - \sum_{i=1}^3 \sum_{n=0_i}^N \sum_{l=1}^{2n+1} (f^{(i)})^\wedge(n, l) y_{n,l}^{(i)}(\eta) \right) d\omega(\eta) \right|. \end{aligned}$$

By applying the Cauchy-Schwarz inequality we are able to estimate for  $x \in \overline{\mathcal{K}}$

$$\begin{aligned} & \left| u(x) - \sum_{i=1}^3 \sum_{n=0_i}^N \sum_{l=1}^{2n+1} (f^{(i)})^\wedge(n, l) v_{n,l}^{(i)}(x) \right| \\ &\leq \left( \int_{\Omega} \sum_{k=1}^3 |\mathbf{g}(x, \eta) \epsilon^k|^2 d\omega(\eta) \right)^{1/2} \left\| f - \sum_{i=1}^3 \sum_{n=0_i}^N \sum_{l=1}^{2n+1} (f^{(i)})^\wedge(n, l) y_{n,l}^{(i)} \right\|_{\ell^2(\Omega)} \\ &\leq C(\mathcal{K}) \left\| f - \sum_{i=1}^3 \sum_{n=0_i}^N \sum_{l=1}^{2n+1} (f^{(i)})^\wedge(n, l) y_{n,l}^{(i)} \right\|_{\ell^2(\Omega)}, \end{aligned}$$

where  $C(\mathcal{K})$  is a constant depending on the set  $\mathcal{K} \subset \Omega_{int}$ .



This implies that

$$\begin{aligned} \sup_{x \in \mathcal{K}} \left| u(x) - \sum_{i=1}^3 \sum_{n=0_i}^N \sum_{l=1}^{2n+1} (f^{(i)})^\wedge(n, l) v_{n,l}^{(i)}(x) \right| \\ \leq C(\mathcal{K}) \left\| f - \sum_{i=1}^3 \sum_{n=0_i}^N \sum_{l=1}^{2n+1} (f^{(i)})^\wedge(n, l) y_{n,l}^{(i)} \right\|_{\ell^2(\Omega)}. \end{aligned}$$

The right hand side tends to 0 as  $N \rightarrow \infty$ , which completes the proof.  $\square$

It should be remarked that the Green tensor kernel

$$\mathbf{g}(x, \eta) = \sum_{i=1}^3 \sum_{n=0_i}^\infty \sum_{l=1}^{2n+1} v_{n,l}^{(i)}(x) \otimes y_{n,l}^{(i)}(\eta), \quad x \in \Omega_{int}, \quad \eta \in \Omega \quad (5.29)$$

can be equivalently written as follows:

$$\begin{aligned} \mathbf{g}(x, \eta) = & \sum_{n=0}^\infty \left\{ \frac{2n+1}{4\pi} \right\} \left\{ \sigma_n^{(1)}(r) \mathbf{p}_n^{(1,1)}(\xi, \eta) \right\} + \sum_{n=1}^\infty \left\{ \frac{2n+1}{4\pi} \right\} \left\{ \tau_n^{(1)}(r) \mathbf{p}_n^{(2,1)}(\xi, \eta) \right\} \\ & + \sum_{n=1}^\infty \left\{ \frac{2n+1}{4\pi} \right\} \left\{ \sigma_n^{(2)}(r) \mathbf{p}_n^{(1,2)}(\xi, \eta) + \tau_n^{(2)}(r) \mathbf{p}_n^{(2,2)}(\xi, \eta) \right\} \\ & + \sum_{n=1}^\infty \left\{ \frac{2n+1}{4\pi} \right\} \left\{ \sigma_n^{(3)}(r) \mathbf{p}_n^{(3,3)}(\xi, \eta) \right\}. \end{aligned} \quad (5.30)$$

Following this decomposition we write that

$$\mathbf{g}_{nor}(x, \eta) = \sum_{n=0}^\infty \left\{ \frac{2n+1}{4\pi} \right\} \left\{ \sigma_n^{(1)}(r) \mathbf{p}_n^{(1,1)}(\xi, \eta) \right\} + \sum_{n=1}^\infty \left\{ \frac{2n+1}{4\pi} \right\} \left\{ \tau_n^{(1)}(r) \mathbf{p}_n^{(2,1)}(\xi, \eta) \right\} \quad (5.31)$$

is associated to the radial displacements of  $f$  on  $\Omega$ , while

$$\begin{aligned} \mathbf{g}_{tan}(x, \eta) = & \sum_{n=1}^\infty \left\{ \frac{2n+1}{4\pi} \right\} \left\{ \sigma_n^{(2)}(r) \mathbf{p}_n^{(1,2)}(\xi, \eta) + \tau_n^{(2)}(r) \mathbf{p}_n^{(2,2)}(\xi, \eta) \right\} \\ & + \sum_{n=1}^\infty \left\{ \frac{2n+1}{4\pi} \right\} \left\{ \sigma_n^{(3)}(r) \mathbf{p}_n^{(3,3)}(\xi, \eta) \right\}. \end{aligned} \quad (5.32)$$

associates the tangential displacements of  $f$  on  $\Omega$ .

### 5.3 A Multiscale Approximation

We begin by introducing an admissibility condition.

### 5.3.1 (Scale Discrete) Cauchy-Navier Scaling Functions

Let  $\ell^2(\overline{\Omega_{int}} \times \Omega)$  denote the set of all square-integrable functions defined on  $\overline{\Omega_{int}} \times \Omega$  equipped with the inner product

$$\langle \mathbf{f}, \mathbf{g} \rangle_{\ell^2(\overline{\Omega_{int}} \times \Omega)} = \int_{\overline{\Omega_{int}}} \int_{\Omega} \mathbf{f}(x, \xi) : \mathbf{g}(x, \xi) \, d\omega(\xi) \, dx. \quad (5.33)$$

We begin our wavelet approach with the following definition (cf. [30]).

**Definition 5.1** *A piecewise continuous function  $\gamma_0 : [0, \infty) \rightarrow \mathbb{R}$  is said to satisfy an admissibility condition, if*

$$\sum_{n=0}^{\infty} \frac{(2n+1)}{4\pi} \left( \sup_{x \in [n, n+1)} |\gamma_0(x)| \right)^2 < \infty. \quad (5.34)$$

We state the following definitions in parallel to the theory developed in [34].

**Definition 5.2** *Let the function  $\varphi_0 : [0, \infty) \rightarrow \mathbb{R}$  satisfy the admissibility condition (5.34) and the following properties:*

- (i)  $\varphi_0$  is monotonically decreasing,
- (ii)  $\varphi_0$  is continuous at 0,
- (iii)  $\varphi_0(0) = 1$ .

*Then the real-valued function  $\varphi_0$  is called the generator of the scale discrete Cauchy-Navier scaling function  $\Phi_0^D : \overline{\Omega_{int}} \times \Omega \rightarrow \mathbb{R}^{3 \times 3}$  defined by*

$$\Phi_0^D(x, \eta) = \sum_{i=1}^3 \sum_{n=0}^{\infty} \sum_{l=1}^{2n+1} (\varphi_0(n)) v_{n,l}^{(i)}(x) \otimes y_{n,l}^{(i)}(\eta), \quad x \in \overline{\Omega_{int}}, \eta \in \Omega. \quad (5.35)$$

**Definition 5.3** *Let  $\varphi_0$  be a generator of a scale discrete Cauchy-Navier scaling function  $\Phi_0^D$  as defined in (5.35). Then, for all  $j \in \mathbb{Z}$ , the dilated generator  $\varphi_j : (0, \infty) \rightarrow \mathbb{R}$ , is defined by*

$$\varphi_j(x) = \varphi_0(2^{-j}x), \quad \text{for all } x \in (0, \infty). \quad (5.36)$$

*Moreover, the Cauchy-Navier scaling function  $\Phi_j^D : \overline{\Omega_{int}} \times \Omega \rightarrow \mathbb{R}^{3 \times 3}$  is given by*

$$\Phi_j^D(x, \eta) = \sum_{i=1}^3 \sum_{n=0}^{\infty} \sum_{l=1}^{2n+1} (\varphi_j(n)) v_{n,l}^{(i)}(x) \otimes y_{n,l}^{(i)}(\eta), \quad x \in \overline{\Omega_{int}}, \eta \in \Omega, j \in \mathbb{Z}. \quad (5.37)$$

Note that the right hand side of (5.37) is well defined, since the condition

$$\sum_{n=0}^{\infty} \frac{(2n+1)}{4\pi} |\varphi_j(n)|^2 < \infty \quad (5.38)$$

holds whenever the admissibility condition (5.34) for  $\varphi_0$  is satisfied (cf. [66]).

As an immediate consequence we are led to the following theorem.

**Theorem 5.2** *Every discrete Cauchy-Navier scaling function  $\Phi_j^D$ ,  $j \in \mathbb{Z}$ , is an element of class  $\ell^2(\overline{\Omega_{int}} \times \Omega)$ .*

**Proof.** To verify this result we reformulate a discrete version of a proof given in [34].

Considering the  $\ell^2(\overline{\Omega_{int}} \times \Omega)$ -inner product (5.33) of two tensors  $v_{n,l}^{(i)} \otimes y_{n,l}^{(i)}$  and  $v_{n',l'}^{(i')} \otimes y_{n',l'}^{(i')}$  we obtain

$$\langle v_{n,l}^{(i)} \otimes y_{n,l}^{(i)}, v_{n',l'}^{(i')} \otimes y_{n',l'}^{(i')} \rangle_{\ell^2(\overline{\Omega_{int}} \times \Omega)} = \delta_{i,i'} \delta_{n,n'} \delta_{l,l'} \|v_{n,l}^{(i)}\|_{\ell^2(\overline{\Omega_{int}})}. \quad (5.39)$$

For all  $n \geq 3$  we get the estimates

$$\begin{aligned} \int_{\Omega_{int}} |v_{n,l}^{(1)}(x)| \, dx &= \int_0^1 r^2 \int_{\Omega} \left( (\sigma_n^{(1)}(r))^2 |y_{n,l}^{(1)}| + (\tau_n^{(1)}(r))^2 |y_{n,l}^{(2)}| \right) d\omega(\eta) \, dr \\ &= \int_0^1 (\sigma_n^{(1)}(r))^2 r^2 \, dr + \int_0^1 (\tau_n^{(1)}(r))^2 r^2 \, dr \\ &\leq \int_0^1 r^{2n-2} (1 + n|\alpha_n|)^2 r^2 \, dr + \int_0^1 \alpha_n^2 (n(n+1)) r^{2n-2} \, dr \\ &\leq \frac{(1+n)^2}{2n+1} + \frac{n(n+1)}{2n+1} = (n+1), \\ \int_{\Omega_{int}} |v_{n,l}^{(2)}(x)| \, dx &= \int_0^1 r^2 \int_{\Omega} \left( (\sigma_n^{(2)}(r))^2 |y_{n,l}^{(1)}| + (\tau_n^{(2)}(r))^2 |y_{n,l}^{(2)}| \right) d\omega(\eta) \, dr \\ &\leq \frac{(n(n+1))^2}{n(n+1)} \int_0^1 r^{2n-2} r^2 \, dr + (1+n)^2 \int_0^1 r^{2n-2} r^2 \, dr \\ &\leq \frac{n(n+1)}{2n+1} + \frac{(1+n)^2}{2n+1} \leq 2(n+1), \\ \int_{\Omega_{int}} |v_{n,l}^{(3)}(x)| \, dx &= \int_0^1 r^{2n+2} r^2 \, dr = \frac{1}{2n+3}. \end{aligned}$$

With the help of orthogonality we finally get the estimate

$$\|\Phi_j^D\|_{\ell^2(\overline{\Omega_{int}} \times \Omega)}^2 = \sum_{i=1}^3 \sum_{n=0_i}^{\infty} \sum_{l=1}^{2n+1} (\varphi_j(n))^2 \|v_{n,l}^{(i)}\|_{\ell^2(\overline{\Omega_{int}})}^2 < \infty.$$

□

**Definition 5.4** *Let  $\{\Phi_j^D\}$ ,  $j \in \mathbb{Z}$ , be a (scale discrete) Cauchy-Navier scaling function of level  $j$ . Suppose that the function  $f$  is of class  $\ell^2(\Omega)$ . Then the convolution of  $\Phi_j^D$  against  $f$ ,  $\Phi_j^D * f$ , is defined by*

$$(\Phi_j^D * f) = \int_{\Omega} \Phi_j^D(\cdot, \eta) f(\eta) \, d\omega(\eta). \quad (5.40)$$

Moreover, the scale space  $v_j$  is defined by

$$v_j = \{\Phi_j^D * f \mid f \in \ell^2(\Omega)\}. \quad (5.41)$$

Now we are able to formulate the following theorem (cf. [34]).

**Theorem 5.3** *Let  $\Xi \in \ell^2(\overline{\Omega_{int}} \times \Omega)$  be a function which is representable in the form*

$$\Xi(x, \eta) = \sum_{i=1}^3 \sum_{n=0_i}^{\infty} \sum_{l=1}^{2n+1} \xi(n) v_{n,l}^{(i)}(x) \otimes y_{n,l}^{(i)}(\eta), \quad (x, \eta) \in \overline{\Omega_{int}} \times \Omega, \quad (5.42)$$

*in the sense of  $\ell^2(\overline{\Omega_{int}} \times \Omega)$ , where  $\xi$  is admissible as defined in (5.34). Then the convolution*

$$\Xi * f = \int_{\Omega} \Xi(\cdot, \eta) f(\eta) d\omega(\eta), \quad f \in \ell^2(\Omega), \quad (5.43)$$

*is an element of  $\ell^2(\overline{\Omega_{int}})$  expandable into a Fourier series as follows:*

$$\Xi * f = \sum_{i=1}^3 \sum_{n=0_i}^{\infty} \sum_{l=1}^{2n+1} \xi(n) \langle f, y_{n,l}^{(i)} \rangle_{\ell^2(\Omega)} v_{n,l}^{(i)}. \quad (5.44)$$

*Moreover, if  $f \in c^{(0)}(\Omega)$ , then this series converges uniformly in every subset  $\mathcal{K} \subset \Omega_{int}$  with  $\text{dist}(\overline{\mathcal{K}}, \Omega) > 0$ .*

**Proof.** Since  $\Xi$  is the  $\ell^2(\overline{\Omega_{int}} \times \Omega)$ -limit of the sequence of the partial sums

$$s_N(x, \eta) = \sum_{i=1}^3 \sum_{n=0_i}^N \sum_{l=1}^{2n+1} \xi(n) v_{n,l}^{(i)}(x) \otimes y_{n,l}^{(i)}(\eta), \quad N \in \mathbb{N}, \quad x \in \overline{\Omega_{int}}, \quad \eta \in \Omega, \quad (5.45)$$

and the field  $f$  is the  $\ell^2(\Omega)$ -limit of the partial sums

$$f_{N'} = \sum_{i=1}^3 \sum_{n=0_i}^{N'} \sum_{l=1}^{2n+1} \langle f, y_{n,l}^{(i)} \rangle_{\ell^2(\Omega)} y_{n,l}^{(i)}, \quad (5.46)$$

we are able to write

$$\begin{aligned} \Xi * f &= \lim_{N, N' \rightarrow \infty} \int_{\Omega} s_N(\cdot, \eta) f_{N'}(\eta) d\omega(\eta) \\ &= \lim_{N, N' \rightarrow \infty} \sum_{i,i'=1}^3 \sum_{n=0_i}^N \sum_{l=1}^{2n+1} \sum_{n'=0_{i'}}^{N'} \sum_{l'=1}^{2n'+1} \xi(n) \langle f, y_{n',l'}^{(i')} \rangle_{\ell^2(\Omega)} v_{n,l}^{(i)} \int_{\Omega} y_{n,l}^{(i)}(\eta) \cdot y_{n',l'}^{(i')}(\eta) d\omega(\eta) \\ &= \sum_{i=1}^3 \sum_{n=0_i}^{\infty} \sum_{l=1}^{2n+1} \xi(n) \langle f, y_{n,l}^{(i)} \rangle_{\ell^2(\Omega)} v_{n,l}^{(i)}. \end{aligned}$$

To show the convergence in  $\ell^2(\Omega_{int})$  we observe that

$$\begin{aligned} &\int_{\overline{\Omega_{int}}} \left| \int_{\Omega} (\Xi - s_N)(x, \xi) f(\eta) d\omega(\eta) \right|^2 dx \\ &\leq \int_{\overline{\Omega_{int}}} \int_{\Omega} |(\Xi - s_N)(x, \eta)|^2 d\omega(\eta) dx \|f\|_{\ell^2(\Omega)}^2 \\ &= \|\Xi - s_N\|_{\ell^2(\overline{\Omega_{int}} \times \Omega)}^2 \|f\|_{\ell^2(\Omega)}^2 \\ &\longrightarrow 0 \quad \text{as } N \longrightarrow \infty, \end{aligned}$$

and

$$\begin{aligned}
& \int_{\overline{\Omega_{int}}} \left| \int_{\Omega} (\mathbf{s}_N(x, \xi)(f - f_{N'}) (\eta) \, d\omega(\eta) \right|^2 dx \\
& \leq \int_{\overline{\Omega_{int}}} \int_{\Omega} |\mathbf{s}_N(x, \eta)|^2 \, d\omega(\eta) \, dx \int_{\Omega} |(f - f_{N'}) (\eta)|^2 \, d\omega(\eta) \\
& \leq \int_{\overline{\Omega_{int}}} \int_{\Omega} |\mathbf{s}_N(x, \eta)|^2 \, d\omega(\eta) \, dx \|f - f_{N'}\|_{\ell^2(\Omega)}^2 \\
& \longrightarrow 0 \quad \text{as } N' \longrightarrow \infty.
\end{aligned}$$

This implies that

$$\|\mathbf{s}_N * f_{N'} - \Xi * f\|_{\ell^2(\overline{\Omega_{int}})} \longrightarrow 0, \quad \text{as } N, N' \rightarrow \infty, \quad (5.47)$$

since

$$\int_{\overline{\Omega_{int}}} \left| \int_{\Omega} \Xi(x, \eta) f(\eta) \, d\omega(\eta) \right|^2 dx \leq \int_{\overline{\Omega_{int}}} \int_{\Omega} |\Xi(x, \eta)|^2 \, d\omega(\eta) \int_{\Omega} |f(\eta)|^2 \, d\omega(\eta) \, dx. \quad (5.48)$$

To prove the locally uniform convergence in  $\Omega_{int}$ , let  $g$  and  $g_N$  be given as follows.

$$g = \sum_{i=1}^3 \sum_{n=0_i}^{\infty} \sum_{l=1}^{2n+1} \gamma(n) < f, y_{n,l}^{(i)} >_{\ell^2(\Omega)} y_{n,l}^{(i)}, \quad (5.49)$$

$$g_N = \sum_{i=1}^3 \sum_{n=0_i}^N \sum_{l=1}^{2n+1} \gamma(n) < f, y_{n,l}^{(i)} >_{\ell^2(\Omega)} y_{n,l}^{(i)}, \quad N \in \mathbb{N}. \quad (5.50)$$

Then it is not difficult to see that

$$\begin{aligned}
|g(\eta) - g_N(\eta)| &= \left| \sum_{i=1}^3 \sum_{n=N}^{\infty} \sum_{l=1}^{2n+1} < f, y_{n,l}^{(i)} >_{\ell^2(\Omega)} y_{n,l}^{(i)}(\eta) \right| \\
&= \left( \sum_{i=1}^3 \sum_{n=N}^{\infty} \sum_{l=1}^{2n+1} < f, y_{n,l}^{(i)} >_{\ell^2(\Omega)}^2 \right)^{1/2} \left( \sum_{i=1}^3 \sum_{n=N}^{\infty} \sum_{l=1}^{2n+1} (\gamma(n))^2 |y_{n,l}^{(i)}(\eta)|^2 \right)^{1/2} \\
&= \left( \sum_{i=1}^3 \sum_{n=N}^{\infty} \sum_{l=1}^{2n+1} < f, y_{n,l}^{(i)} >_{\ell^2(\Omega)}^2 \right)^{1/2} \left( 3 \sum_{n=N}^{\infty} (\gamma(n))^2 \frac{2n+1}{4\pi} \right)^{1/2}. \quad (5.51)
\end{aligned}$$

The right hand side of (5.51) is independent of  $\eta$  and tends to 0 as  $N \rightarrow \infty$ . Hence,  $g$  is an element of  $c(\Omega)$ . In connection with Theorem 3.2, we are able to conclude that the series (5.44) converges in the sense of  $\|\cdot\|_{c(\overline{\mathcal{K}})}$  for every subset  $\mathcal{K} \subset \Omega_{int}$  with  $\text{dist}(\overline{\mathcal{K}}, \Omega) > 0$  and  $\Xi * g \in \text{pot}(\overline{\Omega_{int}})$  is the solution corresponding to the boundary-value problem defined in Theorem 5.1.  $\square$

**Theorem 5.4** *Let  $u$  be the unique solution of the inner displacement boundary-value problem: for a given continuous vector field  $f : \Omega \rightarrow \mathbb{R}^3$ , find  $u \in \text{pot}(\overline{\Omega_{int}})$  so that  $u|_{\Omega} = f$ . Then*

$$\lim_{j \rightarrow \infty} \|\Phi_j^D * f - u\|_{\ell^2(\Omega)} = 0, \quad (5.52)$$

and,

$$\lim_{j \rightarrow \infty} \|\Phi_j^D * f - u\|_{c(\overline{\mathcal{K}})} = 0, \quad (5.53)$$

for all subsets  $\mathcal{K} \subset \Omega_{int}$  with  $\text{dist}(\overline{\mathcal{K}}, \Omega) \geq \gamma > 0$ .

Moreover, if  $\frac{\varphi_j}{\varphi_{j'}}$ ,  $j < j'$ , is also admissible in the sense that

$$\sum_{\substack{n=0 \\ \varphi_{j'}(n) \neq 0}}^{\infty} \frac{2n+1}{4\pi} \left( \frac{\varphi_j(n)}{\varphi_{j'}(n)} \right) < +\infty$$

then the scale spaces form a multiresolution analysis in the sense that

$$\begin{aligned} v_j &\subset v_{j'} \subset \text{pot}(\overline{\Omega_{int}}), \\ \bigcup_{j \in \mathbb{Z}} \overline{v_j}^{\|\cdot\|_{c(\overline{\mathcal{K}})}} &\supset \text{pot}(\overline{\Omega_{int}})|_{\overline{\mathcal{K}}}. \end{aligned}$$

**Proof.** The points of departure are the representations

$$\begin{aligned} u(x) &= \int_{\Omega} \mathbf{g}(x, \eta) f(\eta) \, d\omega(\eta) \\ &= \int_{\Omega} \sum_{i=1}^3 \sum_{n=0_i}^{\infty} \sum_{l=1}^{2n+1} v_{n,l}^{(i)}(x) \otimes y_{n,l}^{(i)}(\eta) f(\eta) \, d\omega(\eta). \end{aligned}$$

Moreover, from Lemma 5.3, we know the estimate

$$|v_{n,l}^{(i)}(x)| \leq 2(1+n)(1-\gamma)^{n-1} \sqrt{\frac{2n+1}{4\pi}}, \quad (5.54)$$

provided that  $x \in \overline{\mathcal{K}}$  and  $n \geq 3$ .

For  $x \in \Omega_{int}$ , we now observe that

$$\begin{aligned} &|(\Phi_j^D * f)(x) - u(x)| \\ &= \left| \int_{\Omega} \Phi_j^D(x, \eta) f(\eta) \, d\omega(\eta) - \int_{\Omega} \mathbf{g}(x, \eta) f(\eta) \, d\omega(\eta) \right| \\ &= \left| \sum_{i=1}^3 \sum_{n=0_i}^{\infty} \sum_{l=1}^{2n+1} \left( \varphi_j(n) \int_{\Omega} y_{n,l}^{(i)}(\eta) \cdot f(\eta) \, d\omega(\eta) - \int_{\Omega} y_{n,l}^{(i)}(\eta) \cdot f(\eta) \, d\omega(\eta) \right) v_{n,l}^{(i)}(x) \right| \\ &= \left| \sum_{i=1}^3 \sum_{n=0_i}^{\infty} \sum_{l=1}^{2n+1} (\varphi_j(n) - 1) \langle f, y_{n,l}^{(i)} \rangle_{\ell^2(\Omega)} v_{n,l}^{(i)}(x) \right| \end{aligned}$$

By the Cauchy-Schwarz inequality it follows that

$$|(\Phi_j^D * f)(x) - u(x)| \leq \left( \sum_{i=1}^3 \sum_{n=0_i}^{\infty} \sum_{l=1}^{2n+1} (\varphi_j(n) - 1)^2 |v_{n,l}^{(i)}(x)|^2 \right)^{1/2} \|f\|_{\ell^2(\Omega)}. \quad (5.55)$$

Since  $0 \leq (\varphi_j(n) - 1)^2 \leq 1$  and  $\sum_{i=1}^3 \sum_{n=0_i}^{\infty} \sum_{l=1}^{2n+1} |v_{n,l}^{(i)}|^2 < \infty$ , the above series is uniformly convergent with respect to  $j$ . Therefore, we are able to formulate

$$\begin{aligned} & \lim_{j \rightarrow \infty} \|\Phi_j^D * f - u\|_{c(\overline{\mathcal{K}})} \\ & \leq \lim_{j \rightarrow \infty} \sup_{x \in \overline{\mathcal{K}}} \left| \int_{\Omega} \Phi_j^D(x, \eta) f(\eta) d\omega(\eta) - u(x) \right| \\ & \leq \lim_{j \rightarrow \infty} \sup_{x \in \overline{\mathcal{K}}} \left( \sum_{i=1}^3 \sum_{n=0_i}^{\infty} \sum_{l=1}^{2n+1} (\varphi_j(n) - 1)^2 |v_{n,l}^{(i)}(x)|^2 \right) \|f\|_{\ell^2(\Omega)}^2 dx \\ & = \sup_{x \in \overline{\mathcal{K}}} \left( \sum_{i=1}^3 \sum_{n=0_i}^{\infty} \sum_{l=1}^{2n+1} \left( \lim_{j \rightarrow \infty} (\varphi_j(n) - 1)^2 \right) |v_{n,l}^{(i)}(x)|^2 \right) \|f\|_{\ell^2(\Omega)}^2 dx \\ & = 0. \end{aligned}$$

To prove the multiresolution analysis, in connection with Theorem 5.3 we notice that  $\Phi_j^D * f$  can be regarded as solution of the displacement problem  $u_j = \Phi_j^D * f \in \text{pot}(\overline{\Omega_{int}})$ ,  $\Phi_j^D * f|_{\Omega} = g_j \in c^{(0)}(\Omega)$ , where

$$g_j = \sum_{i=1}^3 \sum_{n=0_i}^{\infty} \sum_{l=1}^{2n+1} (\varphi_j(n)) \langle f, y_{n,l}^{(i)} \rangle_{\ell^2(\Omega)} y_{n,l}^{(i)}. \quad (5.56)$$

Thus, since  $0 \leq \varphi_j(n) \leq \varphi_{j'}(n)$  for all  $n \in \mathbb{N}_0$ , we may conclude that  $u_j \in v_j$ ,  $u_j|_{\Omega} = g_j \in c^{(0)}(\Omega)$  implies the existence of a function

$$h_{j,j'} = \sum_{i=1}^3 \sum_{\substack{n=0_i \\ \varphi_{j'}(n) \neq 0}}^{\infty} \sum_{l=1}^{2n+1} \left( \frac{\varphi_j(n)}{\varphi_{j'}(n)} \right) \langle f, y_{n,l}^{(i)} \rangle_{\ell^2(\Omega)} y_{n,l}^{(i)} \quad (5.57)$$

in  $c^{(0)}(\Omega)$  due to the requirement that  $\frac{\varphi_j(n)}{\varphi_{j'}(n)}$  is admissible. Obviously,  $\Phi_{j'}^D * h_{j,j'} = \Phi_j^D * f$  such that  $\Phi_j^D * f \in v_{j'}$ .

Finally, for  $u \in \text{pot}(\overline{\Omega_{int}})$  there exists a field  $f \in c^{(0)}(\Omega)$  such that  $u|_{\Omega} = f$  and  $\Phi_j^D * f \rightarrow u$  uniformly on every subset  $\mathcal{K} \subset \Omega_{int}$  with  $\text{dist}(\overline{\mathcal{K}}, \Omega) > 0$ . Since  $\Phi_j^D * f \in v_j$  for all  $j \in \mathbb{Z}$ , we have

$$u \in \overline{\bigcup_{j \in \mathbb{Z}} v_j}^{\|\cdot\|_{c^{(0)}(\overline{\mathcal{K}})}},$$

which completes the proof.  $\square$

### 5.3.2 (Scale Discrete) Cauchy-Navier Wavelets

Next, we introduce scale discrete wavelets which facilitates the multiscale approximation developed in the previous section.

**Definition 5.5** Let  $\varphi_0 : [0, \infty) \rightarrow \mathbb{R}$  be an admissible generator of a Cauchy-Navier scaling function as defined in (5.34). Let  $\psi_0 : [0, \infty) \rightarrow \mathbb{R}$  be a piecewise continuously differentiable function satisfying the admissibility condition (5.34) and the property

$$\psi_0(x) = \varphi_0(x/2) - \varphi_0(x), \quad x \in [0, \infty). \quad (5.58)$$

Then, the function  $\psi_0$  is called a generator of a Cauchy-Navier wavelets  $\Psi_0^D \in \ell^2(\overline{\Omega_{int}} \times \Omega)$  defined by

$$\Psi_0^D(x, \eta) = \sum_{i=1}^3 \sum_{n=0_i}^{\infty} \sum_{l=1}^{2n+1} \psi_0(n) v_{n,l}^{(i)}(x) \otimes y_{n,l}^{(i)}(\eta), \quad (5.59)$$

for  $(x, \eta) \in \overline{\Omega_{int}} \times \Omega$ .

Accordingly, the  $j^{th}$  level Cauchy-Navier wavelet  $\Psi_j^D$  can be formulated as

$$\Psi_j^D(x, \eta) = D_j \tilde{\Psi}_0^D(x, \eta) = \sum_{i=1}^3 \sum_{n=0_i}^{\infty} \sum_{l=1}^{2n+1} (\psi_j(n))^2 v_{n,l}^{(i)}(x) \otimes y_{n,l}^{(i)}(\eta), \quad (5.60)$$

for  $(x, \eta) \in \overline{\Omega_{int}} \times \Omega$  and  $j \in \mathbb{Z}$ .

**Definition 5.6** Let  $\Psi_j^D$  be a discrete Cauchy-Navier wavelet of level  $j$ ,  $j \in \mathbb{Z}$ , as defined above. Suppose that the function  $f$  is of class  $\ell^2(\Omega)$ . Then the scale discretized Cauchy-Navier wavelet transform  $(\mathbf{WT})_j^D : \ell^2(\Omega) \rightarrow \ell^2(\Omega_{int})$  is defined by

$$(\mathbf{WT})_j^D(f)(x) = (\Psi_j^D * f)(x) = \int_{\Omega} \Psi_j^D(x, \eta) f(\eta) d\omega(\eta), \quad (5.61)$$

for all  $x \in \Omega_{int}$ .

Moreover, the corresponding detail space  $w_j$ ,  $j \in \mathbb{Z}$ , to a wavelet  $\Psi_j^D$ , is given by

$$w_j = \{\Phi_j^D * f \mid f \in \ell^2(\Omega)\}. \quad (5.62)$$

It should be remarked that the convolution  $\Phi_j^D * f$  can be understood as a smoothing of the original function  $f$  associated to the scaling function  $\Phi_j^D$  at level  $j$ , interpretable as a low pass filter. The convolution of the wavelet  $\Psi_j^D$  against  $f$  provides the information (detail information) between two successive smoothing  $\Phi_j^D * f$  and  $\Phi_{j+1}^D * f$ , which is known as band pass filter.

Moreover, the definition of the wavelets  $\Psi_j^D$  as the difference of two scaling functions



$\Phi_{j+1}^D$  and  $\Phi_j^D$  enables us to decompose a scaling function  $\Phi_{J+1}^D$  into a scaling function of lower scale  $J_0$ ,  $J_0 \leq J$ , and wavelets  $\Psi_j^D, j = J_0, \dots, J$  of the form

$$\Phi_{J+1}^D(x, \eta) = \Phi_{J_0}^D(x, \eta) + \sum_{j=J_0}^J \Psi_j^D(x, \eta), \quad (x, \eta) \in \Omega_{int} \times \Omega. \quad (5.63)$$

Defining the convolution operators  $\mathbf{p}_j^D$  and  $\mathbf{r}_j^D, j \in \mathbb{N}_0$ , by

$$\mathbf{p}_j^D(f)(x) = (\Phi_j^D * f)(x), \quad (5.64)$$

$$\mathbf{r}_j^D(f)(x) = (\Psi_j^D * f)(x), \quad (5.65)$$

$x \in \Omega_{int}, f \in \ell^2(\Omega)$  we have the following representations for the scale and detail spaces  $v_j, w_j$ , respectively.

$$v_j = \mathbf{p}_j^D(\ell^2(\Omega)), \quad (5.66)$$

$$w_j = \mathbf{r}_j^D(\ell^2(\Omega)). \quad (5.67)$$

To be more explicit, we state the following lemma.

**Lemma 5.5** *Let  $\{\Phi_j^D\}, j \in \mathbb{Z}$ , be a (scale discrete) Cauchy-Navier scaling function and  $\{\Psi_j^D\}$  be the corresponding (scale discrete) Cauchy-Navier wavelets. If  $f \in c(\Omega)$  is given, then for all  $J_1, J_2 \in \mathbb{Z}, J_1 < J_2$ ,*

$$\sum_{j=J_1}^{J_2-1} \Psi_j^D * f = \Phi_{J_2}^D * f - \Phi_{J_1}^D * f \quad (5.68)$$

in  $\ell^2(\Omega)$ -sense. Moreover, the equality (5.68) also hold in the sense of  $\|\cdot\|_{c(\overline{\mathcal{K}})}$  for all subsets  $\mathcal{K} \subset \Omega_{int}$  with  $\text{dist}(\overline{\mathcal{K}}, \Omega) \geq \gamma > 0$ .

**Proof.** We obtain by interchanging the sum and integration

$$\begin{aligned} \sum_{j=J_1}^{J_2-1} (\Psi_j^D * f) &= \sum_{j=J_1}^{J_2-1} \int_{\Omega} \Psi_j^D(\cdot, \eta) f(\eta) \, d\omega(\eta) \\ &= \int_{\Omega} \sum_{j=J_1}^{J_2-1} \Psi_j^D(\cdot, \eta) f(\eta) \, d\omega(\eta) \\ &= \int_{\Omega} \sum_{j=J_0}^J \sum_{i=1}^3 \sum_{n=0_i}^{\infty} \sum_{l=1}^{2n+1} \psi_j(n) v_{n,l}^{(i)} \otimes y_{n,l}^{(i)}(\eta) \, d\omega(\eta). \end{aligned} \quad (5.69)$$

Using the addition theorem for vector spherical harmonics and the property  $\psi_j(0) = 0$  we arrive at a representation of the form

$$\begin{aligned} \sum_{i=1}^3 \sum_{n=0_i}^{\infty} \sum_{l=1}^{2n+1} \psi_j(n) v_{n,l}^{(i)}(x) \otimes y_{n,l}^{(i)}(\eta) &= \sum_{n=1}^{\infty} \left( \frac{2n+1}{4\pi} \right) \psi_j(n) \left\{ \sigma_n^{(1)}(|x|) \mathbf{p}_n^{(1,1)}(\xi, \eta) \right. \\ &\quad + \tau_n^{(1)}(|x|) \mathbf{p}_n^{(1,2)}(\xi, \eta) + \sigma_n^{(2)}(|x|) \mathbf{p}_n^{(2,2)}(\xi, \eta) \\ &\quad \left. + \tau_n^{(2)}(|x|) \mathbf{p}_n^{(2,2)}(\xi, \eta) + \sigma_n^{(3)}(|x|) \mathbf{p}_n^{(3,3)}(\xi, \eta) \right\}, \quad (5.70) \end{aligned}$$

for each fixed  $x \in \overline{\Omega_{int}}$ , where,  $\xi = x/|x|$ .

Using Lemma 5.3 and the property of Legendre tensors that  $|\mathbf{p}_n^{(i,j)}(\xi, \eta) \epsilon^k| < 1$ , for  $i, j = 1, 2, 3$ ,  $k \in \{1, 2, 3\}$  (see [30]), we are able to deduce that the absolute value of each component of the tensor in (5.70) is less than or equal to

$$\begin{aligned} \sum_{n=3}^{\infty} \left( \frac{2n+1}{4\pi} \right) |\psi_j(n)| \{ (1-\gamma)^{n-1} \} \{ (n+1) + (n(n+1))^{1/2} \\ + (n(n+1))^{1/2} + (n+1) + (1-\gamma) \}. \quad (5.71) \end{aligned}$$

Hence, the boundedness can be guaranteed, since  $|1-\gamma| < 1$ . Consequently, the series (5.70) is absolutely convergent, and uniform convergent with respect to  $j$ . Hence, by interchanging the summations in (5.69), we are able to formulate

$$\begin{aligned} \sum_{j=J_1}^{J_2-1} \Psi_j^D * f &= \int_{\Omega} \sum_{i=1}^3 \sum_{n=0_i}^{\infty} \sum_{l=1}^{2n+1} \sum_{j=J_1}^{J_2-1} \psi_j(n) v_{n,l}^{(i)} \otimes y_{n,l}^{(i)}(\eta) d\omega(\eta) \\ &= \int_{\Omega} \sum_{i=1}^3 \sum_{n=0_i}^{\infty} \sum_{l=1}^{2n+1} \sum_{j=J_1}^{J_2-1} (\varphi_{j+1}(n) - \varphi_j(n)) v_{n,l}^{(i)} \otimes y_{n,l}^{(i)}(\eta) d\omega(\eta) \\ &= \int_{\Omega} \sum_{i=1}^3 \sum_{n=0_i}^{\infty} \sum_{l=1}^{2n+1} (\varphi_{J_2-1}(n) - \varphi_{J_1}(n)) v_{n,l}^{(i)} \otimes y_{n,l}^{(i)}(\eta) d\omega(\eta) \\ &= \Phi_{J_2}^D * f - \Phi_{J_1}^D * f, \quad (5.72) \end{aligned}$$

which completes the proof.  $\square$

As a consequence, we finally arrive at the following reconstruction formula, which provides a wavelet representation for the solution of the displacement boundary-value problem.

**Theorem 5.5** *Let  $\{\Phi_j^D\}$ ,  $j \in \mathbb{Z}$  be a (scale discrete) Cauchy-Navier scaling function and  $\{\Psi_j^D\}$  be the corresponding (scale discrete) Cauchy-Navier wavelets. Moreover, let  $u$  be the unique solution of the inner displacement boundary-value problem: for a given*

$f \in c(\Omega)$ , find  $u \in \text{pot}(\overline{\Omega_{int}})$  such that  $u|_{\Omega} = f$ . Then, the equalities

$$\Phi_{J_2}^D * f = \Phi_{J_1}^D * f + \sum_{j=J_1}^{J_2-1} \Psi_j^D * f, \quad (5.73)$$

$$u = (\Phi_{J_1}^D * f) + \sum_{j=J_1}^{\infty} (\mathbf{WT})_j^D(f), \quad (5.74)$$

hold both in the sense of  $\ell^2(\Omega)$  and  $\|\cdot\|_{c(\overline{\mathcal{K}})}$  for all subsets  $\mathcal{K} \subset \Omega_{int}$  with  $\text{dist}(\overline{\mathcal{K}}, \Omega) > 0$ , for all  $J_1, J_2 \in \mathbb{Z}$  with  $J_1 < J_2$ .

**Proof.** In connection with Lemma 5.5 straightforward calculations yield

$$\Phi_{J_1}^D * f + \sum_{j=J_1}^{J_2-1} \Psi_j^D * f = \Phi_{J_1}^D * f + (\Phi_{J_2}^D * f - \Phi_{J_1}^D * f) = \Phi_{J_2}^D * f. \quad (5.75)$$

Since the series

$$\sum_{j=J_1}^J \Phi_j^D * f, \quad J > J_1, \quad (5.76)$$

is uniformly convergent with respect to  $j$  due to Lemma 5.5, the limit exists as  $J$  tends to infinity.

Moreover, we see that

$$\Phi_J^D * f = \Phi_{J_1}^D * f + \sum_{j=J_1}^{J-1} \Psi_j^D * f, \quad J > J_1. \quad (5.77)$$

By virtue of Theorem 5.4 this leads to

$$\|u - \Phi_J^D * f\|_{c(\overline{\mathcal{K}})} = 0 \quad \text{as } J \rightarrow \infty. \quad (5.78)$$

But this implies

$$\Phi_{J_1}^D * f + \sum_{j=J_1}^{\infty} (\Psi_j^D * f) = u \quad (5.79)$$

in the sense of  $\|\cdot\|_{c(\overline{\mathcal{K}})}$  for all  $\mathcal{K}$  with  $\text{dist}(\overline{\mathcal{K}}, \Omega) > 0$ , which gives the desired result  $\square$

It should be remarked that, by letting  $J_1$  tends to  $-\infty$ , we can obtain a fully discrete wavelet reconstruction formula for the solution of the displacement boundary-value problem. However, for numerical purposes, it is worth to consider a wavelet reconstruction of (5.79) along with an initial filtered version  $\Phi_{J_1}^D * f$  with a sufficiently small  $J_1$  (for example,  $J_1 = 0$ ).

### 5.3.3 Computational Aspects

For numerical purposes, we now develop an (exact) fully discrete wavelet representation for the solution of the displacement boundary-value problem. We restrict ourselves to the bandlimited wavelets (for example, Shannon or cubic polynomial wavelets). To calculate the convolutions  $\mathbf{p}_j$  and  $\mathbf{r}_j$  in fully discrete form, we have to use an appropriate numerical integration rule over the sphere (for example, provided by [22],[30]). We construct a tree algorithm (a pyramid scheme) that provides a recursive procedure to compute the wavelet coefficients from level to level. The construction principles are similar to those of the scalar and vectorial cases given in [7],[30],[77].

For simplicity, we suppose that the generator of the scaling function has a support such that

$$\text{supp } \varphi_0 = [0, 1]. \quad (5.80)$$

Accordingly, we have

$$\text{supp } \varphi_j = [0, 2^j], \quad (5.81)$$

$$\text{supp } \psi_j \subset [0, 2^{j+1}]. \quad (5.82)$$

Thus, the resulting scaling functions and wavelets satisfy (cf. [77])

$$\begin{aligned} \Phi_j^D(x, \cdot) \epsilon^i &\in \text{pot}(\overline{\Omega_{int}}), \\ \Psi_j^D(x, \cdot) \epsilon^i &\in \text{pot}(\overline{\Omega_{int}}), \end{aligned}$$

where  $i = 1, 2, 3$  and  $x \in \overline{\Omega_{int}}$ .

Moreover, it is not difficult to show that the corresponding scale and detail spaces with respect to the bandlimited functions in  $\ell^2(\Omega)$  are finite-dimensional subspaces in  $\text{pot}(\overline{\Omega_{int}})$  (cf. [30]).

Assuming that a system  $\{(\eta_k^j, W_k^{N_j}) \in \Omega \times \mathbb{R}, \quad k = 1, \dots, N_j\}$  constitutes an integration rule which is exact of order  $(2^{j+1} - 1)$  within the bandlimited framework of (5.81) such that (cf. [7],[30],[36])

$$\mathbf{p}_j^D(f)(x) = \sum_{k=1}^{N_j} W_k^{N_j} \Phi_j^D(x, \eta_k^j) f(\eta_k^j), \quad x \in \Omega_{int}. \quad (5.83)$$

**Theorem 5.6** *Assume that the scaling functions and the wavelets satisfy the conditions (5.81) and (5.82). Furthermore, suppose that the system  $\{(\eta_k^j, W_k^j) \in \Omega \times \mathbb{R}, \quad k = 1, \dots, N_j\}$  constitutes an integration rule which is exact of order  $2^{j+1} - 1$  for each scale  $j \in \mathbb{N}_0$ . Then the solution of the displacement boundary-value problem has a discrete (exact) wavelet representation*

$$u(x) = (\Phi_0^D * f)(x) + \sum_{j=0}^{\infty} \sum_{k=1}^{N_j} W_k^{N_j} \Psi_j^D(x, \eta_k^j) f(\eta_k^j) \quad (5.84)$$

for all  $x \in \overline{\mathcal{K}}$  for every subset  $\mathcal{K} \subset \Omega_{int}$  with  $\text{dist}(\overline{\mathcal{K}}, \Omega) > 0$ .

Moreover, if  $f$  is assumed to be bandlimited with level  $J \in \mathbb{N}$ , then the above representation can be reduced to

$$u(x) = (\Phi_0^D * f)(x) + \sum_{j=0}^J \sum_{k=1}^{N_j} W_k^{N_j} \Psi_j^D(x, \eta_k^j) f(\eta_k^j), \quad (5.85)$$

where  $J$  is such that  $\langle f, y_{n,l}^{(i)} \rangle_{\ell^2(\Omega)} = 0$  for all  $n \geq 2^{J+1}$ ,  $l = 1, \dots, 2n+1$ ,  $i = 1, 2, 3$ .

Furthermore, we are able to express the  $J^{th}$ -level approximation of  $u$ , denoted by  $u_J$  of the form

$$u(x) = (\Phi_{J_0}^D * f)(x) + \sum_{j=J_0}^J \sum_{k=1}^{N_j} W_k^{N_j} \Psi_j^D(x, \eta_k^j) f(\eta_k^j), \quad J_0 \in \mathbb{N}_0, \quad J_0 \leq J. \quad (5.86)$$

Next we construct a tree algorithm for the computations of wavelet coefficients  $\mathbf{r}_j(f)$ . Basic steps are the well-known *initial step* and the *pyramid step* (cf. [26]).

Assume that for sufficiently large  $J \in \mathbb{N}$  there exist coefficient vectors  $a_k^{N_J} \in \mathbb{R}^3$ ,  $k = 1, \dots, N_J$  such that

$$\mathbf{p}_J^D(f)(\cdot) = \sum_{k=1}^{N_J} \Phi_J^D(\cdot, \eta_k^{N_J}) a_k^{N_J}. \quad (5.87)$$

We want to introduce an algorithm to obtain vector coefficients

$$\mathbf{a}^{N_j} = (a_1^{N_j}, \dots, a_{N_j}^{N_j}) \in \mathbb{R}^{3 \times N_j}, \quad j = J_0, \dots, J$$

such that

- (a) the coefficients  $\mathbf{a}^{N_{j-1}}$  is obtainable from  $\mathbf{a}^{N_j}$ ,  $j = J_0 + 1, \dots, J$ ,
- (b) the expressions  $\mathbf{p}_j^D(f)$  and  $\mathbf{r}_j^D(f)$  can be written as

$$\mathbf{p}_j^D(f)(\cdot) = \sum_{k=1}^{N_j} \Phi_j^D(\cdot, \eta_k^{N_j}) a_k^{N_j}, \quad j = J_0, \dots, J \quad (5.88)$$

$$\mathbf{r}_j^D(f)(\cdot) = \sum_{k=1}^{N_j} \Phi_j^D(\cdot, \eta_k^{N_j}) a_k^{N_j}, \quad j = J_0 + 1, \dots, J. \quad (5.89)$$

For the initial step, we suppose that  $J \in \mathbb{N}$  is sufficiently large and, thus, we see that

$$a_k^{N_J} = W_k^{N_J} f(\eta_k^{N_J}), \quad k = 1, \dots, N_J. \quad (5.90)$$

The aim of the pyramid step is to construct  $\mathbf{a}^{N_{J-1}}$  from  $\mathbf{a}^{N_J}$  by recursion. At this point we follow the procedure known from [77].

For arbitrary (fixed)  $x \in \Omega_{int}$  we consider the convolution

$$(\Phi_{J+1}^D * f)(x) = \int_{\Omega} \Phi_{J+1}^D(x, \eta) f(\eta) d\omega(\eta) \quad (5.91)$$

$$= \sum_{k=1}^{N_J} W_k^J \Phi_{J+1}^D(x, \eta_k^{N_J}) f(\eta_k^{N_J}) \quad (5.92)$$

In connection to the Shannon generators (see Section 5.3.4) and the definition of the scaling function  $\Phi_J^D$  the formula (5.91) can equivalently be written as

$$(\Phi_{J+1}^D * f)(x) = \sum_{k=1}^{N_J} W_k^{N_J} \sum_{i=1}^3 \sum_{n=0_i}^{2^J+1} \sum_{l=1}^{2n+1} v_{n,l}^{(i)}(x) \otimes y_{n,l}^{(i)}(\eta_k^J) f(\eta_k^J). \quad (5.93)$$

In light of (5.90) we are able to write

$$(\Phi_{J+1}^D * f)(\cdot) = \sum_{k=1}^{N_J} \Phi_{J+1}^D(\cdot, \eta_k^{N_J}) a_k^{N_J}. \quad (5.94)$$

Since the coefficients  $a_k^{N_J}$ ,  $k = 1, \dots, N_J$  do not depend on the corresponding scaling function (see, for example, [77]), we are able to formulate

$$(\Phi_J^D * f)(\cdot) = \sum_{k=1}^{N_J} \Phi_J^D(\cdot, \eta_k^{N_J}) a_k^{N_J}. \quad (5.95)$$

Observing the form (5.94) we obtain an expression for  $\Phi_J^D * f$  introducing the values  $a_k^{N_{J-1}}$ ,  $k = 1, \dots, N_{J-1}$  such that

$$(\Phi_J^D * f)(\cdot) = \sum_{k=1}^{N_{J-1}} \Phi_J^D(\cdot, \eta_k^{N_{J-1}}) a_k^{N_{J-1}}. \quad (5.96)$$

Comparing the right hand sides of (5.95) and (5.96) we get the relation

$$\sum_{k=1}^{N_{J-1}} \Phi_J^D(\cdot, \eta_k^{N_{J-1}}) a_k^{N_{J-1}} = \sum_{k=1}^{N_J} \Phi_J^D(\cdot, \eta_k^{N_J}) a_k^{N_J}. \quad (5.97)$$

It is clear that the equation (5.97) has to be solved for  $a_k^{N_{J-1}}$  in terms of  $a_k^{N_J}$ . To obtain an another equivalent form to (5.97) which may easily be solvable, we see that

$$\int_{\Omega} \sum_{k=1}^{N_{J-1}} \Phi_J^D(\xi, \eta_k^{N_{J-1}}) a_k^{N_{J-1}} \cdot y_{n,l}^{(i)} d\omega(\xi) = \int_{\Omega} \sum_{k=1}^{N_J} \Phi_J^D(\xi, \eta_k^{N_J}) a_k^{N_J} \cdot y_{n,l}^{(i)} d\omega(\xi), \quad (5.98)$$

for  $i = 1, 2, 3$ ,  $n = 0_i, \dots, 2^{J-1}$ ,  $j = 1, \dots, 2n + 1$ . It follows that

$$\sum_{k=1}^{N_{J-1}} y_{n,l}^{(i)}(\eta_k^{N_{J-1}}) \cdot a_k^{N_{J-1}} = \sum_{k=1}^{N_J} y_{n,l}^{(i)}(\eta_k^{N_J}) \cdot a_k^{N_J}, \quad (5.99)$$

for  $i = 1, 2, 3$ ,  $n = 0_i, \dots, 2^{J-1}$ ,  $j = 1, \dots, 2n + 1$ . Thus the problem reduces to the solution of the equation (5.99) which leads to the following theorem (cf. [30],[77]).

**Theorem 5.7** *The solution  $a_k^{N_{J-1}}$ ,  $k = 1, \dots, N_{J-1}$  of (5.99) is given by*

$$a_{J-1}^{N_{J-1}} = W_k^{N_{J-1}} \sum_{l=1}^{N_{J-1}} \sum_{i=1}^3 \sum_{n=0_i}^{2^{J-1}} \frac{2n+1}{4\pi} \mathbf{p}_n^{(i,i)}(\eta_l^{N_J}, \eta_l^{N_{J-1}}) a_J^{N_J}. \quad (5.100)$$

**Proof.** The statement of Theorem 5.7 follows by quite analogous steps as given in [34] for the scalar case. For more details concerning the tree algorithm we refer the reader to, for example, [7],[77].

Taking into account the pyramid step (5.100) in connection with the multiscale representation we finally obtain decomposition and reconstruction schemes as follows.

$$\begin{array}{ccccccc} f & \rightarrow & \mathbf{a}^{N_J} & \rightarrow & \mathbf{a}^{N_{J-1}} & \rightarrow & \dots \rightarrow \mathbf{a}^{N_{J_0+1}} & \rightarrow & \mathbf{a}^{N_{J_0}} \\ & & \downarrow & & \downarrow & & \downarrow & & \swarrow \downarrow \searrow \\ & & \mathbf{r}_{\tau_J}^D(f) & & \mathbf{r}_{\tau_{J-1}}^D(f) & & \mathbf{r}_{\tau_{J_0+1}}^D(f) & & \mathbf{r}_{\tau_{J_0}}^D(f) \quad \mathbf{p}_{\tau_{J_0}}^D(f) \end{array}$$

(decomposition scheme)

$$\begin{array}{ccccccc} \mathbf{a}^{N_{J_0}} & & \mathbf{a}^{N_{J_0+1}} & & \mathbf{a}^{N_{J-1}} & & \\ \downarrow & & \downarrow & & \downarrow & & \\ \mathbf{r}_{\tau_{J_0}}^D(f) & & \mathbf{r}_{\tau_{J_0+1}}^D(f) & & \mathbf{r}_{\tau_{J-1}}^D(f) & & \\ \swarrow & & \searrow & & \swarrow & & \searrow \\ \mathbf{p}_{\tau_{J_0}}^D(f) & \rightarrow + \rightarrow & \mathbf{p}_{\tau_{J_0+1}}^D(f) & \rightarrow + \dots + \rightarrow & \mathbf{p}_{\tau_{J-1}}^D(f) & \rightarrow + \rightarrow & \mathbf{p}_{\tau_J}^D(f) \end{array}$$

(reconstruction scheme).

Finally it should be remarked that in the evaluation steps of the tree algorithm, further modifications can be undertaken to reduce the computational time. For example, panel clustering techniques (cf. [44]), domain decomposition, etc. For more details the reader is referred to [30],[44],[49] or the references therein.

### 5.3.4 Examples for Cauchy-Navier Wavelets

In what follows, we present some bandlimited scaling functions and wavelets. In order to realize the localization properties of scaling functions and wavelets we illustrate the

cartesian components and the Frobenius norm of those functions. The numerical implementation shows that the non-diagonal components of both scaling functions and wavelets are dominated by their diagonals. This means that, for numerical purposes, the kernels can be used as diagonal matrices neglecting the non-diagonal terms, when the higher order levels are considered. Three different Cauchy-Navier scaling functions and wavelets up to level 4 are presented. Note that the scaling functions  $\Phi_j^D(x, \cdot)$  and the wavelets  $\Psi_j^D(x, \cdot)$  are considered for a given fixed point  $x \in \Omega$ . Moreover, for the sectional illustrations, we choose  $\varphi = \pi/4$  (fixed).

### Shannon Wavelets

The compactly supported generator  $\varphi_0$  for Shannon wavelets is given by (cf. [30])

$$\varphi_0(x) = \begin{cases} 1 & \text{if } x \in [0, 1] \\ 0 & \text{else} \end{cases} \quad (5.101)$$

and correspondingly the dilates  $\varphi_j$ ,  $j \in \mathbb{Z}$ , have the representation

$$\varphi_j(x) = \begin{cases} 1 & \text{if } x \in [0, 2^j] \\ 0 & \text{else.} \end{cases} \quad (5.102)$$

Via the refinement equation we get the generator  $\psi_j$  of the wavelet of level  $j$ ,  $j \in \mathbb{Z}$ ,

$$\psi_j(x) = \begin{cases} 1 & \text{if } x \in [2^j, 2^{j+1}) \\ 0 & \text{else.} \end{cases} \quad (5.103)$$

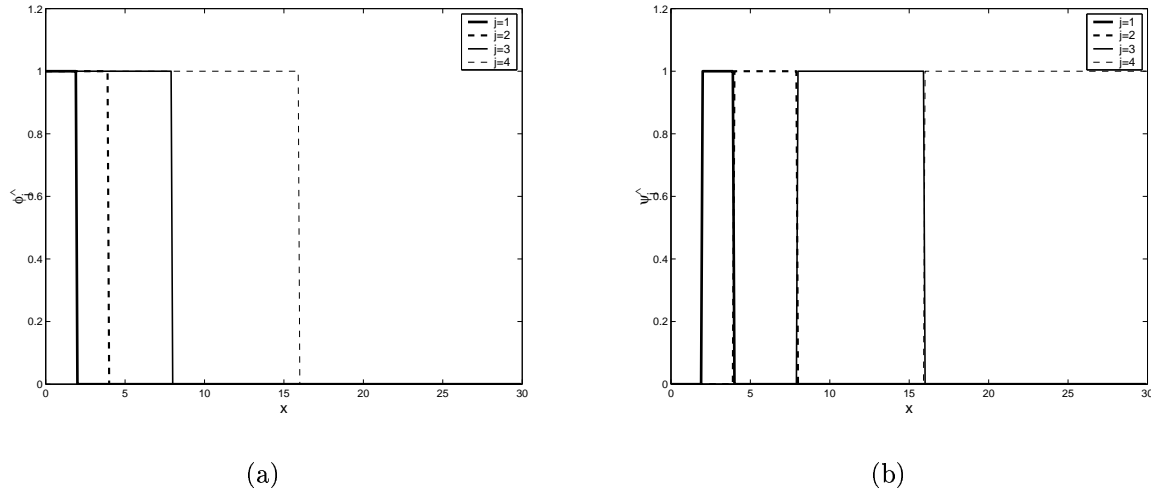


Figure 5.1: Generators for the Shannon scaling functions (left) and for the wavelets (right) at levels  $j = 1, 2, 3, 4$ .



It should be remarked that the Shannon generator provides orthogonal scale and detail spaces. More specifically, we have  $v_{j+1} = v_j + w_j$  with  $v_j \perp w_j$ ,  $j \in \mathbb{Z}$ .

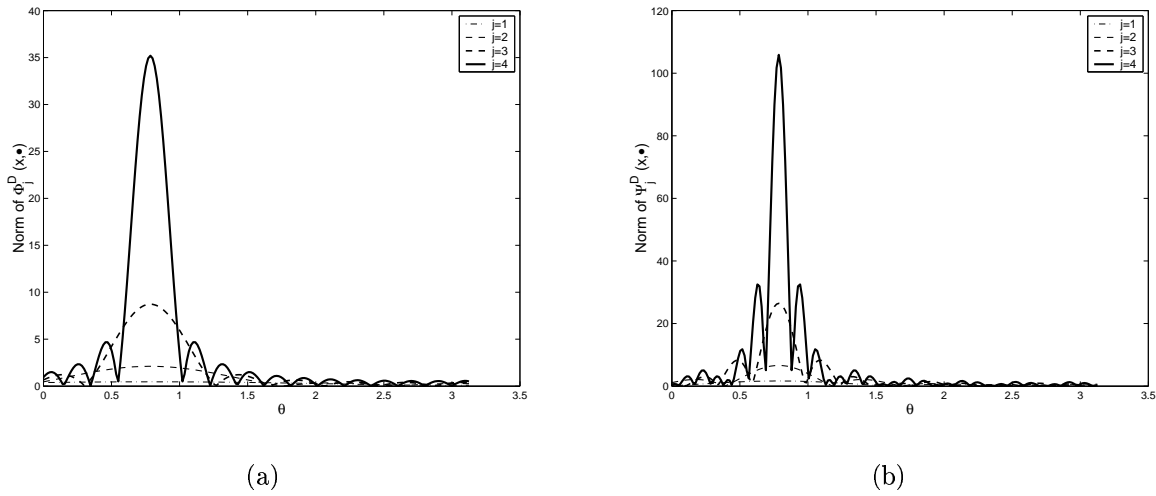


Figure 5.2: Frobenius norm of the Shannon scaling functions (left) and wavelets (right) at levels  $j = 1, 2, 3, 4$ .

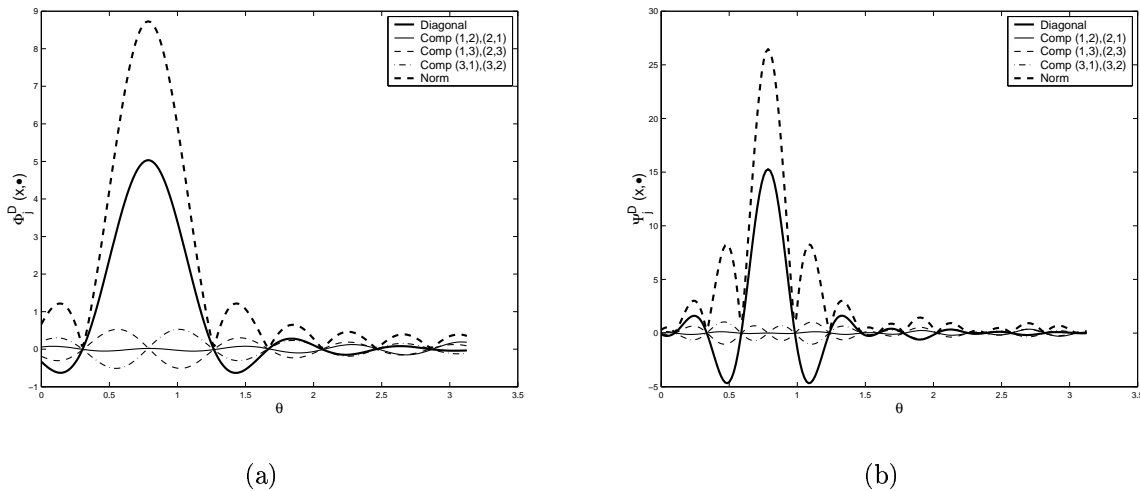


Figure 5.3: Components and the Frobenius norm of the Shannon scaling function (left) and wavelets (right) at level 3.

### Modified Shannon Wavelets

The modified Shannon wavelets have less oscillations than Shannon wavelets ([30]). They may be referred as 'smooth' versions of Shannon wavelets. However, they do not fulfill

the orthogonal properties. More explicitly, the corresponding generator  $\varphi_0$  is given by (cf. [30]),

$$\varphi_0(x) = \begin{cases} 1 & \text{if } x \in [0, h) \\ \frac{1-x}{1-h} & \text{if } x \in [h, 1) \\ 0 & \text{else,} \end{cases} \quad (5.104)$$

where  $h \in (0, 1)$  is an apriori given parameter. Thus, the corresponding dilates  $\varphi_j$ ,  $j \in \mathbb{Z}$  have the representation

$$\varphi_j(x) = \begin{cases} 1 & \text{if } x \in [0, 2^j h) \\ \frac{1-2^{-j}x}{1-h} & \text{if } x \in [2^j h, 2^{j+1} h) \\ 0 & \text{else.} \end{cases} \quad (5.105)$$

For this generator, three cases will be considered.  $h < 0.5$ ,  $h > 0.5$ , and  $h = 0.5$ . Via the refinement equation we can obtain three generators for  $\psi_j$ , in particular, for  $h = 0.5$ , we have

$$\psi_j(x) = \begin{cases} 0 & \text{if } x \in [0, 2^{j-1}) \\ 1 - \left( \frac{1-2^{-j}x}{1/2} \right) & \text{if } x \in [2^{j-1}, 2^j) \\ \left( \frac{1-2^{-j-1}x}{1/2} \right) & \text{if } x \in [2^j, 2^{j+1}) \\ 0 & \text{if } x \in [2^{j+1}, \infty). \end{cases} \quad (5.106)$$

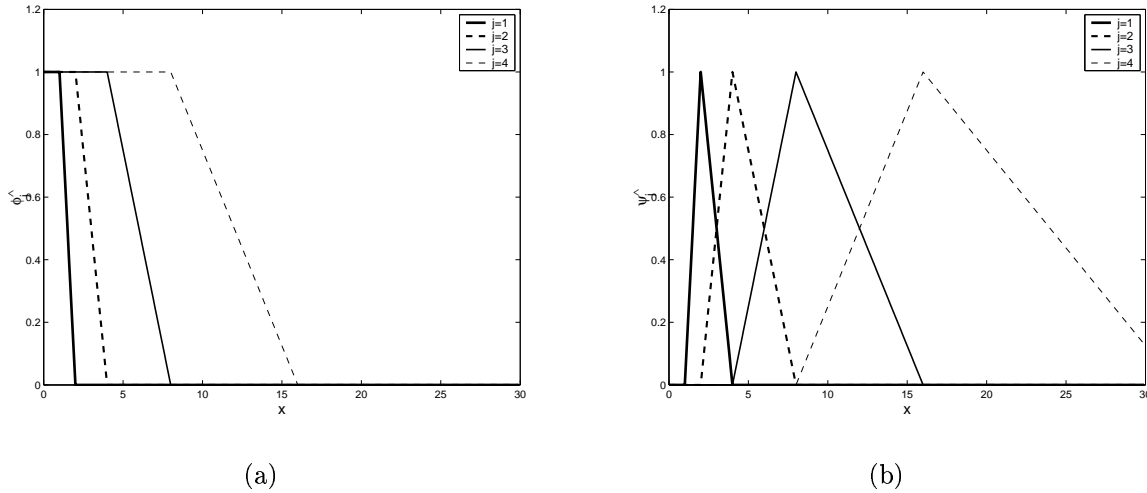


Figure 5.4: Generators for the modified Shannon scaling functions (left) and wavelets (right) at levels  $j = 1, 2, 3, 4$ .

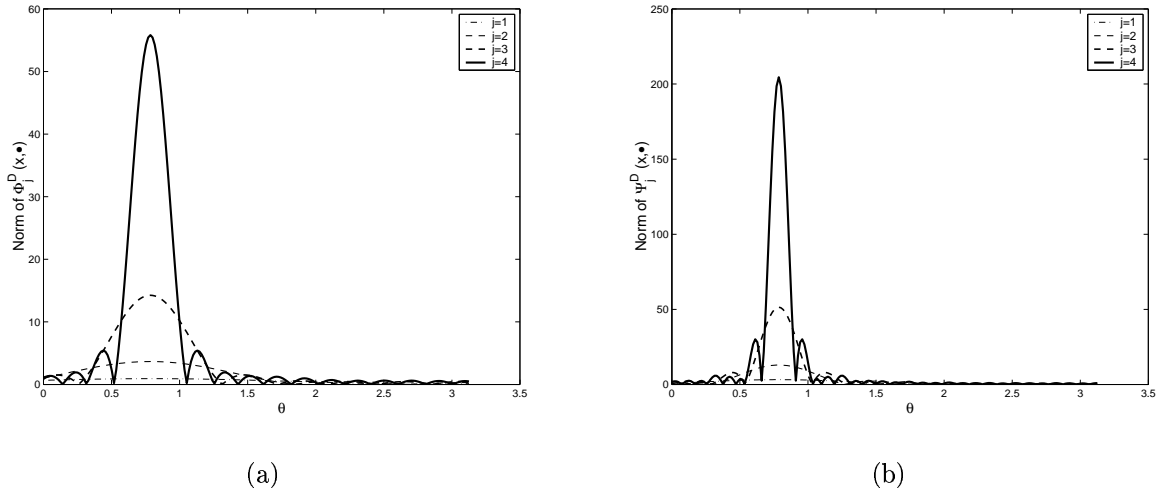


Figure 5.5: Frobenius norm of the modified Shannon scaling functions (left) and wavelets (right) at levels  $j = 1, 2, 3, 4$ .

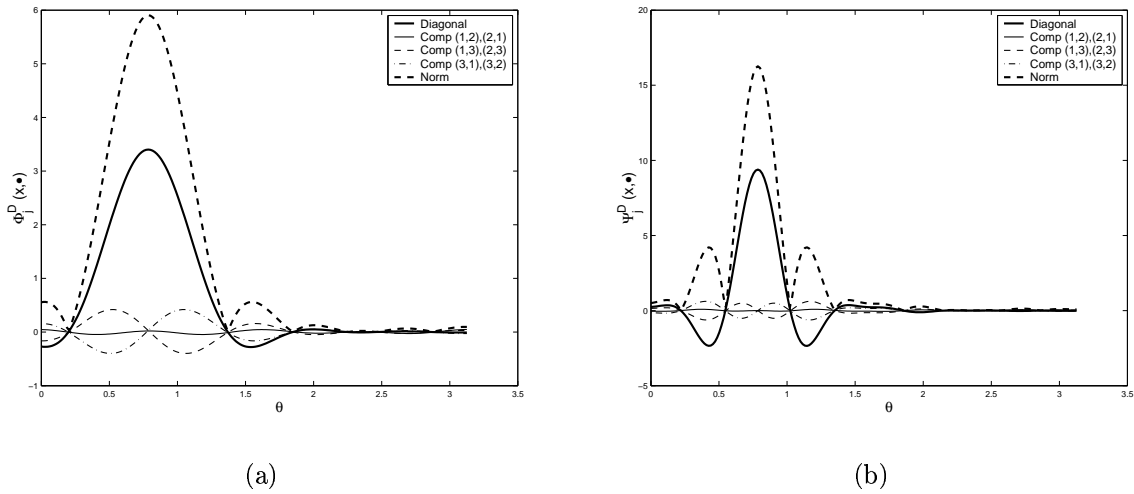


Figure 5.6: Components and the Frobenius norm of the modified Shannon scaling function (left) and wavelets (right) at level 3.

### Cubic Polynomial Wavelets

To avoid the highly oscillating characteristic of the Shannon wavelets one can use alternatively the cubic polynomial wavelets as a modified version, however, losing the property

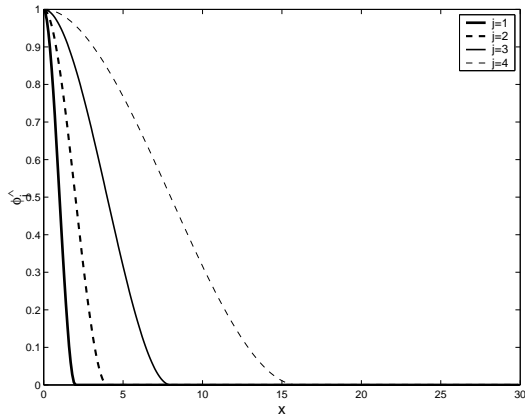
of orthogonality. The generating functions are as follows (cf. [30]):

$$\varphi_0(x) = \begin{cases} (1-x)^2(1+2x) & \text{if } x \in [0, 1) \\ 0 & \text{else} \end{cases} \quad (5.107)$$

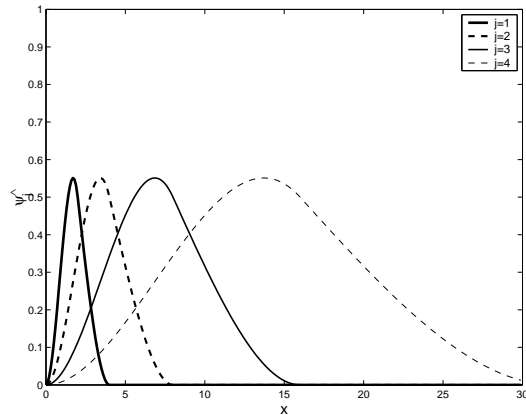
and then the corresponding dilates  $\varphi_j$ ,  $j \in \mathbb{Z}$ :

$$\varphi_j(x) = \begin{cases} (1-2^{-j}x)^2(1+2x^{-j}) & \text{if } x \in [0, 2^j) \\ 0 & \text{else,} \end{cases} \quad (5.108)$$

$$\psi_j(x) = \begin{cases} (1-2^{-j-1}x)^2(1+2^{-j}x) - (1-2^{-j}x)^2(1+2^{-j+1}x) & \text{if } x \in [0, 2^j) \\ (1-2^{-j-1}x)^2(1+2^{-j}x) & \text{if } x \in [2^j, 2^{j+1}) \\ 0 & \text{if } x \in [2^{j+1}, \infty). \end{cases} \quad (5.109)$$



(a)



(b)

Figure 5.7: Generators for the cubic polynomial scaling functions (left) and wavelets (right) at levels  $j = 1, 2, 3, 4$ .

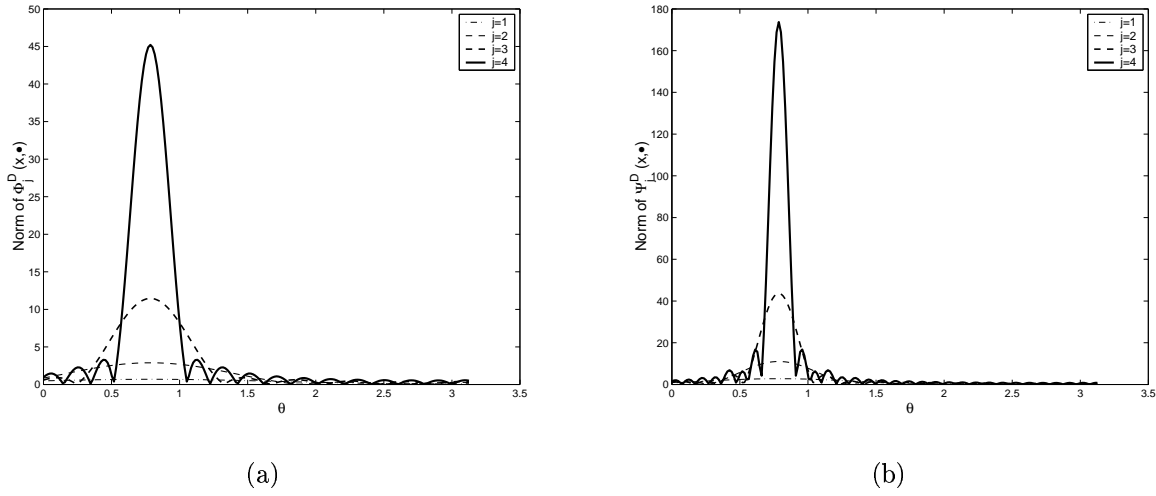


Figure 5.8: Frobenius norm of the cubic polynomial scaling functions (left) and wavelets (right) at levels  $j = 1, 2, 3, 4$ .

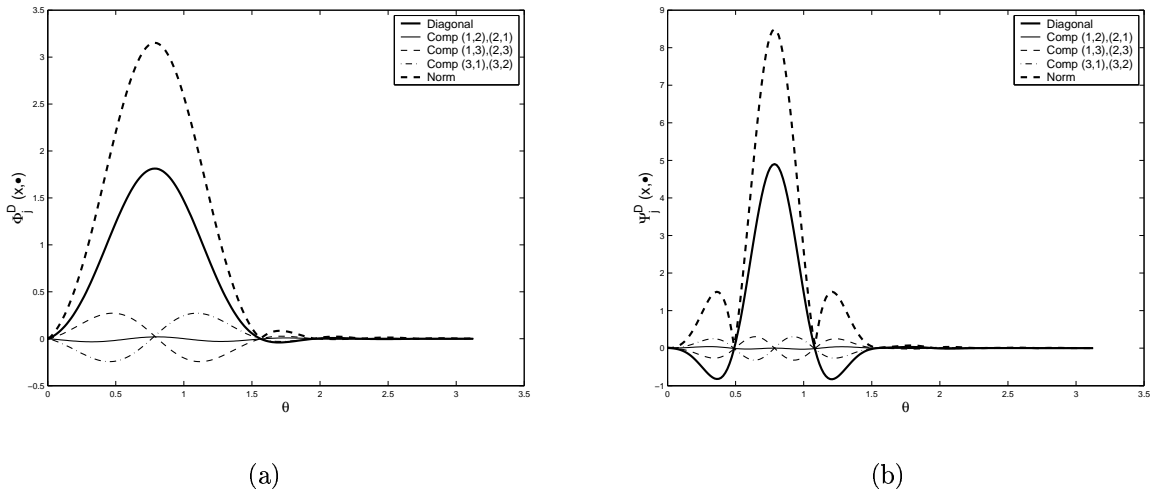


Figure 5.9: Components and the Frobenius norm of the cubic polynomial scaling function (left) and wavelets (right) at level 3.

## 5.4 Green's Function Associated to the Radial Boundary Displacements on the Unit Sphere

Next we are concerned with the particular determination of the Green function associated to radial displacements ([43]). To this end recall the decomposition of the Green function

$\mathbf{g}$  in its normal and tangential splitting  $\mathbf{g} = \mathbf{g}_{nor} + \mathbf{g}_{tan}$  (see, (5.30),(5.31)).

**Lemma 5.6** *Assume that the boundary function  $f : \Omega \rightarrow \mathbb{R}^3$  is a normal vector field to  $\Omega$ , i.e.  $f$  is of the form  $f(\eta) = \eta H(\eta)$  with  $H \in C(\Omega)$ ,  $\eta \in \Omega$ . Then, the unique solution  $u$  of the displacement boundary-value problem can be represented by the integral*

$$u(x) = \int_{\Omega} \mathbf{g}_{nor}(x, \eta) f(\eta) d\omega(\eta), \quad x \in \Omega_{int}. \quad (5.110)$$

**Proof.** It is sufficient to show that the integral  $\int_{\Omega} \mathbf{g}_{tan}(x, \eta) f(\eta) d\omega(\eta)$  vanishes when the boundary function is of the special form  $f(\eta) = \eta H(\eta)$ ,  $\eta \in \Omega$  with  $H \in C(\Omega)$ . Hence, we observe

$$\begin{aligned} \int_{\Omega} \mathbf{g}_{tan}(x, \eta) f(\eta) d\omega(\eta) &= \int_{\Omega} \sum_{n=1}^{\infty} \sum_{j=1}^{2n+1} \left( (v_{n,j}^{(2)}(\xi) \otimes y_{n,j}^{(2)}(\eta)) \eta H(\eta) \right) d\omega(\eta) \\ &\quad + \int_{\Omega} \sum_{n=1}^{\infty} \sum_{j=1}^{2n+1} \left( (v_{n,j}^{(3)}(\xi) \otimes y_{n,j}^{(3)}(\eta)) \eta H(\eta) \right) d\omega(\eta) \\ &= \sum_{n=1}^{\infty} \sum_{j=1}^{2n+1} \left( \int_{\Omega} y_{n,j}^{(2)}(\eta) \cdot \eta H(\eta) d\omega(\eta) (v_{n,j}^{(2)}(\xi)) \right. \\ &\quad \left. + \int_{\Omega} y_{n,j}^{(3)}(\eta) \cdot \eta H(\eta) d\omega(\eta) (v_{n,j}^{(3)}(\xi)) \right), \end{aligned}$$

which completes the proof, since  $y_{n,j}^{(2)}(\eta) \cdot \eta = 0$  and  $y_{n,j}^{(3)}(\eta) \cdot \eta = 0$  for all  $\eta \in \Omega$ .  $\square$

To get an explicit representation for the function  $\mathbf{g}_{nor}$  we recapitulate the following identities (see [43]).

For  $\tau \neq -2$  we have

$$\alpha_n(2n+1) = m_1(\tau) + m_2(\tau) + \frac{m_3(\tau)}{n + \frac{1}{\tau+2}} \quad (5.111)$$

$$\alpha_n n(2n+1) = m_1(\tau) n(2n+1) + \frac{m_2(\tau)}{2} (2n+1) + \quad (5.112)$$

$$\left( m_3(\tau) - \frac{m_2(\tau)}{2} \right) - \frac{m_3(\tau)}{\tau+2} \frac{1}{n + \frac{1}{\tau+2}}, \quad (5.113)$$

where

$$m_1(\tau) = -\frac{\tau}{2(\tau+2)}, \quad (5.114)$$

$$m_2(\tau) = -\frac{(3\tau+4)(\tau+1)}{(\tau+2)^2}, \quad (5.115)$$

$$m_3(\tau) = -m_1(\tau)m_2(\tau). \quad (5.116)$$

Observing well-known properties of Legendre polynomials we obtain

$$\sum_{n=0}^{\infty} P_n(t)r^n = \frac{1}{(1-2rt+r^2)^{\frac{1}{2}}} = F_1(r, t), \quad (5.117)$$

$$\sum_{n=0}^{\infty} (2n+1)P_n(t)r^n = \frac{1-r^2}{(1-2rt+r^2)^{\frac{3}{2}}} = F_2(r, t), \quad (5.118)$$

$$\sum_{n=1}^{\infty} n(2n+1)P_n(t)r^{n-1} = \frac{\partial}{\partial r} F_2(r, t) = F_3(r, t), \quad (5.119)$$

$$\sum_{n=1}^{\infty} \frac{1}{n + (\frac{1}{r+2})} P_n(t)r^{n-1} = r^{-(1+(\frac{1}{r+2}))} \int_0^r \frac{1}{s^{1-(\frac{1}{r+2})}(1-2st+s^2)^{\frac{1}{2}}} ds = F_4(r, t), \quad (5.120)$$

where  $F_1, F_2, F_3$  and  $F_4$  are the abbreviations for the series (5.116)-(5.119), respectively.

Substituting  $t = \xi \cdot \eta$ , we get

$$\mathbf{g}_{nor}(x, \eta) = \frac{1}{4\pi} \sum_{n=0}^{\infty} (r^{n+1} + n\alpha_n r^{n-1}(r^2 - 1))(2n+1)P_n(t)[\xi \otimes \eta] \quad (5.121)$$

$$+ \frac{1}{4\pi} \sum_{n=1}^{\infty} \alpha_n (r^{n-1}(r^2 - 1)P'_n(t)[(\eta - (\xi \cdot \eta)\xi) \otimes \eta]. \quad (5.122)$$

Set

$$A_1 = \sum_{n=0}^{\infty} (2n+1)r^{n+1}P_n(t), \quad (5.123)$$

$$A_2 = \sum_{n=0}^{\infty} n(2n+1)\alpha_n(r^{n+1} - r^{n-1})P_n(t), \quad (5.124)$$

$$A_3 = \sum_{n=0}^{\infty} (2n+1)\alpha_n(r^{n+1} - r^{n-1})P'_n(t). \quad (5.125)$$

Hence, we have

$$\mathbf{g}_{nor}(x, \eta) = \frac{1}{4\pi} ((A_1 + A_2)[\xi \otimes \eta] + A_3[(\eta - (\xi \cdot \eta)\xi) \otimes \eta]). \quad (5.126)$$

With the above notations we find

$$A_1 = \sum_{n=0}^{\infty} (2n+1)r^{n+1}P_n(t) = rF_1(r, t) \quad (5.127)$$

$$\begin{aligned} A_2 &= \sum_{n=0}^{\infty} \left[ m_1(\tau)n(2n+1) + \frac{m_2(\tau)}{2}(2n+1) + \left( m_3(\tau) - \frac{m_2(\tau)}{2} \right) - \frac{m_3(\tau)}{\tau+2} \frac{1}{n + \frac{1}{\tau+2}} \right] \\ &= m_1(\tau)(r^2 - 1)F_3(r, t) + \frac{m_2(\tau)}{2} \left( \frac{1}{r} - 1 \right) F_2(r, t) \\ &\quad + \left( m_3(\tau) - \frac{m_2(\tau)}{2} \right) \left( r - \frac{1}{r} \right) F_1(r, t) + \frac{m_3(\tau)}{\tau+2} \left( r - \frac{1}{r} \right) F_4(r, t) = F_5(r, t), \end{aligned} \quad (5.128)$$

$$\begin{aligned} A_3 &= \sum_{n=0}^{\infty} \alpha_n(2n+1)(r^{n-1}(r^2 - 1)P'_n(t)) \\ &= \frac{\partial}{\partial t} \frac{1}{4\pi} \sum_{n=0}^{\infty} \alpha_n(2n+1)(r^{n-1}(r^2 - 1)P_n(t)) \\ &= \frac{\partial}{\partial t} \frac{1}{4\pi} \sum_{n=0}^{\infty} \left( m_1(\tau) + m_2(\tau) + \frac{m_3(\tau)}{n + \frac{1}{\tau+2}} \right) (r^{n+1} - r^{n-1})P_n(t) \\ &= \frac{\partial}{\partial t} \left[ m_1(\tau) \left( r - \frac{1}{r} \right) F_2(r, t) + m_2(\tau) \left( r - \frac{1}{r} \right) F_1(r, t) + m_3(\tau) \left( r - \frac{1}{r} \right) F_4(r, t) \right] \\ &= \left( r - \frac{1}{r} \right) \left( m_1(\tau) \frac{\partial}{\partial t} F_2(r, t) + m_2(\tau) \frac{\partial}{\partial t} F_1(r, t) + m_3(\tau) \frac{\partial}{\partial t} F_4(r, t) \right) = F_6(r, t). \end{aligned} \quad (5.129)$$

This finally leads to the representation

$$\mathbf{g}_{nor}(x, \eta) = \frac{1}{4\pi} (rF_2(r, t) + F_5(r, t))[\xi \otimes \eta] + \frac{1}{4\pi} F_6(r, t)[(\eta - (\xi \cdot \eta)\xi) \otimes \eta]. \quad (5.130)$$

Altogether, if only radial displacements are prescribed on the spherical boundary, the above explicit form can be used efficiently to solve the displacement boundary-value problems by numerical integration. Finally, it should be remarked that, in order to obtain an implementable representation for the complete Green function including tangential parts, further investigations are required.



# Chapter 6

## Numerical Results

In this chapter we are concerned with the numerical realization of the wavelet approximations developed in previous sections.

### 6.1 A Test Example - Use of Cauchy-Navier Wavelets Associated to Layer Potentials

We present some test examples for the geoscientifically important case of a sphere (i.e.,  $\Sigma = \Omega$ ).

#### 6.1.1 Spherical Approximation of Vector Fields by Layer Potentials

For this purpose, we first consider the vector field  $f : \Omega \longrightarrow \mathbb{R}^3$  given by

$$f(\xi) = \begin{cases} 0\epsilon^3 & , \quad -1 \leq \xi \cdot \epsilon^3 \leq h \\ \frac{3}{2} \left( \frac{h - \xi \cdot \epsilon^3}{h-1} \right)^2 \epsilon^3 & , \quad h \leq \xi \cdot \epsilon^3 \leq \frac{2+h}{3} \\ \left( 1 - 3 \left( \frac{\xi \cdot \epsilon^3 - 1}{h-1} \right)^2 \right) \epsilon^3 & , \quad \frac{2+h}{3} \leq \xi \cdot \epsilon^3 \leq 1 \end{cases} \quad (6.1)$$

with  $h = 1/2$  (cf. [37]).

The third component of the boundary function  $f$  is illustrated in Figure 6.1.

We are particularly interested in approximating (the third component) of the vector function  $f$  by our wavelet approach based on layer potentials (as prescribed above). Figure 6.2 shows the sectional illustration of approximations of the boundary function corresponding to the  $\Sigma$ -scaling function  $\Phi_{\tau_j}^{(5)}$  for different levels, i.e.  $\tau_j = 2^{-j}$ ,  $j = 1, 2, 3, 4$ . Note that, in each evaluation step, a sufficiently large number of equiangular longitude-latitude grid

points on the unit sphere has been used in order to avoid oscillations in the approximation process.

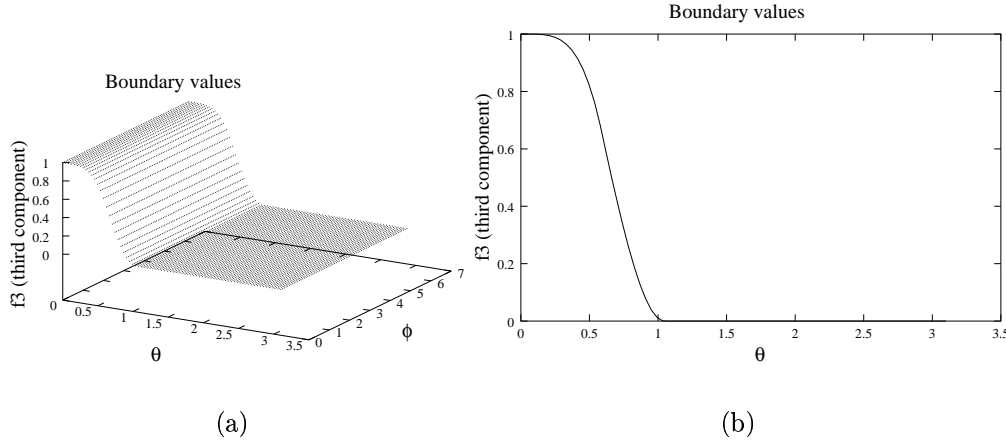


Figure 6.1: Functional values of  $f$  (third component): (a) on a longitude-latitude grid of points on  $\Omega$  (b) one-dimensional sectional illustration.

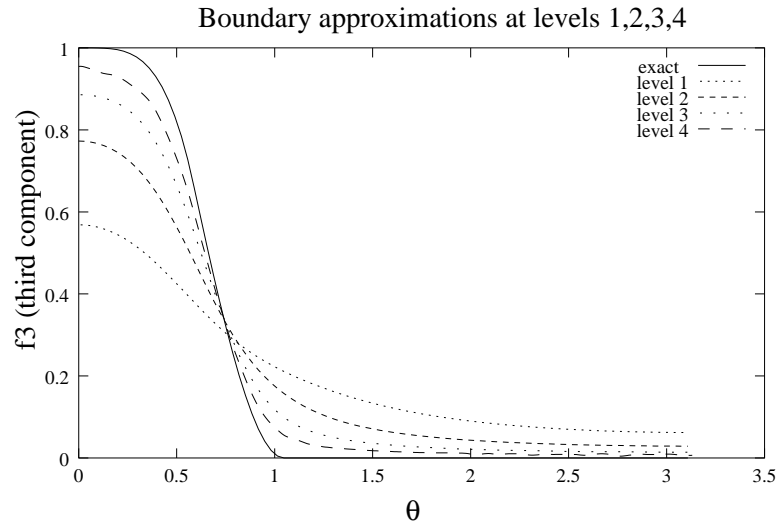


Figure 6.2: Sectional illustration of the scale approximations of  $f$  (third component) associated to the  $\Sigma$ -scaling function  $\Phi_{\tau_j}^{(5)}$  for  $j = 1, 2, 3, 4$ .

In accordance with Theorem 4.1 it may be expected that our multiscale procedure also provides a good approximation of  $u \in \text{pot}(\overline{\Omega_{int}})$  with  $u|_{\Omega} = f$  inside  $\Omega$ . However, we did not make effort to make a more detailed quantitative description.

## 6.2 Test Examples - Use of Cauchy-Navier Wavelets Associated to Vector Spherical Harmonics

In this section, we apply our multiscale procedure (i.e. the spectral approach to wavelets) for a simple inner displacement boundary-value problem, of which the boundary is assumed to be the unit sphere  $\Omega$  and an analytical solution is explicitly known for  $\overline{\Omega_{int}}$ . In contrast to the test problems, where only the boundary function is known (for example, Section 6.1 or real geophysically relevant problems), this test example enables us to check the accuracy of the approximation in the inner space  $\Omega_{int}$ . For simplicity, we investigate the obtained accuracy of the solution on the surface of  $\Omega_{1/2} \subset \Omega_{int}$  and the scale approximations of given boundary function. To be more explicit, we consider the solution  $u \in pot(\overline{\Omega_{int}})$  corresponding to the boundary field  $u|_{\Omega} = f$  given by

$$f(x) = \frac{x_1 x_2}{2} \epsilon^1 - \frac{\sigma}{2(\sigma + 3)} (x_1^2 + x_2^2 + x_3^2) \epsilon^2 + \frac{x_2 x_3}{2} \epsilon^3, \quad \sigma \neq 0. \quad (6.2)$$

We choose, in particular,  $\sigma = 2.5$  (i.e.  $\lambda = 2$ ,  $\mu = 3$ ).

The following figure shows the exact boundary displacements under the displacement function  $f$ .

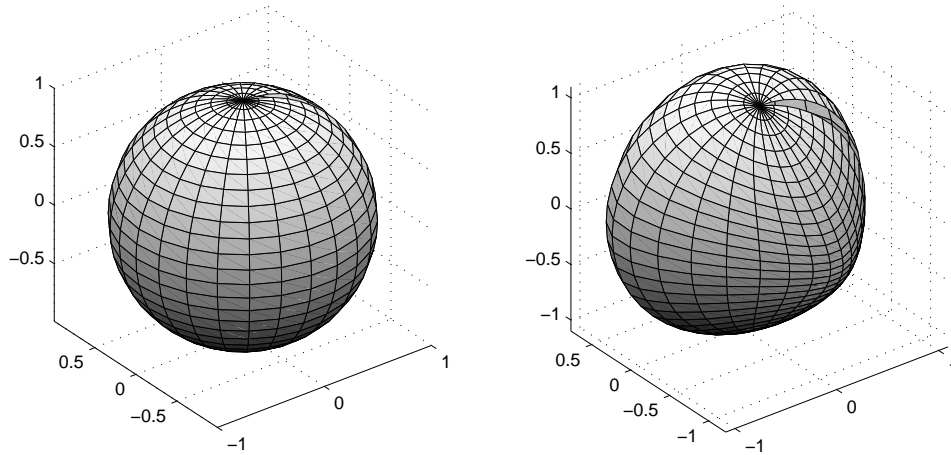


Figure 6.3: The reference (left) and the deformed (right) configurations of the unit sphere  $\Omega$  associated to the displacement function  $f$ .

We compute the multiscale approximations of the inner displacements on the sphere  $\Omega_{1/2}$  for the first five levels by means of three different type of wavelets, namely, Shannon,

modified Shannon and cubic polynomials wavelets. For the quantitative analysis of the accuracy, the radial and tangential displacements are taken into account. Following figures show the exact radial displacement quantities and tangential displacement vectors on  $\theta-\varphi$  plane, by gray scale colormaps and arrows, respectively.

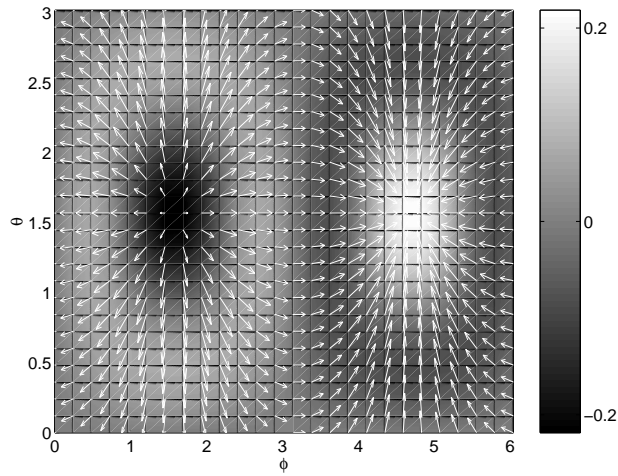


Figure 6.4: The (exact) radial and tangential boundary displacements on the unit sphere  $\Omega$ .

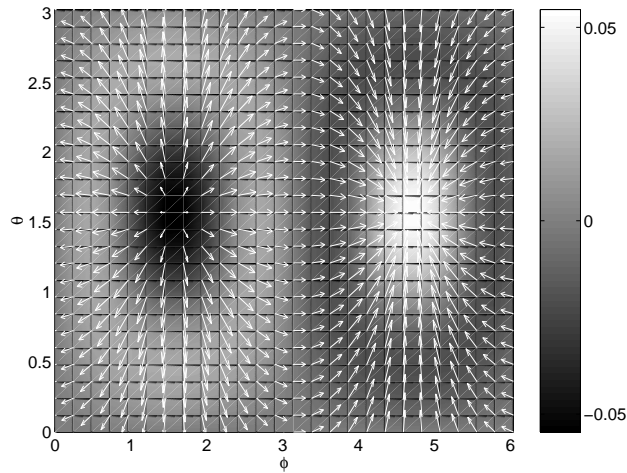


Figure 6.5: The (exact) radial and tangential displacements on the sphere  $\Omega_{1/2}$ .

### 6.2.1 Multiscale Approximation - Scale and Detail Reconstructions (Global)

In what follows, we approximate the displacements over the sphere  $\Omega_{1/2}$  using the boundary displacements over the whole unit sphere  $\Omega$ . Since the evaluation of wavelet coefficients naturally consists of integrations over the unit sphere  $\Omega$ , we have to use an appropriate integration rule. We use an equiangular longitude-latitude grid system where the integration weights are explicitly known (see, for example, [22]). Moreover, assuming that the wavelets are bandlimited, we are able to use an exact integration rule as mentioned in Chapter 5.

Assuming that the boundary displacement function is bandlimited, we compute our multiscale approximations by using three different bandlimited wavelets mentioned above. In each case, the multiscale approximations are observed until the detail information are almost negligible. Moreover, at each level  $j$ , a sufficiently large number of equiangular grid points are used for numerical integration so that the exact integration is assured (see, for example, [22],[30]). The following series of Figures 6.6-6.13 show multiscale reconstructions.

It should be remarked that we use gray scale colormaps for the radial displacements and arrows for the tangential displacement vectors of each approximation. Moreover, in order to show the quantitative properties of results, we scale the size of arrows at each level taking the exact tangential displacement vectors as the reference size.

#### Multiscale Analysis Using Shannon Wavelets

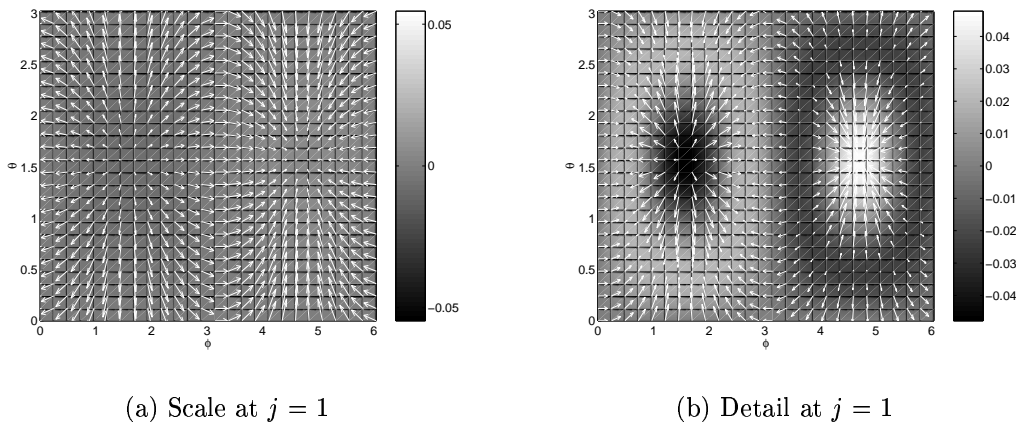


Figure 6.6: Scale and detail reconstructions by Shannon wavelets.

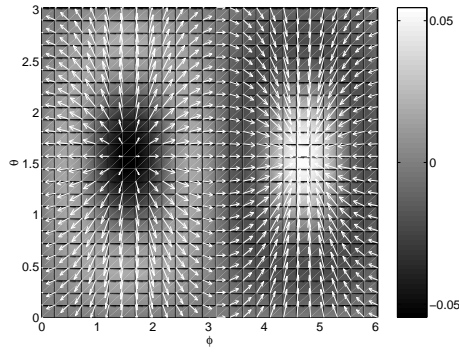
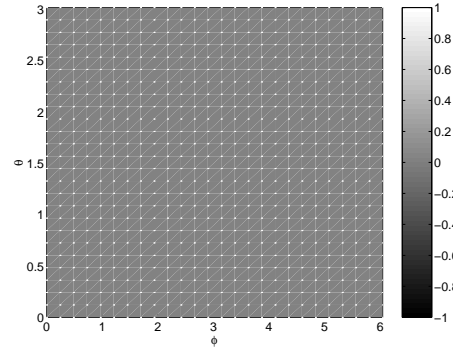
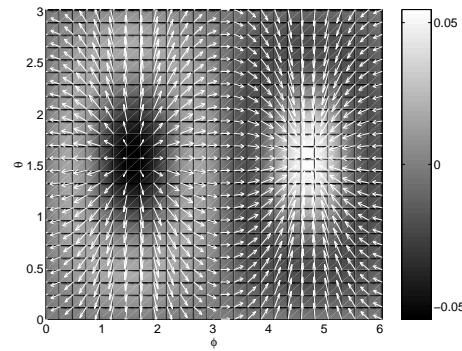
(a) Scale at  $j = 2$ (b) Detail at  $j = 2$ (c) Scale at  $j = 3$ 

Figure 6.7: Scale and detail reconstructions by Shannon wavelets.

### Multiscale Approximation Using Modified Shannon Wavelets

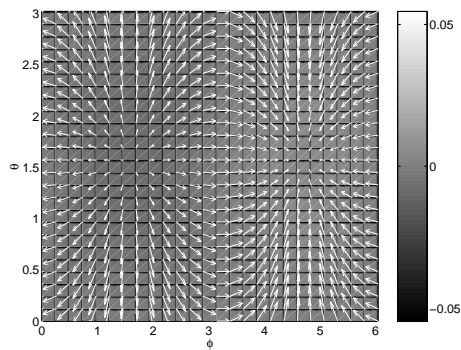
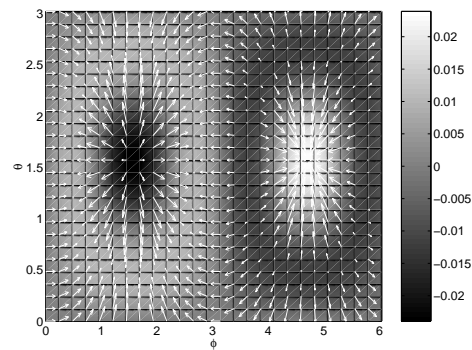
(a) Scale at  $j = 1$ (b) Detail at  $j = 1$ 

Figure 6.8: Scale and detail reconstructions by modified Shannon wavelets.

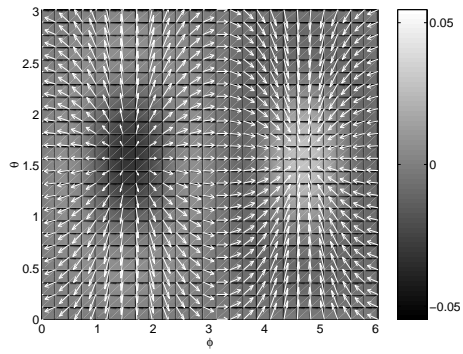
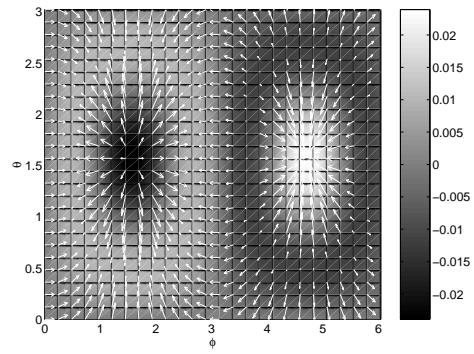
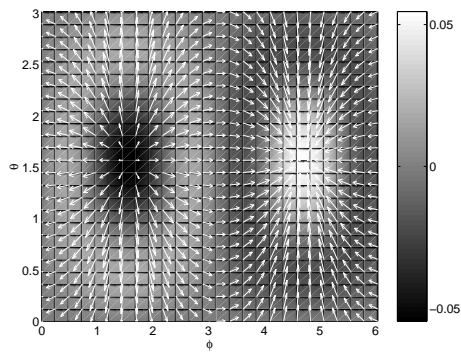
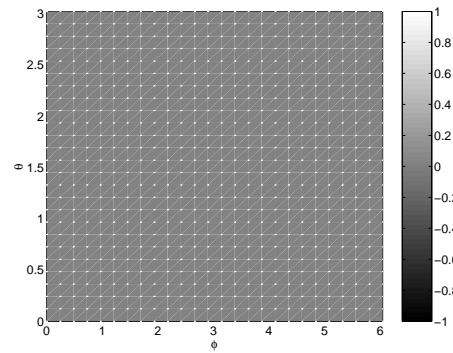
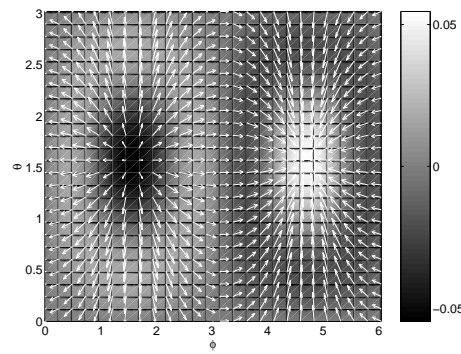
(a) Scale at  $j = 2$ (b) Detail at  $j = 2$ (c) Scale at  $j = 3$ (d) Detail at  $j = 3$ (e) Scale at  $j = 4$ 

Figure 6.9: Scale and detail reconstructions by modified Shannon wavelets.

## Multiscale Approximation Using Cubic Polynomial Wavelets

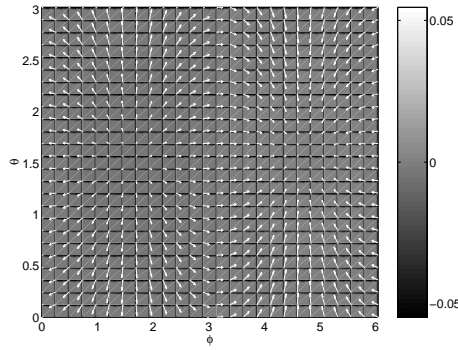
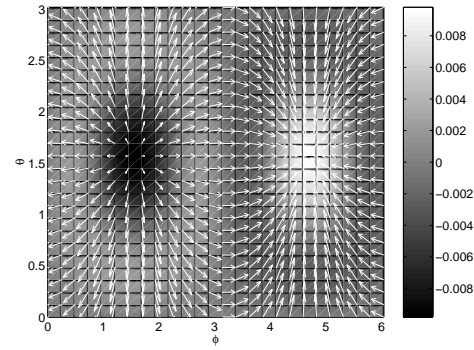
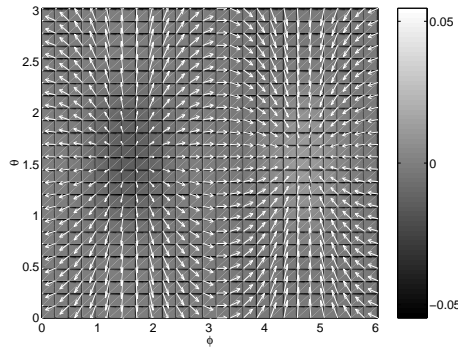
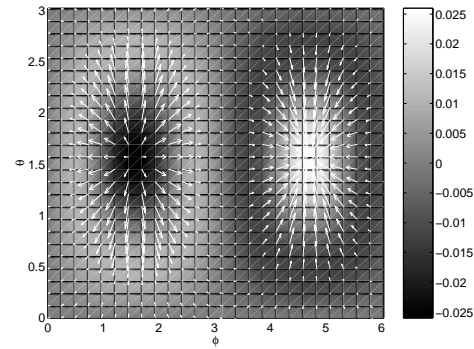
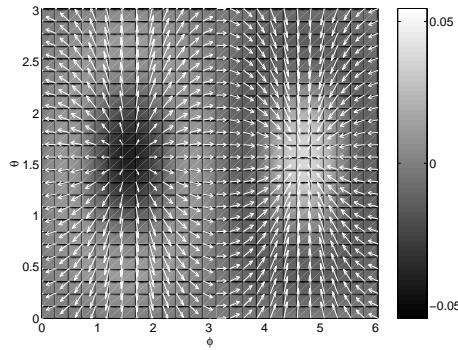
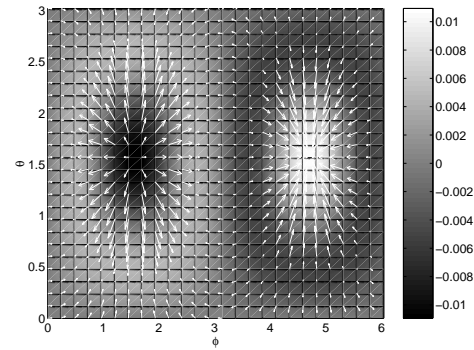
(a) Scale at  $j = 1$ (b) Detail at  $j = 1$ (c) Scale at  $j = 2$ (d) Detail at  $j = 2$ (e) Scale at  $j = 3$ (f) Detail at  $j = 3$ 

Figure 6.10: Scale and detail reconstructions by cubic polynomial wavelets.



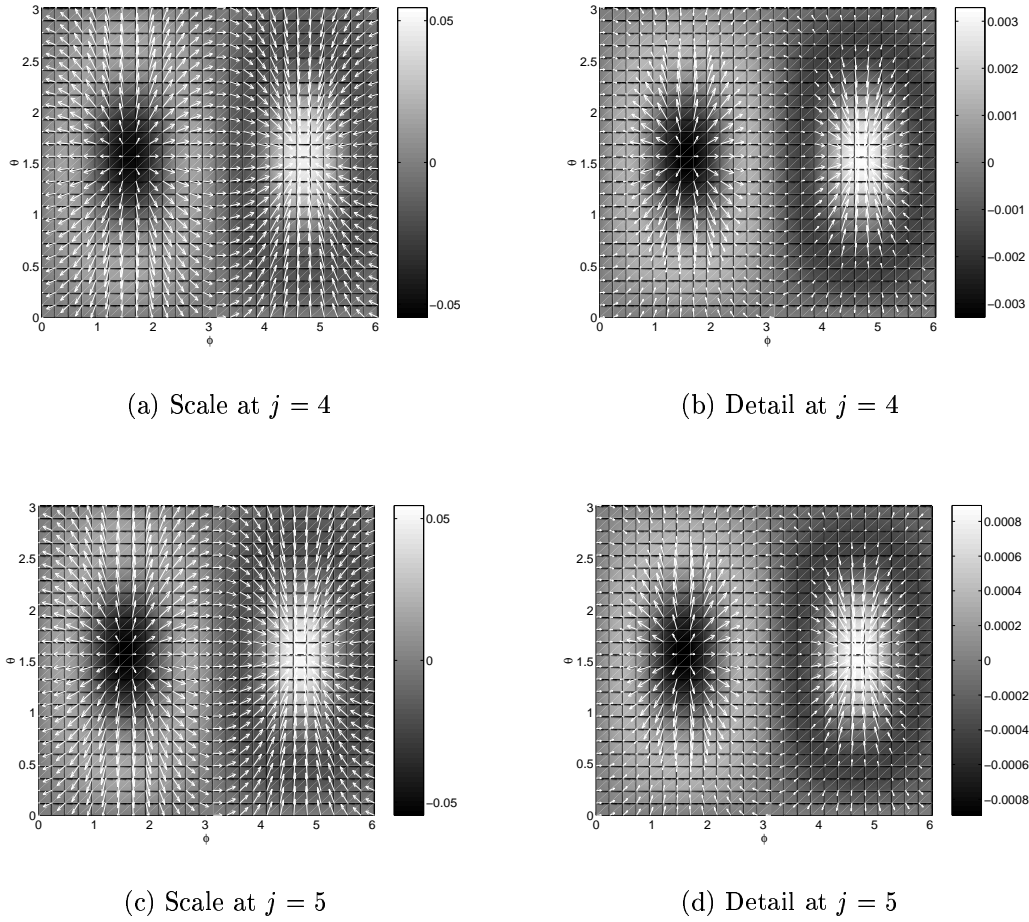


Figure 6.11: Scale and detail reconstructions by cubic polynomial wavelets.

Next we evaluate the scale approximations for boundary displacements (i.e. displacements on  $\Omega$ ) by using cubic polynomial wavelets up to level 5. For the purpose of comparing those results with the scale approximations of inner displacements, we plot the results together with scale approximations obtained on  $\Omega_{1/2}$ . The Figures 6.12 - 6.13 illustrate the radial and tangential displacements. It should be noted, once again, that the arrows of tangential displacement vectors are scaled taking the exact values on  $\Omega$  and  $\Omega_{1/2}$ , respectively, as the reference scales.

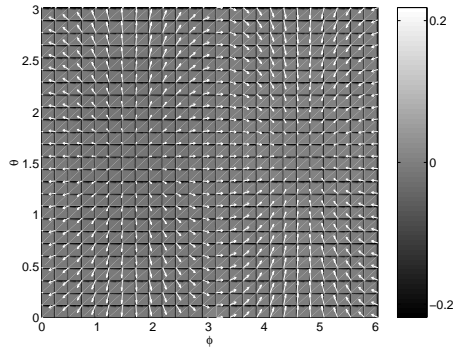
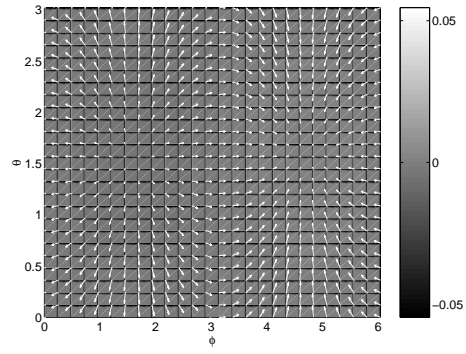
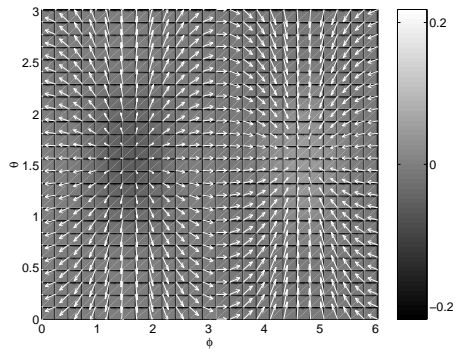
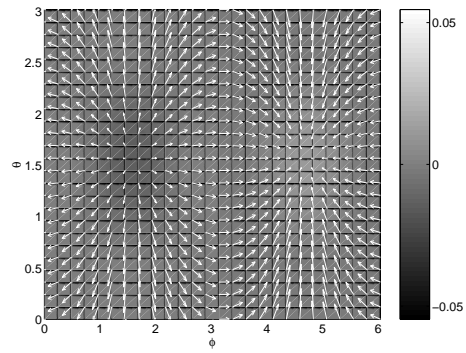
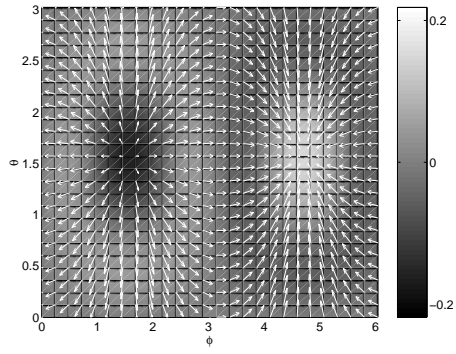
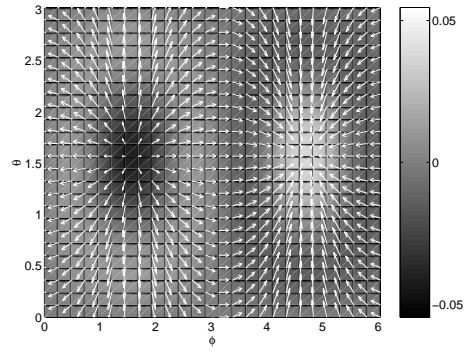
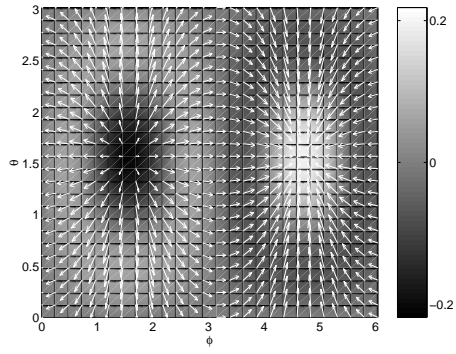
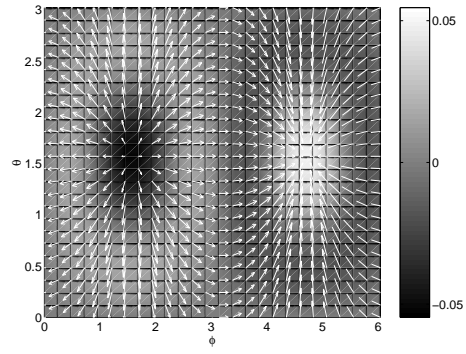
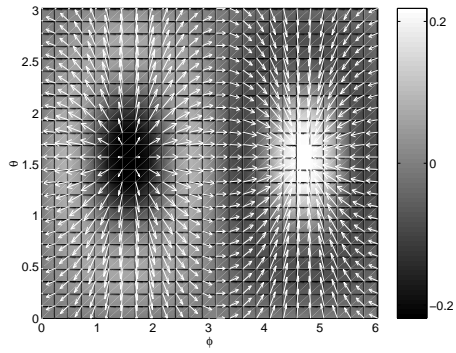
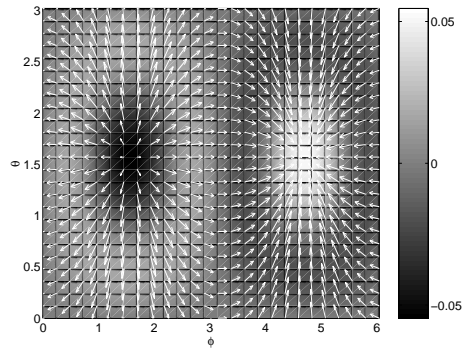
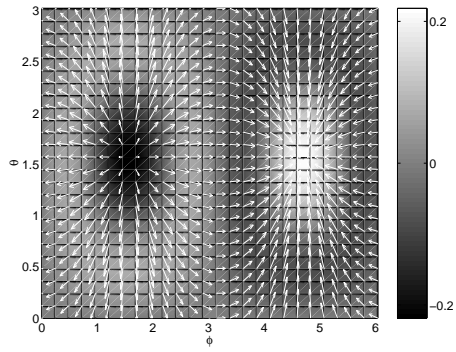
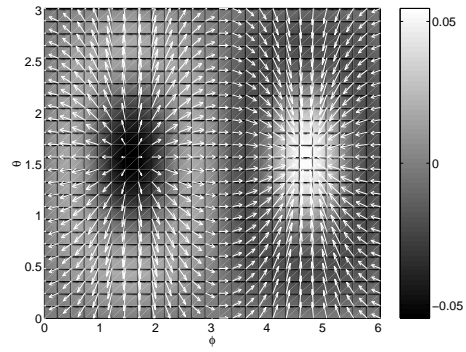
(a) Scale at  $j = 1$ (b) Scale at  $j = 1$ (c) Scale at  $j = 2$ (d) Scale at  $j = 2$ (e) Scale at  $j = 3$ (f) Scale at  $j = 3$ 

Figure 6.12: Scale approximations by cubic polynomial wavelets at levels 1,2,3, on  $\Omega$  (left) and on  $\Omega_{1/2}$  (right).

(a) Scale at  $j = 4$ (b) Scale at  $j = 4$ (c) Scale at  $j = 5$ (d) Scale at  $j = 5$ 

(e) Exact



(f) Exact

Figure 6.13: Scale approximations by cubic polynomial wavelets at levels 4,5 and exact displacements on  $\Omega$  (left) and on  $\Omega_{1/2}$  (right).

In conclusion, the Shannon wavelet approximation has provided a fast convergence process where the detail information is rapidly decreased. One may conclude that, this is due to orthonormal property of the Shannon wavelets. Since the spectral coefficients of Shannon wavelets are either 0 or 1, whole information of the boundary data are covered up to a certain degree in terms of vector spherical harmonics (see, Figure 5.1). However, a major drawback of Shannon wavelets is the oscillating characteristic in the detail reconstructions. It may happen in higher level resolutions due to the sharp cutting of the wavelets in the frequency domain.

Furthermore, a smooth version of bandlimited wavelets, i.e. the cubic polynomial wavelets give a slowly decreasing but smooth process in detail reconstruction. However, higher level resolutions are required to get a better approximation.

For the quantitative analysis of the accuracy, one can consider different types of error measures, in particular, we use the mean absolute error  $e_{abs}$  defined by

$$e_{abs} = \frac{1}{n} \sum_{\substack{x \in B \\ \#B=n}} |u(x) - \tilde{u}(x)|, \quad (6.3)$$

where  $B$  denotes the point set which contains  $n$  points.

The vector fields  $u$  and  $\tilde{u}$  are the exact and approximate displacements, respectively. Error behaviour of our three different wavelet approximations on  $\Omega_{1/2}$  is given by the following figure.

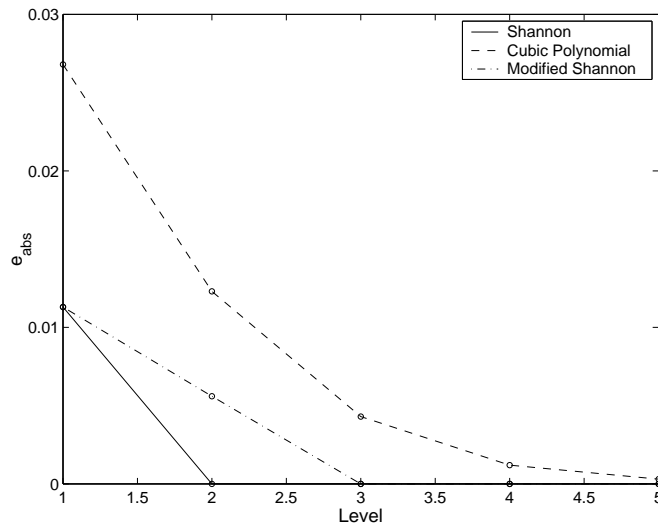


Figure 6.14: Mean absolute errors ( $e_{abs}$ ) of three different wavelet approximation of the inner displacements on  $\Omega_{1/2}$ .

### 6.2.2 Multiscale Approximation - Scale and Detail Reconstructions (Local)

In the remaining part of our numerical realization, we illustrate the multiresolution in terms of cubic polynomial wavelets. Since the cubic polynomial wavelets are smoother and localize in the space domain, we expect to obtain a better local resolution for the scale approximations of the displacement field.

In what follows, we consider again the same displacement boundary-value problem (i.e. the test example of Section 6.2.1) using only a part of the boundary displacements on the sphere  $\Omega$ . More specifically, we use the boundary function to be given for the region  $\phi \in [0, 2.09439]$  ( $= [0^\circ, 120^\circ]$ ),  $\theta \in [0, 1.04719]$  ( $= [0^\circ, 60^\circ]$ ) on  $\Omega$ . For simplicity, we only approximate the (inner) displacements for the region prescribed by  $\phi \in [0.8901, 1.2043]$  ( $= [51^\circ, 70^\circ]$ ),  $\theta \in [0.4450, 0.6221]$  ( $= [25^\circ, 35^\circ]$ ) on the surface  $\Omega_{0.99}$  (see Figure 6.15). Moreover, to avoid the boundary effect to the approximate solutions (i.e. Gibb's phenomenon), a sufficiently large number of boundary data, that covered the evaluation area, are used for the boundary integrations.

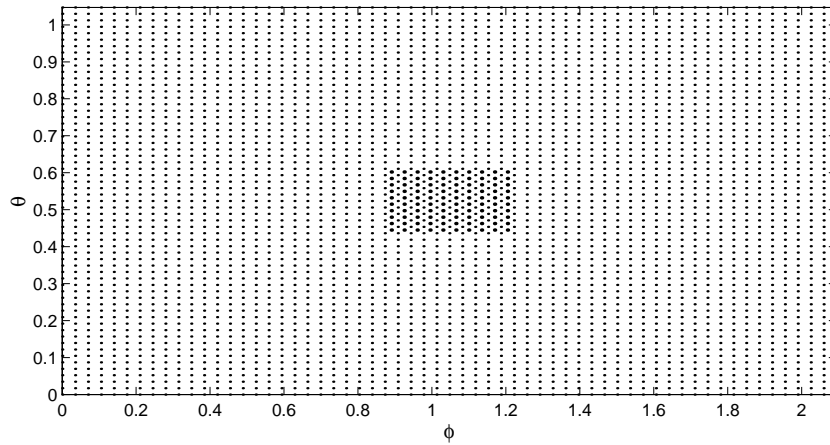


Figure 6.15: The test region of the multiscale approximation (local). The dark points in the middle describe where the approximations are evaluated.

In order to illustrate the multiresolution idea, we plot a series of pictures of scale approximations and detail reconstructions (see Figures 6.16 - 6.17). In those pictures, the quantities of inner displacements are presented by their magnitudes (i.e. by using the Euclidean norm).

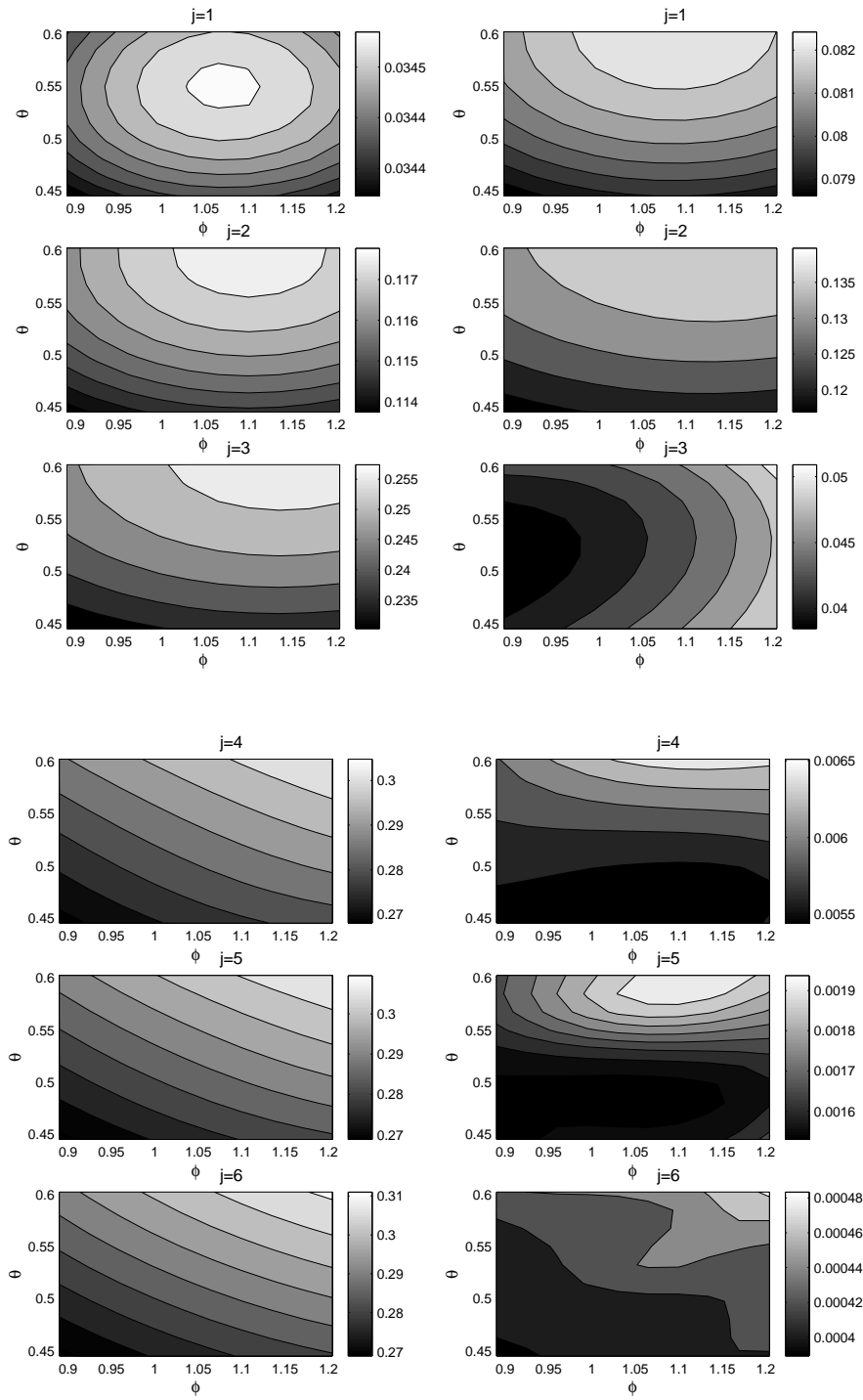


Figure 6.16: Multiscale approximation of displacements on  $\Omega_{0.99}$  at levels from 1 to 6. The Euclidean norm of the scale (left) and detail (right) reconstructions of the displacement vectors.

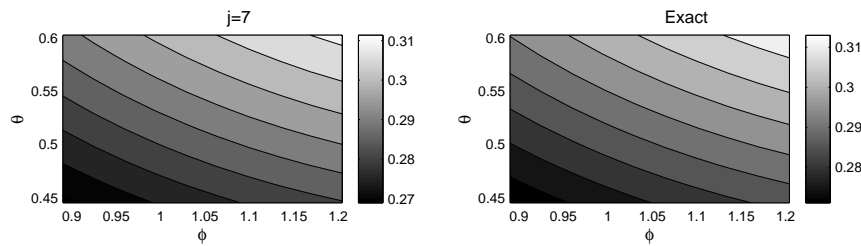


Figure 6.17: Scale approximation and exact values. Euclidean norm of the scale approximation at level 7 (left) and the exact displacements (right).

Looking at the above results, we see that the detail information at level 6 is nearly negligible. Hence, we conclude that a better approximation can be obtained locally, within the first 7 resolutions by cubic polynomial wavelets.

### 6.3 An Application to Deformation Analysis of the Earth

In what follows, we are concerned with an application of our Cauchy-Navier wavelet approach developed in Chapter 5. The deformation analysis of the Earth's interior near to the surface is approximated from displacements on the spherical Earth's surface assumed to be spherical. The boundary displacement vectors under consideration are computed from mean velocity displacements obtained from GPS satellite measurements (see, for example, [16]).

As it is well-known, the Earth is a deformable body and its shape is continuously undergoing changes; thus the relative positions of the points on the Earth's surface change continuously. Three-dimensional movements (displacements) on the Earth's surface and the interior are a consequence of various physical and anthropogenic processes within the Earth's system. For many areas, the Earth's surface is subject to small but important displacements known as Earth's deformations, like uplift, lateral movements, elastic deformation, etc. Those can be understood in a sense of (spatial) global and local changes of the relative positions and occur due to many reasons such as tidal forces, active tectonic processes, Earth rotation and polar motion and crustal loading and unloading. The movements of the tectonic plates due to the tidal forces may cause to change the Earth gravity field and the shape of the Earth as a rigid body, whereas the time varying surface loads cause to crustal deformations (locally) which may create cracks in the Earth's crust (that are, however, not considered of this work).

### 6.3.1 Crustal Deformation

The Earth's crust is composed by lithospheric plates with varying thickness from 10 to 80 km having the average density of  $\rho = 2.67g/cm^3$ . This crust is affected by various (regional) loading and unloading processes. Being considering the Earth's material simply as a solid the Earth's crust exhibits the non-linear stress-strain behaviour. Practically, in some regions, the Earth's materials may behave strain-rate sensitive obeying the Hooke's law and, thus, the Earth's deformation can be modelled by using the the concepts of *elasticity theory*. Many crustal rocks exhibit (linear or nonlinear) elastic properties with a Young modulus dependent on the confining pressure having a Poisson's ratio in a range from 1/10 to 1/2 (for the most of rocks it is 0.27 (cf. [50])). In this context, the study of the elastic deformations of the Earth crust plays a considerable role in the Earth sciences.

Even though most surface displacements have minor effect on landscapes and ecosystems, there are several advantages such as the determination of where drainage channels are suddenly displaced by faults, where the highest displacements occur which exceed the elastic limits and cause a crack (known as crack problems). Another important example is the deformation analysis of lake areas, where the displacements may occur due to the changes of the water load on it. Such an analysis had been done by Tücks, ([81]) for deformation analysis of the Blåsjø lake, in Norway by satellite and terrestrial data. The crustal deformation analysis based on classical geodetic measurements has been subject to a large number of research directions (see, for example, [19]). Many other possible problems have been discussed by several scientists (see, for example, [13],[21],[54],[83]).

### 6.3.2 Deformation Analysis for the Nevada Area Using GPS Measurements

In this study, we use the Nevada region (USA) as our test area for modelling the elastic deformation. This area lies between the longitudes 125.0W and 115.0W and latitudes 32.5N and 42.5N. From Geophysical point of view, the choice of this area is justified, because it has found that the Nevada region located in the North American tectonic plate is a most active deformable area in the USA. During the past decade, three considerable Earthquakes and several minor movements occurred in this area ([72]). In our approach we determine the elastic deformation in the Nevada region using the mean surface displacement velocities measured during the time period 1994-2000 determined by GPS (Global Positioning System) geodetic measurements. Mean velocities are used to calculate the mean surface displacement rates in which the several stations, spread evenly throughout the considered area, are selected. It is worth to mention that the geodetic measurements with GPS are widely applied in geophysical studies. At present short-term crustal deformation can be detected within the accuracy of  $2mm$  by using space techniques. For more detailed informations on numerous applications, the reader is referred to, for example, [17],[19],[70],[78],[82]. However, our work is restricted only to the analysis of mean deformation of the interior using readily available boundary data.

At this point it is worth mentioning the well-known datum problem. Roughly speak-



ing, a geodetic datum defines the size and shape of the Earth as well as the origin and orientation of the coordinate systems used to map the Earth. The technological advancements that have made possible global positioning measurements with sub-meter accuracies require careful datum selection between coordinates. Referencing geodetic coordinates to the wrong datum can result into large position errors. The commonly chosen coordinate system is the latitude, longitude, and height system. The Prime Meridian and the Equator are the reference planes used for defining longitudes and latitudes. Moreover, three-dimensional positions can be determined in an Earth fixed coordinate system with respect to the center of mass. For more details about the datum problem, the reader is referred to geodetic literature.

In our consideration, we start from boundary displacements which are available in cartesian coordinates for a certain subarea of the Earth. To be more specific, we consider a set of nodes to be given in an Earth's fixed coordinate system such that every displacement vector is associated to one of the members of the nodal system (see Appendix C). Necessary information and data are available in the web site <http://quake.wr.usgs.gov/research/deformation/gps/auto/CL.html> maintained by the USGS-Earthquake Hazards Program- Northern California.

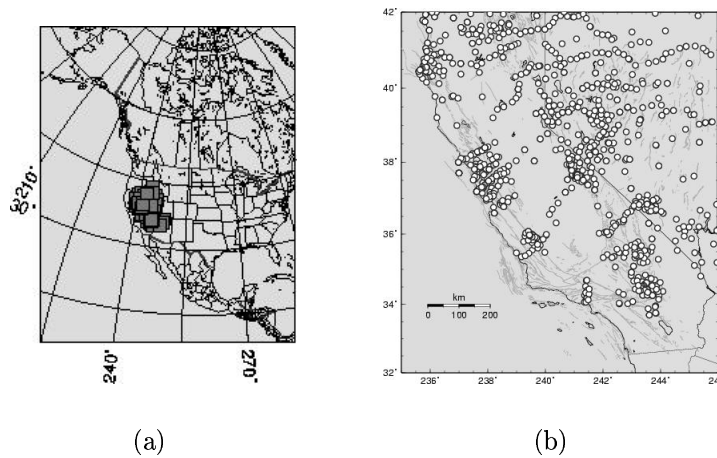


Figure 6.18: California and Nevada areas (USA) and GPS stations - the test area. (Source: USGS - Earthquake Hazards Program- Northern California).

It is worth mentioning that one can use the (original) scattered data set (see Figure 6.19(a)) directly for wavelet approximations introducing an appropriate integration procedure. However, for simplicity, we wish to apply a readily available numerical integration rule which we have used in previous test examples. For this purpose, as it is essential to have boundary data on equiangular grid points, we evaluate the mean boundary displacements on each equiangular grid point by taking the average of given displacements at neighbouring points. The Figures 6.23(a)-6.23(b) show the scattered data and the

estimated values of them on equiangular grid points.

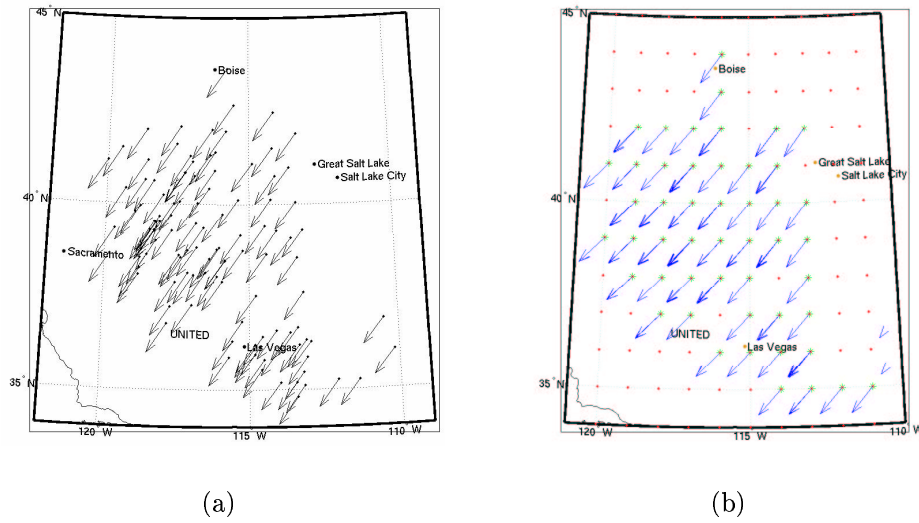


Figure 6.19: (a) 1994-2000 average horizontal velocities of the crustal deformation at 115 points measured using GPS (source : USGS - Earthquake Hazards Program- Northern California). (b) 1994-2000 average horizontal velocities of the crustal deformation transformed to equiangular longitude-latitude grids.

Missing boundary data in the considered region are filled up by using appropriate linear interpolation and extrapolation procedures. The complete set of boundary displacement vectors is shown in Figures 6.20(a)-6.20(b). In these figures, the gray colormaps show the Euclidean norm of the boundary displacements, whereas the arrows represent the horizontal displacements.

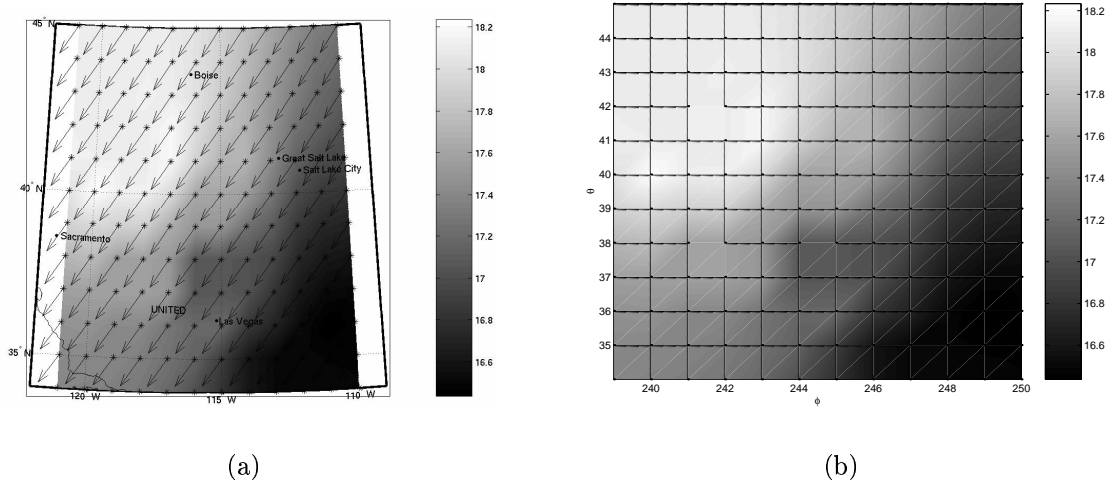


Figure 6.20: (a) 1994-2000 average crustal deformation of the region covered by latitudes  $34^{\circ}N - 45^{\circ}N$  and longitudes  $121^{\circ}W - 110^{\circ}W$  (i.e.  $\phi \in [239^{\circ}, 250^{\circ}]$ ,  $\theta \in [34^{\circ}, 45^{\circ}]$ ) including extended (interpolated and extrapolated) data. The gray colormap represents the magnitude of the mean deformation in  $mm$  and the horizontal displacements are prescribed by arrows. (b) Magnitude (Euclidean norm) of the mean displacements in  $mm$  on  $\theta - \phi$  plane.

We use the above boundary displacement vectors and our wavelet technique with cubic polynomial wavelets to approximate displacement fields in the region covered by latitudes  $38^{\circ}N - 41^{\circ}N$  and longitudes  $117^{\circ}W - 112^{\circ}W$  (i.e.  $\theta \in [38^{\circ}, 41^{\circ}]$ ,  $\phi \in [241^{\circ}, 246^{\circ}]$ ).

For this particular data set (see Appendix C), we see that the radial displacements are nearly negligible compared to horizontal displacements. Therefore, for simplicity, we transform the data onto a spherical boundary. We use a spherical Earth's surface with mean radius  $6731Km$  and approximate the displacements in the interior on the spherical area of radius  $0.999 \times 6731Km$  covered by the above longitude-latitude boundaries.

The following figures show the multiscale approximations up to level 8. We present our results in two different forms: using the magnitudes of the approximate displacement vectors and considering the tangential displacements. For more convenience, we scale the vectorial quantities of scale approximations as in previous sections taking the results at level 8 as reference scale. Moreover, in the representation of detail information, we use the detail reconstruction at level 1 as reference values. The Euclidean norm of displacements vectors (the magnitudes) is represented by gray colormaps. It should be remarked that the arrows in Figures 6.21-6.23 (i.e. the horizontal displacements) are appeared in one direction, because, the changes of the directions are almost negligible compare to the size of the displacement vectors.

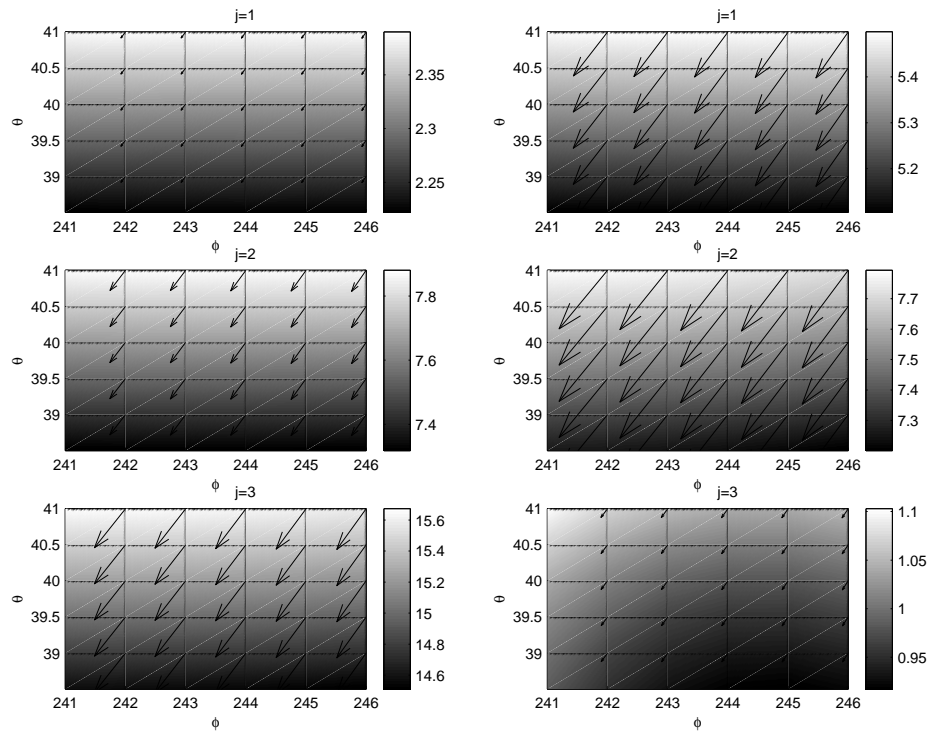


Figure 6.21: Multiscale approximation of displacements at levels 1, 2, 3. The magnitude (gray colormap) and tangential displacements (arrows) of scale (left) and detail (right) reconstructions.

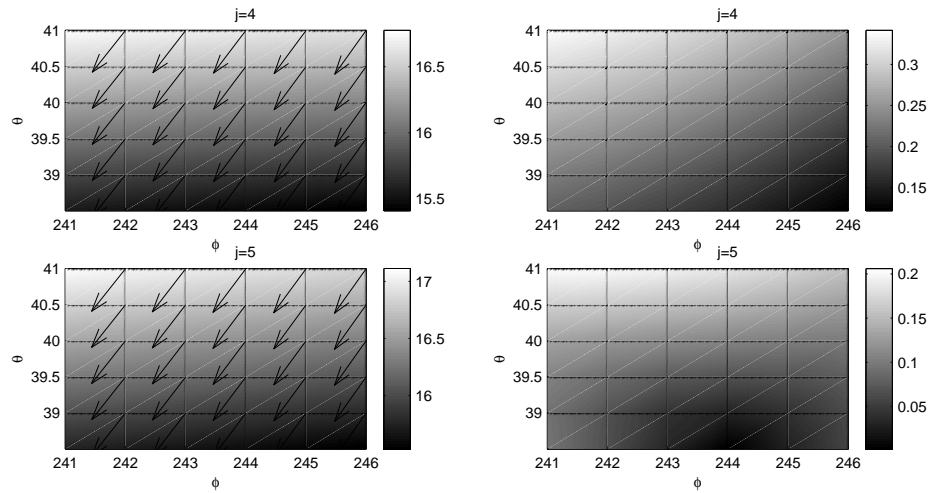


Figure 6.22: Multiscale approximation of displacements at levels 4, 5. The magnitude (gray colormap) and tangential displacements (arrows) of scale (left) and detail (right) reconstructions.

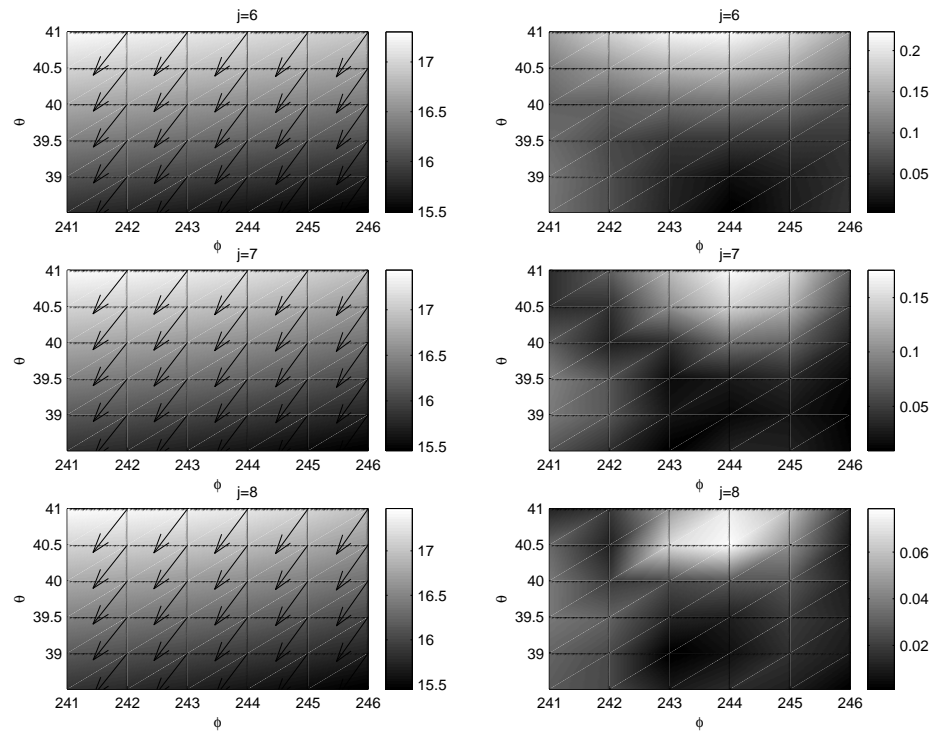


Figure 6.23: Multiscale approximation of displacements at levels 6, 7, 8. The magnitude (gray colormap) and tangential displacements (arrows) of scale (left) and detail (right) reconstructions.

# Chapter 7

## Concluding Remarks

The focus of this work had been to develop two families of wavelet solvers for the inner displacement boundary-value problem of elastostatics. The methods we developed are particularly suitable for the deformation analysis corresponding to geoscientifically relevant (regular) boundaries like sphere, ellipsoid or the actual Earth's surface.

The principal idea of our spatial approach to Cauchy-Navier wavelets discussed in Chapter 4, is based on the classical limit and jump relations of elastostatics. The overall approach can be viewed as a first attempt to 'short-wavelength modelling', i.e. high resolution of the fine structure of displacement fields. The method is restricted to the homogeneous and isotropic case of linear elasticity, hence, it should be formulated under more complex (geo)physical assumptions in future investigations. We believe that the 'zoom in' procedure as presented here will become a flexible and useful technique of microstructural analysis of elastic displacement fields on regular boundaries. It is a drawback for complicated geometries that we have to resort a suitable linear system solver to obtain the wavelet coefficients of the resulting integral equations for solving the boundary-value problem for inner displacements. The difficulties can be overcome by establishing integration rules over regular boundaries. But it should be noted that, the multiscale structure together with the pyramid scheme dramatically reduce the computational effort.

It has been shown that the spectral approach to Cauchy-Navier wavelets provides an efficient numerical procedure to approximate the solution of the inner displacement boundary-value problem associated to spherical boundaries. The resulting algorithms are simple and efficient. In contrast, solving the associated linear systems, the inherent advantage of this method is that we need only boundary integrations to approximate the inner displacements. Moreover, the use of the wavelet strategy provides a 'zoom in' property to handle the problems locally, which is of practical significance in many geoscientific problems for (local) deformation analysis. The method provides sufficiently accurate solutions only within less multiresolution steps when compared to the exact solutions for the test problems considered. Moreover, it is demonstrated in numerical examples that the cubic polynomial wavelets are particularly well suited in both global and local problems. The

test problem we dealt with real data can be viewed as the first step towards practical applications, and illustrates the large potential of the method. The method is ready to take on the challenge for solving more applied geoscientifically relevant problems in a straightforward manner.

In order to accelerate the evaluation process of tensorial kernel functions appearing in both approaches, the knowledge of, for example, Fast Multipole Methods and Domain Decomposition Techniques can be applied with necessary modifications. That is, however, beyond the scope of this work. Moreover, there are a number of ways to extend the methods presented in this thesis. The following avenues of research show particular promise: (i) The spatial approach to Cauchy-Navier wavelets has originated from the concept of fundamental solutions. In doing so, the method can also be established for the solution of problems which have more complicated fundamental solutions such as problems involving anisotropic materials, where, however, the corresponding limit and jump relations have to be specified in close adaptation to the physical reality. (ii) The spectral approach can be formulated on non-spherical regular boundaries as well, in which a complete reformulation according to the Cauchy-Navier theory and non-trivial modifications are essential. This is a challenge for future work.

# Appendix A

## Further Results on Cauchy-Navier Scaling Functions and Wavelets

In this section we present a graphical representation of Cauchy-Navier scaling functions and wavelets considering the tensors componentwise. We consider the Shannon and the cubic polynomial functions at the levels 1,2,3 and 4. The corresponding scaling and wavelet functions  $\Phi_j^D(x, \cdot)$ ,  $\Psi_j^D(x, \cdot)$  are evaluated over the  $\theta - \phi$  plane being  $x \in (-1, 1, 0)$  fixed. (i.e. the fixed point  $x$  is represented by polar coordinates as  $r = 1, \phi = \pi, \theta = \pi/2$ .)

### A.1 Shannon Scaling Functions and Wavelets

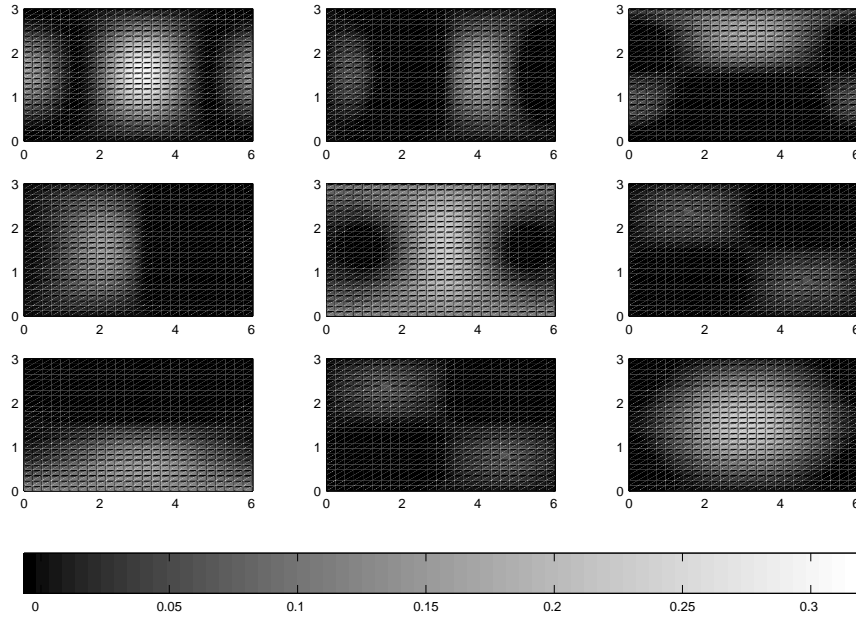


Figure A.1: Shannon scaling function at level 1.



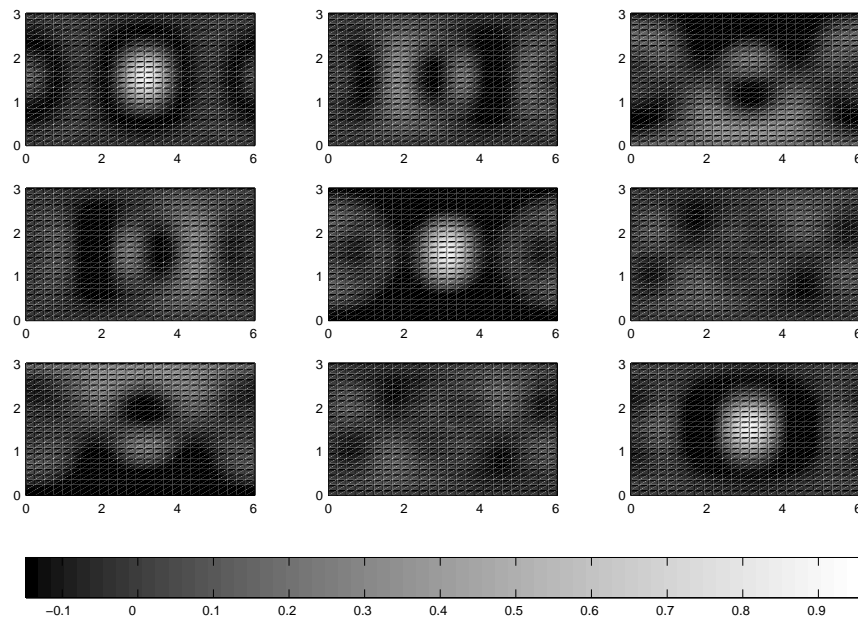


Figure A.2: Shannon wavelet at level 1.

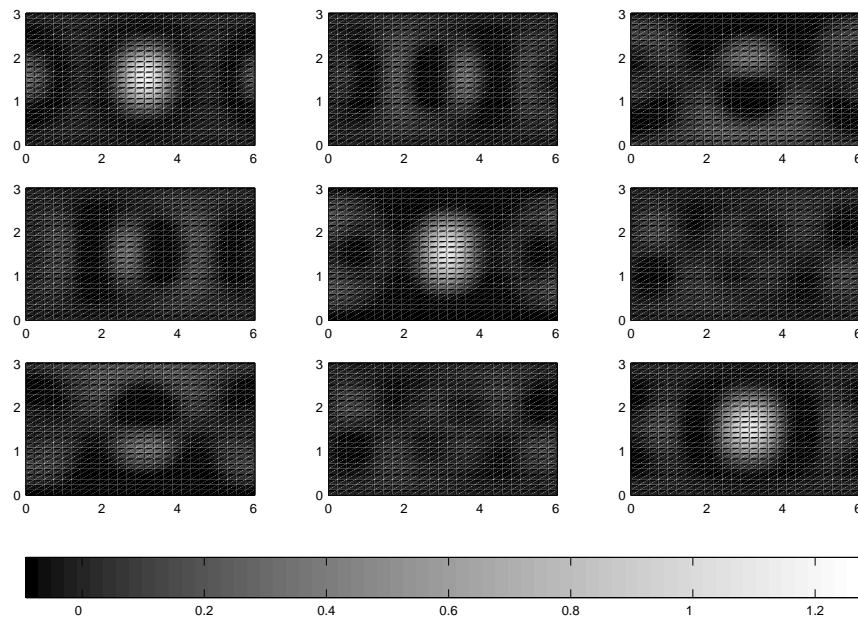


Figure A.3: Shannon scaling function at level 2.

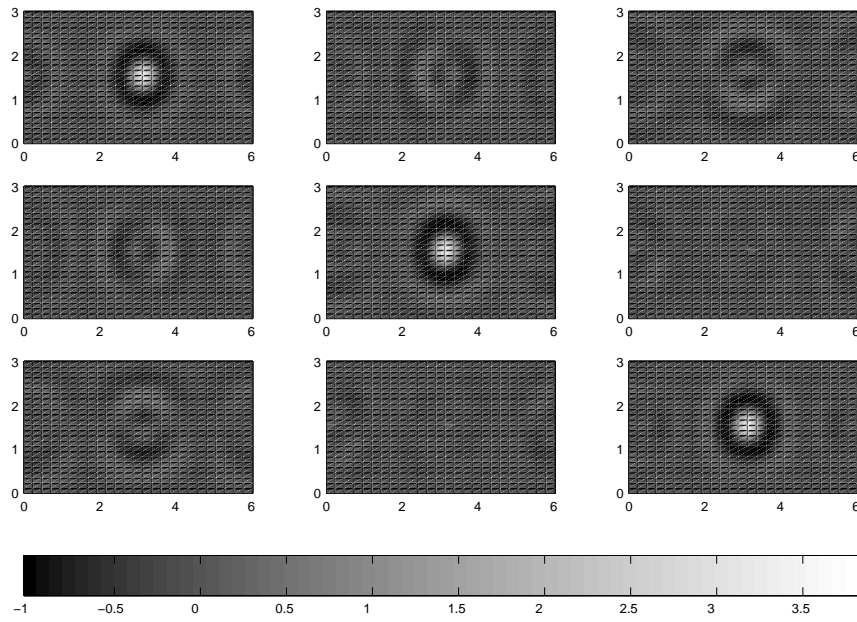


Figure A.4: Shannon wavelet at level 2.

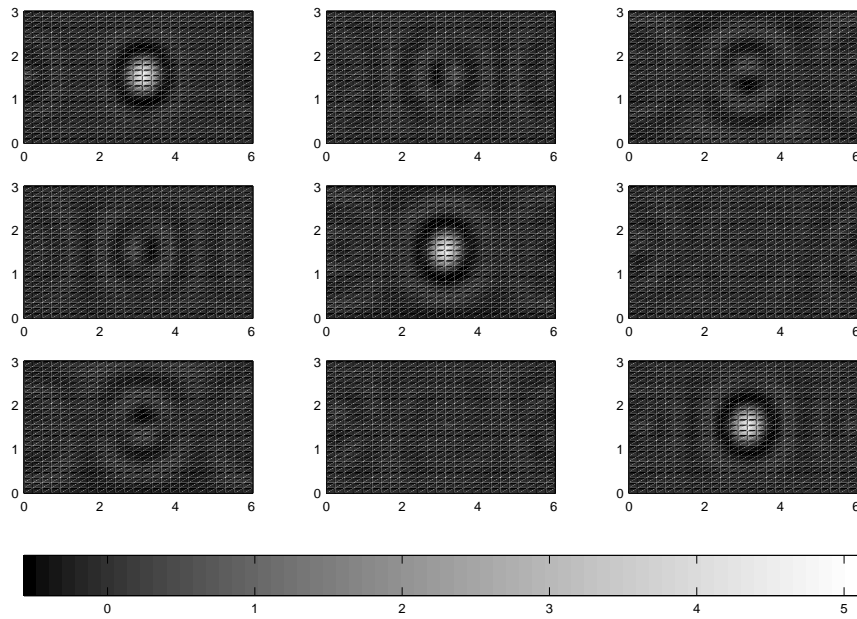


Figure A.5: Shannon scaling function at level 3.

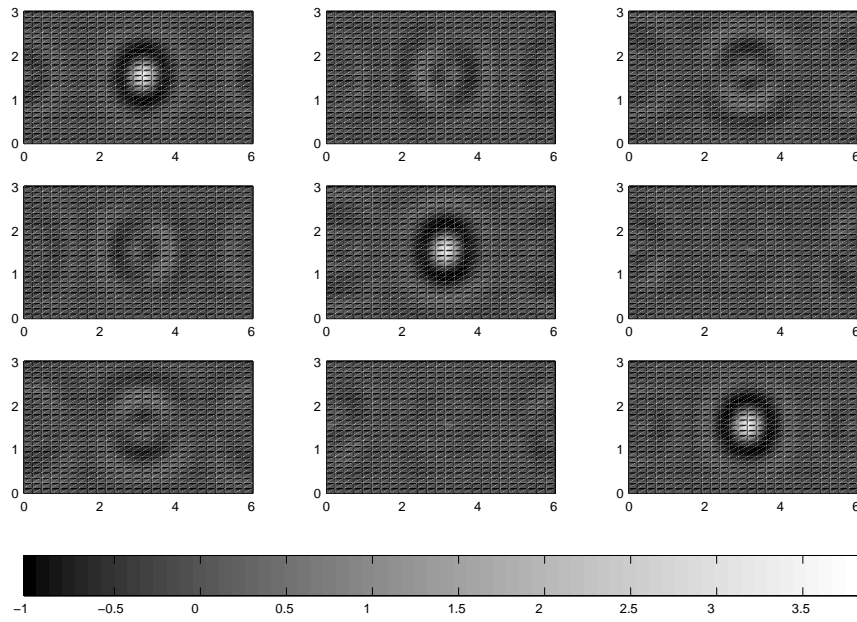


Figure A.6: Shannon wavelet at level 3.

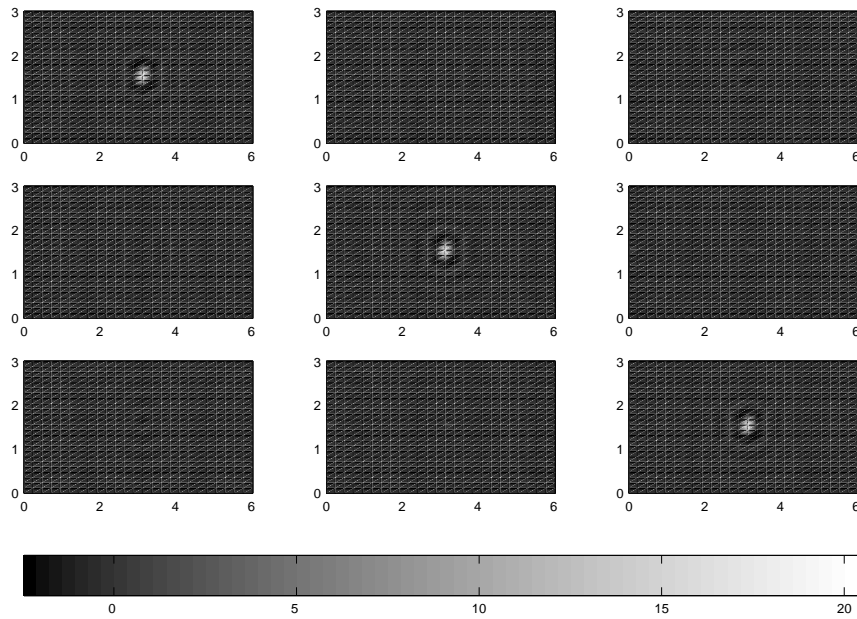


Figure A.7: Shannon scaling function at level 4.

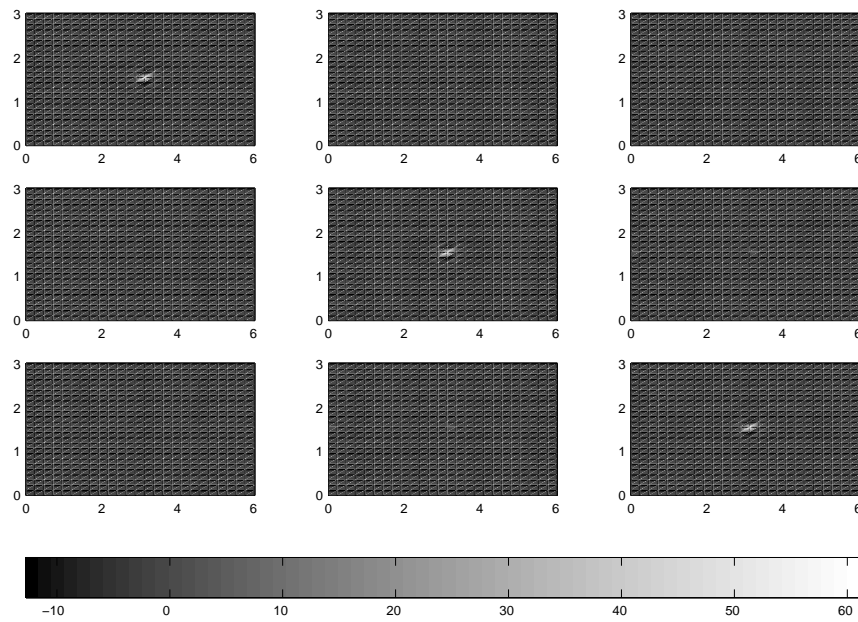


Figure A.8: Shannon wavelet at level 4.

## A.2 Cubic Polynomial Scaling Functions and Wavelets

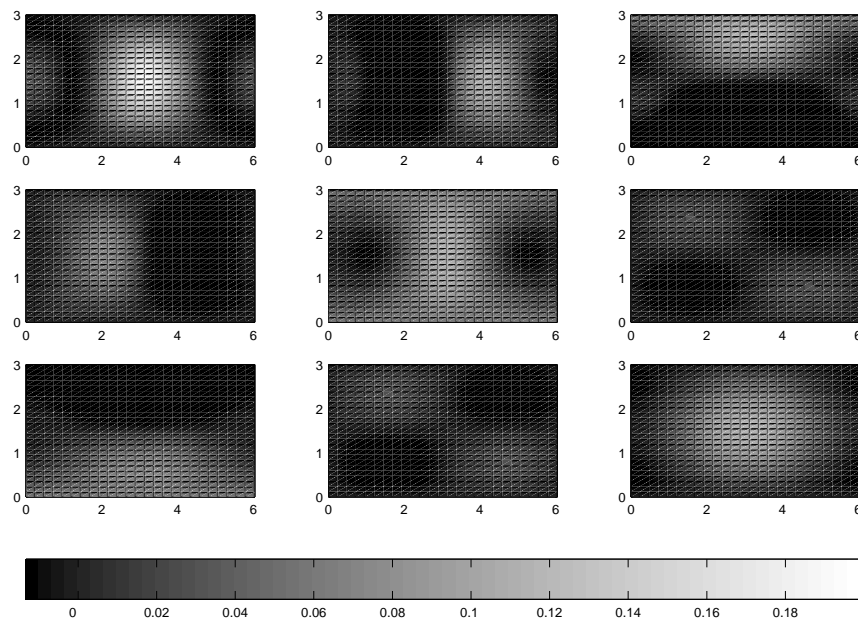


Figure A.9: Cubic polynomial scaling function at level 1.

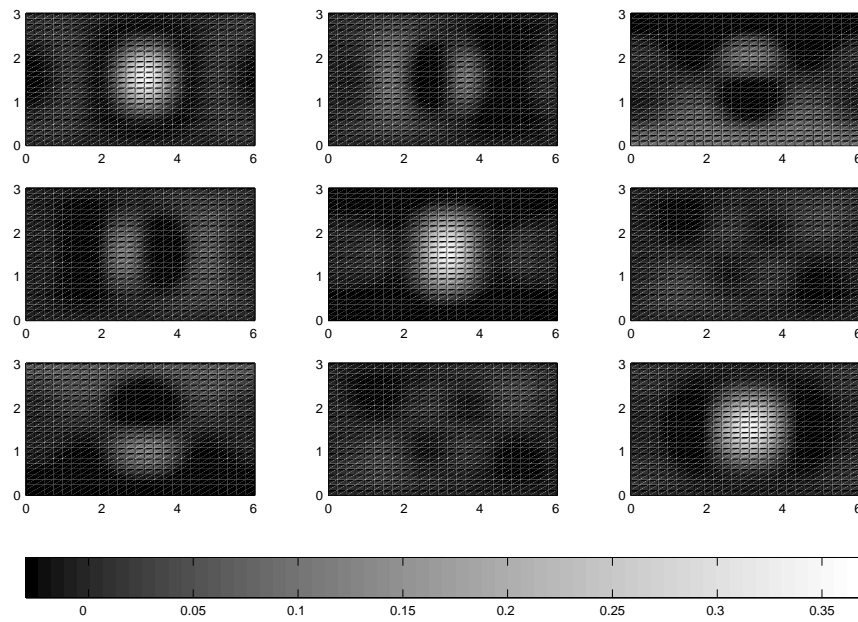


Figure A.10: Cubic polynomial wavelet at level 1.

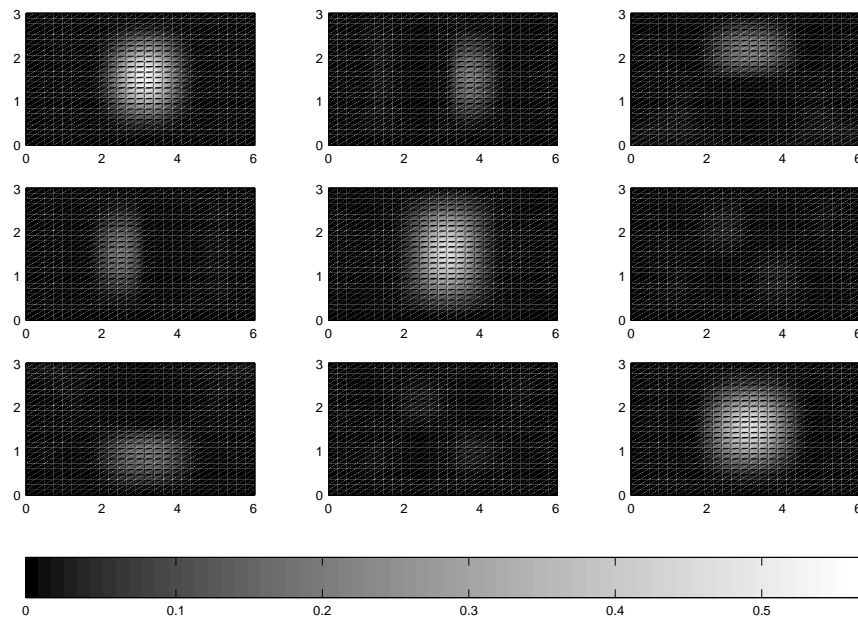


Figure A.11: Cubic polynomial scaling function at level 2.

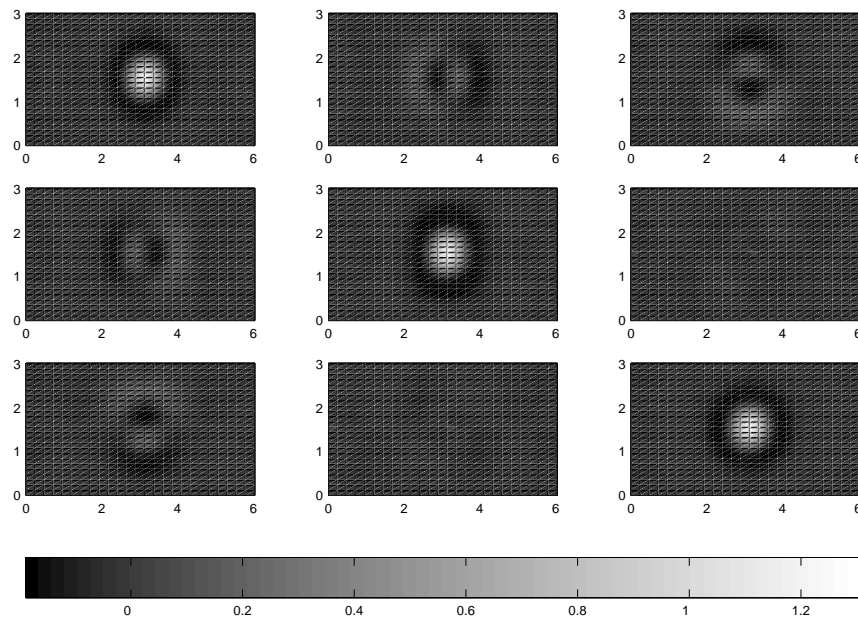


Figure A.12: Cubic polynomial wavelet at level 2.

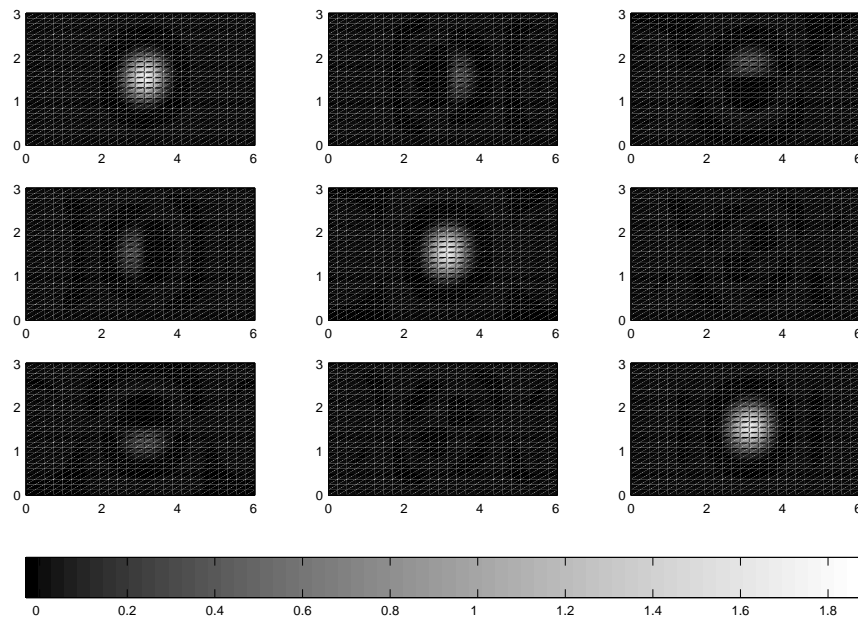


Figure A.13: Cubic polynomial scaling function at level 3.

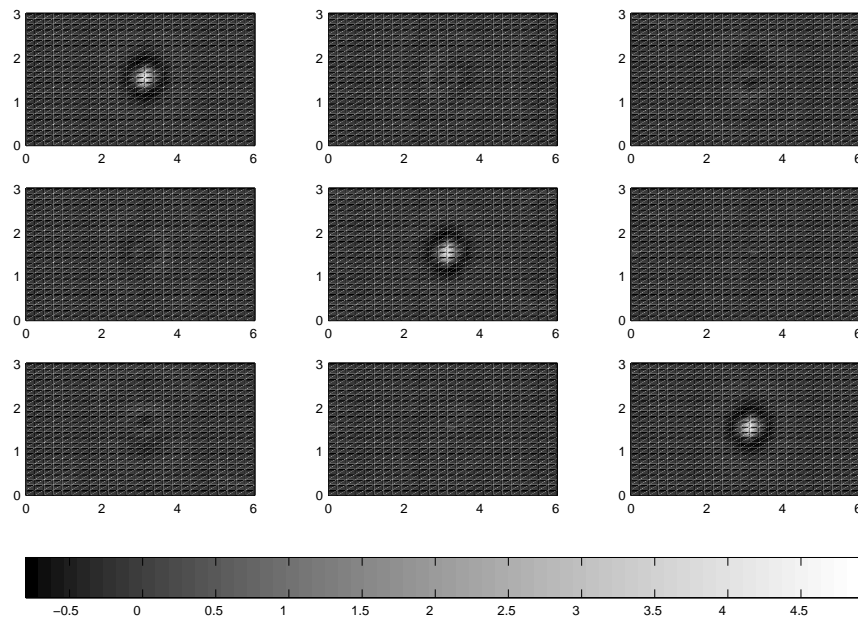


Figure A.14: Cubic polynomial wavelet at level 3.

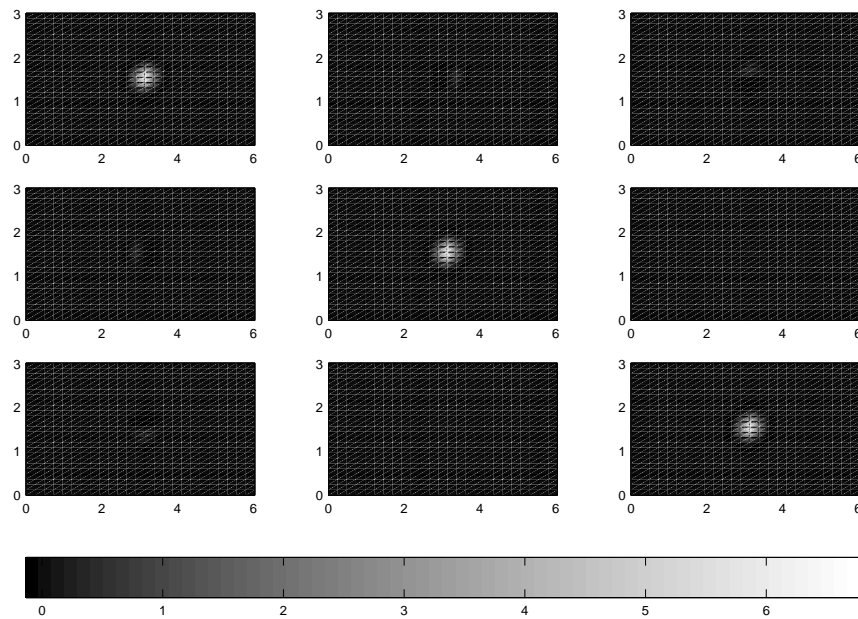


Figure A.15: Cubic polynomial scaling function at level 4.

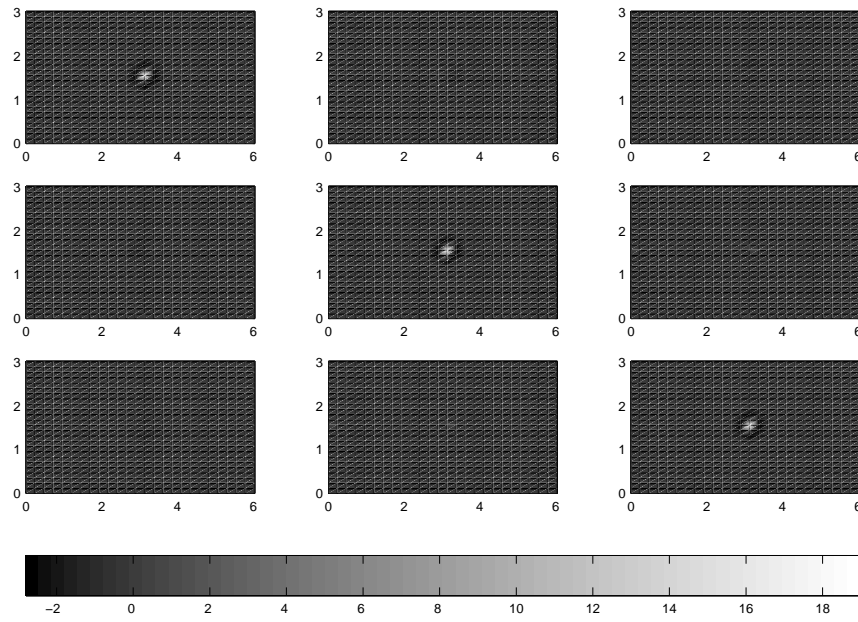


Figure A.16: Cubic polynomial wavelet at level 4.



# Appendix B

## Auxiliary Results

### B.1 Partial Sums of Legendre Series via Clenshaw's Algorithm

The general problem is to compute the sums of the kind

$$S_N(t) = \sum_{n=0}^N A_n T_n(t), \quad (\text{B.1})$$

with the constant coefficients  $A_n$ . The function  $T_n(t)$  is assume to satisfy the difference equation

$$T_n(t) - a_n(t)T_{n-1}(t) - b_n(t)T_{n-2}(t) = 0, \quad b_n \neq 0, \quad n = 2, \dots, N. \quad (\text{B.2})$$

To the above problem the well-known Clenshaw's algorithm is given by

$$U_{N+1} = U_{N+2} = 0, \quad (\text{B.3})$$

$$U_n = A_n + a_{n+1}U_{n+1} + b_{n+2}U_{n+2}, \quad \text{for } n = N, N-1, \dots, 1, \quad (\text{B.4})$$

$$S_N = (A_0 + b_2U_2)T_0 + U_1T_1. \quad (\text{B.5})$$

In case of calculating the coefficients of Legendre tensors associated with the scaling functions and wavelets in Chapter 5, the problem is to compute the finite sums which are similar to the form (B.1) in which  $T_n$  represents the Legendre polynomials. Therefore, in what follows we construct a modified form of the Clenshaw's algorithm for the partial sums (B.1) where the function  $T_n$  is replaced by the Legendre function  $P_n$  and its first two derivatives. Our purpose is to go through the complete proof of the algorithm for the general setting given by

$$S_N(t) = \sum_{n=m}^N A_n P_n^{(m)}(t), \quad (\text{B.6})$$

where  $m$  represents the order of the derivative of  $P_n$  with respect to  $t$  and  $m = 0, 1, 2$ . Note that for each  $m$ , the function  $P_n^{(m)}(t)$  satisfies the difference equation (B.2) and thus the method can be applied as well. Hence we state the following.

**Lemma B.1** *Let  $P_n$  be the Legendre polynomial of degree  $n$ . Then the followings hold:*

$$P_n(t) - \left(\frac{2n-1}{n}\right)tP_{n-1}(t) - \left(\frac{n-1}{n}\right)P_{n-2}(t) = 0, \quad n \in \mathbb{N} \setminus \{0, 1\} \quad (\text{B.7})$$

$$P'_n(t) - \left(\frac{2n-1}{n-1}\right)tP'_{n-1}(t) - \left(\frac{n}{n-1}\right)P'_{n-2}(t) = 0, \quad n \in \mathbb{N} \setminus \{0, 1, 2\} \quad (\text{B.8})$$

$$P''_n(t) - \left(\frac{2n-1}{n-2}\right)tP''_{n-1}(t) - \left(\frac{n+1}{n-2}\right)P''_{n-2}(t) = 0 \quad n \in \mathbb{N} \setminus \{0, 1, 2, 3\}. \quad (\text{B.9})$$

Moreover, considering the above three equations the general form can be written as

$$P_n^{(m)}(t) - a_n^m(t)P_{n-1}^{(m)}(t) - b_n^m P_{n-2}^{(m)}(t) = 0, \quad (\text{B.10})$$

where

$$a_n^m(t) = \frac{2n-1}{n-m}t, \quad b_n^m(t) = \frac{n+m-1}{n-m} \text{ and } n \in \mathbb{N} \setminus \{0, 1, \dots, m+1\}, m \in \mathbb{N}_0.$$

**Lemma B.2** *Let the recurrence relation of the derivatives of the Legendre functions  $P_n^{(m)}$ ,  $m \in \mathbb{N}_0$  be given by (B.10). Then the partial sum*

$$S_N = \sum_{n=m}^N A_n P_n^{(m)}(t) \quad (\text{B.11})$$

*with the constant coefficients  $A_n$  is given by the Clenshaw's algorithm of the form*

$$\begin{aligned} U_{N+1} &= U_{N+2} = 0, \\ U_k &= A_k + a_{k+1}U_{k+1} + b_{k+2}U_{k+2}, \quad \text{for } k = N, N-1, \dots, m+1, \\ S_N &= (A_m + b_{m+2}U_{m+2})P_m^{(m)}(t) + U_{m+1}P_{m+1}^{(m)}. \end{aligned}$$

This lemma can easily be proved using the technique given in [18].

**Proof.**

Recall the difference equation

$$P_n^{(m)}(t) - a_n^m(t)P_{n-1}^{(m)}(t) - b_n^m P_{n-2}^{(m)}(t) = 0, \quad (\text{B.12})$$

$$m = 0, 1, \dots, \quad n = m+2, m+3, \dots$$

Assume that, for instance,  $P_m^{(m)}(t) \neq 0$  for all  $t \in [-1, 1]$ . Then the fraction

$$\frac{P_{m+1}^{(m)}(t)}{P_m^{(m)}(t)} = a_{m+1}^m$$

can be defined.

Observing the equations

$$P_m^{(m)}(t) = P_m^{(m)}(t) \quad (\text{B.13})$$

$$P_{m+1}^{(m)}(t) - a_{m+1}^m P_m^{(m)}(t) = 0 \quad (\text{B.14})$$

together with (B.11) we obtain the linear system of equations

$$M q = r, \quad (\text{B.15})$$

where

$$M = \begin{pmatrix} 1 & 0 & & & \\ -a_{m+1}^m & 1 & 0 & & \\ -b_{m+2}^m & -a_{m+2}^m & 1 & 0 & \\ 0 & -b_{m+3}^m & -a_{m+3}^m & 1 & \\ & & \ddots & \ddots & \ddots \\ & & & -b_N^m & -a_N^m & 1 \end{pmatrix},$$

$$q = \begin{pmatrix} P_m^{(m)}(t) \\ P_{m+1}^{(m)}(t) \\ \vdots \\ P_N^{(m)}(t) \end{pmatrix} \quad \text{and} \quad r = \begin{pmatrix} P_m^{(m)}(t) \\ 0 \\ \vdots \\ 0 \end{pmatrix}.$$

Since  $\det(M) \neq 0$ ,  $M^{-1}$  exists.

Letting  $a^T = (A_m, A_{m+1}, \dots, A_N)^T$  and  $u^T = (U_m, U_{m+1}, \dots, U_N)^T$  we get the sum

$$S_N = \sum_{n=m}^N A_n P_n^{(m)}(t) = a^T q = a^T (M^{-1} r) = (M^{-T} a)^T r. \quad (\text{B.16})$$

Taking the vector  $u$  such that  $M^T u = a$  we obtain,

$$S_N = (M^{-T} a)^T r = u^T r = U_m P_m^{(m)}(t). \quad (\text{B.17})$$

Observing the linear system  $M^T u = a$  we find for  $k = N, N-1, \dots, m+1$ ,

$$U_k = A_k + a_k^m U_{k+1} + b_k^m U_{k+2}. \quad (\text{B.18})$$

Substituting the relations  $U_m = A_m + a_{m+1}^m U_{m+1} + b_{m+1}^m U_{m+2}$  and (B.14), finally we obtain

$$\begin{aligned} S_N &= U_m P_m^{(m)}(t) \\ &= (A_m + a_{m+1}^m U_{m+1} + b_{m+2}^m U_{m+2}) P_m^{(m)}(t) \\ &= (A_m + b_{m+2}^m U_{m+2}) P_m^{(m)}(t) + a_{m+1}^m U_{m+1} P_{m+1}^{(m)}(t) / a_{m+1}^m \\ &= (A_m + b_{m+2}^m U_{m+2}) P_m^{(m)}(t) + U_{m+1} P_{m+1}^{(m)}(t). \end{aligned} \quad (\text{B.19})$$

Now the assumption  $P_m^{(m)}(t) \neq 0$  can be relaxed. Then the results in (B.18) and (B.19) together with the auxiliary conditions  $U_{N+2} = U_{N+1} = 0$  complete the desired proof.  $\square$

Finally, corresponding to our computational work we state the following corollary.

**Corollary B.1** *Let the conditions of Lemma B.2 be given. Then the partial sums*

$$S_N = \sum_{n=m}^N P_n^{(m)}(t), \quad m = 0, 1, 2, \quad N > m, \quad (\text{B.20})$$

*are given by the following three forms of the Cleschew's algorithm:*

*(a) For  $m = 0$ ,*

$$\begin{aligned} U_{N+1} &= U_{N+2} = 0, \\ U_k &= A_k + a_{k+1}U_{k+1} + b_{k+2}U_{k+2}, \quad \text{for } k = N, N-1, \dots, 1, \\ S_N &= (A_0 + b_2U_2) + tU_1. \end{aligned}$$

*(b) For  $m = 1$ ,*

$$\begin{aligned} U_{N+1} &= U_{N+2} = 0, \\ U_k &= A_k + a_{k+1}U_{k+1} + b_{k+2}U_{k+2}, \quad \text{for } k = N, N-1, \dots, 2, \\ S_N &= (A_1 + b_3U_3) + 3tU_2. \end{aligned}$$

*(c) For  $m = 2$ ,*

$$\begin{aligned} U_{N+1} &= U_{N+2} = 0, \\ U_k &= A_k + a_{k+1}U_{k+1} + b_{k+2}U_{k+2}, \quad \text{for } k = N, N-1, \dots, 3, \\ S_N &= 3(A_2 + b_4U_4) + -15tU_3. \end{aligned}$$

# Appendix C

## Crustal Deformation Data

### C.1 GPS Measurements

GPS measurements of 1994-2000 average surface displacements in Nevada region

Station	Lati(d)	Long(d)	Hight(m)	M.O.T	N(mm)	E(mm)	Up(mm)	X	Y	Z	Ux	Uy	Uz
1	39.2847	-118.3031	2006.9270	1994.4562	-13.98	-11.26	-0.05	-2404910.5840	-4165374.5876	4176899.7850	-14.14	-2.08	-10.85
2	41.1622	-119.9997	1360.4360	1994.5274	-14.06	-11.61	-0.05	-2437640.4098	-4223066.8570	4099566.8889	-14.66	-2.18	-10.62
3	40.2450	-118.0056	1210.8115	1996.8161	-14.06	-11.41	-0.05	-2084794.6061	-4306501.9368	4206355.6756	-14.41	-2.13	-10.76
4	41.5111	-114.1682	1907.2390	1997.8949	-12.81	-12.33	-0.04	-2230787.5469	-4693201.7419	3687325.6562	-14.78	-2.24	-9.62
5	35.5410	-114.5772	777.2983	1997.1104	-12.69	-10.99	-0.04	-2449777.5147	-4295450.8655	4018103.1284	-13.08	-1.91	-10.35
6	35.1132	-113.1716	660.9141	1994.3753	-12.50	-10.96	-0.04	-2193462.2846	-4740922.6764	3648524.7953	-12.95	-1.89	-10.25
7	38.6145	-118.5481	1745.9064	1994.4507	-13.91	-11.15	-0.05	-2454286.5379	-4346454.0845	3960058.1163	-13.95	-2.05	-10.89
8	38.1351	-117.1216	2042.5556	1994.4452	-13.74	-11.12	-0.04	-2426735.5753	-4399939.5798	3918510.8777	-13.82	-2.02	-10.83
9	38.6334	-119.8233	2316.1411	1999.3466	-14.12	-11.04	-0.05	-2508640.9979	-4314311.2222	3962053.0336	-13.96	-2.04	-11.06
10	38.7333	-115.2236	2103.4195	1994.4369	-13.10	-11.57	-0.04	-2245135.9437	-44449170.3527	3970579.2131	-14.00	-2.08	-10.25
11	42.6564	-115.5345	1846.0452	1994.5329	-13.00	-12.48	-0.04	-2094268.4785	-4206793.1350	4300755.0431	-15.09	-2.30	-9.59
12	41.2995	-117.0804	1322.3656	1994.5274	-13.74	-11.81	-0.05	-2321048.0578	-4201171.9136	4188339.9307	-14.71	-2.20	-10.36
13	40.6543	-118.6533	1171.9475	1994.5132	-13.87	-11.60	-0.05	-2375276.8624	-4224618.7885	4134135.2920	-14.53	-2.16	-10.55
14	41.1732	-118.5814	1739.2059	1999.3675	-13.89	-11.70	-0.05	-2362243.6484	-4189123.3924	4178068.5050	-14.67	-2.19	-10.49
15	41.9047	-113.2988	1575.3807	1999.4088	-12.46	-12.58	-0.04	-1987147.9538	-4320139.2265	4238786.3346	-14.89	-2.27	-9.30
16	36.5851	-114.0889	1071.4782	1997.5204	-12.84	-11.18	-0.04	-2241004.3375	-4612884.0786	3781158.7450	-13.39	-1.97	-10.33
17	36.0981	-113.9557	869.5820	1994.3767	-12.25	-11.30	-0.04	-2102521.4807	-4712541.6786	3737505.6592	-13.25	-1.96	-9.92
18	40.8478	-117.2708	1257.6970	1999.3658	-13.69	-11.74	-0.05	-2322890.9369	-4237726.6781	4150476.1659	-14.58	-2.18	-10.38
19	38.4602	-115.8468	1801.8606	1999.3749	-12.91	-11.59	-0.04	-2204845.7048	-4490095.4201	3946691.1870	-13.93	-2.07	-10.14
20	41.0994	-114.8900	1728.3791	1997.2602	-12.59	-12.34	-0.04	-2043132.2156	-4359633.3790	4171884.8705	-14.67	-2.23	-9.51
21	40.7661	-114.0811	1507.0519	1999.3988	-12.84	-12.15	-0.04	-2115003.0062	-4352023.0028	4143768.9491	-14.58	-2.20	-9.75
22	40.7566	-116.9194	1359.5044	1994.4973	-13.19	-11.97	-0.04	-2203060.9377	-4308763.8899	4142873.8804	-14.57	-2.19	-10.02
23	38.2594	-118.7767	1946.8583	1999.3438	-13.84	-11.10	-0.05	-2448970.4902	-4377741.9958	3929295.9899	-13.85	-2.03	-10.89
24	41.5097	-119.4994	1322.8858	1999.3630	-14.21	-11.60	-0.05	-2428237.9157	-4122224.1935	4205858.4164	-14.76	-2.20	-10.67
25	37.5293	-114.7803	1142.7954	1997.8530	-12.62	-11.50	-0.04	-2158286.7110	-4582508.5966	3864838.2367	-13.66	-2.03	-10.03
26	40.9052	-116.1966	1289.7152	1994.5035	-13.41	-11.90	-0.04	-2252186.9369	-4271038.5024	4155312.8201	-14.60	-2.19	-10.17
27	39.5135	-118.1243	1479.7453	1994.4619	-14.03	-11.28	-0.05	-2454936.5270	-4273450.0169	4037398.8268	-14.21	-2.09	-10.85
28	38.0309	-116.1145	1389.9839	1997.8295	-13.44	-11.24	-0.04	-2353225.5221	-44447181.6675	3909003.7566	-13.80	-2.03	-10.61
29	39.3512	-116.5816	1901.5700	1994.4722	-13.30	-11.61	-0.04	-2274868.9066	-4385225.3172	4023751.8431	-14.17	-2.11	-10.31
30	38.0843	-118.8247	2529.4349	1994.4507	-13.83	-11.07	-0.05	-2451384.0337	-4390683.9161	3914369.9201	-13.81	-2.02	-10.91
31	38.8251	-116.8100	1728.1434	1999.3575	-13.23	-11.53	-0.04	-2274145.8190	-4426908.1566	3978289.6691	-14.03	-2.08	-10.33
32	36.1547	-114.6369	961.7476	1999.3222	-12.67	-11.15	-0.04	-2208876.9377	-4659621.6622	3742632.9806	-13.26	-1.95	-10.25
33	36.4148	-114.5484	1039.6217	1994.3880	-12.69	-11.20	-0.04	-2208753.6397	-4640836.2022	3765949.3728	-13.34	-1.96	-10.24
34	38.8141	-116.0313	1371.0670	1994.4507	-13.46	-11.41	-0.04	-2334324.4529	-4396023.1607	3977116.3253	-14.02	-2.07	-10.52
35	35.2004	-113.4250	214.4424	1994.3752	-12.42	-11.01	-0.04	-2170008.2901	-4745176.8923	3656178.2357	-12.98	-1.90	-10.17
36	36.2859	-112.9345	1427.1133	1999.3347	-11.94	-11.47	-0.04	-2017070.3236	-4736856.6856	3754659.2235	-13.31	-1.98	-9.65
37	38.7599	-116.1161	1943.1227	1994.4371	-13.44	-11.41	-0.04	-2329790.5089	-4403195.6949	3972786.0689	-14.00	-2.07	-10.51
38	39.2822	-118.4497	1302.1140	1994.4562	-13.93	-11.28	-0.05	-2438592.4397	-4301386.1971	4017441.3595	-14.14	-2.08	-10.81
39	37.6152	-113.1582	1449.7864	1994.4178	-12.50	-11.57	-0.04	-2125679.4188	-4591587.2633	3872582.1589	-13.69	-2.04	-9.93
40	37.8938	-115.9418	1504.9239	1997.4686	-12.88	-11.47	-0.04	-2214370.2114	-4528450.7231	3897075.8141	-13.77	-2.04	-10.19
41	37.8854	-117.5445	1732.1005	1999.3411	-13.61	-11.13	-0.04	-2402210.1421	-4432529.0011	3896473.8304	-13.75	-2.01	-10.77
42	39.0740	-113.5626	1783.0670	1994.4288	-12.38	-11.97	-0.04	-2051757.0054	-4515230.0786	3999822.3134	-14.11	-2.12	-9.63
43	39.2932	-113.1570	1886.2495	1999.3991	-12.50	-11.96	-0.04	-2077236.4154	-4486712.7324	4018753.7034	-14.17	-2.13	-9.70
44	39.2932	-113.1573	1886.0737	1994.4288	-12.50	-11.96	-0.04	-2077220.0168	-4486722.0267	4018751.5381	-14.17	-2.13	-9.70
45	35.4759	-113.1872	707.8818	1999.3186	-12.49	-11.05	-0.04	-2182429.1746	-4720446.6766	3681401.8777	-13.06	-1.91	-10.20
46	39.2699	-114.0470	1817.3094	1999.3886	-12.85	-11.80	-0.04	-2164461.8547	-4447052.5441	4016707.8623	-14.16	-2.12	-9.97
47	39.9437	-118.7973	1887.2176	1994.4731	-13.83	-11.47	-0.05	-2389819.9799	-4275608.0631	4074407.6190	-14.33	-2.12	-10.63
48	39.0012	-118.2458	1408.8700	1999.3530	-13.99	-11.18	-0.05	-2463701.7752	-4309849.9578	3993309.9978	-14.06	-2.06	-10.90

49	39.2699	-114.0470	1817.2895	1994.4325	-12.85	-11.80	-0.04	-2164461.8316	-4447052.5341	4016707.8540	-14.16	-2.12	-9.97
50	36.5300	-113.6178	540.9993	1994.3909	-12.36	-11.37	-0.04	-2118456.9262	-4673964.3828	3775930.2218	-13.38	-1.98	-9.95
51	41.3978	-116.1749	1266.2660	1997.9819	-13.42	-12.00	-0.04	-2236984.1799	-4238325.3133	4196501.3176	-14.74	-2.22	-10.09
52	39.7929	-118.9818	1218.9705	1999.3572	-13.77	-11.47	-0.05	-2380999.2097	-4292219.3796	4061126.2864	-14.29	-2.12	-10.61
53	35.1967	-113.9591	1119.9905	1994.5524	-12.25	-11.08	-0.04	-2126078.3605	-4766086.2045	3656370.8931	-12.98	-1.91	-10.04
54	40.1283	-114.2348	1715.6164	1994.4918	-12.79	-12.03	-0.04	-2123366.6665	-4399211.5741	4089995.4411	-14.40	-2.17	-9.81
55	40.1204	-115.3872	1732.2251	1997.8437	-13.05	-11.90	-0.04	-2188472.5169	-4367837.6499	4089332.7363	-14.39	-2.16	-10.01
56	42.0941	-117.4271	1254.3314	1996.2938	-13.64	-12.03	-0.05	-2267475.5691	-4163524.8489	4254209.6597	-14.92	-2.25	-10.15
57	38.7449	-117.1417	2063.0374	1994.4397	-13.73	-11.26	-0.04	-2404883.1823	-4363933.7250	3971561.6958	-14.00	-2.06	-10.74
58	41.9624	-115.8126	1617.5236	1997.9680	-12.92	-12.37	-0.04	-2096656.9105	-4263328.5773	4243582.5863	-14.90	-2.26	-9.64
59	38.0754	-116.9256	1632.9292	1997.4452	-13.19	-11.37	-0.04	-2288737.3327	-4477509.3837	3913040.7163	-13.81	-2.04	-10.41
60	39.4956	-118.2316	1316.0629	1994.4562	-14.00	-11.29	-0.05	-2447490.0360	-4279031.3911	4035759.9585	-14.20	-2.09	-10.83
61	43.6339	-115.7697	795.3233	1994.5537	-12.93	-12.73	-0.04	-2043814.2834	-4148038.0151	4379286.0766	-15.34	-2.35	-9.39
62	35.2516	-112.0650	1023.2675	1999.3181	-12.22	-11.11	-0.04	-2115808.1541	-4766727.1247	3661287.4166	-13.00	-1.91	-10.00
63	36.7808	-117.8153	1186.3664	1999.3384	-13.53	-10.92	-0.04	-2416152.5264	-4508989.7285	3798651.6194	-13.43	-1.95	-10.86
64	36.3411	-113.0821	706.5798	1994.3880	-12.53	-11.25	-0.04	-2167361.2357	-4665364.2169	3759167.4487	-13.32	-1.96	-10.11
65	36.3044	-115.5835	594.1058	1999.3259	-12.99	-11.05	-0.04	-2289662.3498	-4609166.7095	3755819.4108	-13.30	-1.94	-10.49
66	40.9847	-113.5792	1743.0836	1998.2583	-12.37	-12.41	-0.04	-1994008.5219	-4391522.6052	4162283.2793	-14.64	-2.23	-9.36
67	36.8662	-110.4966	1313.6177	1999.3164	-11.44	-11.81	-0.04	-1873091.8002	-4754290.7819	3806312.4877	-13.49	-2.03	-9.17
68	40.0580	-113.3754	1806.2454	1999.4012	-12.43	-12.17	-0.04	-2037500.3580	-4445244.7289	4084077.2188	-14.39	-2.17	-9.54
69	36.0789	-114.8391	623.8815	1994.3811	-12.60	-11.16	-0.04	-2194405.5911	-4671630.0092	3735640.1155	-13.24	-1.95	-10.21
70	38.5229	-116.3643	1720.6295	1994.4373	-13.36	-11.39	-0.04	-2318233.0326	-4427651.0633	3952094.2641	-13.94	-2.06	-10.48
71	38.5406	-113.3484	1811.1182	1999.3966	-12.44	-11.81	-0.04	-2084115.6877	-4541284.6688	3953683.6272	-13.96	-2.09	-9.76
72	40.0716	-117.4393	1166.2577	1994.4731	-13.64	-11.60	-0.05	-2337137.1809	-4293609.4899	4084823.6551	-14.37	-2.14	-10.47
73	41.9970	-118.6458	1844.7475	1999.3642	-13.87	-11.89	-0.05	-2327798.7734	-4138901.6931	4246588.1960	-14.90	-2.23	-10.34
74	39.6885	-117.7303	1433.5936	1994.4671	-13.55	-11.56	-0.04	-2328309.6573	-4329631.4238	4052349.8054	-14.26	-2.12	-10.46
75	39.3673	-118.2099	1859.5301	1994.4619	-14.00	-11.26	-0.05	-2453813.4794	-4286322.3165	4025101.0678	-14.17	-2.08	-10.86
76	39.0012	-118.2458	1408.8597	1994.4618	-13.99	-11.18	-0.05	-2463701.7413	-4309849.9941	3993309.9632	-14.06	-2.06	-10.90
77	38.1392	-116.5033	1437.2229	1999.3384	-13.32	-11.33	-0.04	-2319584.6427	-4456507.8036	3918491.2788	-13.83	-2.04	-10.50
78	36.6717	-113.3750	480.5140	1998.0032	-12.43	-11.37	-0.04	-2134312.0014	-4656381.6194	3788516.8816	-13.42	-1.98	-10.00
79	39.1620	-115.3080	2024.7513	1994.4288	-13.08	-11.68	-0.04	-2225109.9908	-4425681.9042	4007553.3886	-14.13	-2.10	-10.17
80	38.6409	-114.4070	1433.1466	1997.8325	-12.74	-11.71	-0.04	-2155315.4446	-4499901.3104	3962151.1523	-13.98	-2.09	-9.97
81	41.1467	-116.9776	1401.0726	1997.8285	-13.17	-12.07	-0.04	-2185800.0533	-4285725.9305	4175626.2373	-14.67	-2.21	-9.95
82	40.4242	-116.3914	1417.3176	1997.3949	-13.35	-11.82	-0.04	-2253831.6700	-4309600.1487	4114877.1015	-14.47	-2.16	-10.19
83	40.4182	-119.3322	1344.9263	1999.3603	-14.26	-11.34	-0.05	-2480803.4748	-4183502.0302	4114323.1341	-14.45	-2.13	-10.89
84	36.0408	-110.1697	2262.6113	1999.3164	-11.55	-11.56	-0.04	-1920710.3147	-4794770.9167	3733182.3483	-13.25	-1.98	-9.36
85	34.8066	-113.3960	184.9426	1999.3164	-12.43	-10.91	-0.04	-2182829.9096	-4766839.0062	3620380.8103	-12.86	-1.88	-10.23
86	37.2326	-117.7062	1178.1281	1994.4579	-13.56	-11.00	-0.04	-2410422.5717	-4477802.7104	3838686.7425	-13.56	-1.98	-10.82
87	38.5305	-118.7826	2028.5630	1994.4535	-13.84	-11.16	-0.05	-2439427.6469	-4361732.0061	3952938.5840	-13.93	-2.04	-10.85
88	38.4711	-115.8334	1796.1912	1994.4266	-12.92	-11.59	-0.04	-2205561.9618	-4488897.2096	3947638.3133	-13.93	-2.07	-10.14
89	35.8670	-115.6997	408.9289	1999.3219	-12.96	-10.96	-0.04	-2292911.1993	-4639296.0967	3716484.4239	-13.17	-1.92	-10.52
90	41.3189	-116.3787	1335.4038	1994.5223	-13.36	-12.02	-0.04	-2224609.2076	-4251426.2117	4189971.8873	-14.72	-2.21	-10.06
91	36.8279	-115.2537	886.9527	1997.3377	-13.09	-11.13	-0.04	-2300683.7472	-4565212.8995	3802655.8203	-13.45	-1.97	-10.51
92	35.2508	-111.3652	1571.6181	1999.3164	-11.81	-11.26	-0.04	-2007295.9003	-4813968.9596	3661531.8221	-13.01	-1.93	-9.66
93	40.8560	-117.2509	1219.7918	1998.3492	-13.69	-11.74	-0.05	-2324067.7827	-4236366.8016	4151142.7064	-14.59	-2.18	-10.39
94	39.7310	-115.9311	1769.8163	1994.4288	-12.88	-11.89	-0.04	-2159121.6750	-4413371.3083	4056193.5675	-14.29	-2.14	-9.94
95	39.6648	-118.1280	1514.2215	1994.4699	-14.03	-11.31	-0.05	-2449335.9098	-4264343.5226	4050375.1623	-14.25	-2.10	-10.83
96	39.4791	-116.8454	1724.3595	1997.1597	-13.22	-11.68	-0.04	-2250477.2045	-4387510.4333	4034607.7156	-14.21	-2.12	-10.23
97	41.6142	-117.5640	1363.0717	1999.3722	-13.60	-11.95	-0.05	-2274497.2707	-4200282.7462	4214572.6682	-14.80	-2.22	-10.20
98	35.8719	-113.0716	492.6006	1994.3804	-12.53	-11.13	-0.04	-2181074.3712	-4692637.3927	3716971.8359	-13.18	-1.94	-10.18
99	37.2743	-116.9724	1192.8002	1997.5084	-13.18	-11.19	-0.04	-2309616.6677	-4527486.5862	3842382.3609	-13.58	-1.99	-10.51
100	40.0342	-116.8077	1498.3484	1994.4918	-13.23	-11.80	-0.04	-2235271.5929	-4350804.3239	4081855.6953	-14.37	-2.15	-10.16
101	35.9400	-114.8169	780.6572	1994.3932	-12.61	-11.12	-0.04	-2200133.2632	-4679092.7091	3723261.9491	-13.20	-1.94	-10.23
102	40.6218	-118.3504	1242.6312	1999.3631	-13.96	-11.55	-0.05	-2398763.2654	-4214090.7529	4131445.9352	-14.52	-2.16	-10.63
103	40.1283	-114.2348	1715.6165	1999.3909	-12.79	-12.03	-0.04	-2123366.7220	-4399211.5741	4089995.4791	-14.40	-2.17	-9.81
104	35.8055	-114.5138	1542.7123	1994.3767	-12.71	-11.05	-0.04	-2228883.6202	-4675844.6507	3711609.7329	-13.16	-1.93	-10.33
105	42.4659	-114.1104	1489.9065	1994.5438	-12.83	-12.53	-0.04	-2058014.1812	-4240273.6721	4284925.2333	-15.04	-2.29	-9.49
106	39.4021	-114.4442	1956.2216	1994.4288	-12.73	-11.89	-0.04	-2129604.7097	-4453651.1183	4028156.3252	-14.20	-2.13	-9.86
107	39.3172	-119.6823	2045.7410	1999.3548	-14.16	-11.17	-0.05	-2495030.1085	-4266709.2082	4020922.9375	-14.15	-2.08	-10.98
108	36.2096	-113.3350	542.5158	1999.3224	-12.45	-11.25	-0.04	-2150298.5750	-4682611.1319	3747304.5662	-13.28	-1.96	-10.07
109	36.2102	-114.8015	639.1268	1994.3822	-12.61	-11.18	-0.04	-2193817.5277	-4662424.0971	3747414.7180	-13.28	-1.95	-10.20
110	39.5330	-118.3020	1403.9912	1994.4615	-13.98	-11.31	-0.05	-2440955.2997	-4279795.5630	4039023.2209	-14.21	-2.09	-10.81
111	38.5529	-117.3679	1241.7538	1999.3440	-13.66	-11.25	-0.04	-2393705.2346	-4384517.3664	3954401.2412	-13.94	-2.05	-10.71
112	38.6061	-117.4231	1290.9834	1994.4507	-13.64	-11.27	-0.04	-2387740.9827	-4383622.6176	3959044.5250	-13.96	-2.05	-10.69
113	40.0154	-117.6290	1295.9590	1999.3631	-13.58	-11.62	-0.04	-2324858.9996	-4304943.6158	4080132.7485	-14.35	-2.13	-10.43
114	39.2738	-117.6893	1278.9855	1999.3499	-13.56	-11.46	-0.04	-2345240.4077	-4353638.5629	4016704.4299	-14.15	-2.09	-10.53
115	42.0131	-116.2842	1343.1736	1996.8936	-13.38	-12.15	-0.04	-2207775.9481	-4202375.4458	4247583.4600	-14.91	-2.25	-9.97

# List of Figures

1.1	An illustration of a regular surface. . . . .	17
4.1	Sectional illustration of scale discrete $\Sigma$ -scaling function $\Phi_j^{D;(5)}(x, \cdot)$ at levels 1,2 and 3 with $\theta$ variable and $\varphi = \pi/4$ and $x$ fixed. $\Phi_j^{D;(5)}(x, \cdot) = \Phi_{\tau_j}^{(5)}(x, \cdot)$ for $\tau = 2^{-j}$ , $j = 1, 2, 3$ . Frobenius norm, diagonal components (left) and non-diagonal components (right). . . . .	42
4.2	Sectional illustration of scale discrete $\Sigma$ -wavelet $\Psi_j^{D;(5)}(x, \cdot)$ at levels 1,2 and 3 with $\theta$ variable and $\varphi = \pi/4$ and $x$ fixed. $\Psi_j^{D;(5)}(x, \cdot) = \Psi_{\tau_j}^{(5)}(x, \cdot)$ for $\tau = 2^{-j}$ , $j = 1, 2, 3$ . Frobenius norm, diagonal components (left) and non-diagonal components (right). . . . .	43
5.1	Generators for the Shannon scaling functions (left) and for the wavelets (right) at levels $j = 1, 2, 3, 4$ . . . . .	79
5.2	Frobenius norm of the Shannon scaling functions (left) and wavelets (right) at levels $j = 1, 2, 3, 4$ . . . . .	80
5.3	Components and the Frobenius norm of the Shannon scaling function (left) and wavelets (right) at level 3. . . . .	80
5.4	Generators for the modified Shannon scaling functions (left) and wavelets (right) at levels $j = 1, 2, 3, 4$ . . . . .	81
5.5	Frobenius norm of the modified Shannon scaling functions (left) and wavelets (right) at levels $j = 1, 2, 3, 4$ . . . . .	82
5.6	Components and the Frobenius norm of the modified Shannon scaling function (left) and wavelets (right) at level 3. . . . .	82
5.7	Generators for the cubic polynomial scaling functions (left) and wavelets (right) at levels $j = 1, 2, 3, 4$ . . . . .	83
5.8	Frobenius norm of the cubic polynomial scaling functions (left) and wavelets (right) at levels $j = 1, 2, 3, 4$ . . . . .	84

5.9	Components and the Frobenius norm of the cubic polynomial scaling function (left) and wavelets (right) at level 3. . . . .	84
6.1	Functional values of $f$ (third component): (a) on a longitude-latitude grid of points on $\Omega$ (b) one-dimensional sectional illustration. . . . .	89
6.2	Sectional illustration of the scale approximations of $f$ (third component) associated to the $\Sigma$ -scaling function $\Phi_{\tau_j}^{(5)}$ for $j = 1, 2, 3, 4$ . . . . .	89
6.3	The reference (left) and the deformed (right) configurations of the unit sphere $\Omega$ associated to the displacement function $f$ . . . . .	90
6.4	The (exact) radial and tangential boundary displacements on the unit sphere $\Omega$ . . . . .	91
6.5	The (exact) radial and tangential displacements on the sphere $\Omega_{1/2}$ . . . . .	91
6.6	Scale and detail reconstructions by Shannon wavelets. . . . .	92
6.7	Scale and detail reconstructions by Shannon wavelets. . . . .	93
6.8	Scale and detail reconstructions by modified Shannon wavelets. . . . .	93
6.9	Scale and detail reconstructions by modified Shannon wavelets. . . . .	94
6.10	Scale and detail reconstructions by cubic polynomial wavelets. . . . .	95
6.11	Scale and detail reconstructions by cubic polynomial wavelets. . . . .	96
6.12	Scale approximations by cubic polynomial wavelets at levels 1,2,3, on $\Omega$ (left) and on $\Omega_{1/2}$ (right). . . . .	97
6.13	Scale approximations by cubic polynomial wavelets at levels 4,5 and exact displacements on $\Omega$ (left) and on $\Omega_{1/2}$ (right). . . . .	98
6.14	Mean absolute errors ( $e_{abs}$ ) of three different wavelet approximation of the inner displacements on $\Omega_{1/2}$ . . . . .	99
6.15	The test region of the multiscale approximation (local). The dark points in the middle describe where the approximations are evaluated. . . . .	100
6.16	Multiscale approximation of displacements on $\Omega_{0.99}$ at levels from 1 to 6. The Euclidean norm of the scale (left) and detail (right) reconstructions of the displacement vectors. . . . .	101
6.17	Scale approximation and exact values. Euclidean norm of the scale approximation at level 7 (left) and the exact displacements (right). . . . .	102
6.18	California and Nevada areas (USA) and GPS stations - the test area. (Source: USGS - Earthquake Hazards Program- Northern California). . . . .	104



6.19	(a) 1994-2000 average horizontal velocities of the crustal deformation at 115 points measured using GPS (source : USGS - Earthquake Hazards Program- Northern California). (b) 1994-2000 average horizontal velocities of the crustal deformation transformed to equiangular longitude-latitude grids. . . . .	105
6.20	(a) 1994-2000 average crustal deformation of the region covered by latitudes $34^{\circ}N - 45^{\circ}N$ and longitudes $121^{\circ}W - 110^{\circ}W$ (i.e. $\phi \in [239^{\circ}, 250^{\circ}]$ , $\theta \in [34^{\circ}, 45^{\circ}]$ ) including extended (interpolated and extrapolated) data. The gray colormap represents the magnitude of the mean deformation in $mm$ and the horizontal displacements are prescribed by arrows. (b) Magnitude (Euclidean norm) of the mean displacements in $mm$ on $\theta - \phi$ plane. . . . .	106
6.21	Multiscale approximation of displacements at levels 1, 2, 3. The magnitude (gray colormap) and tangential displacements (arrows) of scale (left) and detail (right) reconstructions. . . . .	107
6.22	Multiscale approximation of displacements at levels 4, 5. The magnitude (gray colormap) and tangential displacements (arrows) of scale (left) and detail (right) reconstructions. . . . .	107
6.23	Multiscale approximation of displacements at levels 6, 7, 8. The magnitude (gray colormap) and tangential displacements (arrows) of scale (left) and detail (right) reconstructions. . . . .	108
A.1	Shannon scaling function at level 1. . . . .	111
A.2	Shannon wavelet at level 1. . . . .	112
A.3	Shannon scaling function at level 2. . . . .	112
A.4	Shannon wavelet at level 2. . . . .	113
A.5	Shannon scaling function at level 3. . . . .	113
A.6	Shannon wavelet at level 3. . . . .	114
A.7	Shannon scaling function at level 4. . . . .	114
A.8	Shannon wavelet at level 4. . . . .	115
A.9	Cubic polynomial scaling function at level 1. . . . .	115
A.10	Cubic polynomial wavelet at level 1. . . . .	116
A.11	Cubic polynomial scaling function at level 2. . . . .	116
A.12	Cubic polynomial wavelet at level 2. . . . .	117
A.13	Cubic polynomial scaling function at level 3. . . . .	117
A.14	Cubic polynomial wavelet at level 3. . . . .	118
A.15	Cubic polynomial scaling function at level 4. . . . .	118

---

A.16 Cubic polynomial wavelet at level 4. . . . .	119
---	-----

# Bibliography

- [1] M.K. Abeyratne, W. Freeden and C. Mayer, *Multiscale Deformation Analysis by Cauchy-Navier Wavelets*, AGTM Report, No. 247, Department of Mathematics, Geomathematics Group, University of Kaiserslautern, 2002.
- [2] N. I. Achieser and I.M. Glasman, *Theorie der linearen Operationen in Hilbert-Räumen*, Akademie Verlag, Berlin, 1981.
- [3] B. Alpert, G. Beylkin, R. Coifman and V. Roklin, *Waveletlike Bases for the Fast Solution of Second-kind Integral Equations*, SIAM J. Sci. Statist. Comput., **14**, 159-184, 1993.
- [4] E. Argyropoulos and K. Kiriaki, *A Modified Green's-Function Technique for the Exterior Dirichlet Problem in Linear Elasticity*, Quart. J. Mech. Appl. Math., **52**, 275-295, 1998.
- [5] H. Bauch, *Approximationssätze für die Lösungen der Grundgleichung der Elastostatik*, Dissertation, RWTH Aachen, Institut für Reine und Angewandte Mathematik, 1981.
- [6] M. Bayer, *Geomagnetic Field Modelling From Satellite Data by First and Second Generation Vector Wavelets*, Ph.D. Thesis, Department of Mathematics, Geomathematics Group, University of Kaiserslautern, Shaker, Aachen, 2000.
- [7] M. Bayer, S. Beth and W. Freeden, *Geophysical Field Modelling By Multiresolution Analysis*, Acta. Geod. Geoph. Hung., **33(2-4)**, 289-319, 1998.
- [8] E.B. Becker, G.F. Carey and J. T. Oden, *Finite Elements: An Introduction*, Volume 1, Prentice-Hall, 1981.
- [9] B. Bertram, *Numerical Solution of Fredholm Integral Equations Using Simple Wavelet Expansions*, Integral Methods in Science and Engineering, C. Constanda (ed.), Longman Scientific, 50-53, 1997.
- [10] S. Beth, *Multiscale Approximation by Vector Radial Basis Functions on the Sphere*, Ph.D. Thesis, Department of Mathematics, Geomathematics Group, University of Kaiserslautern, Shaker, Aachen, 2000.

- [11] C. A. Brebbia, J. Dominguez, *Boundary Elements: An Introductory Course*, Computational Mechanics Publications, 2 Edition, 1992.
- [12] C. S. Burrus, R. Gopinath and H. Guo, *Introduction to Wavelets and Wavelet Transforms*, Prentice Hall, Upper Saddle River, NJ, 1998.
- [13] P.J. Clarke, R.R. Davies, P.C. England, B. Parsons, H. Billiris, D. Paradissis, G. Veis, P.A. Cross, P.H. Denys, V. Ashkenazi, R. Bingley, H.-G. Kahle, M.-V. Muller and P. Briole, *Crustal Strain in Central Greece from Repeated GPS Measurements in the Interval 1989-1997*, Geophys. J. Int., **135**(1), 195-214, 1998.
- [14] W. Dahmen, *Wavelet and Multiscale Methods for Operators*, Acta Numerica, Cambridge University Press, 55-228, 1997.
- [15] W. Dahmen, A. Kunoth and R. Schneider, *Wavelet Least Squares Methods for Boundary Value Problems*, SIAM J. Numer. Anal., **39** (6), 1985-2013, 2002.
- [16] J.L. Davis, W.H. Prescott, J.L. Svarc and K.J. Wendt, *Assessment of Global Positioning System Measurements for Studies of Crustal Deformation*, J. Geophys. Res., **94**, 13 635-13 650, 1989.
- [17] S.C.R. Davis and L. Quartapelle, *Spectral Algorithms for Vector Elliptic Equations in a Spherical Gap*, J. Comput. Physics, **61**, 218-241, 1985.
- [18] P. Deuffhard, *On Algorithms for the Summation of Certain Special Functions*, Bericht 7407, Gruppe Numerische Mathematik, Technische Universität München, 1974.
- [19] D. Dong, T.A. Herring and R.W. King, *Estimating Regional Deformation from a Combination of Space and Terrestrial Geodetic Data*, J. of Geodesy, **72**(4), 200-214, 1998.
- [20] D. Donoho, *Nonlinear Wavelet Methods for Recovery of Signals, Densities, and Spectra from Indirect and Noisy Data*, Different Perspectives on Wavelets, Proceeding of Symposia in Applied Mathematics, **47**, I. Daubechies (ed.), Amer. Math. Soc., Providence, R.I., 173-205, 1993.
- [21] H. Dragert and R. D. Hyndman, *Continuous GPS Monitoring of Elastic Strain in the Northern Cascadia Subduction Zone*, Geophys. Res. Letters, **22**, 755-758, 1995.
- [22] J.R. Driscoll and D.H. Healy, *Computing Fourier Transforms and Convolutions on the 2-Sphere*, Adv. Appl. Math., **15**, 202-250, 1994.
- [23] A.H. England, *Complex Variable Methods in Elasticity*, Wiley-Interscience, 1971.

- [24] W. Freeden, *On the Approximation of External Gravitational Potential With Closed Systems of (Trial) Functions*, Bull. Géod., **52**, 165-175, 1980.
- [25] W. Freeden, *Least Squares Approximation by Linear Combinations of (Multi-)poles*, OSU Report No. 3444, Dep. Geod. Sci., Columbus, 1983.
- [26] W. Freeden, *Multiscale Modelling of Spaceborne Geodata*, B.G. Teubner, Stuttgart, Leipzig, 1999.
- [27] W. Freeden, *Lecture Notes in Elasticity*, Department of Mathematics, Geomathematics Group, University of Kaiserslautern, 2001.
- [28] W. Freeden and T. Gervens, *Vector Spherical Spline Interpolation (Basic Theory and Computational Aspects)*, Math. Meth. in the Appl. Sci., **16**, 151-183, 1991.
- [29] W. Freeden, T. Gervens and J. C. Mason, *A Minimum Norm Interpolation Method for Determining the Displacement Field of a Homogeneous Isotropic Elastic Body from Discrete Data*, IMA Journal of Appl. Math., **44**, 55-76, 1990.
- [30] W. Freeden, T. Gervens and M. Schreiner, *Constructive Approximation on the Sphere (With Application to Geomathematics)*, Oxford Sci. Publ., 1998.
- [31] W. Freeden, O. Glockner and M. Schreiner, *Fast Multiscale Evaluation of Geopotentials by Harmonic Wavelets*, in: Progress in Geodetic Science, W. Freeden (ed.), Shaker, 237-257, 1998.
- [32] W. Freeden and C. Mayer, *Wavelets Generated by Layer Potentials*, Appl. Comp. Harm. Anal., **5**, 195-237, 2003.
- [33] W. Freeden and V. Michel, *Constructive Approximation and Numerical Methods in Geodetic Research Today - an Attempt at a Categorization Based on on Uncertainty Principle*, J. of Geodesy, **73**, 452-465, 1999.
- [34] W. Freeden and V. Michel, *Multiscale Potential Theory (with Applications to Earth's Sciences)*, Birkhäuser, Boston, Basel, Berlin, (submitted), 2003.
- [35] W. Freeden and S. Pereverzev, *Spherical Tikhonov Regularization Wavelets in Satellite Gravity Gradiometry with Random Noise*, J. of Geodesy, **74**, 730-736, 2001.
- [36] W. Freeden and R. Reuter, *Remainder Terms in Numerical Integration Formulas of the Sphere*, Internat. Series Numer. Math., **62**, 151-170, 1982.
- [37] W. Freeden and R. Reuter, *A Constructive Method for Solving the Displacement Boundary-Value Problem of Elastostatics by Use of Global Basis Systems*, Math. Meth. in the Appl. Sci., **5**, 105-128, 1990.

- [38] W. Freeden and F. Schneider, *Wavelet Approximation on Closed Surfaces and Their Application to Boundary-Value Problems of Potential Theory*, Math. Methods Appl. Sci., **21**, 129-163, 1998.
- [39] W. Freeden and M. Schreiner, *New Wavelet Methods for Approximating Harmonic Functions*, Geodetic Theory Today, F. Sansó, (ed.), International Association of Geodesy Symposia, Springer, **114**, 112-121, 1995.
- [40] W. Freeden and M. Schreiner, *Orthogonal and Nonorthogonal Multiresolution Analysis, Scale Discrete and Exact Fully Discrete Wavelet Transform on the Sphere*, Constr. Approx., **14**, 493-515, 1998.
- [41] W. Freeden and U. Windheuser, *Spherical Wavelet Transform and its Discretization*, Adv. Comput. Math., **5**, 51-94, 1995.
- [42] Y.C. Fung, *Foundation of Solid Mechanics*, Prentice-Hall, Englewood Cliffs, N.J., 1965.
- [43] T. Gervens, *Vektorkugelfunktionen mit Anwendungen in der Theorie der elastischen Verformungen für die Kugel*, Ph.D. Thesis, RWTH Aachen, Institut für Reine und Angewandte Mathematik, 1989.
- [44] O. Glockner, *On Numerical Aspects of Gravitational Field Modelling from SST and SGG by Harmonic Splines and Wavelets (With Application to CHAMP Data)*, Ph.D. Thesis, Department of Mathematics, Geomathematics Group, University of Kaiserslautern, Shaker, Aachen, 2002.
- [45] J. Goswami and A. Chan, *Fundamentals of Wavelets: Theory, Algorithms, and Applications*, John Wiley Interscience, New York, 1999.
- [46] M.E. Gurtin, *Theory of Elasticity*, Handbook der Physik, **VI**, 2nd ed., Springer, Berlin, 1991.
- [47] W. Hackbusch and Z.P. Nowak, *On the Fast Matrix Multiplication in the Boundary Element Method by Panel Clustering*, Numer. Math., **54**, 463-491, 1989.
- [48] F. Hartmann, *Elastostatics*, In C. A. Brebbia (ed.), Progress in Boundary Element Methods, **1**, Plymouth : Pentech Press, 1981.
- [49] K. Hesse, *Domain Decomposition Methods in Multiscale Geopotential Determination from SST and SGG*, Ph.D. Thesis, Department of Mathematics, Geomathematics Group, University of Kaiserslautern, Shaker, Aachen, 2002.
- [50] J.C. Jaeger and N.G. Cook, *Fundamentals of Rock Mechanics*, Chapman and Hall, London, ed 3, 1979.
- [51] S. Jaffard, *Wavelet Methods for Fast Resolution of Elliptic Problems*, SIAM J. Numer. Anal., **29**(4), 965-986, 1992.

- [52] M.A. Jawson and G.T. Symm, *Integral Equation Methods in Potential Theory and Elastostatics*, Academic Press, London, New York, San Francisco, 1977.
- [53] G. Kaiser, *A Friendly Guide to Wavelets*, Birkhäuser, Cambridge, MA, 1994.
- [54] J. Kakkuri and Z.T. Wang, *Structural Effect of the Crust on the Geoid Modelled by Using Deep Seismic Sounding Interpretations*, Geophys. J. Int., **135**, 495-504, 1998.
- [55] A. Karageorghis, G. Fairweather, *Method of Fundamental Solutions for Axisymmetric Elasticity Problems*, Comput. Mech., **25**, 524-532, 2000.
- [56] R. Klees and R. Hagmans, *Wavelets in the Geosciences*, (eds.), Lecture Notes in Earth's Sciences, Springer, Berlin, Heidelberg, New York, 1999.
- [57] M.A. Knops and L.E. Payne, *Uniqueness Theorems in Linear Elasticity*, Springer, Berlin, Heidelberg, New York, 1971.
- [58] V.D. Kupradze, *Potential Methods in the Theory of Elasticity*, Moskau, 1963; Israel Programme for Scientific Translations, Jerusalem, 1969.
- [59] P.D. Lax, *Symmetrizable Linear Transformations*, Comm. Pure and Appl. Math., **7**, 633-647, 1954.
- [60] L.A. Ljusternik and W.I. Sobolev, *Elemente der Funktionalanalysis*, Akademie Verlag, Berlin, 1955.
- [61] A. Lurje, *Räumliche Probleme der Elastizitätstheorie*, Akademie Verlag, Berlin, 1963.
- [62] T. Maier, *Multiscale Geomagnetic Field Modelling from Satellite Data - Theoretical Aspects and Numerical Applications*, Ph.D. Thesis, Department of Mathematics, Geomathematics Group, University of Kaiserslautern, 2003.
- [63] Y. Mayer, *Wavelets Algorithms and Applications*, Philadelphia, PA, SIAM Press, 1993.
- [64] J.E. Marsden and T.J.R. Hughes, *Mathematical Foundation of Elasticity*, Dover Publications, Inc., New York, 1994.
- [65] Y. Melnikov, *Green's Functions in Applied Mechanics*, Comput. Mech. Publ., Southampton, Great Britain, 1994.
- [66] V. Michel, *A Multiscale Method for the Gravimetry Problem - Theoretical and Numerical Aspects of Harmonic and Anharmonic Modelling*, Ph.D. Thesis, Department of Mathematics, Geomathematics Group, University of Kaiserslautern, Shaker, Aachen, 1999.

- [67] M H. Murray and P. Segall, *Modeling Broadscale Deformation in Northern California and Nevada from Plate Motions and Elastic Strain Accumulation*, American Geophysical Union, Geophys. Res. Letters, **28**, 4315-4318, 2001.
- [68] C. Müller, *Foundations of the Mathematical Theory of Electromagnetic Waves*, Springer, Berlin, Heidelberg, New York, 1969.
- [69] H. Nutz, *A Unified Setup of Gravitational Field Observations*, Ph.D. Thesis, Department of Mathematics, Geomathematics Group, University of Kaiserslautern, Shaker, Aachen, 2002.
- [70] S. Owen, P. Segall, M. Lisowsky, A. Miklius, R. Denlinger and M. Sako, *Rapid Deformation of Kilauea Volcano: Global Positioning System Measurements Between 1990 and 1996*, J. Geophys. Res., **105 (B8)**, 18983 - 18998, 2000.
- [71] F.F. Pollitz, *Coseismic Deformation from Earthquake Faulting on a Layered Spherical Earth*, Geophys. J. Int., **125**, 114, 1996.
- [72] W.H. Prescott, J.C. Savage, J.L. Svarc and D. Manaker, *Deformation Across the Pacific-North America Plate Boundary Near San Francisco, California*, J. Geophys. Res., **106**, 66736682, 2001.
- [73] A. Rathsfeld, *A Wavelet Algorithm for the Boundary Element Solution of a Geodetic Boundary Value Problem*, Comput. Methods Appl. Mech. Eng. **157**, 267-287, 1998.
- [74] J.N. Reddy, *Applied Functional Analysis and Variational Methods in Engineering*, McGraw-Hill, 1986.
- [75] A.S. Saada, *Elasticity Theory and Applications*, Pergamon Press, Inc., New York, 1974.
- [76] A.M. Sändig, *Variational Methods for Elliptic Boundary Value Problems*, AGTM Report, No. 201, Department of Mathematics, University of Kaiserslautern, 1998.
- [77] M. Schreiner, *Tensor Spherical Harmonics and Their Application in Satellite Gradiometry*, Ph.D. Thesis, Department of Mathematics, Geomathematics Group, University of Kaiserslautern, 1994.
- [78] P. Segal, *GPS Applications for Geodynamics and Earthquake Studies*, Ann. Rev. Earth and Planet. Sci. **25**, 301-36, 1997.
- [79] I.N. Sneddon and D.S. Berry, *The Classical Theory of Elasticity*, Encyclopedia Phys., **6**, Springer, 1958.
- [80] I.S. Sokolnikoff, *Mathematical Theory of Elasticity*, 2nd ed., MacGraw-Hill Book Company, New York, 1956.



- [81] M.W. Tücks, *Navier-Splines und ihre Anwendung in der Deformationsanalyse*, Ph.D. Thesis, Department of Mathematics, Geomathematics Group, University of Kaiserslautern, Shaker, Aachen, 1996.
- [82] O.N. Ucan, S. Seker, A. M. Albora and A. Ozmen, *Separation of Magnetic Fields in Geophysical Studies Using a 2-D Multi-resolution Wavelet Analysis Approach*, J. Balkan Geophys. Soc., **3(3)**, 53-58, 2000.
- [83] P. Vanicek and E.J. Krakiwsky, *Geodesy : The Concepts*, 2nd ed., Elsevier Science, North Holland, Amsterdam, 1986.
- [84] K. Washizu, *Variational Methods in Elasticity and Plasticity*, Pergamon Press, 1975.
- [85] K. Yoshida, *Functional Analysis*, Springer, Berlin, Heidelberg, New York, 1965.

## Wissenschaftlicher Werdegang

- |             |  |
|-------------|--|
| 1965        | Geboren in Kahawattha, Sri Lanka   |
| 1970 - 1979 | Primary/Secondary School in Maha Pannila, Rakwana, Sri Lanka   |
| 1979        | General Certificate of Education (Ordinary Level)  |
| 1980 - 1983 | Gankande Central College in Pelmadulla, Sri Lanka  |
| 1983        | General Certificate of Education (Advanced Level)  |
| 1984 - 1987 | Studium der Mathematik/Physik an der<br>Universität Ruhuna in Matara, Sri Lanka  |
| 1987 - 1991 | Studium der Mathematik an der<br>Universität Kelaniya, Sri Lanka   |
| 1991        | B.Sc. (Special) Hons. Degree in Mathematics  |
| 1991 - 1995 | Wissenschaftlicher Mitarbeiter an der<br>Universität Ruhuna in Matara, Sri Lanka   |
| 1995 - 1997 | Studium der Technomathematik an der<br>Universität Kaiserslautern, Deutschland;<br>gefördert als DAAD-Stipendiat                           |
| 1997        | M.Sc. nat. (Industrial Mathematics)  |
| 1997 - 2000 | Wissenschaftlicher Mitarbeiter an der<br>Universität Ruhuna in Matara, Sri Lanka   |
| 2000 - 2003 | Doktorand der AG Geomathematik an der<br>Universität Kaiserslautern, Deutschland;<br>gefördert vom DAAD und der Universität Kaiserslautern |

### **Eidesstattliche Erklärung**

Hiermit erkläre ich an Eides statt, dass ich die vorliegende Arbeit selbst und nur unter Verwendung der in der Arbeit genannten Hilfen und Literatur angefertigt habe.

.....

Kaiserslautern, 07, July 2003.